Examining the impact of anti-inflammatory and anti-viral treatments in human brain cell infection models for *Herpes Simplex* virus encephalitis

‘Thesis submitted in accordance with the requirements of the University of Liverpool for the degree of Doctor in Philosophy by Jeoffrey Vincent Ginès François Segura’

June 2018

PhD Thesis title: **Examining the impact of anti-inflammatory and anti-viral treatments in human brain cell infection models for *Herpes Simplex* virus encephalitis**

Submitted by: **Jeoffrey Vincent Ginès François Segura.**

Primary Supervisor: **Dr Michael J Griffiths**

Secondary supervisor: **Prof Tom Solomon**

Abstract

Herpes Simplex Encephalitis (HSE) is a lethal brain inflammation induced by *Herpes Simplex* virus (HSV), mainly HSV-1 subtype. Brain damage associated with HSE is reported to be caused directly by the virus and indirectly by the host immune responses.

Aciclovir, the gold standard anti-viral therapy, targets HSV replication but not brain inflammation. Hence, administration of anti-inflammatory drugs alongside aciclovir may improve outcome in HSE patients. However, clinicians worry that immune-modulating drugs may enhance HSV replication during acute HSE. A few small clinical studies have demonstrated that administering glucocorticoids in combination with aciclovir improve patient outcome. However, change in HSV viral load was not examined. Interestingly, tumor necrosis factor alpha (TNF-α), a known pro-inflammatory mediator, exhibits high levels in cerebrospinal fluid among HSE patients. To date, there are no studies examining anti-TNF therapy in HSE patients or human models. Further studies need to be performed to investigate the effect of anti-TNF agents and glucocorticoids on human brain cell survival and HSV viral load, to support future clinical studies.

In my thesis, I have studied the impact of dexamethasone (a glucorticoid) and infliximab (an anti-TNF agent) in acute (up to 72 hours post-infection) HSV-1-infected human brain cell models. My study shows dexamethasone and infliximab administered in combination with aciclovir were not detrimental to cell viability or cell activity (as measured by mitochondrial activity) among HSV-1-infected neuroblastoma or microglia. I also showed these drugs do not enhance HSV-1 replication in these cells. Interestingly, Infliximab (in a single dose) was protective against HSV-1 infection in neuroblastoma and microglia cells. It led to a rapid reduction of HSV DNA abundance in the culture medium of the infected cells and slowed reduction in live cell number and activity. Nonetheless, neither dexamethasone nor infliximab showed a significant benefit in combination with aciclovir compared to aciclovir alone. I have also developed co-culture

models of HSE using primary astrocytes or neuroblastoma cells co-cultured with microglial cells to begin to enable evaluation of drug therapies in more complex models.

My results highlight that adjunctive anti-inflammatory therapies do not enhance HSV replication during acute infection of human brain cells. My findings also suggest infliximab may have potential, in different dose regimens, as a future adjunctive therapy in HSE.

Acknowledgements

This thesis became a reality with the great support and help of many individuals. I would like to deeply express my sincere thanks to:

-My first supervisor Dr Mike Griffiths. I would like to thank Mike for his guidance over the last four years. I have definitely learnt a lot from my sessions with him. I am now a better researcher and scientist compared to the day we met. And now, I can also understand his "welsh" accent and his jokes too.

-My second supervisor Prof Tom Solomon. Tom has been supportive and really useful for helping to choose the right directions of my PhD project.

-The Kirkby Foundation. I would like to deeply thank the Kirkby Foundation for having funded this PhD. It was always a pleasure to see Janet and Stuart and talk with them. They were supportive and friendly every time we met.

-Dr Gosia Wnek. I would like to thank Gosia for teaching everything I had to know in the lab when I started. She always was patient and opened to answer my questions. I am also grateful for her help in the gene expression studies performed in microglial cells.

-Dr Janet Flatley and Dr Tessa Prince. Thanks to my colleagues and friends Janet and Tessa for her kindness and support. I will never forget the time you spent in helping to make this thesis easier to read. Neither I will forget the good moments we had outside the IGH, during lunch time or in A&J on the Friday evenings.

-All the other members of the Brain Infection Group (Lance, Fiona, Lutfi…). It was nice to be a member of the Brain Infection Group. I am a grateful for all the support and feedbacks I got from everyone especially during presentations, meetings…I also got brilliant memories for the retreats (games, dinners, walks…) we had together.

-Dr Antoine Barbieri (University of Bordeaux). Many thanks for your supervision in the statistics part. It was always a pleasure to talk with you.

-Dr Kukhanova et al. Thank you very much for accepting I use your figure (figure 1.1) in my thesis.

-My PhD advisors. Thank you to Britta Urban and Neil Blake for their precious advices and help during this PhD.

-My friends from IGH. I would like to thank all my friends from IGH (Alessandra, Ana, Charlene, Libby, Lindsay, Marie, Marion, Noon, Raquel, Rong, Shadia, Amer, Dinos, Filippo, John, Jordan, Stavros…). We shared so many things together, good and bad moments, in the lab and outside. My life in Liverpool would not have been the same without them. I have special thoughts for the ones that are ending their PhD now (Charlene, Lindsay, Marion, Raquel) and wish them good luck.

-The "Old Bank crew". I remember with great pleasure my first year in Liverpool in this "Old Bank" that became a home thanks to four wonderful ladies (Bibi, Klaudia, Lisa, Rachel). I am glad we keep in touch and I wish them the best of luck in their lives.

-My family. I would like to thank my family for all the support they sent me over the phone, by skype, by texts, by email or for sure when they came to visit me. All of them were supportive and gave me a lot of strength to handle the difficult moments. I am happy to be back home and looking forward to spend a nice summer together since we could not do that over the last years. *Merci à toute ma famille.*

-My friends back home. I am also grateful to have such good friends back home for so many years now. I am proud we all kept in touch for all these years. It is always a pleasure to meet up in Montpellier or Vinassan. *Et oui Vinassan est le plus des villages. Merci à tous.*

Declaration

Except for the assistance outlined in the acknowledgements, the work described is my own work and has not been submitted for a degree or other qualification to this or any other university.

List of abbreviations

Acv	Aciclovir
ACV-TP	Aciclovir-triphosphate
AM	Acetoxymethyl
Bcl-2	B-cell lymphoma 2
β-2M	β-2 Microglobulin
CD	Cluster of differentiation
CMC	Carboxymethyl cellulose
CNS	Central nervous system
CSF	Cerebrospinal fluid
CXC	C-X-C motif chemokine
Dex	Dexamethasone
DMEM	Dulbecco's modified Eagle's medium
DNA	Deoxyribonucleic acid

ELISA	Enzyme-linked immunosorbent assay
ERK	Extracellular signal-regulated kinase
gD	glycoprotein D
gH	glycoprotein H
gJ	glycoprotein J
gL	glycoprotein L
HA	Human astrocytes
HeLa	Henrietta Lacks
HEp-2	Human epithelial type-2
HSV	*Herpes Simplex* virus
HSE	*Herpes Simplex* virus encephalitis
Ifx	Infliximab
IP-10	Interferon γ-induced protein 10
Ig	Immunoglobin
ICP	Infected cell polypeptide
IL	Interleukin
INF-β	Interferon-β
IFN-γ	Interferon-γ
iNOS	inducible nitric oxide synthase
JE	Japanese encephalitis

JEV	Japanese encephalitis virus (JEV)
JNK	Jun nuclear kinase
LAT	Latency-associated transcripts
LPS	Lipopolysaccharide
MAPK	Mitogen-activated protein kinase
MEK	MAPK/ERK kinase
MG	Microglia
MOI	Multiplicity of infection
MRI	Magnetic resonance imaging
NAD	Nicotinamide adenine dinucleotide
NADH	Nicotinamide adenine dinucleotide + hydrogen
NADP	Nicotinamide adenine dinucleotide phosphate
NADPH	Nicotinamide adenine dinucleotide phosphate + hydrogen
NB	Neuroblastoma cells
NF-κB	Nuclear factor κ-light-chain-enhancer of activated B cells
NO	Nitric oxide
PBS	Phosphate Buffered Saline
PCR	Polymerase Chain Reaction
Pi	Post-infection
PI	Propidium iodide

Pt	Post-treatment
RANTES	Regulated on activation, normal T cell expressed and secreted (also known as CCL5)
RHIM	Receptor-interacting protein homotypic interaction motif
RIP3	Receptor-interacting protein 3
RNA	Ribonucleic acid
sCD8	soluble cluster of Differentiation 8
sFas	soluble Fas (Fas is also known as CD95)
sIL2R	soluble interleukin-2 Receptor
t	time
TG	Trigeminal ganglion
TLR	Toll-Like Receptor
TNF	Tumor Necrosis Factor
TNFR	TNF Receptor
US3	Ser/Thr Kinase kinase coded by HSV-1 in the Unique Short (US) region
UK	United-Kingdom
WST-1	Water-Soluble Tetrazolium-1

List of figures and tables

Table of contents

Chapter 1

1.1. Herpes Simplex Virus type 1 (HSV-1)

1.1.1. Classification and structure of HSV-1

HSV-1 (*Herpes Simplex* virus type 1) is a double-stranded (ds) DNA virus, belonging to the group I of the Baltimore classification. It is a member of the *Herpesvirales* order, *Herpesviridae* family and *Alphaherpesvirinae* subfamily, along with *Varicella Zoster* virus (VZV). Like *Herpes Simplex* virus-2 (HSV-2), its genus is *simplex virus*. The full particle of HSV is spherical with a diameter of around 225 nm[1]. It consists of a central core, an icosahedral nucleocapsid containing 152-155 kilo base-pairs (kbp) of dsDNA, which is surrounded by an amorphous matrix of viral proteins called the tegument, and the envelope (fig 1.1A). The envelope, the outer layer of the viral particle includes a lipid bilayer derived from the host cell, in which 600 to 750 surface glycoproteins, such as gB, gD, gH, or gL are anchored and form numerous spikes[1]. Surface glycoproteins are essential for HSV entry in host cells. gD is the main entry receptor of HSV and although it is able to bind both the surface molecules nectin-1 and Herpes Virus Entry Mediator (HVEM) on the host cell plasma membrane, the binding to nectin-1 appears to have a more crucial role in Herpes Simplex virus Encephalitis (HSE) pathogenesis in mice[2]. gB is a fusion protein that is only functional when partnered with the heterodimer gH/gL[3,4]. The HSV genome consists of two DNA blocks: one short and one long, each containing a unique sequence flanked by inverted repeat regions (fig1.1B). The HSV genome consists of four different DNA isomers encoding at least 84 multifunctional proteins that play a crucial role in viral replication and immune evasion.

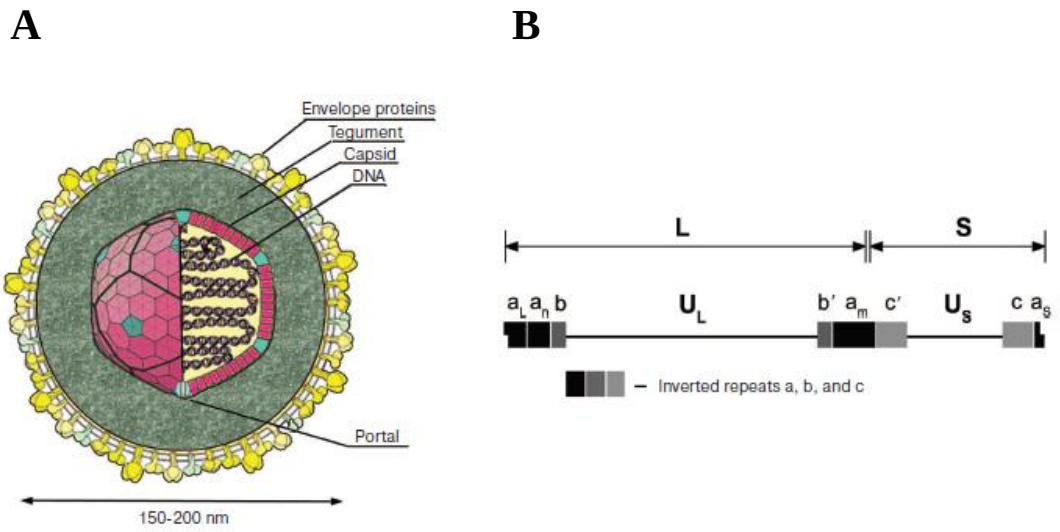

Figure 1.1. Structure of Herpes Simplex Virus type 1 (HSV-1). Source: Kukhanova et al. (*Biochemistry*, 2014, vol. 79, No. 13, pp. 1635-1652)[5]. (**A**) **Structure of HSV-1.** The HSV-1 particle contains a central core, the capsid or nucleocapsid in which the viral DNA is packaged. The capsid is surrounded by an amorphous matrix of proteins called the tegument and by a lipid envelop originated from the host cell and in which viral envelop proteins are anchored. (**B**) **Genome of HSV-1.** (U_L) Long Unique region, (U_S) Short Unique region, (IR_L and TR_L) Long Inverted Repeat sequences, (IR_S and TR_S) Short Inverted Repeat sequences. HSV-1 genome consists of 2 unique sequences, one short (U_S) and one long (U_L), that are both flanked by inverted repeat sequences (IR and TR).

1.1.2. Life cycle of HSV

The HSV life cycle consists of (i) a lytic phase in which viral replication and production of virions in host cells occurs and ultimately leads to cellular destruction and (ii) a latent phase whereby the virus remains dormant within nerve cells (i.e. sensory ganglia such as the trigeminal ganglion).

1.1.2.1. Lytic HSV replication in host cells

HSV replication is the process whereby the virus replicates its genome and synthesises new viral proteins within host cells in order to produce new HSV particles[6]. This process is aided by the ability of the virus to hijack the host cell machinery. It is lytic as it leads to the

destruction of host cells. Finally, the newly formed particles are released in the extra-cellular matrix and disseminated in the tissue for new host cell infections[6].

Once HSV gD binds host receptors, the viral envelope fuses with the plasma membrane thanks to the "fusogenic core" including the viral proteins gB and gH/gL[3,4]. The fusion allows the penetration of both the capsid and some viral tegument proteins into the host cell cytoplasm. Once the capsid reaches the nuclear pores, the HSV genome is released inside the nucleus[6]. The viral DNA is then replicated thanks to seven viral proteins including a DNA polymerase and transcribed by the host RNA polymerase II in the nucleus. New virions are also assembled inside the nucleus after translation of viral proteins in the cytoplasm. "Lytic" genes are HSV genes whose expression leads to the "lytic programme". This programme drives HSV replication in host cells by (i) replicating the genome, (ii) producing viral proteins and (iii) assembling new HSV particles including viral genome and proteins. Transcription of "lytic genes" occurs as a temporal cascade[6]. Firstly, immediate early (α) genes are transcribed; then early (β) genes and finally late (γ) genes. The α-gene products, such as ICP4, ICP22, ICP27, ICP47 and Us1.5 are involved in the β-gene transcription but also in the regulation of HSV replication[7]. The regulation of viral replication (and reactivation) is also ensured by other viral proteins such as the thymidine kinase or the ribonucleotide reductase[8, 9, 10, 11]. The expression of α-genes is necessary for a successful lytic viral replication, and their transcription is mainly triggered by the viral protein and transcriptional activator VP16[12, 13, 14]. The α-gene products not only promote lytic infection but also allow for the viral evasion of the host immune system. For example, *in vivo*, ICP27 is able to inhibit host mRNA translation while ICP47 can evade $CD8^+$ T cell recognition by inhibiting the activity of the transporter protein TAP (Transporter associated with Antigen Processing) [15]. The γ-proteins play a crucial role in the assembly of the capsid, tegument and envelope. Once the replicated viral DNA is packaged into the capsid, virions undergo steps of envelopment/de-envelopment by the membrane of the nucleus and Endoplasmic Reticulum (ER)[6, 16]. After the release into the cytoplasm, the capsid acquires a

mature envelop during the process of budding into endosome or Trans Golgi Network (TGN)-derived vesicles[16]. The anterograde movement of HSV virions into the cytoplasm to the cell periphery is dependent on the action of microtubules aided by kinesin motor proteins[16]. Overall, HSV productive infection destroys host cells and allows the release of infectious particles into the tissue and subsequent infection of nearby cells. This occurs during symptomatic HSV infections of mucosal tissue for example, lips, oral cavity etc.

1.1.2.2. Latency and reactivation

HSV infections can also be non-replicative and lead to latency establishment like in nerve cells. This can happen in the trigeminal ganglion (TG) (or the sacral ganglion following genital infection) once HSV particles infect neurons and travel along sensory fibres.

Latency is the ability of the virus to become dormant meaning the virus cannot replicate within the host cells during this phase. It allows the formation of stock of viruses within cells that can evade the host immune system. Latency is reversible, and reactivation is the process by which a latent infection turns back into a productive one, allowing the transmission to new hosts. Reactivation can be triggered by many stimuli such as stress, fever, immunosuppression and trauma[6]. HSV reactivation can result, for instance, in the virus travelling back from the Trigeminal Ganglion (TG), through sensory nerves, to the cutaneous nerve endings where a localized vesicular eruption can occur. This phenomenon of reactivation is well-described for patients with recurrent episodes of *Herpes labialis.* Latent infection is characterised by the circularization of the viral DNA into an episome (DNA mainly silenced). The elevated expression of Latency-Associated Transcripts (LATs) associated with a repressed expression of lytic genes has been described in a crucial subset of HSV-1-latently-infected neurons both in mice and human[6, 17, 18, 19]. Interestingly, *in vivo*, it has been shown that the LATs expressed during latent infections originated from the same HSV-1 genome regions in both central nervous system (CNS) and peripheral nervous system (PNS) tissues[20].

In a mouse model, LATs RNA were shown to play a role in maintaining the pool of latently-infected neurons in the TG with their absence leading to a significant loss of this pool[21]. LATs are thought to promote cell survival potentially through an anti-apoptotic activity, which has been mapped to 3'-end of the first exon and the 5'-end of the stable 2kb LAT intron[22]. In mouse HSV-1-latently-infected neurons, LATs induced not only a decrease in expression of lytic genes but also a reduced viral reactivation after exposure to one stress stimulus[23]. Another study confirmed this result but also showed that following multiple stress stimuli, LAT-null viruses but not LAT-positive viruses lost their capacity to reactivate over time[24].

Overall, it seems that the expression of LATs in HSV-1-latently-infected neurons in the TG leads to (i) the repression of lytic gene expression, (ii) the maintenance of a pool of latently infected neurons and (iii) the maintenance of the competence of reactivation over time but used at low frequency. Interestingly, most scientists accept that LATs are not translated *in vivo* into functional proteins, thus emphasizing their interest in the latent HSV transcriptome to better understand the mechanisms of latency and reactivation during HSV infection[7].

1.1.3. Pathological manifestations of HSV infection

Humans are the natural host of HSV. HSV infections occur worldwide and are not influenced by seasonality[6]. HSV transmission is thought to occur through close contact involving mucosal surfaces (i.e. oral cavity, genital mucosa) [6]. Most HSV infections are asymptomatic and sub-clinical, with the virus establishing latency in nerve cells (i.e. TG or sacral ganglia). The seropositivity of HSV-1 is extremely high and reached around 68% of the United States population in the period 1988-1994[25 26]. In the same study, the seropositivity of HSV-2 and the seropositivity for both HSV-1 and HSV-2 were around 22% and 17% respectively[26]. In 2012, the HSV-2 prevalence among 15-49 years old was estimated around 10% worldwide[27]. One third of the world's population is estimated to be affected by recurrent HSV (symptomatic) infections[6]. The main pathological manifestations of HSV infection includes

oral herpes, ocular herpes, genital herpes and herpes encephalitis. Oral herpes (known as cold sore, fever blister) is a rash of the skin and mucous membranes around the mouth, especially the lips (*labialis herpes*) characterised by lesions, blisters and mainly induced by HSV-1[28]. In Europe, the incidence and prevalence of *labialis herpes* are estimated to be respectively at 1.6 and 2.5 per 1000 patients and per year[28]. Herpetic gingivostomatitis is a specific presentation of oral herpes, within the mouth, describing an inflammation of both the oral mucosa and gingiva. In general, herpetic gingivostomatitis occurs in young children during a primary infection with HSV-1. Ocular herpes infection includes a spectrum of manifestations (i.e. stromal keratitis, endothelitis, superficial epithelial disease) depending on the part of the eye infected with HSV[29]. It is among the leading causes of visual morbidity[29]. In the United States, half a million of active ocular *herpes simplex* infections are diagnosed every year[30]**.** Genital herpes is clinically characterized by lesions and inflammation around the genital area, mainly the vulva and vagina for women and the shaft and the glans of penis for men. Five hundred million people are reported to live with genital herpes but this seems to be widely underestimated as there is an high proportion of patients unaware of their genital infection by HSV[31]. It is a very frequent sexually transmitted infection (STI) induced mainly by HSV-2 but also by HSV-1 for a high percentage of emerging first time cases. HSV-2 is mainly responsible for recurrent genital herpes infections. HSV-1 and 2 can also infect the nervous central system and cause other infectious diseases such as herpes simplex encephalitis and herpes simplex meningitis. Herpes simplex meningitis is an inflammation of the meninges, frequently recurrent, and usually caused by HSV-2[32]. Finally, herpes encephalitis is an inflammation of the brain parenchyma induced by HSV-1 (mainly) and 2 and presenting the most severe and lethal type of HSV infections.

1.2. Herpes Simplex Encephalitis (HSE)

1.2.1. HSE from a clinical perspective

1.2.1.1. Clinical definition of HSE

During the 1940's, the first cases of HSE, inflammation of the brain due to HSV, were demonstrated in both adults and neonates thanks to the detection of intranuclear inclusion bodies and the isolation of HSV from brains affected by encephalitis during post-mortem studies[33, 34]. The most characteristic pathological findings in the autopsy of the brain of the adult affected by HSE were necrosis, gliosis, perivascular cuffs of lymphocytes, multiple small haemorrhages and intranuclear inclusions of the herpetic type[33]. Crucially, these changes were asymmetrical as they were mainly observed in one temporal lobe and represented late-stage HSE. A picture of perivascular infiltrates is shown in the figure 1.2.

In a biopsy study of 12 subjects in 1984, very early signs of HSE in adult brain, including gliosis, glia nodules, perivascular inflammation and meningeal inflammation were described as being in mainly one temporal lobe of patient brain[35]. This is considered to correspond to the first week of neurological dysfunction in HSE[35]. Interestingly, at this stage of infection, neither necrosis nor haemorrhage were found in any of the brains of HSE patients. However, studies presenting acute HSE, and later stages of infection, revealed both the presence of necrosis and haemorrhages. Thus, in another clinical study, biopsy or necropsy of 22 acute HSE patients were done and revealed a majority of necrotizing encephalitis[36]. Furthermore, focal haemorrhages in the brain tissues could also be observed in this study. More recently, pictures of a brain biopsy of a HSE-affected 16-year-old male diagnosed and observed by Dr Dennis K. Burns (UT Southwestern Medical Center, Dallas, TX, United-States), showing brain necrosis in the right temporal cortex, was thoroughly described in the review of Kim et al[37].

Interestingly, brain haemorrhages can also be a feature of HSE acute phase, despite normal results of CSF analysis, as shown by a case-report of Lever et al[38].

It is now thought that both necrosis and inflammation peak about 2-3 weeks after HSV brain infection, while viral antigen detection declines within the brain tissue[35, 39]. Beyond necrosis and haemorrhages, within the brain tissue, the HSE acute phase can exhibit frequent Cowdry A intranuclear inclusions (masses of acidophilic material surrounded by clear halos within nuclei) in neurons, other direct signs of inflammation (i.e gliosis), vessel congestion, neuronophagia (destruction of neurons by phagocytosis), presence of cavitation and swellings in the temporal lobe[36]. In most HSE cases, liquefactive necrosis of the brain tissue occurs, which is a type of necrosis characterized by a liquid viscous mass of pus and other fluid remains.

In HSE, the inter-human transmission of HSV is thought to occur via contact with mucosal surfaces or abraded skin essentially involving the area of the mouth. It was recently shown that HSV-1 could enter human keratinocytes by a mechanism of nectin-1-dependent plasma membrane fusion (at low temperature)[40]. Of note, HSV particles consequently undergo a retrograde transport, by a mechanism shared with pseudorabies virus[41]. Hence, by nerve axonal flow, HSV may establish latency in the dorsal root ganglion or in the CNS targeting the TG, the olfactory bulb or the brain as shown *in vivo*[42]. However, direct productive infection of the brain following HSV primo-infection is possible[43, 44, 45]. The majority of HSE patients contracting a primary infection are under 18 years old[45]. Although, HSE can be the result of a primary infection, HSE is mainly due to reactivation of HSV from latency into nerves. Reactivation of HSV in CNS may occur in the brain tissue, olfactory bulb and trigeminal ganglia.

Animal studies demonstrate that the route of HSV access to the brain includes both olfactory and trigeminal nerves pathways. In humans, the main hypothesis favours the route through the

olfactory nerves. Contrary to the trigeminal nerve pathway, the olfactory pathway leads to both temporal lobes and limbic areas, which are probably the main sites of brain tissue damage during HSE. This hypothesis has been further reinforced by the demonstration of HSV particles in necrotic olfactory bulbs in HSE cases[46].

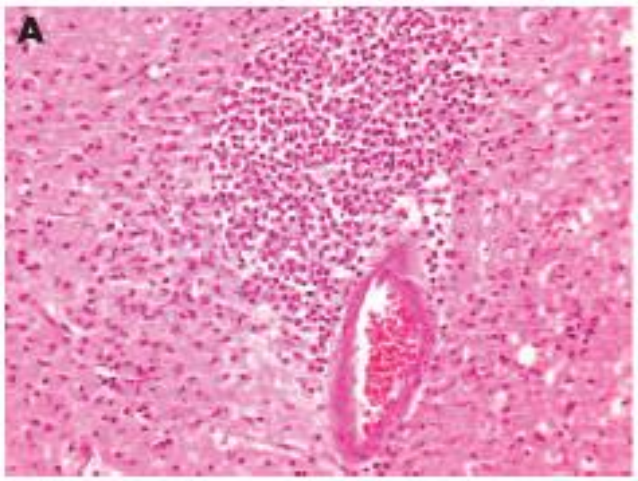

Figure 1.2. Histopathological changes of the temporal cortex in a patient who died from HSE. Source: Prof T. Solomon[47], pictures originally from Dr D. Crooks. Important perivascular infiltrate (activated microglia, macrophages and lymphocytes). Staining by Haematoxylin-Eosin. 20 x magnification.

1.2.1.2. Epidemiology

HSE is the most commonly diagnosed viral encephalitis in western countries and the most common infectious cause of sporadic encephalitis worldwide[43]. However, it is a rare disease with an annual incidence of 1 in 250,000 - 500,000 individuals worldwide[43]. A very recent study estimated the annual hospitalisation rate for HSE at 10.3 ± 2.2 cases/million in neonates, 2.4 ± 0.3 cases/million in children and 6.4 ± 0.4 cases/ million in adults in the US[48]. Excluding very young children (under 3 years of age), HSE peaks over the age of 50 and affects both sexes equally[43]. Currently, HSV-1 accounts for around 90% of HSE cases[49].

1.2.1.3. Clinical manifestations

The most frequent clinical signs associated with HSE include fever, severe headache, nausea, vomiting, lethargy, altered mental state, focal neurological deficit, behavioural changes, seizures and evidence of brain inflammation such as cerebro-spinal fluid (CSF) pleocytosis (≥ 5 nucleated cells/ml)[32, 45, 43]. Magnetic Resonance Imaging (MRI) of brains affected by HSE usually demonstrates specific abnormalities, such as focal enhancement in the temporal lobe or adjacent structures (fig 1.3) [39, 47]. In 45 HSE patients, MRI has shown that the areas of involvement were mainly the temporal lobe (87.5%) but also the insula (70%), the frontal lobe (67.5%) and the thalamus (27.5%)[50]. By this same technique, HSE due to HSV-2 has shown more heterogeneous spread compared to the HSV-1 encephalitis. Furthermore, MRI is more sensitive than Computed Tomography (CT) scanning for detecting early changes of HSE[200]. In another HSE clinical study, favourable initial Electroencephalogram (EEG) findings were correlated with good 6-month clinical outcomes[51].

CNS complications such as seizures (38%), status epilepticus (5.5%), acute respiratory failure (20.1%), ischemic stroke (5.6%) and intracranial hemorrhages (2.7%) were found relatively frequent among HSE patients and associated with mortality[48].

Of note, some patients seem to develop HSE after having received neurosurgical procedures, CNS radiation therapy or immune therapies especially natalizumab or TNF inhibitors[39]. HSE can also affect immunocompromised patients, however there is no evidence that HSE is more prevalent in this population[39]. HSE in immunocompromised patients exhibits less extensive CSF pleocytosis, more widespread CNS lesions and higher mortality rate[39].

Without treatment, more than 70% of HSE patients die and less than 3% completely recover a normal neurologic status[52]. The most frequent neurological sequelae observed in HSE are memory impairment, personality and behavioral changes, speech abnormalities, epileptic

seizures and anosmia[53]. HSE survivors can also experience permanent seizure disorder or motor deficit[32].

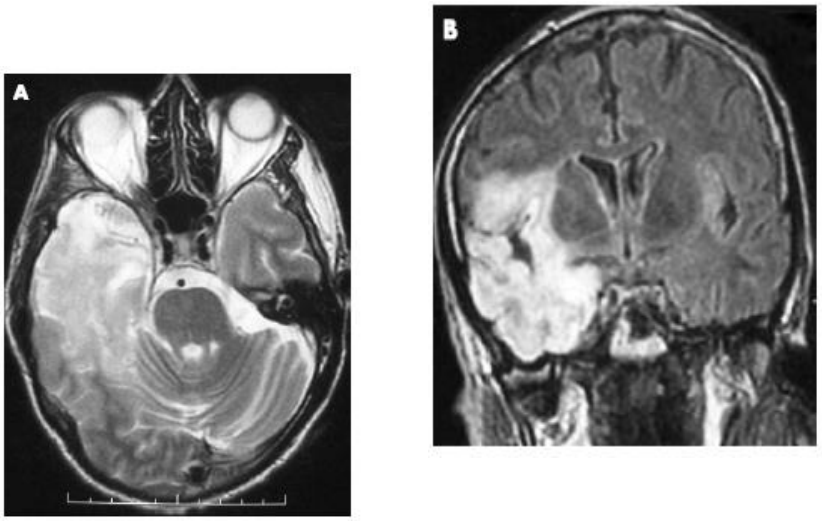

Figure 1.3. Right temporal lobe hyperintensity observed by T2-weighted MRI in a patient with HSE. Source: Prof T.Solomon[47].

1.2.2. HSE pathogenesis

1.2.2.1. HSV pathogenesis at the cellular level

HSV-1 modulates major cellular functions including mitochondrial functions, mRNA and protein synthesis and synaptogenesis during the infection of brain cells.

Following HSV-1 lytic infection, a shutoff of host mRNA has been observed in diverse mammalian non-CNS cells. This appeared to be due to several actions of viral proteins on host cellular machinery such as (i) host mRNA degradation by virion host shutoff (vhs) protein, (ii) impairment of the host mRNA splicing induced by ICP27 and (iii) suppression of host mRNA synthesis by targeting RNA polymerase II activity, particularly through ICP22[54, 55, 56, 57, 58, 59]. In the host cell machinery, PP1-α has the ability to induce protein synthesis as it leads to the dephosphorylation of eiF2-α so as to reverse the PKR-induced inhibition of protein synthesis[60]. Regarding the modulation of protein synthesis by HSV-1, it was shown that the interaction

between the viral protein ICP34.5 and eiF2-α is crucial for the specific dephosphorylation of eiF2-α by PP1[61]**.** Hence, HSV-1 is able to modulate protein synthesis potentially to facilitate viral replication.

Interestingly, the amino-terminally truncated form of the viral protein UL12 could induce a complete depletion of the mitochondrial DNA leading to higher requirements in pyruvate and uridine cell consumption[62]. A post-mortem transcriptomic study showed a preferential reduction in expression of mitochondrial genes such as cytochrome c oxidase 1 (CO1) in HSE cases compared to control subjects[63]. The loss of CO1 gene expression was confirmed in *in vitro* HSV-1 infection of primary human astrocytes and shown to be prior to the decrease in the nuclear DAD-1 gene expression. In mitochondria, the loss of enzymatic activity of mitochondrial genome-encoded CO1 was also seen before that of the nuclear genome-encoded mitochondrial enzyme SDH. The infection was associated with temporal sequence of mitochondrial integrity damage (i.e. loss of granularity, membrane fragmentation) starting prior to the nuclear morphologic changes. Altogether, this suggests that the alteration of mitochondrial functions in brain cells may be an early event of HSE pathogenesis. Interestingly, the antibiotic drug minocycline was found to increase cell viability, CO1 gene expression and mitochondrial activity in HSV-1-infected astrocytes[63].

In neurons, HSV-1 was shown to induce microtubule dynamic alterations, τ hyperphosphorylation and resulting axonal disruption[64]. HSV-1-infected neurons are also affected by a synaptic dysfunction characterized by (i) a reduced production of presynaptic proteins, (ii) an impaired synaptic transmission and (iii) a reduced plasticity due to GSK-3 activation and a subsequent intraneuronal accumulation of amyloid-β proteins[65].

Hence, during HSE, neurons and other brain cells undergo diverse and various alterations of their organelles (microtubules, mitochondria, nucleus) and functions (energy production, cytoskeleton intracellular transport, mRNA splicing, protein synthesis). Ultimately, these

pathogenic changes can lead to the brain cell death and liquefactive necrosis of targeted regions of the brain tissue affected by HSE.

1.2.2.2. Immune response involved in HSE pathogenesis

It has been demonstrated that the severity of histopathologic changes and neurological clinical signs does not correlate well with the viral load in the CSF[66]. However, HSV replication is in balance with the immune response suggesting the latter can also be involved in detrimental brain cell damage and HSE pathogenesis[67].

1.2.2.2.1. Leukocyte infiltration, microglia activation and Blood Brain Barrier (BBB) permeability following HSV-1 brain infection and their role in HSE pathogenesis

The phenotypes and kinetics of leukocyte infiltration have been assessed in an *in vivo* model of HSE[68]. Macrophages and neutrophils were the first immune cells to invade the brain several days after infection, followed by T lymphocytes (2-4 weeks after the infection) at a $(CD8^+)/(CD4^+)$ ratio of 3/1[68]. In parallel, within the brain tissue, microglia, the resident macrophages, markedly up-regulated their MHC II expression (2-4 weeks after infection), as a sign of their activation. In response to HSV-1, lymphocytes, macrophages and microglia presented a marked increase in the gene expression of one key pro-inflammatory molecule each: IFN-γ, TNF-α and IL-1β, respectively[68]. Crucially, the transfer of activated immune cells in an *in vivo* model of HSE led to an earlier mortality[68]. Similarly, Lundberg *et al.* have shown after HSV-1 corneal inoculation that (i) mice susceptible to HSE, but not the resistant counterparts, presented intense focal inflammatory brain stem lesions of primarily F4/80+ macrophages and Gr-1^+ neutrophils and (ii) the depletion of these cells in the susceptible mice led to an enhancement of their survival[69]. Finally, in response to an *in vivo* intranasal HSV infection, there were also significant increases in the percentage of macrophages and INF-γ-

producing CD8 T cells in the trigeminal ganglion[70]. Altogether, this suggests that leukocyte infiltration and microglia activation may participate in HSE pathogenesis**.**

In HSE patients, the levels of two markers of T cell activation, sIL-2R and sCD8, peaking at convalescence stage, suggest that the immune response following leucocyte infiltration may also play a role in patient outcome after the acute phase both in relapse and neurological sequelae[71]. Interestingly, B-cells have been shown to decrease the susceptibility to HSE in mice by reducing viral multiplication, most probably through antibody secretion[72]. Among patients with proven HSE, a high proportion (74-84%) presented with at least a 4-fold increase in CSF IgG[73]. However, CSF anti-HSV-IgG levels did not influence the outcome of HSE-patients treated with ACV[74].

Leukocyte infiltration is dependent on the blood brain barrier (BBB) permeability. Of note, a retrospective study demonstrated that the BBB permeability was negatively correlated with CSF IL-10 among patients with encephalitis and, interestingly CSF IL-10 was positively correlated with a normal coma score at admission[75]. This suggests that an increased BBB permeability may reflect the high degree of unconsciousness at admission among patients with encephalitis.

1.2.2.2.2. TLRs, signalling pathways and some pro-inflammatory cytokine profiles associated to detrimental or protective effects during HSE

Among transmembrane proteins, Toll-like receptors (TLRs) are pattern-recognition receptors (PRR) found in innate immune cells such as neutrophils and macrophages (like microglial cells in the brain) [76]. Their role is to recognize a very wide repertoire of pathogen-associated patterns (PAMPS) and, upon activation, to initiate the immune response to infectious agents.

In humans, 10 TLRs have been discovered (TLR1-TLR10)[76]. They own an extracellular leucine-rich domain especially mediating the immune response to bacterial surface-associated

PAMPS such as LPS or viral structural proteins. The leucine-rich TLR binding surface has been structurally characterized and appears to be 10-fold greater than the ones of antibodies or T-cell receptors[77]. TLR1, 2, 4, 5 and 6 are found on the plasma membrane[76]. TLR3, 7, 8 and 9 are observed within the cells, on the surface of endosomes and can target bacterial or viral nucleic acids[76]. For instance, TLR3 responds to double-stranded RNA and activate the PI3K-Akt pathway while TLR9 is activated following viral CpG DNA recognition[78, 79].The cooperation between different TLRs such as TLR2 and 6 is essential for host response against invading agents like bacteria or yeast[80].

Other PRRs such as C-type lectin receptors, NOD-like receptors, RIG-I-like receptors or cytosolic DNA sensor (i.e. cGAS) have been discovered more recently. Their cross-talk with the TLRs is essential for innate immune initiation[76, 81, 82]. For example, it was shown that NOD-1 combined with TLR7 induced a higher proliferative response in peripheral B cells compared to the effect of TLR7 alone[82]. PRRs are also involved in the activation of the adaptative immune system by inducing dendritic cells (DCs) maturation. It is the case of TLR5 following bacterial flagellin challenge[83].

The TLR activation triggers different intracellular signalling pathways modulated by kinases (such as Mitogen Activated Protein Kinases (MAPK) including c-Jun N-terminal Kinase (JNK) or p38 mitogen-activated protein kinases) and leads to the expression of different transcription factors including NF-kB or Interferon Regulatory Factor 3 (IRF3). In turn, it leads to the production of cytokines, chemokines and Reactive Oxygen Species. As an illustration, epithelial TLR5, after flagellin challenge, induces p38 activation that leads, in turn, to an increase in IL-8 expression[84].

Lokensgard *et al.* showed that HSV-1-infected human foetal microglia underwent a limited viral replication but release considerable amounts of TNF-α, IL1-β, CXCL10/IP-10 and RANTES whereas (human foetal) astrocytes and neurons were fully permissive to HSV but

did not release any of the aforementioned cytokines or chemokines [85]. Other scientists found that the cytokines IL-1β, IL-6, TNF-α, IL-18, IL-12β and CXCL2 were produced, in a TLR2-dependent way, by murine microglia following *in vitro* HSV infection [86].

$CD118^{-/-}$ mice, compared to WT, showed a pathological enlargement of lateral ventricles associated with their absence of type I INF pathway in microglia[87]. The worse outcome in this $CD118^{-/-}$ population was associated with an increase in CXCL1 and CXCL10 levels in the CSF, an increased TNF-α expression in the ependymal region and a brain invasion of neutrophils[87]. Another *in vivo* study revealed that the absence of the adaptor MyD88, inducer of NF-κB, was associated with a decrease in macrophages TNFα production and severe encephalitis in mice [88]. Cyclic GMP-AMP synthase (cGAS) is a PRR that can sense viral DNA in the cytosol and induce a type I IFN response through the adaptor protein stimulator of type I INF genes (STING). In an ocular HSE mice model, it was found that mice deficient in cGAS-STING presented a higher susceptibility to HSE with an impaired antiviral defence [89]. *In vitro*, the same authors showed that the administration of IFN α/β at the time of infection induced a decrease in viral titres in neurons (only for WT mice), astrocytes (WT and "STING KO" mice) and microglia cells (WT and "STING KO" mice) [89]. Hence, this suggests a crucial role of type I IFN for the initial control of HSV-1 replication *in vivo* induced by the cGAS-STING activation. Furthermore, IFN- α/β Receptor knock-out (IFN α/β KO) mice were shown to present earlier mortality, higher brain viral titres and increased brain IFN- β expression in another HSE *in vivo* model[90]. This same study showed that both $TLR2^{-/-}$ and WT mouse populations exhibited similarly a low mortality and few signs of encephalitis after HSV-1-infection[70]. However, $TLR9^{-/-}$ and $TLR2/9^{-/-}$ mice were much more affected with 60% and 100% mortality respectively. They exhibited considerable histopathological changes such as intense leptomeningitis associated with oedema, white matter vacuolization, endothelial reactivity, perivascular oedema and focal encephalitis (characterized by mononuclear cell infiltrates, activated microglia and perivascular cuffing). The most significant changes seen in

microscopy concerned the TLR2/9$^{-/-}$ population. Regarding the gene expression profile, the bad outcome in TLR2/9$^{-/-}$ was associated with increased CCL2/MCP-1, CXCL10/IP-10 and decreased IL-1β and INF-γ levels in both brain and TG.

Nevertheless, other researchers found the absence of TLR2 to be protective in HSE *in vivo* models. Thus, it was observed that HSV-1 intraperitoneally-infected TLR2$^{-/-}$ mice, independently of the virus titers in brain, exhibited a blunted cytokine/chemokine response associated with reduced levels of serum IL-6, brain MCP-1/CCL2, fewer histopathological changes, a reduced inflammation in cerebellum and a decreased mortality[91].

The unclear outcome of TLR activation and its upstream release of pro-inflammatory cytokines and chemokines following *in vivo* HSV-1 infection in CNS could be due to the difference in mice strains, CNS regions studied, HSV-1 administration mode (intranasal vs intraperitoneal), HSV-1 strains or MOI used in the *in vivo* models. Alternatively, this may just reflect the fact that effects of cytokine and chemokine effects following HSV-1-brain infection are the results of a sum of interactions between cytokines and chemokines up or down regulated rather than that of an action of one individual pro-inflammatory molecule.

Ex vivo brain slices showed that HSV-1 infection induced a slight increase in IFN-β gene expression and a more marked increase concerning the expression level of the Interferon-stimulated-gene Mx1[92].

In HSE-affected patients, it has been found that during the acute phase (first week of illness), the CSF pro-inflammatory molecules IL-6 and IFN-γ levels were elevated[71]. Then, during a convalescence stage, high levels of TNF-α, sIL2R and sCD8 were observed. Another study showed that high CSF values of INF-γ at the time of admission and high maximum CSF value of IL-6 (10^3-10^4 pg/ml) were predictors of poor outcome[93]. A significant increase in the CSF levels of two markers of immune system activation, neopterin and β2M, has also been

observed in HSE patients compared to a group of patients affected by other neurological diseases (mainly non-HSV encephalitis) during the acute phase[94]. Crucially, high levels of neopterin correlated with worse outcomes during this phase. Finally, high levels of this molecule were still found in the CSF of HSE patients in the convalescent phase emphasizing the persistence of immune activation, after the acute phase, in HSE. Hence, clinical studies associate high CSF levels of some key pro-inflammatory molecules with HSE and potentially with clinical bad outcome.

On the other hand**,** innate defects in the pro-inflammatory TLR3 signalling pathway have been correlated with a reduced anti-HSV-1 response and high susceptibility to HSE[95, 96, 97]. Among a cohort of sixteen adult patients with HSE, different mutations in molecules associated with the TLR3 or IFN receptor pathways (IRF3, TRIF, STAT1, TLR3 and TBK1) in PBMCs were identified by whole-exome sequencing[95]. Most of these patients exhibited PBMCs with impaired expression in IFN-β**,** CXCL10 and/or TNF α. Moreover, TLR3 mutations were also associated with HSE in children[97]. Altogether, this suggests that defects in the early innate immune response to HSV-1 could lead to HSE predisposition.

1.2.2.2.3. Role of ROS and associated pro-inflammatory cytokines in HSE pathogenesis

Reactive oxygen species (ROS) are chemical molecules containing oxygen, produced by cells under normal conditions with crucial functions in cell signalling and homeostasis[98]. During an infection, their production is increased and they have been shown to have antimicrobial properties. However, an excessive production of ROS can lead to oxidative stress and cell damage[98].

Concerning HSE, it has been found that (i) an increase in oxidative products and (ii) a high inducible-Nitric Oxide Synthase (iNOS) and Heme Oxygenase (HO)-1 transcript abundance were associated with brain damage following *in vivo* HSV-1 brain infection[98]. HO-1 catalyses

heme degradation. The major source of the related nitric oxide (NO) production was the population of microglia $CD45^{(int)}/CD11b^{(+)}$ [98]. *In vitro*, increased intracellular production of ROS after HSV-1 infection has been observed in wild-type (WT) microglia compared to the $TLR2^{-/-}$ ones[99]. This TLR2-dependent production of ROS in microglia was associated with the activation of the p38 MAPK-p44/42 signalling pathways and with neural oxidative damage and toxicity[99].

However, other researchers have found a protective role for iNOS and NO in HSE. Indeed, $iNOS^{-/-}$ mice, after HSV-1 infection, presented with earlier mortality and showed an increased gene expression of the viral transcript VP16 as well as the TNF-α, MCP-1, RANTES and IP-10 host pro-inflammatory molecules compared to the WT counterparts in the TG[100]. Interestingly, an *in vitro* study showed that ROS can drive the TNF-α, IL-1β cytokine and the CCL2 or CXCL10 chemokine expression through p38 MAPK-p44/42 activation in HSV-1-infected microglia[101].

Altogether, the data suggests a HSV-1-induced and TLR2-dependent ROS production by microglia/macrophages, which can be either detrimental or beneficial to the brain tissue during HSE. This dual effect of ROS in HSV-1-infected brain cells could be dependent on (i) its variable concentration into their brain tissue and/or (ii) its ability to induce the expression of different pro-inflammatory molecules depending on the infection stage and the microenvironment and/or (iii) the different models, cell lines and Multiplicity of Infection (M.O.I) used from one experiment to another.

1.2.2.2.4. Programmed cell death following HSV-1-infection and its role in HSE pathogenesis

Both HSV-1 and HSV-2 can trigger or block apoptosis, depending on the cell type. Many *in vitro* and *in vivo* studies reported diverse HSV proteins as modulators of apoptosis. In Hep-2 strain of HeLa cervical adenocarcinoma cells, HSV-1 triggered apoptosis and later blocked it

by *de novo* protein synthesis at a critical time period called the "prevention window" [102]. The expression of the HSV immediate early gene ICP0 seems to play a key role in initiating apoptosis[103]. Nevertheless, the viral proteins ICP27 (indirectly), gD, gJ, Us3, latency-associated transcript (LAT) and ribonucleotide reductase large subunit (R1) were shown to exhibit anti-apoptotic functions. These anti-apoptotic functions were induced by: (i) activation of NF-kB signalling and subsequent expression of anti-apoptotic genes[103] and/or (ii) inactivation of caspase-3 activation and/or (iii) inactivation by phosphorylation of Bcl-2 family pro-apoptotic proteins[103]. During HSV-1 latent infection of neuron-like cells, Latency-Associated Transcripts (LATs) were abundantly expressed and could counteract apoptosis induced by T-cells by interfering in the "caspase 3/granzyme B" interaction[104].

In an *in vitro* study using HSV-infected human hippocampal neurons, HSV-1 triggered apoptosis through c-Jun/Jnk pathway activation while HSV-2, inducing neither increase in apoptosis nor HSE, highly activated the MEK/ERK1/2 survival pathway but not c-Jun/Jnk[105]. Interestingly, HSV-1 and HSV-2 replicated similarly in hippocampal neurons suggesting that the induction of apoptosis only by the subset HSV-1 is independent of the viral replication but due to specific "HSV-1 versus host brain cells" molecular interactions leading to c-Jun/Jnk pathway and caspase-3 activation. In human HSE brain slices, there was also a good correlation between areas of HSV-1 infection, apoptosis and JNK activation[105]. An *in vitro* study from murine cells showed HSV-1-induced apoptosis in microglia cells was dependent on TLR2[106]. We could hypothesize for c-Jun/Jnk a role of mediator of TLR2 activation in HSV-infected microglia since this has already been shown in human corneal epithelial cells following TLR2 ligand challenge[107].

The difference in activation of c-Jun/JNK and MEK/ERK1/2 signalling pathways in hippocampal neurons between HSV-1 and HSV-2 infection leading to a higher induction of apoptosis and HSE with HSV-1 could be explained by the anti-apoptotic activity of the viral

protein kinase (PK) ICP10 only possessed by HSV-2[108]. Indeed, HSV-2 ICP10 PK decreased apoptosis by phosphorylating ERK1 and ERK2 and increasing the expression of the anti-apoptotic proteins c-Raf-1 and Bag-1. Meanwhile, HSV-1 ICP6, homologue of HSV-2 ICP10, had no effect on apoptosis in neurons. The difference in apoptosis between HSV-1 and HSV-2 infection in hippocampal neurons was confirmed in cortical neurons. Interestingly, apoptosis in HSE is triggered both by the external (FasL, TNF) and the internal/mitochondrial (c-Raf-1 and Bag-1) apoptotic pathways.

In the majority (75%) of HSE brains studied by Aurelian *et al.*, neuronal apoptosis was observed and the sites of apoptosis matched with the location of viral antigens suggesting a HSV-1-induced apoptosis in neurons[67]. Another study also showed that, in general, the brain regions with high rates of apoptotic brain cells matched with areas of productive viral infection but did not co-localize with immune CD3+ cells[109]. Interestingly, in the latter study, not all the apoptotic brain cells expressed viral antigens suggesting that apoptosis in HSE may be due to viral infection but also to bystander mechanisms triggering apoptosis in uninfected cells nearby infected cells.

The presence of apoptosis in neurons and glia cells and high level of HSV particles in patient brain tissue are only restricted to the acute phase of HSE[109]. Interestingly, apoptotic microglial and satellite cells were also found in human HSE-affected brains[110].

Crucially, more severe outcomes were observed for HSE patients with a high increase in the CSF level of sFas, a soluble protein involved in apoptosis initiation by the external apoptosis pathway, over the course of infection[111]. Moreover, INF-γ protected against detrimental HSE by decreasing apoptosis in mice brain[112]. Altogether, this suggests a role of HSV-1-induced apoptosis modulated by the immune response of brain cells in HSE neuropathogenesis.

Necroptosis can be considered as a programmed necrosis, a back-up process to eliminate cells when apoptosis is altered. TNF-α is an initiator of necroptosis in a mouse fibrosarcoma cell line[113]. Interestingly, in the presence of apoptosis inhibitors, TNF-α in murine embryonic fibroblasts but also FasL, activated TNF-R1, Fas or TRAIL-R in Jurkat cells can also trigger necroptosis initiation[113]. Following initiation, an activation of the receptor-interacting kinase 3 (RIP3 or RIPK3) is needed to complete necroptosis. Interestingly, HSV R1 protein has been revealed as an actor influencing necroptosis signalling through a RHIM-dependent modulation of RIP3 suggesting necroptosis could be another mechanism triggering HSE pathogenesis and dependent on the immune response[114].

1.2.2.2.5. Analysis of the HSE studies and their models published in the literature

In conclusion, HSE is not only due to brain cell lysis via HSV but also to the subsequent inappropriate immune response as seen in numerous *in vivo* and *in vitro* aforementioned studies. CSF studies from HSE patients also suggest a detrimental immune response is involved into HSE pathogenesis. However, other studies have shown that some immune responses, especially from innate immunity, such as the activation of TLR3 pathway and **subsequent type I IFN production** in patients or *in vivo* models, are protective against HSE. This emphasizes the fact that the timing of HSV-1 infection is a key factor to consider and targeting the immune response too early in order to improve HSE treatment could be inefficient. Thus, an *in vivo* study showed that delayed but not early treatment of glucocorticoids was protective against HSE[115]. Finally, the presence of HSV-1-induced apoptosis during HSE also supports that HSE pathogenesis is not solely due to HSV lytic replication.

The numerous differences between the models, cell lines and MOI used in HSE studies, likely explain, in part, the differences seen regarding the effect of pro-inflammatory molecules in HSE pathogenesis.

In *in vivo* studies, the differences in pathogenesis and HSE susceptibility observed between mouse models can be partly related to the animal genetic background. Indeed, while the C57BL/6 mouse strain was shown resistant to HSE, other strains including A/J, BALB/c or 129S6SvEv/Tac were associated with more severe outcome[116, 117. 118, 119].

Of note, a more recent study showed that HSV-1 replication in the eyes, viral spread and the ability of inducing latent viral genomes in the TG were similar between C57BL/6 and BALB/c mice although the survival rate was still significantly higher for the C57BL/6 population[120]. In this study, severe combined immunodeficient (SCID) mice were also used to assess the differences in replication, spread and virulence of HSV-1 between mice with C57BL/6 and BALB/c genetic background. Based on the data obtained, the differences in genetic background between the two populations did not lead to significant changes in the resistance of SCID mice to HSV-1 pathogenesis. Since, SCID mice lack mature lymphocytes but not the components of the innate system, the authors suggested that "the resistance of C57BL/6 mice to HSV-1 pathogenesis is absolutely dependent on both (i) the development of a rapid IFN-α/β response and (ii) the T-lymphocyte-mediated suppression of HSV-1 replication in infected tissues".

The inoculation route is also a key determinant of pathogenesis and severity in HSE mouse models. In mice, HSE can be induced by intracranial, intranasal, ocular, intraperitoneal or intravenous inoculation of HSV-1. Nevertheless, the two latter, although leading to lethal encephalitis, do not exhibit HSV titers in brain tissue and therefore seem less relevant for mimicking human HSE[121]. Intranasal inoculation is frequently used in HSE mice models and has been shown 100-fold more efficient than oral[122]. From the nasal epithelium, HSV-1 reaches the brain though either olfactory or trigeminal nerves. The limitations of the nasal inoculation include the potential outbreak of lung infection leading to undesired systemic immune responses and the variation of animal breathing intensity potentially altering the

reproducibility of the experiment[123]. The direct inoculation of HSV into the CNS to mimic human HSE in mice can be preferred to the other methods of inoculation. Indeed it decreases the variations of HSE susceptibility due to genetic background and age by bypassing peripheral immunity[123].

Kollias et al. and Mancini et al. recently reviewed the literature from HSE mouse models and discussed in depth these differences between models, as well as the current understanding of HSE pathogenesis in these animals[123, 121].

1.3. Herpes Simplex Encephalitis (HSE) treatment

1.3.1. Antiviral aciclovir as gold standard therapy for HSE treatment

Currently, intravenous aciclovir (ACV, acycloguanosine) (10mg/kg, three times daily, for 14 days) is the recommended treatment for HSE in the UK and should be started before the results of laboratory analysis when HSE is clinically suspected[39, 124]. Research studies and clinical trials have shown that aciclovir (intravenous, 10mg/kg, three times daily, 14 days) has the best efficacy relative to other used drugs such as vidarabine[125, 53]. It has reduced HSE mortality from 70% to 14-19%[126]. Of note, for patients with creatinine clearance <50mL/min, aciclovir dose should be adjusted. Moreover, oral valaciclovir should only be prescribed instead of intravenous aciclovir for patients presenting with clinical conditions precluding intravenous therapy.

Aciclovir is a molecule that *in vivo* is both converted by HSV and cellular thymidine kinases to Aciclovir-TriPhosphates (ACV-TP). ACV-TP, in turn, is incorporated into the HSV DNA inhibiting the viral DNA synthesis and, thereby limiting HSV propagation and brain damage.

1.3.2. The limitations of aciclovir monotherapy

Treatment of HSE with aciclovir does not guarantee survival since the mortality rate of patients treated with aciclovir is still as high as 14-19%[126]. Furthermore, a clinical study showed that 45-60% of HSE survivors exhibited neurological sequelae, one year after the completion of aciclovir treatment[126]. In a similar study, a long-term examination showed that among survivors 69% had memory impairment, 45% experienced personality or behavioural abnormalities, and 20-35% lived with severe anxiety, impaired concentration, insomnia, irritability, fatigue, poor motivation or emotional lability[53]. Outcome assessment at 6-months post hospitalization on 97 HSE patients treated with aciclovir showed 8% died, 23% had no sequelae, 32% experienced mild sequelae, 19% moderate sequelae and 19% severe sequelae[127]. "Mild sequelae" were defined by "minor disability (…), able to work and function autonomously"; moderate sequelae by "major disability (…), cannot sustain a regular job" and "severe sequelae" by "major neuropsychiatric disability or chronic care patient (…), need constant help for daily routine". A long duration of disease before hospital admission and extensive MRI brain involvement were associated with poor prognosis in this same retrospective study[127]. Although the majority of HSE survivors treated with aciclovir exhibited good recovery and regained independence in daily activities, most of them had persistent neurological sequelae.

Despite the outcome of HSE-affected patients being markedly improved with the therapeutic use of aciclovir, the still possible fatal outcome and the high percentage of incomplete recovery in treated patients emphasises the need to identify new adjunctive therapies. Aciclovir only targets HSV replication through inhibition of viral DNA synthesis. Thus, in an *in vivo* model of HSE, aciclovir treatment was shown to reduce viral titers but not inflammation or mortality[69] while HSE seems to be partly due to detrimental immune response (discussed

above). Altogether, this emphasises the interest of anti-inflammatory adjunctive therapy combined with aciclovir to improve HSE treatment.

1.3.3. Adjunctive treatment in HSE

1.3.3.1. Glucocorticoids

Glucorticoids are used as medicines in a wide range of inflammatory, auto-immune and allergic diseases (e.g. rheumatoid polyarthritis, asthma) as inhibitors of the pro-inflammatory response. A case report showed a positive effect of high-dose of methylprednisolone, a member of the glucocorticoids, after aciclovir therapy improved the outcome of a HSE patient[128]. In children affected by HSE and treated with aciclovir, multiple case reports have suggested steroids improve cognitive and motor function as well as seizure frequency[129]. More compelling, a multiple logistic regression analysis performed retrospectively on 45 patients with HSE, defined corticosteroid treatment in combination with aciclovir as one of the predictors of good outcome[130].

In vivo, following HSV-1 infection, delayed administration of both corticosterone and dexamethasone but not early administration of corticosterone resulted in a significant increase in mouse survival (with a greater impact for dexamethasone) [115]. Interestingly, the effects of dexamethasone were correlated with a decrease in both the expression of pro-inflammatory genes (MCP-1, TNF-α, IL-1β, IP-10, iNOS) and viral replication. Another HSE *in vivo* study also showed that the combination of aciclovir/glucocorticoids did not influence viral replication but did significantly reduce the presence of MRI abnormalities compared to aciclovir alone or untreated counterparts[131]. Finally, a recent clinical study suggested corticosteroids decreased temporal lobe and total oedema volumes in HSE patient brains treated with aciclovir[132].

1.3.3.2. TNF inhibitors (Etanercept, Infliximab)

TNF protein and gene expression were shown to increase following HSV-1 infection in human foetal microglia[85]. Furthermore, TNF-α protein levels were elevated in HSE patient CSF during the convalescence stage[71]. This high CSF TNF level in the convalescence stage may indicate a detrimental immune response could persist after the acute phase HSE and induce either relapse or persistent neurological sequelae. Hence, the administration of TNF inhibitors together with aciclovir could benefit HSE patient outcome by targeting the TNF production of the HSE post-acute phase (or convalescence stage) starting around 7-10 days after the beginning of the acute phase.

Today, TNF inhibitors such as infliximab (Remicade), etanercept (Enbrel), adalimumab, and certolizumab are used to also treat a wide range of inflammatory conditions including rheumatoid arthritis, psoriasis, ankylosing spondylitis, Crohn's disease and ulcerative colitis. Biologically, these anti-TNF drugs prevent TNF from inducing biological responses through host cell surface TNF receptors (TNFR). Infliximab is a chimeric human/mice monoclonal antibody targeting the soluble and transmembrane human TNF-α protein. Etanercept is a dimeric fusion protein consisting of (i) the extracellular ligand-binding portion of human TNF receptor and (ii) the Fc portion of human IgG1. A treatment combining the antiviral valacyclovir and etanercept, significantly increased mouse survival following intranasal HSV-1 challenge compared to untreated counterparts or mice treated with only one of these two drugs [133]. Interestingly, mice treated with both therapies exhibited a decrease in brain TLR2 and CCL2 gene expression compared to the group treated with antiviral only. Of note, in a mouse model of Japanese Encephalitis, etanercept was shown to significantly increase survival while reducing brain Japanese Encephalitis Virus (JEV) load and inflammation. The reduction of inflammation induced by etanercept was characterised by the restoration of blood-brain barrier integrity and the reduction of glial activation, glial nodule number, neuronal death and

perivascular cuffing number[134]. These observations are of major importance and may suggest a potential use of etanercept or other anti-TNF drugs for HSE treatment as the signs of inflammation induced by JEV inside the brain, and reduced by the drug, are similar to the ones characterised in HSE. Furthermore, the use of this same treatment in JEV-infected microglia-neuronal cultures led to a decrease in the protein expressions of TNF-α, IL1-β, IL-6 and CCL2; all of them have also been shown increased in HSE or HSE models.

1.4. Rationale, aim and objectives of my PhD project

1.4.1. Summary of the rationale

The limitation of aciclovir monotherapy in HSE and the need of adjunctive therapies have already been mentioned. Evidence of the involvement of detrimental immune responses in HSE pathogenesis has also been discussed. However, among the anti-inflammatory drugs, only a few glucorticoids have been assessed in HSE patients and, there is a lack of clear data to validate their impact on patient outcome and to understand the mechanisms of their potential effect[128, 130]. Interestingly, a beneficial effect of adjunctive anti-TNF therapy in a mouse model of HSE has been observed[133]. Therefore, although seen in a single *in vivo* experiment, we can hypothesize that anti-TNF therapies may also be of interest as adjunctive therapy for HSE treatment in human. They may have a positive impact on long-term outcome (i.e. neurological sequelae) potentially by targeting the high CSF TNF production during the convalescence stage (starting 7-10 days after the beginning of the acute phase)[71]. Crucially, the effects of both drug types, combined with aciclovir, in adult human brain cells infected by HSV-1 have never been assessed before this PhD project. Studying these effects is of major interest as it could give crucial insights to determine the importance of clinically assessing such drugs as adjunctive therapies for HSE treatment.

1.4.2. Hypothesis

The main hypothesis of this work was that administering the anti-inflammatory drugs dexamethasone and infliximab in HSV-1-infected brain cells treated with aciclovir could improve their survival.

1.4.3. Aim and main objectives

Hence, the aim of this PhD was to assess the effects of these anti-inflammatory drugs, from glucocorticoid and anti-TNF families, combined with aciclovir in HSV-1-infected human brain cells.

The main objectives of my PhD were:

a) Establishing *in vitro* models of HSV-1-infection using human brain cells

a1) Models using single cultures of human brain cells (Chapter 3)

The human brain cells used in single culture to set up HSE models were neuroblastomas, immortalised microglia and primary astrocytes. Neuroblastomas were chosen as neuron-like cells. Neurons are extensively damaged during HSE both by necrosis and apoptosis[39, 67]. Astrocytes also undergo HSV-1-induced cell death during HSE by both ways[39, 67]. Microglia cells are the brain resident macrophages representing probably both the first line of defence against HSV-1 in the brain tissue and a source of damage to this same tissue through an overwhelming and detrimental release of ROS species, pro-inflammatory cytokines and chemokines[98, 86, 87, 91]. Hence, the long-term action of microglia cells during HSE could participate in the pathogenesis. Altogether, understanding better the effects of HSV-1 on neuroblastoma cells, astrocytes microglia cells is crucial for improving HSE therapy.

Hence, I set up *in vitro* models of HSE using single cultures of these three human brain cell types targeted/eliminated by HSV-1 and/or potentially contributing to HSE pathogenesis.

These cell culture models were used to observe the effects of HSV-1 on (i) cell viability and morphology, (ii) viral replication and (iii) expression of inflammatory markers (TNF, INF-γ) during time-course experiments.

a2) Models using co-culture of human brain cells (chapter 7)

These particular models have been set up both (i) to get closer to *in vivo* models by getting two types of brain cells communicating together and (ii) to understand better the role of microglia following HSV-1-infection of nearby cells such as neuroblastomas and astrocytes. Indeed, as mentioned previously, the role of microglia cells in HSE is not fully understood with studies showing they are essential to protect brain cells from HSV-1 infection and others finding they are a source of detrimental immune response damaging these same cells [98, 86, 87, 91].

Using co-culture systems, HSV-1 replication and cell viability were assessed in all cell types at different time-points following infection.

b) Assessment of anti-inflammatory drugs as adjunctive therapies for HSE treatment *in vitro* (chapters 4-6)

For practical reasons and because of the time limitation of a PhD project, adjunctive therapies were assessed only in neuroblastomas and microglia monocultures.

The anti-inflammatory drugs used, combined with aciclovir (effect of aciclovir alone in chapter 4), have been dexamethasone (chapter 5) and infliximab (chapter 6). Dexamethasone is used to treat inflammatory diseases such as rheumatoid arthritis, osteoarthritis, psoriasis, cerebral oedema etc. This corticosteroid drug was chosen because different studies suggested a potential positive impact of dexamethasone and other corticosteroids in HSE treatment both *in vivo* and in clinical retrospective studies[115, 131, 128, 130]. Infliximab (Remicade) is a monoclonal antibody targeting human TNFα used clinically to treat various auto-immune diseases such as

Crohn’s disease, ulcerative colitis, rheumatoid/psoriatic arthritis, ankylosing spondylitis, plaque psoriasis. The choice of this particular human TNF inhibitor has been guided by practical reasons regarding access to anti-TNF drugs. Treatments with aciclovir, dexamethasone and infliximab were performed following HSV-1-infection (24h pi). Subsequently, viral replication, brain cell morphology and viability as well as TNF gene expression were performed from 30 h to 72 h pi (6 h-48 h post-treatment).

Chapter 2 Materials and Methods

2.1. Introduction

The main aim of my PhD is to assess the effects of dexamethasone and infliximab as adjunctive therapies to aciclovir. *In vitro* culture of human brain cells infected with HSV-1 has been used as model of HSE. During the first part of my PhD, I had to establish *in vitro* models of HSE using human brain cells both in single and co-culture. Then, I could assess the effects of dexamethasone and infliximab as adjunctive therapies for HSE treatments in some of these *in vitro* HSE models. These effects were assessed by measurement of cell viability, viral replication and host gene expression of key pro-inflammatory molecules (TNF-α, INF-γ).

In this chapter, the materials and methods needed to fulfil these objectives are described. They include cell culture, HSV-1-infection, drug administration and assessments of cell viability, viral replication and the pro-inflammatory response.

2.2. Materials and Methods

2.2.1. Cell culture

2.2.1.1. Cell incubation and storage

2.2.1.1.1. Incubation of cells cultured

Cells cultured were incubated in a humidified incubator (37 ℃, 5% CO2).

2.2.1.1.2. Cell freezing

After centrifugation (5 min, 300 x g) of the cell suspension, cell pellet was resuspended on ice in a solution of 90% FBS and 10% DMSO at a density of 1-2 x 10^6/mL (1-2 mL). This cell

suspension containing FBS and DMSO was then frozen in cryogenic vials for 24 h, at -80℃. Subsequently, they were frozen and stored in liquid nitrogen (-196 ℃).

2.2.1.1.3. Cell Defrosting

Cryogenic vials were defrosted in a water bath, at 37 ℃. Once defrosted, the cell suspension from one cryogenic vial was added to a pre-warmed adequate cell culture medium in one T75 flask, which was then incubated at 37 ℃, 5% CO_2. Twenty-four hours after incubation, cell culture medium was changed to preserve cells from DMSO toxicity.

2.2.1.2. Mycoplasma assessment

All primary cells and cell lines were tested for mycoplasma on a regular basis by qPCR testing on cell culture medium (every 2-3 months minimum) by the technical team of the Institute of Infection and Global Health (University of Liverpool).

2.2.1.3. Primary astrocytes culture

2.2.1.3.1. Pre-coating with poly-L-lysine

Primary human astrocytes (HAs; Sciencell, Caltag, SC-1800-5) were semi-adherent and needed the use of a coating agent, poly-L-lysine (PLL), to facilitate their attachment and adherence to the flask surface. Pre-coating consisted of adding 1 mL of PLL (15 µg/mL) per 25 cm^2 of the flask surface, followed by 1-2 hours incubation (at 37 ℃, 5% $CO_{2)}$ prior to addition of cells.

2.2.1.3.2. Primary astrocyte culture

Following pre-coating, flasks were filled with 15 mL of pre-warmed Dulbecco's Modified Eagle's Medium (DMEM)/ Ham's Nutrient Mixture F12 (Sigma-Aldrich) in the presence of 5% FBS, 1% Penicillin/Streptomycin (Sigma-Aldrich, 100X) and 1% L-Glutamine solution

(Sigma-Aldrich, 200 mM). Subsequently, a volume of 2-3mL of primary astrocytes, at a concentration of 10^6 cells/mL, was added into the flasks. Astrocytes were passaged at 80-100% confluence using Tryspin-EDTA 1X (1-2min at 37℃) solution to detach the cells. In all experiments, astrocytes used were between passages 3 and 9.

2.2.1.4. Microglia culture

The microglia cells used were SV40 immortalized human microglia cells (>99% purity) derived from primary human microglia cells (ABM company). They still have microglia markers such as CD68 and NGF. They were adherent cells and cultured with DMEM (Sigma-Aldrich) in the presence of 10% FBS, 1% Penicillin/Streptomycin (Sigma-Aldrich, 100 X), 1% L-Glutamine solution (Sigma-Aldrich, 200 mM). They were sub-cultured at 100% confluence using Tryspin-EDTA 1X (1-2 min at 37 ℃) solution to detach the cells.

2.2.1.5. Kelly neuroblastomas culture

Kelly neuroblastomas (Sigma, 92110411) were adherent and cultured with RPMI 1640 (Sigma-Aldrich) in presence of 10% FBS, 1% Penicillin/Streptomycin (Sigma-Aldrich, 100X), 1% L-Glutamine solution (Sigma-Aldrich, 200mM) and incubated in a humidified incubator at 37 ℃. They were sub-cultured at 80% confluence using Tryspin-EDTA 1 X (1-2 min at 37℃) solution to detach the cells.

2.2.1.6. Vero cell culture

Vero cells (Public Health England, culture collections, 84113001) were adherent and cultured with DMEM (Sigma-Aldrich) in presence of 10% FBS, 1% Penicillin/Streptomycin (Sigma-Aldrich, 100 X), 1% L-Glutamine solution (Sigma-Aldrich, 200 mM). They were sub-cultured at 100% confluence using Tryspin-EDTA 1 X (1-2min at 37℃) solution to detach the cells.

2.2.1.7. Co-culture of astrocytes/microglia and neuroblastomas/microglia

Co-culture of microglia with astrocytes or neuroblastomas was performed in 12 well-plates by using inserts (12 mm transwell with 0.4 µm pores, Corning (Sigma)) to create a top compartment in each well. Neuroblastomas or primary astrocytes were seeded at the bottom of the well (bottom compartment) while microglia were seeded in the insert (fig 2.1). The insert includes a membrane containing 0.4 µm pores that allows passage of fluid, small molecules and viruses from bottom to top compartment and vice-versa.

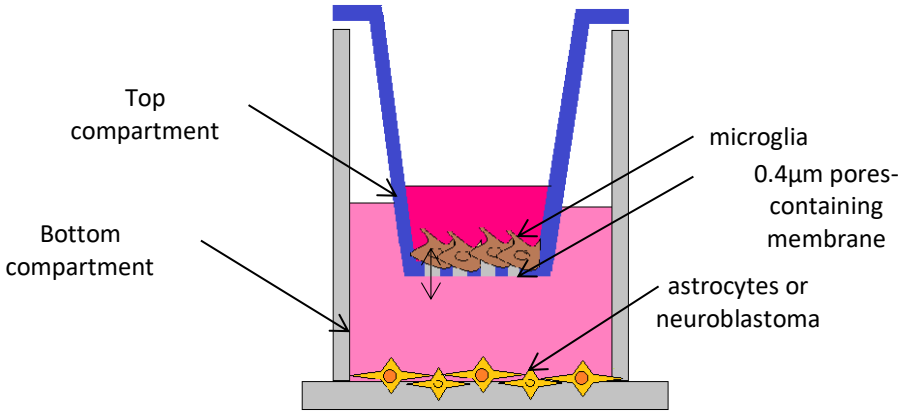

Figure 2.1. Scheme of the co-culture of microglia with astrocytes or neuroblastomas.

2.2.2. HSV-1-infection

2.2.2.1. HSV-1 stocks and viral load quantification by plaque-assay

2.2.2.1.1. Propagation and stocks of HSV-1 in Vero cells

Herpes Simplex type 1 strain 17+ virus particles were propagated in Vero cells from the original virus stock (Public Health England, 0104151v). The infection was performed by removing medium from one confluent T75 flask of Vero cells and adding 2 mL of fresh medium containing 10 µL of the initial batch of HSV-1. After incubating for 1 h (at 37 °C, 5% CO2), 13 mL of medium was added (t=0 of infection). Cells were then monitored every 24 h. When more than 50% of the cells displayed effects of cytopathology (at 72 h pi), the cell

monolayer was detached using Trypsin. The cells and the culture medium were harvested and removed from the flask together. Following centrifugation of the cell suspension (500 x g, 5 min), the supernatant was removed and the pellet was resuspended in 1 mL of fresh medium before being frozen in aliquots of 10-20 µL (-80 °C). Viral stocks were subsequently titered by plaque-assay to quantify the virus concentration.

2.2.2.1.2. Quantification of HSV-1 by plaque-assay

HSV-1 infection was performed using 500 µl of stock HSV-1 ten-fold serial dilutions in 6 well-plates containing confluent Vero cells to assess viral titres. After 1h of incubation (37 °C, 5% CO_2), a solution of carboxymethyl cellulose (CMC) 0.6%- DMEM (2 mL) was added in each well and then incubated at room temperature (RT) for 30 min-1 h at room temperature (RT). Plates were then incubated at 37 °C, 5% CO2 for 48 h-72 h until plaques (rounded gaps in the monolayer due to HSV-1) were visible. The overlay was then removed and 10% formalin added (under fume hood). After 30 min at RT, formalin (Sigma) was removed (under fume hood) and wells stained with toluidine blue for 10 min. Plates were then washed carefully with water, dried and plaques counted. The counting of plaques results in an accurate quantification of the number of HSV-1 infectious particles in plaque-forming units (pfu) contained in the HSV-1 solution.

2.2.2.2. HSV-1-infection time-course experiments in human brain cells

2.2.2.2.1. Cell preparation before HSV-1-infection

2.2.2.2.1.1. Coating with fibronectin for astrocyte attachment

Experiments using astrocytes were performed in 12-well plates pre-coated with a solution of fibronectin-gelatin to facilitate their attachment. The solution of fibronectin-gelatin was prepared by diluting 1 mL of Fibronectin (Sigma-Aldrich, 1 mg/mL) in 199 mL of 0.02% gelatin (Sigma). Plates were incubated for 2 hours at 37 °C, 5% CO2 with 500 µL of

Fibronectin-0.02% gelatin per well. Then, the solution of fibronectin-gelatin were carefully removed and cells seeded.

2.2.2.2.1.2. Brain cell seeding in culture models of HSE

For HSV-1-time-course experiments, two different plates were used. For cell counting using Trypan Blue exclusion staining, host gene expression and viral replication studies, HSV-1-infection time-course experiments were performed in 12 well-plates. For WST-1 assay, the experiments were performed in 96 well-plates.

The number of cells seeded, the volume of medium per well, the time between seeding and infection, the use of a potential coating agent to facilitate cell attachment (for astrocytes) were optimised to obtain even monolayers 80-100% confluence and presenting no signs of cellular stress or cell death (Tables 2.1 and 2.2).

Table 2.1 summarises all of the cell seeding settings used for HSV-1-infection in single culture of brain cells.

	Single culture				
Cells	Neuroblastomas		Astrocytes	Microglia	
Plates	12 well	96 well	12 well	12 well	96 well
Number of cells/well	1x10^6	5-10 x10^4	4x10^5	4x10^5	1.5-3 x10^4
Volume of medium/well	1mL	100uL	1mL	1mL	100uL
Time before infection (h)	36	24	15	15	15
Coating agent	No		Fibronectin	No	

Table2.1. Summary of the different parameters used for brain cell seeding in single culture models of HSE.

For co-cultures, the seeding of neuroblastomas and microglia in co-culture differed only in that the volume was slightly smaller (800 µL) to decrease the chance of media cross-contamination between the two compartments. Table 2.2 summarises all of the cell seeding parameters used for HSV-1-infection in co-culture of brain cells.

	Co-culture		
	Bottom compartment (well)		Insert
Cells	Neuroblastomas	Astrocytes	Microglia
Plates	12 well	12 well	Insert (12 well-plate)
Number of cells/well	1x10^6	4x10^5	0.5-3x10^5
Volume of medium/well	800uL	800uL	500uL
Time before infection (h)	36	15	14 (with astrocytes) 35 (with neuroblastomas)
Coating agent	No	Fibronectin	No

Table2.2. Summary of the different parameters used for brain cell seeding in co-culture models of HSE.

2.2.2.2.2. HSV-1-infection

HSV-1 infection of monocultures in plates was performed in two steps. Firstly, just after removing culture medium, a small volume of HSV-1 solution (200 µL/well in 12 well-plates and 30 µL/well in 96 well-plates) was added in each well, to the cell monolayer. This small volume of HSV-1 contained appropriate cell culture medium and the number of viruses needed per monolayer (or well) to match the M.O.I (Multiplicity of Infection) chosen. The M.O.I, representing the number of viruses added per cells, was 0.01 (1 virus for 100 cells) for the majority of experiments. Cells were then incubated one hour (37 °C, 5% CO_2). Following the incubation, the second step consisted in topping up each well with medium (800 µL/well in 12 well-plates and 70 µL/well in 96 well-plates).

In co-cultures, infection was done only in the bottom compartment (neuroblastomas and astrocytes) following the same steps but topping up with 600 µL in the second step rather than 800 µL to avoid cross-contamination between the two compartments (only in 12 well-plates).

2.2.3. Treatments

2.2.3.1. Aciclovir

Aciclovir powder (Sigma) was dissolved in PBS at 400 µM before being added to the cells. In 12 well-plates, per well, 50 µL of 400 µM of aciclovir in PBS was added to the cells in 950 µL of culture medium. In 96 well-plates, per well, 5 µL of 400 µM aciclovir in PBS was added to the well containing cells in 95 µL of culture medium. Therefore, the final concentration of aciclovir used was 20 µM. The choice of this concentration was explained in the chapter 4 (Introduction).

2.2.3.2. Dexamethasone

Dexamethasone (Dex)-soluble powder (Sigma) was dissolved in PBS before being added to cells. In 12 well-plates, per well, 50 µL of 20 X Dex in PBS was added to the cells in 950 µL of culture medium. In 96 well-plates, per well, 5 µL of 20X dexamethasone in PBS was added to the cells in 95 µL of culture medium. Different final concentrations (X) were assessed especially in the range 0.5-10 µM. However**,** the optimisation experiments determined that 0.5 µM of dexamethasone was the best concentration to work with (detailed in chapter 5).

2.2.3.3. Infliximab

Infliximab powder (Remicade, 100mg) was dissolved in PBS before being added to cells. In 12 well-plates, per well, 50 µL of 20X infliximab in PBS was added to the cells in 950 µL of culture medium. In 96 well-plates, per well, 5 µL of 20 X infliximab in PBS was added to the cells in 95 µL of culture medium. Different final concentrations (X) were assessed in the range

of 0.5-10 mg/mL. However, optimisation experiments determined that the concentration of 0.5 mg/mL of infliximab was the best to work with (detailed in the chapter 6).

2.2.4. Assessment of HSV-1 effects in human brain cells using microscopy and molecular biology techniques

2.2.4.1. Quantification of HSV-1-replication by qPCR

A way to assess the HSV-1-infection-time course and its severity is through detection of the viral genome from culture medium and cells by qPCR. Dual-labeled qPCR probe from the company Sigma was used to quantify HSV DNA (figure 2.2). Each assay consisted of (i) unlabelled primers, (ii) a probe with a FAM dye on the 5'end, and a nonfluorescent quencher (NFQ) on the 3'end, and (iii) a TaqMan gene expression master mix containing a Taq DNA polymerase and dNTPs (Thermofisher). The HSV-1 DNA primers (HSV-1 Forward: 5'-GCAGTTTACGTACAACCACATACAGC-3'; HSV-1 Reverse: 5'-AGCTTGCGGGCCTCGTT-3') and the probe (5'-CGGCCCAACATATCGCGTTGACATGGC-3'**;** Synthesis: 0.05 HPLC; 5'reporter dye: 6fAM; 3'quencher dye: TAMRA; OD:1) were chosen to target HSV gene gB.

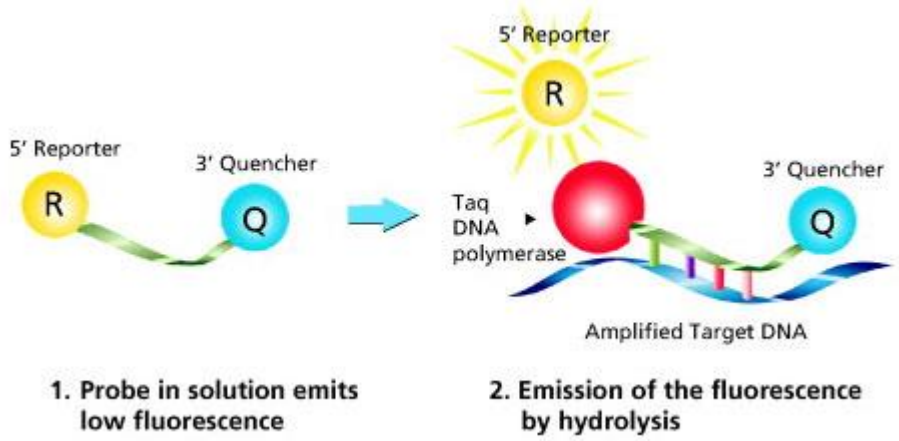

Figure 2.2. Gene expression assay using a dual-labeled probe (Sigma). Source: Sigmaaldrich.com. (1) A Dual-labeled Probe is a single-stranded oligonucleotide labeled with two different dyes. A reporter dye is located at the 5' end and a quencher molecule located

at the 3' end. The quencher molecule inhibits the natural fluorescence emission of the reporter by fluorescence resonance energy transfer (FRET). (2) The primer is elongated by the polymerase and the probe binds to the specific DNA template. Hydrolysis releases the reporter from the probe/target hybrid, causing an increase in fluorescence. The measured fluorescence signal is directly proportional to the amount of target DNA.

2.2.4.1.1. From brain cell nucleic acid extracts

Nucleic acid extraction was performed using Phenol-chloroform extraction method. PCR reactions were performed in 96-well plates (Biorad). For one PCR reaction (25 µL) per well, 12.5 µL of Master Mix (Thermofisher), 9.25 µL of nuclease-free-H2O, 0.5 µL of each HSV-F and R primers and 0.25 µL of probe (Sigma) were added to samples of 100 ng of nucleic acid in 2 µL (measured by Nanodrop). The plate was centrifuged (20s, speed: 1000 x g) and placed in the thermal cycler (Biorad CFX connect). PCR parameters were : 95 °C for 10 min followed by a second step consisting of 15 s at 95 °C, 30 s at 50 °C and 30 s at 72 °C, which was repeated for 44 cycles.

2.2.4.1.2. From cell culture medium

PCR reactions were performed in 96-well plates (Biorad). For one PCR reaction (25 µL) per well, 12.5 µL of Master Mix (Thermofisher), 6.25 µL of nuclease-free-H2O, 0.5 µL of each HSV-F and R primers and 0.25 µL of probe (Sigma) were added to samples of 5 µL of cell culture medium. The plate was centrifuged (20s, speed: 1000 x g) and placed in the thermal cycler (Biorad CFX connect). PCR parameters were : 95 °C for 10 min followed by a second step consisting of 15 s at 95 °C, 30 s at 50 °C and 30 s at 72 °C, which was repeated for 44 cycles.

In a preliminary experiment, I studied the correlation between the number of active HSV-1 particles estimated by plaque-essay in Vero cell culture and the Ct value obtained by HSV

DNA qPCR from culture medium. This is represented by the Figure 2.3. The correlation was statistically defined by a Pearson r coefficient of -0.94 and a R square of 0.88.

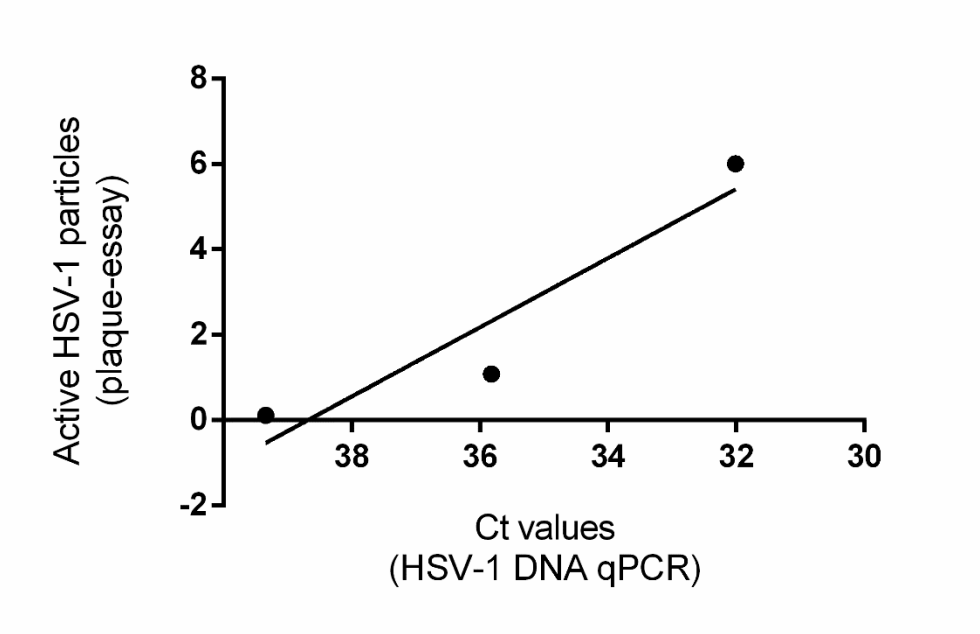

Figure 2.3. Correlation between the number of HSV-1 particles in plaque-essay and the Ct values obtained by HSV DNA qPCR. HSV-1 infection was done in Vero cells at different dilutions from the HSV-1 original stock (10^{-8}-10^{-5}). Plaque essay and HSV DNA qPCR from cell culture medium were performed at 72 h pi following the protocols described in the previous parts. Data from only one preliminary experiment. Pearson r = -0.94; R square = 0.88 (correlation).

2.2.4.2. Assessment of HSV-1-induced damage in human brain cells

2.2.4.2.1. By light microscopy

Clear signs of infection in HSV-1-infected brain cell monolayer can be easily detected by light microscopy from a 4x magnification. The most common signs are (i) cells rounding up and forming clusters, (ii) rounded gaps in the monolayer, (iii) high proportion of cells floating and (iv) syncitium-like-stuctures (multi-nuclei giant cells). The proportion of these signs varies by cell type and the MOI used. This will be described in the results chapters.

A protocol was used to quantify the area of attached cells in microscopy pictures (4 x magnification) using the software “ImageJ”. It was widely adapted from a protocol of “FITC-dextran exclusion assay analysis using ImageJ software” done by S.Panagiotou and L.Jacques (Institute of Infection and Global Health, University of Liverpool). The image had first to be opened with “ImageJ” and “RGB color” was then selected. Subsequently, the image was adjusted to 8-bit to be converted into greyscale. The threshold was then adjusted. Once the threshold applied, the picture appeared in black and white (negative picture) with cells still attached to the well (and presumably alive) colored in black and spaces between them in white. The percentage of the black area on the picture could be measured by “ImageJ” and as a result be an estimation of attached cell area and cell viability. An example of the estimation of attached cell areas of HSV-1-infected neuroblastomas using the software “ImageJ” was performed using three different microscopy pictures and is presented in the figure 2.4.

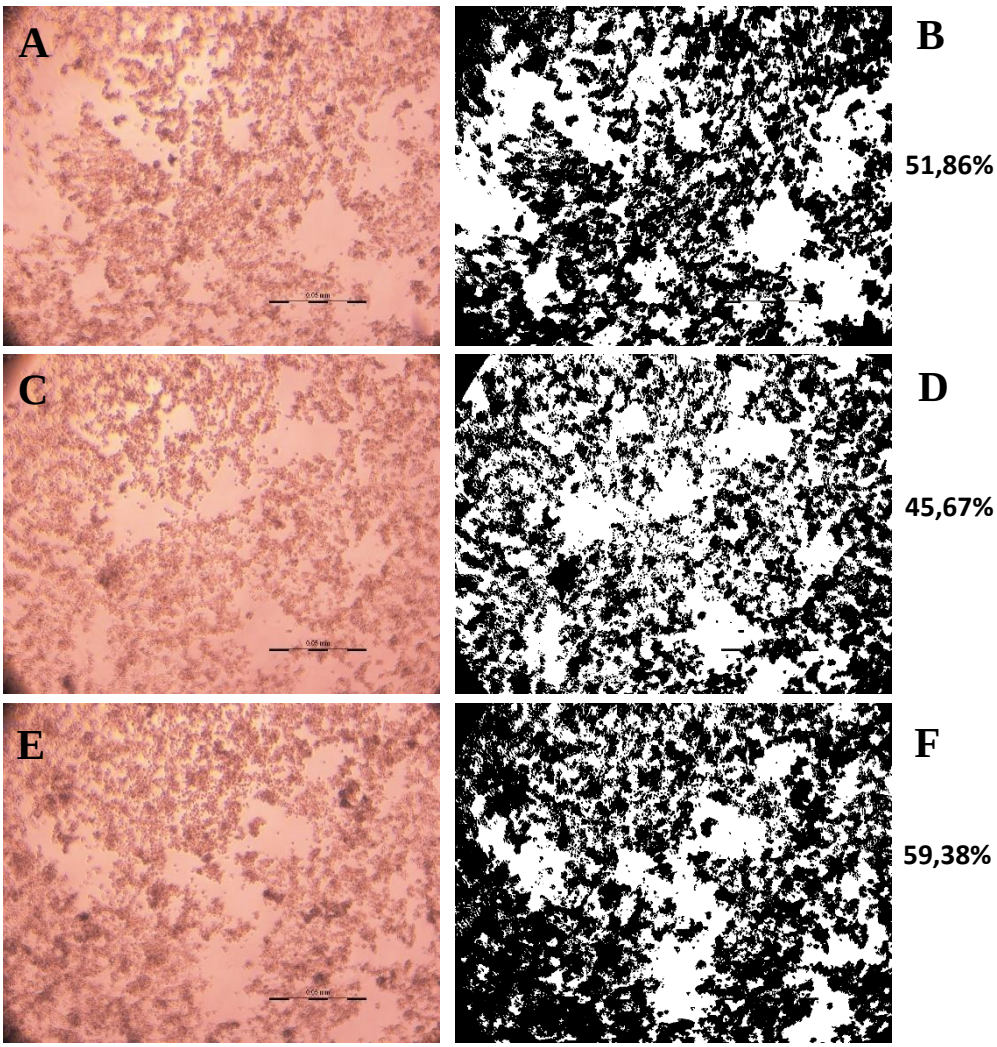

Figure 2.4 Estimation of live cell area of HSV-1-infected cells of microscopy pictures using the software "ImageJ". (A), **(C)** and **(E)** are the original microscopy pictures (4 x magnifications) assessed for live cell areas. **(B)**, **(D)** and **(F)** are the negative images of (A), (B) and (E) respectively. They were obtained following the protocol described above. The estimation of live cell areas for each of the three pictures was written on the right side.

2.2.4.2.2. Cell counting by Trypan blue exclusion staining and automated cell counter (Luna FL)

Live and dead cells were counted using Trypan blue exclusion staining. Once the cells were homogeneously resuspended in culture medium, a 1/10 dilution in fresh culture medium

followed by a 1/2 dilution in Trypan blue was performed. After 1-2 min in presence of Trypan blue, live cells (unstained) and dead cells (blue) were counted manually using a Neubauer chamber or automatically using the Luna FL automated cell counter.

2.2.4.2.3. Calcein-AM and Propidium Iodide (PI) staining

Calcein-AM (Sigma) is a cell-permeant fluorogenic dye which stains only live cells in green (emission at 520 nm) after hydrolysis by active cellular esterases following excitation at 490 nm (figure 2.5).

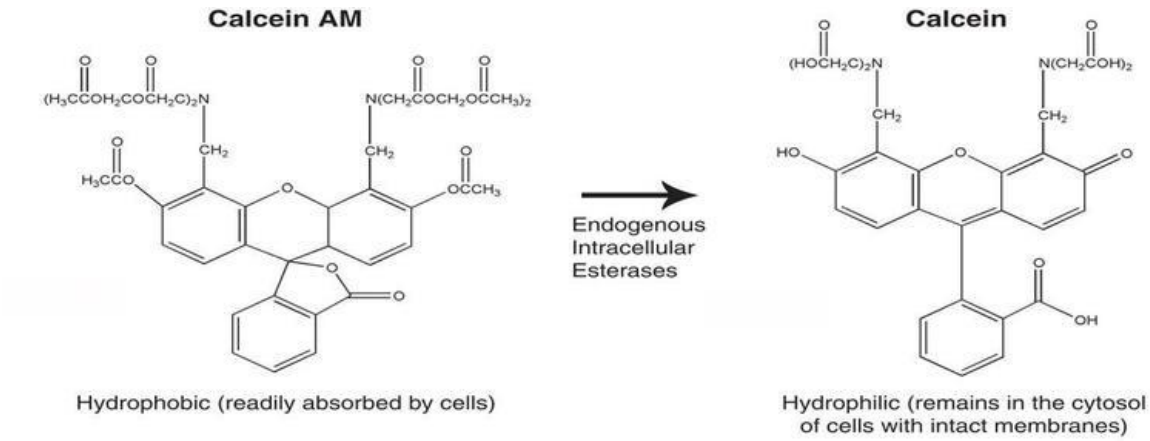

Figure 2.5. Conversion of calcein-AM in green fluorescent calcein by esterases of live cells. Source: R&D (Sigma) data sheet "calcein-AM, cell viability assay, catalog number: 4892-010-K".

A calcein-AM stock solution of 2 mM was made by resuspending 50 µg of calcein-AM powder (Lifetechnologies) with 25 µL of DMSO. The working solution (c=0.5 µM) was made by diluting the stock solution 1 in 4000 clear DMEM medium (Sigma). After removing medium and washing cells with PBS, cells were incubated with 0.5 µM calcein-AM solution for 30min at 37 °C, 5% CO_2. Cells were then washed twice before the addition of clear DMEM medium.

Fluorescence could be directly quantified in plates using the FLUOstar Omega microplate reader or observed by fluorescent microscopy.

Propidium Iodide (P.I) (Invitrogen) is a non-permeant dye, only penetrating dead cells (with a compromised plasma membrane). P.I is an intercalating agent that stains in red nucleic acid of dead cells red (617 nm) following excitation at 535 nm. P.I stock was made in deionized water at 1.5 mM (1 mg/mL). The working dilution (c=0.5 µM) was made by a 1/3000 dilution of the stock solution in clear DMEM medium (Sigma). After removing medium and PBS wash, cells were incubated with 0.5 µM P.I solution for 5 min at 37 °C, 5% CO_2. Cells were then washed twice before the medium was replaced. Fluorescence could be directly quantified in plates using the FLUOstar Omega microplate reader or observed in fluorescent microscopy.

Dual staining with calcein-AM and P.I was also performed using the same working concentrations of both dyes. After removing medium and PBS wash, cells were incubated with 0.5 µM calcein-AM solution for 25 min at 37 °C, 5% CO_2. Cells were washed again twice with PBS before a 5 min staining step at 37 °C, 5% CO_2 with 0.5 µM P.I solution. Cells were then washed twice before being put in presence with clear DMEM medium. Fluorescence of both calcein-AM and PI could be directly quantified in plates using the FLUOstar Omega microplate reader or observed in fluorescent microscopy.

2.2.4.2.4. WST-1

The WST-1 assay is colorimetric and designed to assess cell proliferation, viability and cytotoxicity by spectrophotometric quantification. The cell proliferation reagent WST-1 (Roche-Sigma) is a tetrazolium salt associated with an electron coupling agent (figure 2.6). This assay is based on the ability of viable cells to produce NAD(P)H through glycolysis by the mitochondrial succinate-tetrazolium-reductase system (respiratory chain complex). When NAD(P)H is produced in presence of WST-1, slightly red, the latter is cleaved to soluble

formazan, revealing a dark red colour. As a result, the production of this dark red dye directly correlates to the number of cells metabolically active.

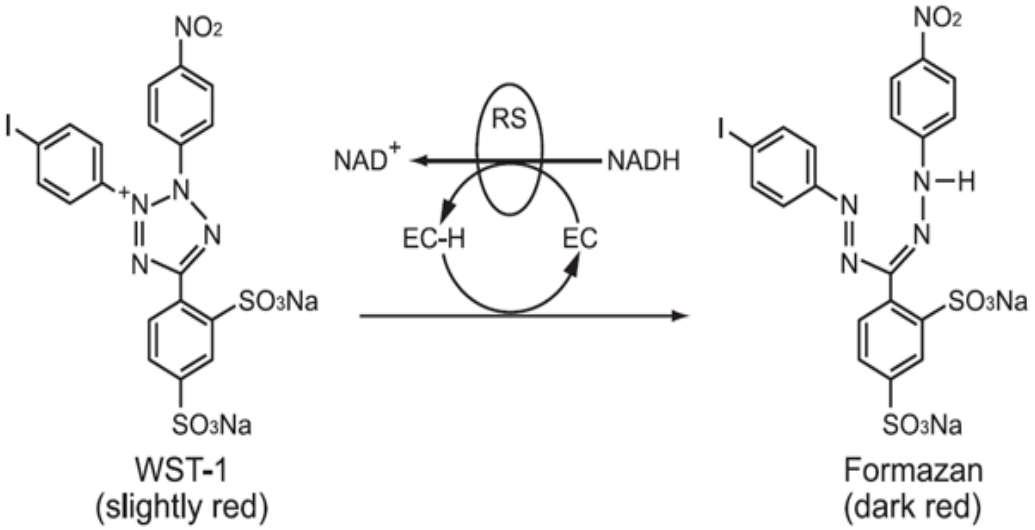

Figure 2.6. Conversion of WST-1 to formazan by the respiratory chain of healthy cells. Source: Roche, data sheet. EC: electron coupling agent; RS: mitochondrial succinate-tetrazolium-reductase system.

In this end-point assay, cells were grown in 96-well plates. At the end-point, cells were stained with 10 µL of WST-1 (Roche) per well and incubated (37 °C, 5% CO2) for 30 min before the plate was read at 450 nm (with wavelength correction at 600 nm) using a spectrophotometer.

2.2.4.2.5. qRT-PCR targeting the housekeeping gene DAD-1

DAD-1 is a housekeeping gene involved in the N-glycosylation process in eukaryotes. It was already validated in a published *in vitro* study of HSE[135]. qRT-PCR targeting DAD-1 can also estimate cell viability in samples although with low sensitivity. The technical details of the qRT-PCR targeting DAD-1 are described together with the ones of the qRT-PCR targeting pro-inflammatory genes in the part 2.2.4.3.3.

2.2.4.3. Assessment of host gene response by qRT-PCR

2.2.4.3.1. Cell collection in 12 well-plates using Trizol

In each well, culture medium was collected and centrifuged 5 min, at 300 x g to collect cells detached from the monolayer. After centrifugation, without touching the cell pellet, supernatant was discarded. The pellet containing the cells was then resuspended in 100 µL of culture medium. Cells still attached to the monolayer were trypsinised (150 µL per well) and resuspended in 850 µL of culture medium (volume total: 1 mL). This cell suspension of 1 mL was then pooled with the 100 µl of cell suspension from culture medium. After centrifugation of this cell suspension mixture, the supernatant was discarded and the pellet was resuspended in 50 µL of culture medium. Then 600 µL of Trizol (Sigma) was added to this last cell suspension before being vortexed and frozen at -80C.

2.2.4.3.2. Nucleic acid (RNA) extraction

The samples containing Trizol were defrosted at RT and vortexed. 100 µL of chloroform was added to the samples before vortexing (under fume hood). After phase separation, samples were centrifuged (4 °C, 21000 x g, 30 min) before taking off the aqueous phase (under fume hood). A volume of 5 M NaCl equal to 10% of the aqueous phase, 10 µL of glycogene and 500 µL of isoprapanol were then added to the aqueous phase before vortexing and placing the samples for 1 h at -80 °C. After defrosting at RT, they were centrifuged again (30 min, 21000 x g, 4 °C) and the supernatant was removed. The pellet was then washed with 500 µL of 80% ethanol before a new step of centrifugation (10 min). The last two steps (wash and centrifugation) were then repeated again before drying the pellet. Once resuspended in 20 µL of nuclease-free water, nucleic acid was quantified (ng/uL), and the A260:280 and A260:230 ratios were assessed by Nanodrop.

2.2.4.3.3. qRT-PCR targeting IL-1β, TNF-α, INF-γ, IL-6 and DAD-1

2.2.4.3.3.1. The Reverse Transcription

All of the RNA samples were diluted in 10 µL to get a RNA concentration of 100 ng/uL. To each diluted RNA sample, 10 µL of master mix was added. The master mix consisted of 2 µL of oligodT primers, 2 µL of 10 X RT buffer, 4 µL of dNTP mix, 1 µL of RNase inhibitor and 1 µL of MMLV RT enzyme. The samples were subsequently placed in a thermocycler for 1 h at 44 ℃, 10 min at 92 ℃ and 10 min at 4 ℃.

2.2.4.3.3.2. qPCR step

TaqMan technology was used for this qPCR step (figure 2.7). After reverse transcription, 1µL of cDNA solution (100 ng) was used with 19uL of a mix for one qPCR reaction. The mix was composed of 10 µL of TaqMan gene expression Master Mix (Lifetechnologies, 4369016), 8 µL of H_2O and 1µL of a commercial combination of target gene primers and TaqMan dual-labelled probe (Sigma: Hs02912874_m1 DAD1 FAM-MGB; Hs00174128_m1 TNF FAM-MGB; Hs00985639_m1 IL-6 FAM-MGB). After preparation of the reactions, the 96-wells plate was centrifuged (20s, speed: 1000) and placed in the thermocycler (Biorad, CFX-connect). The cycle parameters were as follows: one 10 min step at 95℃, then 60 cycles of 15 s at 95 ℃, 30 s at 50 ℃ and 30 s at 72℃.

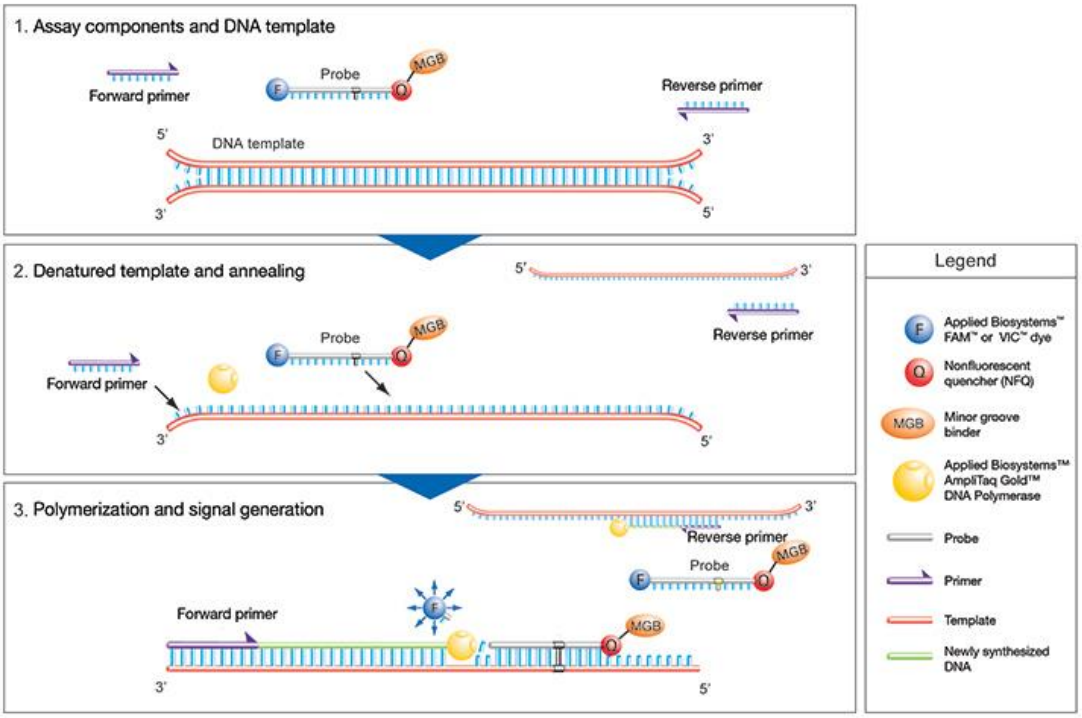

Figure 2.7. TaqMan gene expression assay process. Source: Thermofisher.com. (1) Denaturation of the double-stranded cDNA as temperature is raised. The signal from FAM on the 5'end of the TaqMan probe is still quenched by the non-fluorescent quencher (NFQ) on the 3'end. (2) Annealing of primers and probe to their specific target sequences as temperature is lowered. (3) Synthesis of new strands by the Taq DNA polymerase thanks to the unlabelled primers and template. When the polymerase reaches a TaqMan probe, the polymerase 5' nuclease activity leads to the cleavage of the probe. The latter results in the release of the fluorescent FAM finally separated from the NFQ. With each PCR cycle, there is an increase in fluorescence intensity proportional to the amount of amplicon synthesized.

2.2.4.4. ELISA targeting TNF protein

A commercial kit (Peprotech; 900-K25) of ELISA sandwich was used to measure human TNF-α protein from culture medium of uninfected and HSV-1-infected cells in my cell culture experiments. The ELISA assay was performed according to the manufacturer's instructions (Preprotech). The principle of the ELISA sandwich is described in the figure 2.8. Briefly, the colour development was monitored with an ELISA plate reader at 405 nm with a wavelength correction at 600 nm. The concentration of TNF in samples was calculated using the TNF standards provided. The range of TNF detection of this kit was 31-2000 pg/ml.

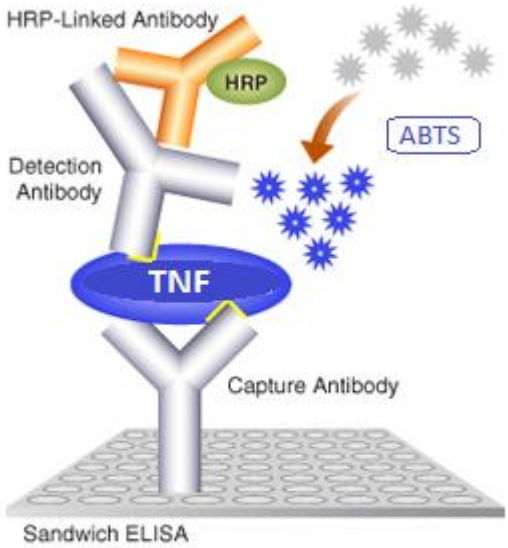

Figure 2.8 Sandwich ELISA mechanism. Source (online)**:** Ozyme.fr (adapted). The sandwich ELISA detects and measures the amount of TNF proteins released by cells in the culture medium. Capture antibody (in grey), attached to the bottom of the well, can bind TNF. TNF is then bound to a second (primary) antibody (in grey), the detection antibody, recognized itself by a secondary antibody (in orange) conjugated to the enzyme horseradish peroxidase (HRP). Then, the cleavage of the substrate ABTS by HRP leads to the apparition of a green final product that can be measured by a spectrophotometer. The apparition of the final green product is proportional to the amount of TNF in the culture medium.

2.3. Statistics

The statistical significance of the results of qPCR, WST-1, ELISA and attached cell area analysis by “ImageJ” was assessed by the Student's test (t-test) and the analysis of variance (ANOVA test) using the software “GraphPad Prism”. ANOVA test was performed to statistically highlight the existence of differences between the means of different treatment groups at each time-point and with more than two groups considered. If an ANOVA test showed significant differences, t-test (for one time-point experiments) or multiple t-test (for multiple time-point experiments) were then applied to compare between two distinct groups. Each test was considered as statistically significant when the p-value was below 0.05.

As classically done, data of the biological replicates of multiple experiments was pooled to get more information and increase the power of statistical tests. For qPCR, every biological replicate was divided in two technical replicates read by the thermocyler. The average of the values of two technical replicates was used as final data for every biological replicate.

Chapter 3 HSV-1-infection in human brain cells

3.1. Introduction

As previously mentioned, Herpes Simplex Encephalitis (HSE) is a rare but fatal disease. It is characterised by important lymphocyte infiltration at the brain tissue, activated microglia, necrosis and neuronophagia (phagocytosis of neurons by microglia) in some brain areas[37, 39]. Areas affected typically include the temporal lobe, the infero-frontal lobe and the insular cortex of cerebral hemispheres in an asymmetrical way. In HSE, necrosis affects multiple types of brain cells, including neurons and astrocytes[39].

As described in chapter one, this brain damage is not only the result of HSV-1-induced cell death but also of a secondary immune response to the virus. Microglial cells, the brain resident macrophages, have been described as having both a protective effect against HSV infection and also playing a role in this detrimental immune response. On one hand, they were shown, via the functional type I INF pathway, to decrease mouse brain lateral ventricle enlargement in an *in vivo* model of HSE[87]. Microglial cells, through IL-6 secretion, also induce a rescue of neuronal precursor cell number following HSV-1-infection of neural progenitor cells[136]. Conversely, following HSV-1-infection, they were also shown to be detrimental for neurons by secreting Reactive Oxygen Species (ROS) following TLR2 activation[99]. Another study showed that the drug corilagin reduced inflammation both in HSV-1-infected mouse brain as seen by microscope observations and in HSV-1-infected murine microglia cells as shown by the decrease in NO, TNF-α and IL-1β concentrations in microglia cell supernatant[137]. An increase in microglial cell apoptosis following corilagin administration after HSV-1-infection was also reported. Altogether, this suggests the beneficial effect of corilagin on reducing

mouse brain inflammation, following HSV-1-infection, could be due to the reduction of cytokine production and the induction of microglial cell apoptosis.

In HSE-affected brains, extensive HSV-induced neuronal death is widely observed[39]. In my experiments, Kelly neuroblastoma cells were used to create a model of neuron-like cells. This avoids all the issues raised by culture of primary neurons *per se*, particularly the fact they do no divide. These neuroblastoma cells were isolated from a patient and underwent N-MYC amplification to correlate with the clinical progression of neuroblastoma. Subtypes of these cells have been studied and it was shown that Kelly neuroblastoma cells, similarly to another neuroblastoma cell type SH-SY5Y, consisted of more than 90% neuroblasts and less than 10% non-neuronal cells[138]. More recently, Shipley et al. have differentiated the SH-SY5Y neuroblastomas cells in a reductionist model of "HSV-1 vs neurons" interactions[139]. A few *in vitro* studies have used Kelly neuroblastoma cells including one assessing the gene expression level of MYC, C-KIT and VEGFA as these genes could be interesting targets for neuroblastoma treatment[201]. However, to my knowledge, Kelly neuroblastomas have never been used in an HSV-1 or brain infection *in vitro* model.

Astrocytes play a role in brain tissue homeostasis and provision of nutrients to neurons. A cross-talk between microglia and astrocytes was observed in pathological conditions in the CNS[140]. Co-culture with astrocytes was shown to be protective for neurones in a thiamine deficiency *in vitro* model[141]. In an *in vitro* model of HSE using monoculture, extensive cell death and decrease in cytochrome c oxidase (CO) expression were observed in primary astrocytes following HSV-1 infection[135].

There is a lack of data and understanding about the effects of HSV-1 on Kelly neuroblastomas, microglia and astrocyte cell types individually. In this chapter, I set up *in vitro* models of HSE using single cultures of these three human brain cell types targeted and eliminated by HSV-1 and/or potentially contributing to HSE pathogenesis. Hence, in these cells following HSV-1

infection, viral load, cell viability/death and expression of key pro-inflammatory cytokines (TNF and INF-γ) were assessed in this chapter.

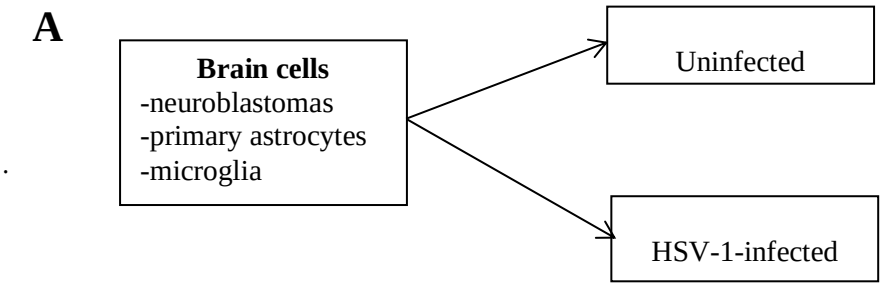

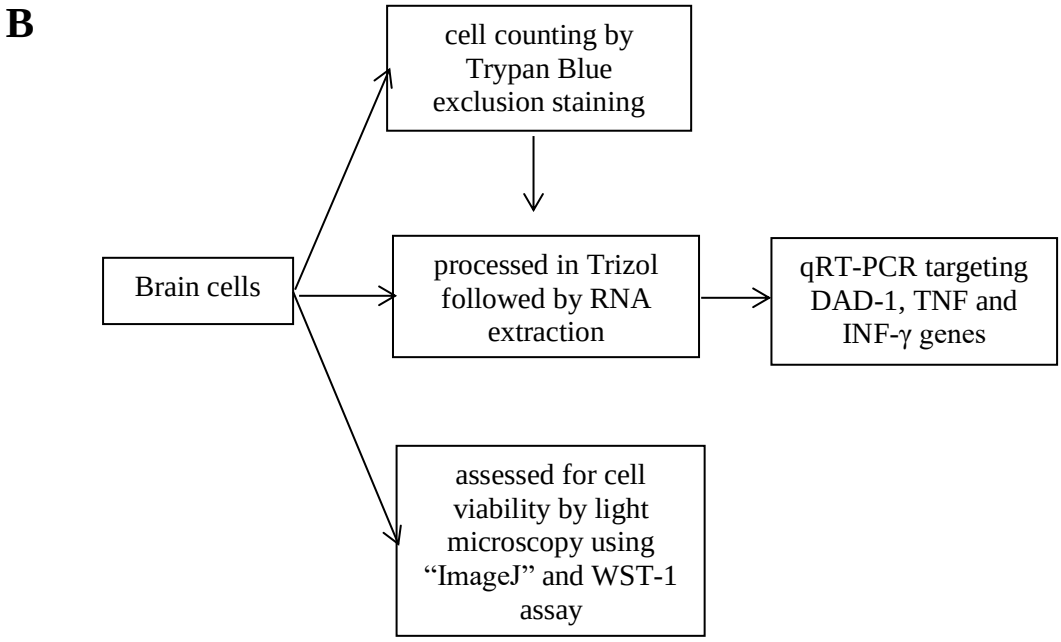

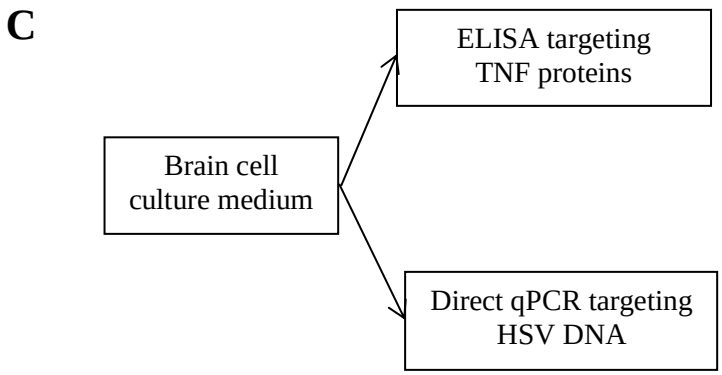

Figure 3.1. Experimental design for Chapter 3 "HSV-1-infection in human brain cells". (**A)** Brain cell populations used. **(B)** Techniques performed on brain cells following HSV-1-infection. **(C)** Techniques performed on brain cell culture medium following HSV-1-infection.

3.2. Results

3.2.1. HSV-1-infection of neuroblastoma cells

3.2.1.1. HSV-1 replicates and is associated with cell death in neuroblastoma cells

The effects of HSV-1 on neuroblastoma cells were first assessed by light microscopy at MOI=0.01. Uninfected neuroblastomas presented with a "fibroblast-like" morphology that became less obvious with time. These cells are highly proliferative and quickly became confluent (fig 3.2A, C, E). At 24 h post-infection (pi), the monolayer of infected cells exhibited their first signs of infection, which included a loss of attachment of the confluent monolayer (with more gaps appearing between cells) and the first appearance of rounded cells on the surface of the plate (fig 3.2B). At 48 h and 72 h pi (respectively fig 3.2D and F), all infected cells possessed a "rounded" morphology and there were a higher number of gaps between them. These combined observations demonstrated the ability of HSV-1 to lead to cell death in neuroblastomas. These microscopy pictures together with other replicate experiments were analysed by the software "ImageJ" and it was quantitatively shown that HSV-1 was associated with a reduction in attached neuroblastoma cell area at 72 h pi (fig 3.3). Using the dye calcein-AM, staining live cells in green, there was decrease in neuroblastoma live cell staining following HSV-1 infection (MOI=0.01) at 72 h pi (fig 3.4).

At MOI=0.001, a significant decrease in both (i) RNA yield, following acid nucleic extraction, and (ii) cell viability, by cell counting following Trypan blue exclusion staining, was also observed in HSV-1-infected neuroblastomas compared to the uninfected cells (data not shown). qRT-PCR analysis that targeted the expression of the reference gene DAD-1, as a proxy marker of neuroblastomas viability, showed that the presence of HSV-1 was associated

with a decrease in DAD-1 gene expression (higher Ct values) from 30 h to 72 h pi (MOI=0.01) (fig 3.5). Similarly, WST-1 assay also showed a decrease in cellular activity of dehydrogenases (mitochondrial metabolism), another proxy marker of cell viability, in the infected population (MOI=0.01), at 48 h and 72 h pi (fig 3.6). Additionally, evidence of viral replication of HSV-1 in neuroblastomas was demonstrated by an increase in viral load in cell culture medium over time from 24 h to 72 h pi (MOI=0.01) (fig 3.7).

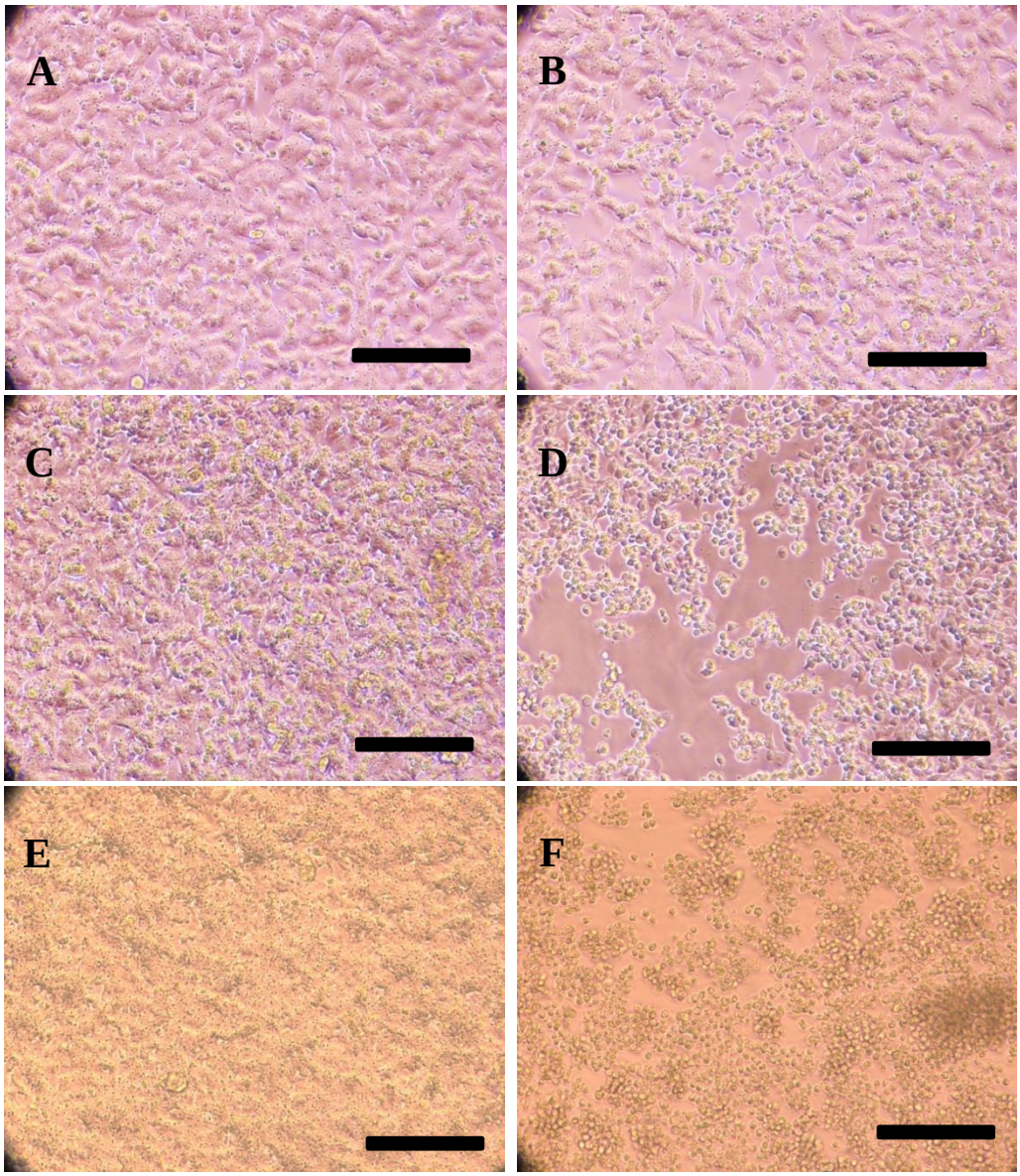

Figure 3.2. Representation of HSV-1-infected neuroblastoma cell culture. HSV-1 infection was done at MOI=0.01. On the left panel, the uninfected neuroblastomas are represen ted at 24 h (**A**), 48 h (**C**) and 72 h (**E**) after time of infection for the infected cells. The monolayer of these uninfected cells is 100% confluent at all time-points with number of cells increasing over time (as cells look smaller at 48 h and 72 h). (**B**), (**D**) and (**F**) represent HSV-1-infected neuroblastoma cells respectively at 24 h, 48 h and 72 h post-infection (h pi). Infected cells start to lose confluence at 24 h pi with gaps in the monolayer and some round cells appearing (**B**). At 48 h pi (**D**) and 72 h pi (**F**), the infection has progressed since there are bigger gaps between cells and all cells seem round. 10 x magnification. Scale bar: 50 µm.

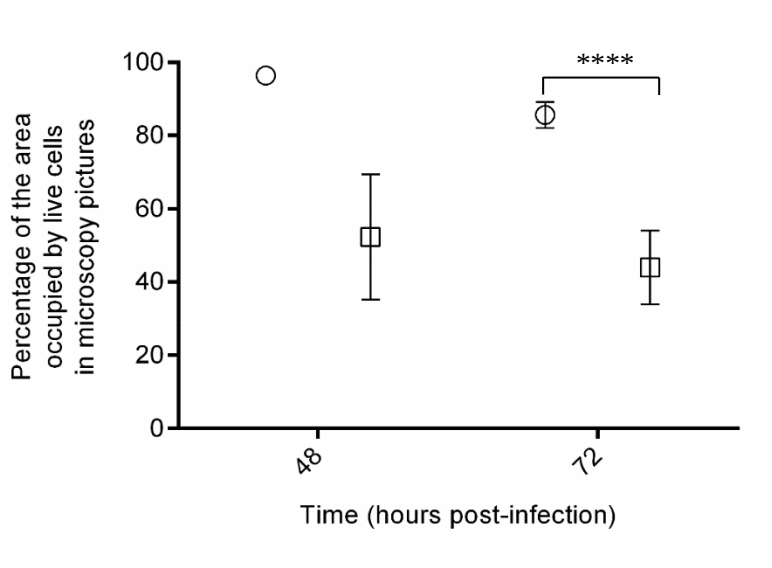

Figure 3.3. Percentage of attached cell area in microscopy pictures of HSV-1-infected neuroblastoma cells. HSV-1-infection was done at MOI=0.01. Areas of attached neuroblastoma cells were measured by the software "ImageJ" from pictures taken at 48 h and 72 h post-infection of uninfected (circles) or infected (squares) neuroblastoma cells. Data are expressed as mean of the area of live cells + 95% CI and were obtained as described in chapter 2 (Material and methods). At 48 h pi, one picture was used for uninfected and three for HSV-1-infected. At 72 h pi, nine pictures from three replicates were used for the uninfected cells and twenty-four pictures from 3 replicates for the HSV-1-infected ones. (****) $p<0.0001$ (multiple t-tests).

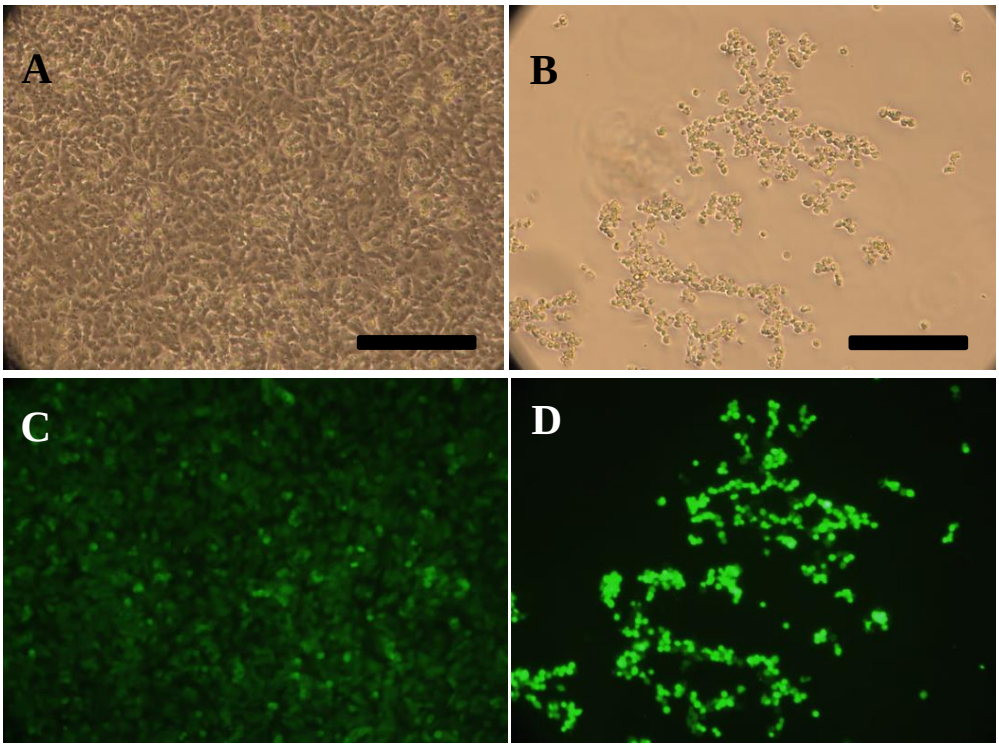

Figure 3.4. Live cell pictures by fluorescent microscopy in HSV-1-infected neuroblastoma cells. HSV-1 infection was done at MOI=0.01. (**A**) Uninfected neuroblastomas monolayer observed by light microscopy. The cells are "fibroblast-like" and the monolayer is 100% confluent. (**B**) HSV-1-infected neuroblastomas observed 72 h pi by light microscopy. There is no monolayer anymore, only few round cells are left. (**C**) Same picture as (A) observed by fluorescence microscopy following staining with the live cell dye calcein-AM (0.5 µM; excitation at 495 nm). (**D**) Same picture as (B) observed by fluorescence microscopy following staining with the live cell dye calcein-AM (0.5 µM; excitation at 495 nm). 10 x magnification. Scale bar: 50 µm.

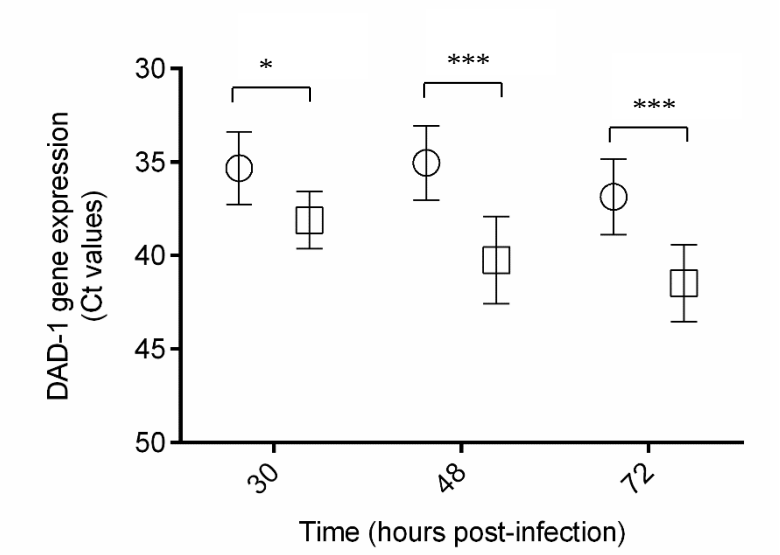

Figure 3.5. DAD-1 gene expression in HSV-1-infected neuroblastoma cells. HSV-1 infection was done at MOI=0.01. The values represent Ct values after qRT-PCR targeting DAD-1 from 1 µg of RNA extracts of uninfected (circles) or HSV-1-infected (squares) neuroblastomas at 30, 48, 72 h pi. Data are expressed as mean + 95% Confidence Interval (C.I) of 9 replicates from 3 independent experiments. (*) $p<0.05$; (***) $p<0.005$ (multiple t-tests).

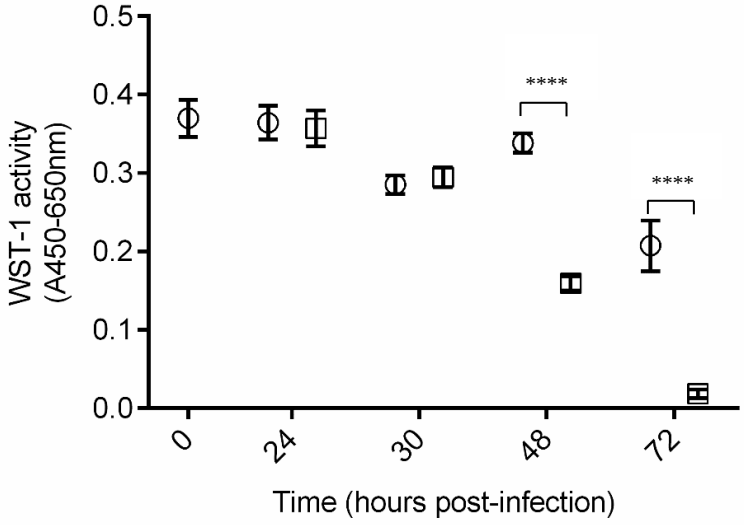

Figure 3.6. Mitochondrial activity in HSV-1-infected neuroblastoma cells. HSV-1 infection was done at MOI=0.01. The values represent WST-1 activity (absorbance at 450 nm (A450 nm) normalised by subtraction of the background (A650 nm) after addition of WST-1) of uninfected neuroblastomas (circles) and HSV-1-infected neuroblastomas (squares) at different time-points (0-72 h post-infection). Data are expressed as mean + 95% CI of 30 replicates from 3 independent experiments. (****) $p<0.0001$ (multiple t-tests).

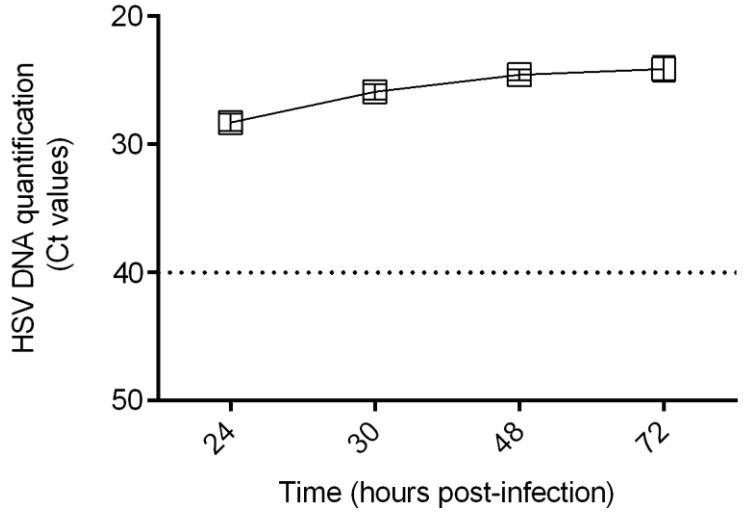

Figure 3.7. HSV DNA abundance in culture medium of HSV-1-infected neuroblastoma cells. HSV-1 infection was done at MOI=0.01. The values represent Ct values after HSV DNA qPCR from culture medium of HSV-1-infected neuroblastomas at 24, 30, 48 and 72 h pi. Each point represents the mean + 95% CI of data from at least 3 independent experiments. Triplicates were used for each point-time in each experiment.

3.2.1.2. Neuroblastoma cells exhibit an increase in TNF and INF-γ relative gene expression following HSV-1 infection

HSV-1 infection was associated in these cells with a significant increase in relative gene expression of the key pro-inflammatory cytokine TNF as early as 30 h pi and still present at 48 h and 72 h pi (fig 3.8). Interestingly, a single experiment showed that IFN-γ relative gene expression was also significantly increased in neuroblastomas following HSV-1 infection at 39 h pi (data not shown, only experiment and one time point).

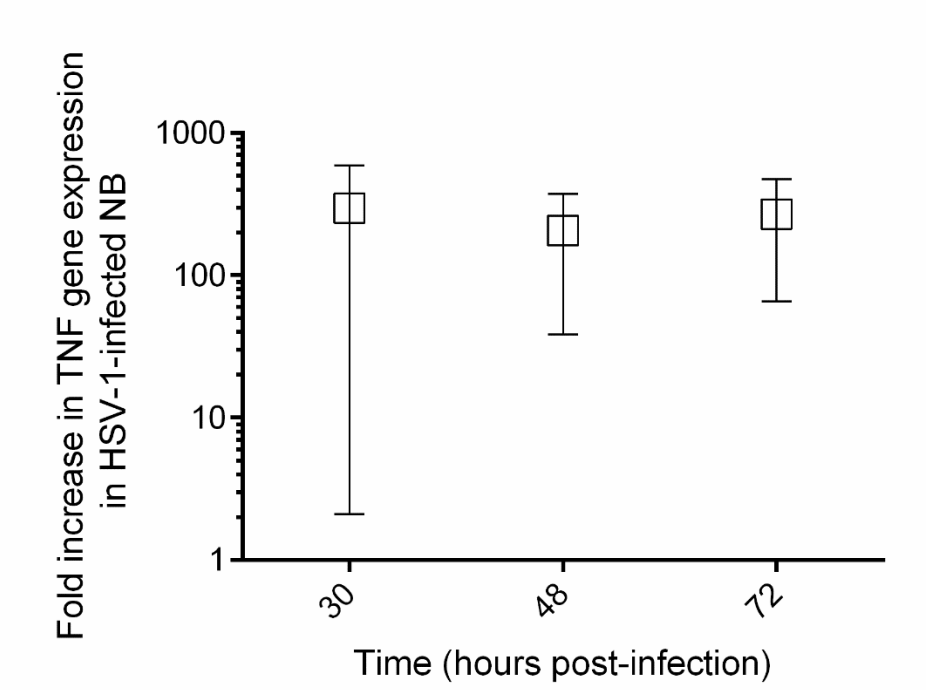

Figure 3.8. TNF relative gene expression in HSV-1-infected neuroblastoma cells. HSV-1 infection was done at MOI=0.01 in neuroblastoma cells. The data represent TNF relative gene expression expressed as mean +/- 95% CI of $2^{-\Delta\Delta Ct}$ values at 30 h, 48 h and 72 h post-infection. The scale is logarithmic. $2^{-\Delta\Delta Ct}$ values were obtained following qRT-PCR of TNF and DAD-1 genes. DAD-1 gene was used as reference (housekeeping) gene. From qRT-PCR Ct values of DAD-1 and TNF, ΔCt values [Ct (TNF)-Ct(DAD-1]) were obtained for both uninfected and HSV-1-infected cells. ΔΔ Ct values represented $[(\Delta Ct)_{HSV} - (\Delta Ct)_{uninfected}]$. Data were obtained from 3 independent experiments.

3.2.1.3. An increase in secreted TNF was not detected in neuroblastoma cell culture medium in response to HSV-1

TNF expression was also assessed at the protein level by ELISA test in the culture medium of HSV-1 infected neuroblastomas in T75 flasks, at different time-points (-6 to 72 h pi). Following HSV-1 infection, there was no detectable increase in TNF observed at any time point in flasks containing 8 mL (fig 3.9A) or 16 mL of culture medium (fig 3.9B).

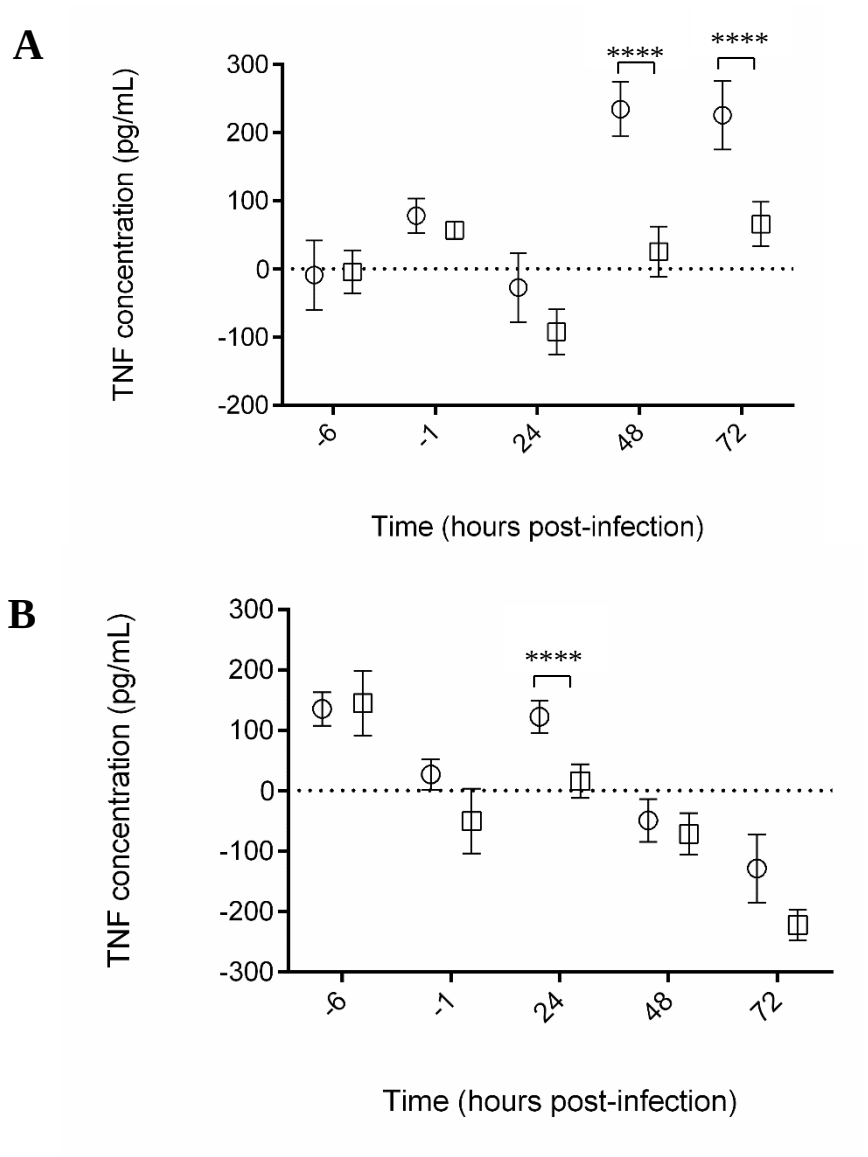

Figure 3.9. TNF protein concentration in culture medium of HSV-1-infected neuroblastoma cells. (A) TNF protein concentration in neuroblastoma cell culture medium (V= 8 mL). TNF concentration obtained by ELISA in culture medium of uninfected (circles) and HSV-1-infected neuroblastoma cells (squares) at 6, -1, 24, 48 and 72 h pi. TNF concentration was detected by spectrophotometer at 405 nm with correction at 650 nm. Values are expressed as mean of TNF concentration (pg/mL) + 95% CI. Each point is the mean of 4 replicates, each replicate was read twice by the spectrophotometer. (****) $p<0.0001$ (multiple t-tests). **(B) TNF protein concentration in neuroblastoma cell culture medium (V= 16mL).** TNF concentration obtained by ELISA in culture medium of uninfected (circles) and HSV-1-infected neuroblastoma cells (squares) at -6, -1, 24, 48 and 72 h pi. TNF concentration was detected by ELISA plate reader at 405 nm with correction at 650 nm. Values are expressed as mean of TNF concentration (pg/mL) + 95% CI. Each point is the mean of 4 replicates, each replicate was read twice by the spectrophotometer. (****) $p<0.0001$ (multiple t-tests).

3.2.2. HSV-1-infection of microglial cells.

3.2.2.1. HSV-1 replicates and is associated with cell death in microglia

The effect of HSV-1 on microglial cells was first assessed by light microscopy using three different MOI (0.001, 0.01 and 0.1). At 24 h post-infection (pi), the infected cells were 100% confluent for all the MOI tested (fig 3.11A; fig3.12A; fig 3.13A). The first signs of infection appeared at 24h pi. Some of the cells lost their "ovoid" shape to become rounder, smaller and brighter while the uninfected cell monolayer continued to present normal ovoid-shaped microglial cells (fig 3.10A). This phenomenon was linked with the viral load as the proportion of round cells increased with higher MOI. At 48h pi, in addition to a higher proportion of round cells, gaps in the monolayer could be observed for all MOI tested (fig 3.11B; fig 3.12B; fig 3.13B) while the uninfected cells were still 100% confluent and "ovoid" (fig 3.10B). These gaps indicate HSV-1-induced cell death in microglia. Again, cell of death (gaps) increased with MOI. Finally, at 72 h pi, all the infected cells appeared rounded at all MOI. The majority of cells had detached from the monolayer at MOI=0.1 (fig 3.13C). At MOI=0.001 (fig 3.11C) and 0.01 (fig 3.12C), more round cells were still attached compared to MOI=0.1 but the monolayer was still highly altered compared to uninfected (fig 3.10C). These microscopy pictures were then analysed by the software "ImageJ" and it was again observed that HSV-1 induced a reduction in the area of attached microglial cells at MOI=0.01 although the results were not statically significant (due to the low number of pictures suitable for "ImageJ" analysis) (fig 3.14).

The decrease in microglial cell viability was linked to higher HSV-1 viral load (MOI). This was confirmed by cell counting using Trypan Blue exclusion staining (fig 3.15). The lowest number of live cells (fig 3.15A) and the highest percentage of cell death (fig 3.15D) were seen at the highest MOI (0.1) at 72 h pi (not statistically significant). At MOI=0.01, HSV-1 was associated with a decrease in live cell number at 72 h pi and 96 h pi (fig 3.16A). The

percentage of dead cells was again elevated in presence of HSV-1 at these two time-points (fig 3.16D). Abundance of DAD-1 (housekeeping gene) was lower at 48 and 72 h pi (fig 3.17). Again this indicates reduced live cell number and/or reduced cell viability. A reduction of mitochondrial metabolism was also shown by WST-1 assay following HSV-1-infection at 72 h pi (fig 3.18). HSV viral load continued to increase over time. HSV DNA measured in culture medium demonstrated a steadily increase in abundance from 30 to 72 h pi (fig 3.19).

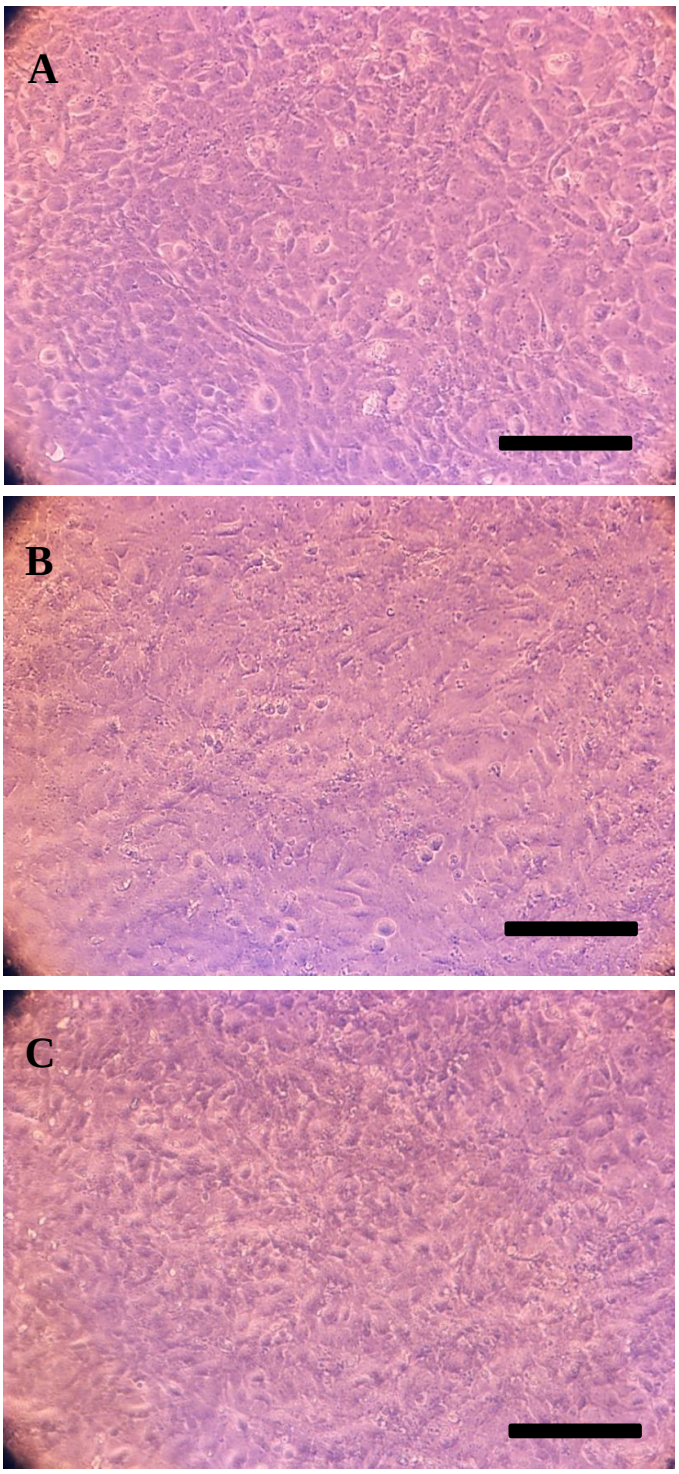

Figure 3.10. Microscopy pictures of (uninfected) microglia culture. Microscopy pictures of microglial cells at (**A**) 24 h, (**B**) 48 h and (**C**) 72 h after time of infection for the infected cells. These uninfected microglia show the same "ovoid" morphology and 100% confluency through the 3 time-points. 10 x magnification. Scale bar: 50 µm.

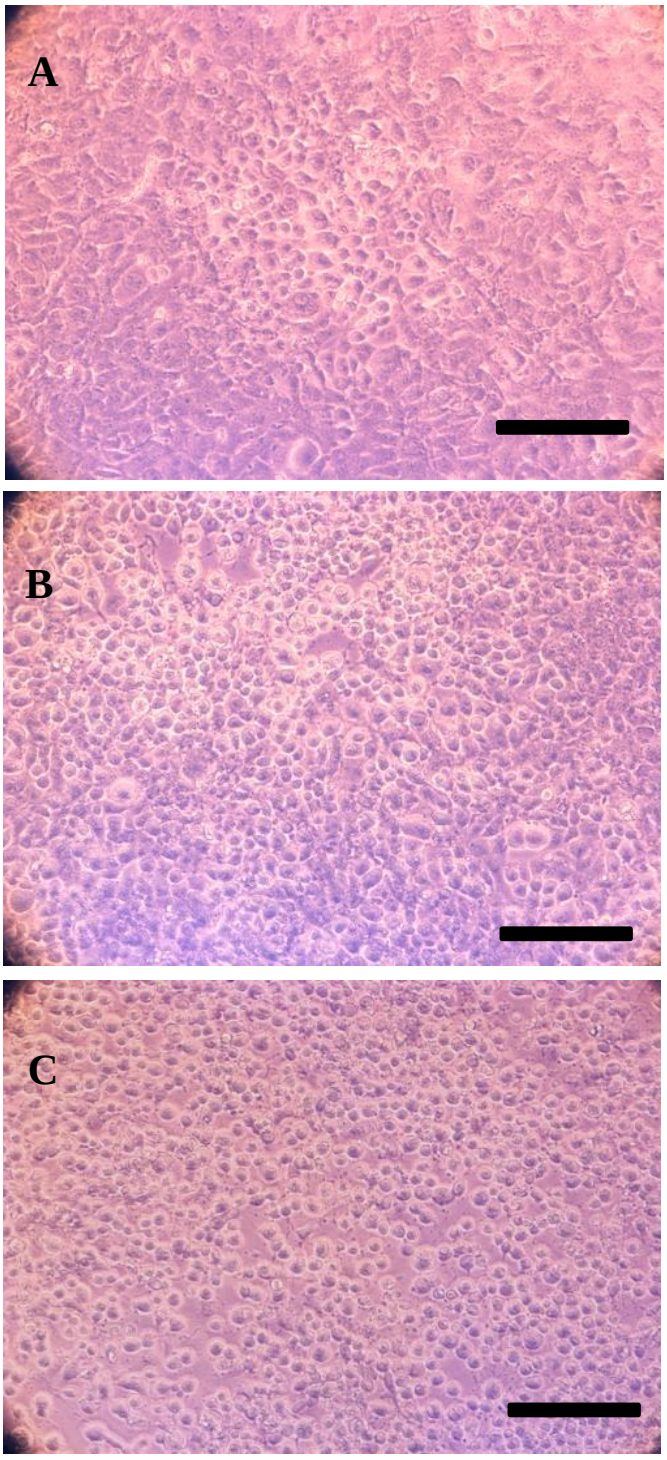

Figure 3.11. Microscopy pictures of HSV-1-infected microglia culture at MOI=0.001. (**A**) 24 h post-infection (pi). First round cells appear in the middle. (**B**) 48 h pi. More cells are round and the first gaps appear in the monolayer. (**C**) 72 h pi. All cells seem round and gaps are more frequent. 10 x magnification. Scale bar: 50 µm.

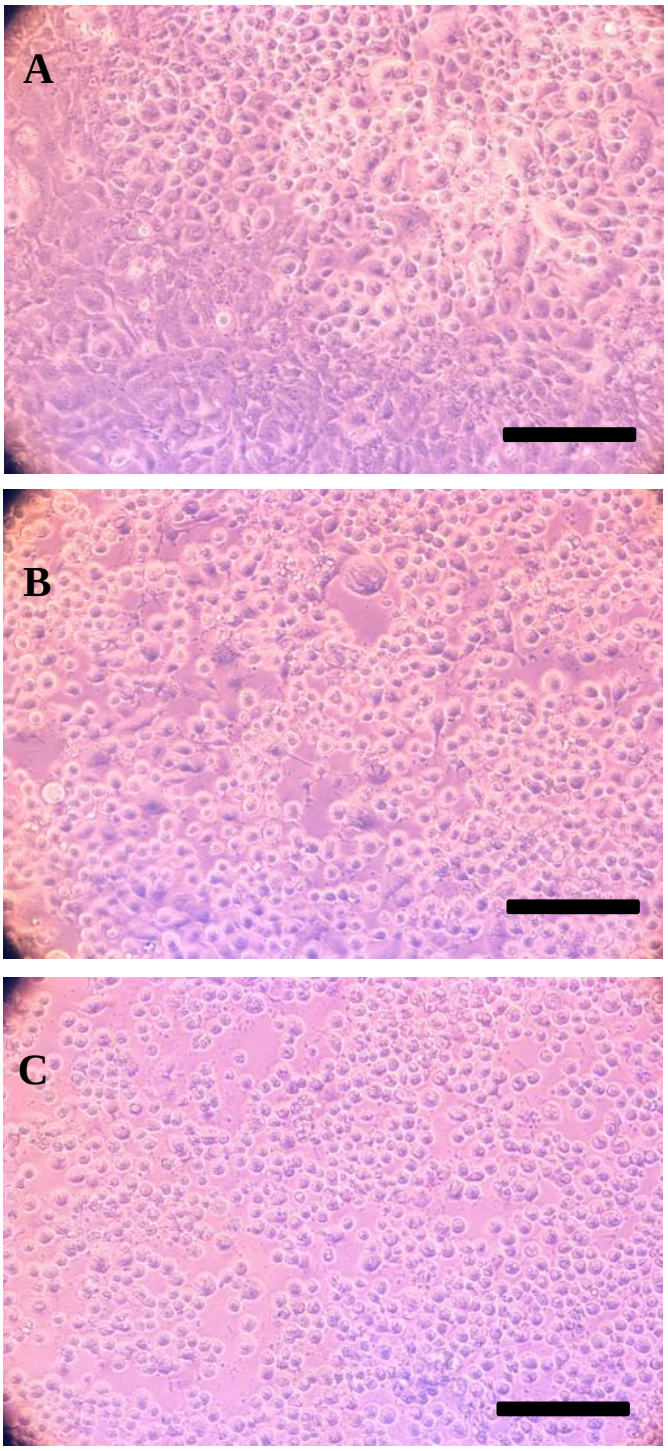

Figure 3.12. Microscopy pictures of HSV-1-infected microglia culture at MOI=0.01. (**A**) 24 h post-infection (pi). Half of the cells seem round. (**B**) 48 h pi. The proportion of round cells increase while frequent gaps in the monolayer appear. (**C**) 72 h pi. All cells are round and there are more gaps in the monolayer. 10 x magnification. Scale bar: 50 µm.

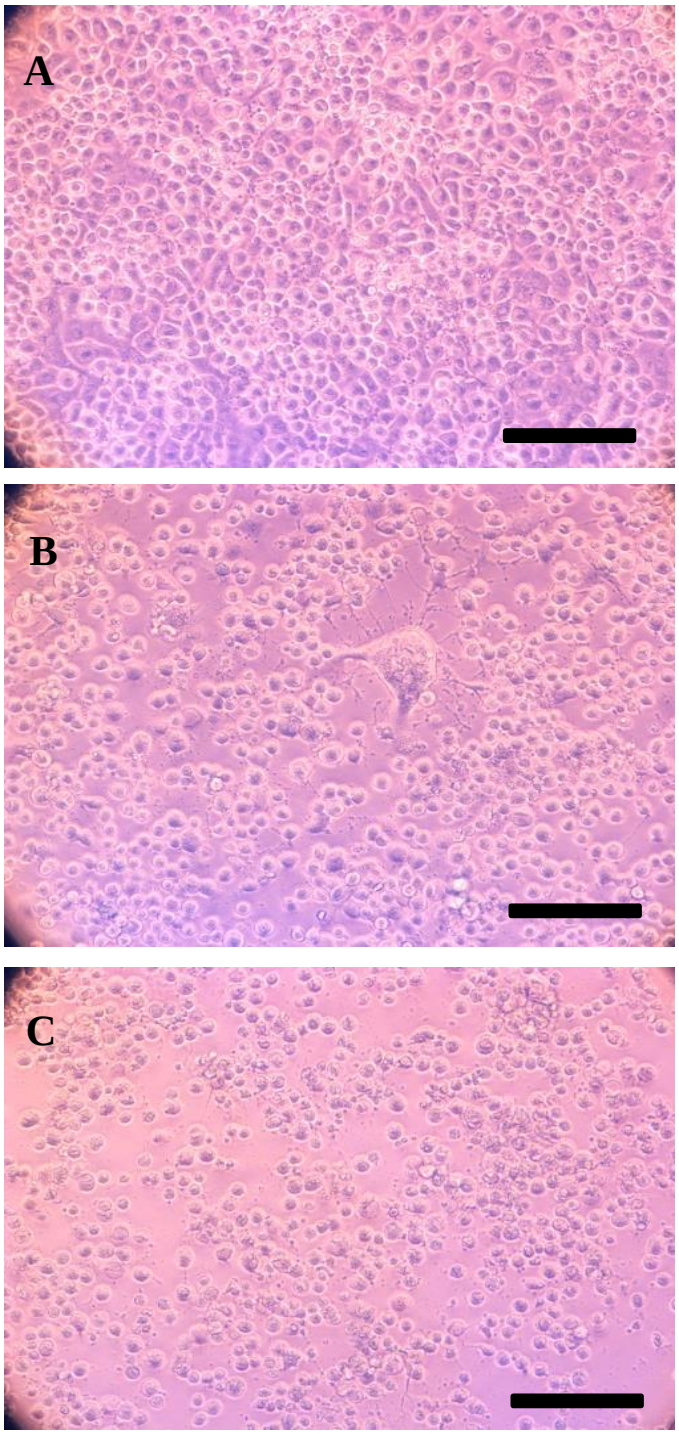

Figure 3.13. Microscopy pictures of HSV-1-infected microglia culture at MOI=0.1. (**A**) 24 h post-infection (pi). Most cells seem round. (**B**) 48 h pi. A lot of gaps in the monolayer appear. A giant cell, syncytia-like structure appears in the middle. (**C**) 72 h pi. All cells are round and most of cells detached from the surface. 10 x magnification. Scale bar: 50 µm.

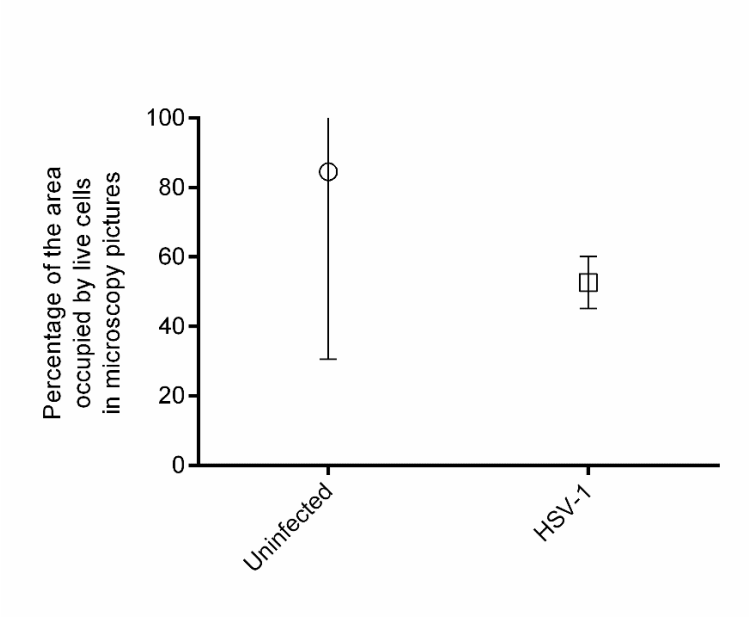

Figure 3.14. Percentage of attached cell area in microscopy pictures of HSV-1-infected microglial cells. HSV-1-infection was done at MOI=0.01. Areas of attached cells were measured by the software ImageJ from pictures taken at 72 h post-infection. Two 4 x magnification microscope pictures for uninfected and four for infected were analysed. Statistical tests were not relevant due to a number of replicates too low.

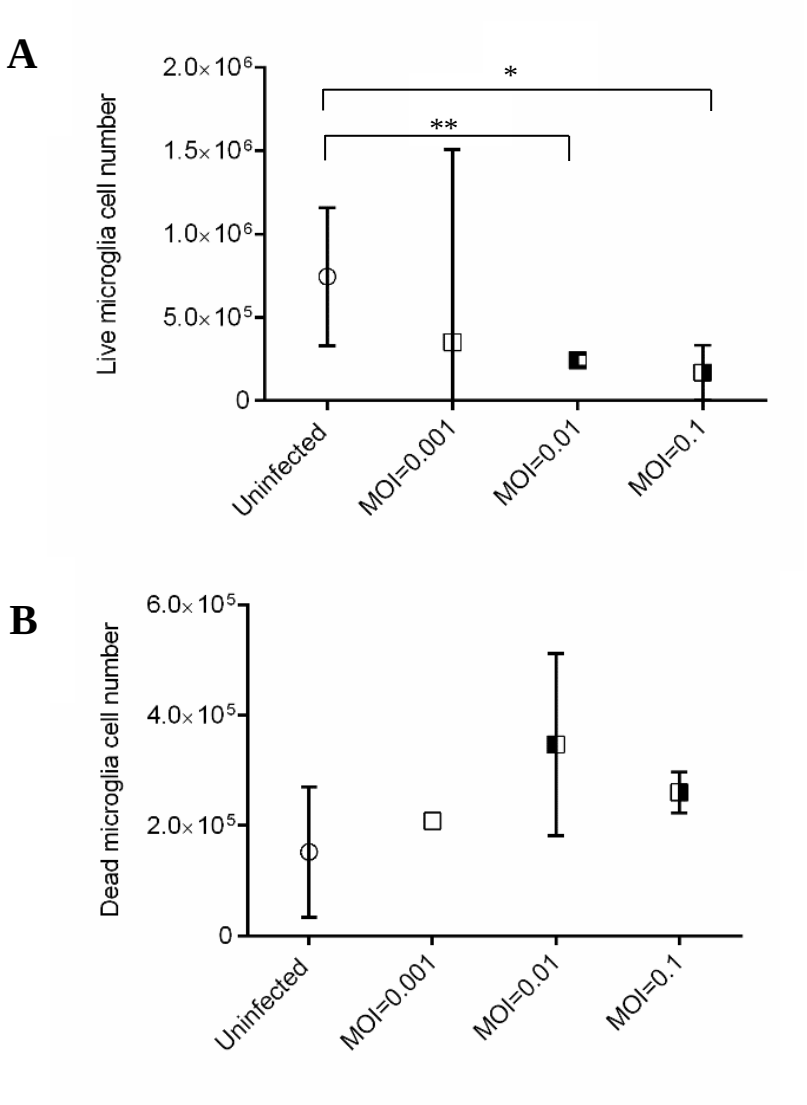

Figure 3.15. Figures 3.15B-C and legend next page.

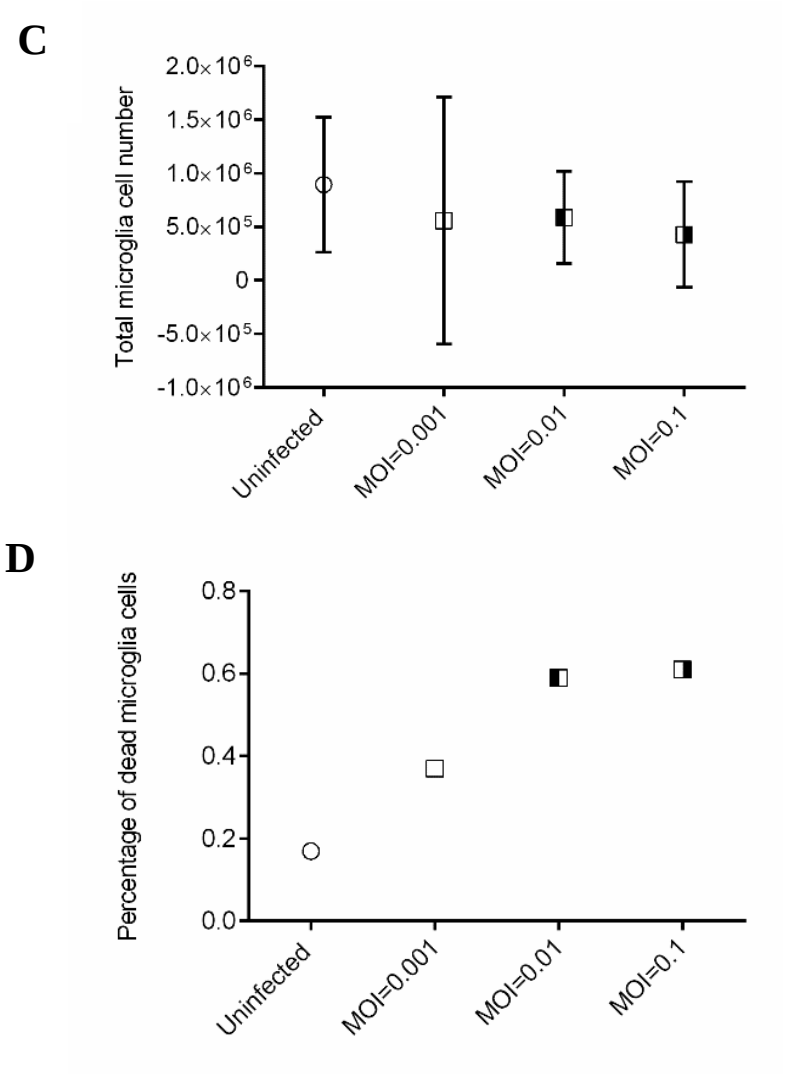

Figure 3.15. Live and dead cell number in HSV-1 infected microglial cells at 72 h pi at different MOI. The infection was done at MOI=0.001 (unfilled squares), MOI=0.01 (squares half-filled on the left side) or MOI=0.1 (squares half-filled on the right side). Cell counting at 72 h pi by trypan blue exclusion staining of the number of live cells (**A**), the number of dead cells (**B**), the total number of cells (**C**) and the percentage of dead cells (**D**) in uninfected (circles) and HSV-1-infected microglial cells (squares). Data is expressed as the mean of cell counting + 95% CI (except for figure (D) that represents mean of percentage of dead cells (without 95% CI)). Each condition was assessed in triplicates in only one experiment. ANOVA test statistically showed significant differences between the means of the different conditions for live cell counting (A) ($p<0.005$) but not for dead cell counting (B) or total cell counting (C) ($p>0.05$). (*) $p<0.05$; (**) $p<0.01$ (t-tests).

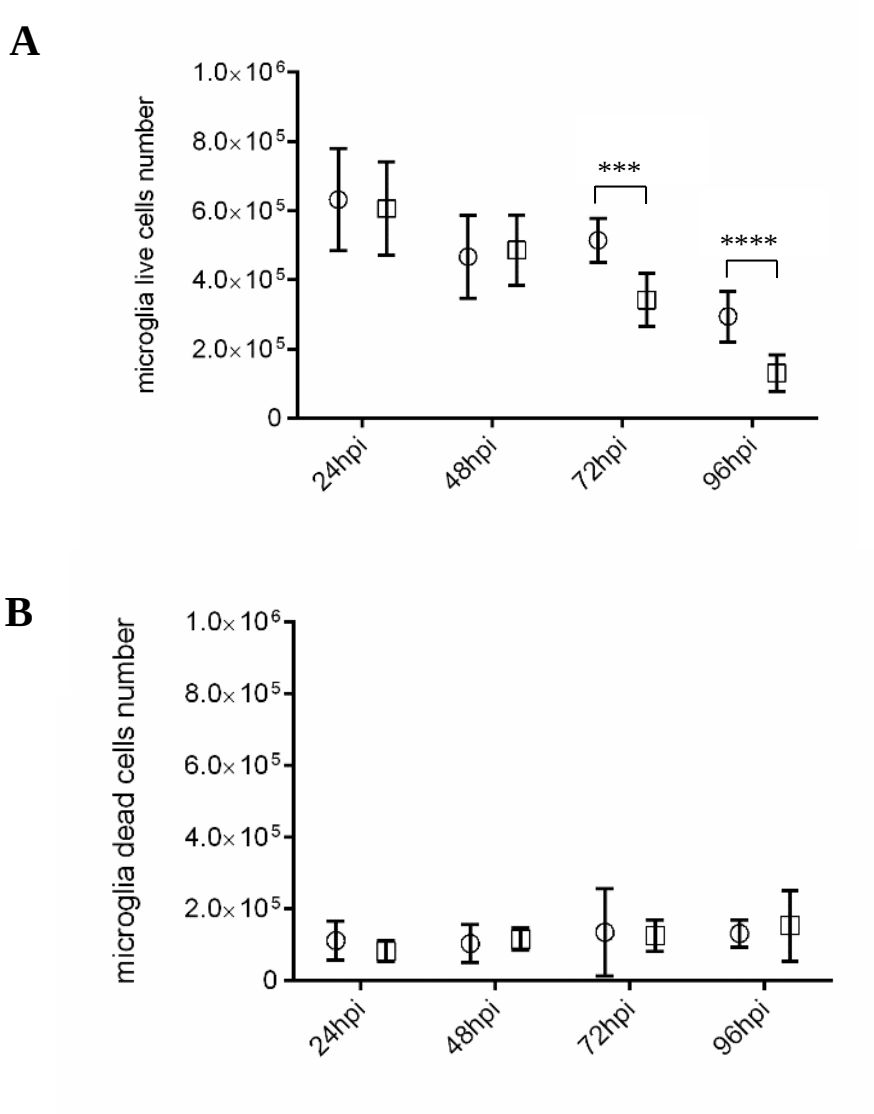

Figure 3.16. Legend and figures 3.16C-D next page.

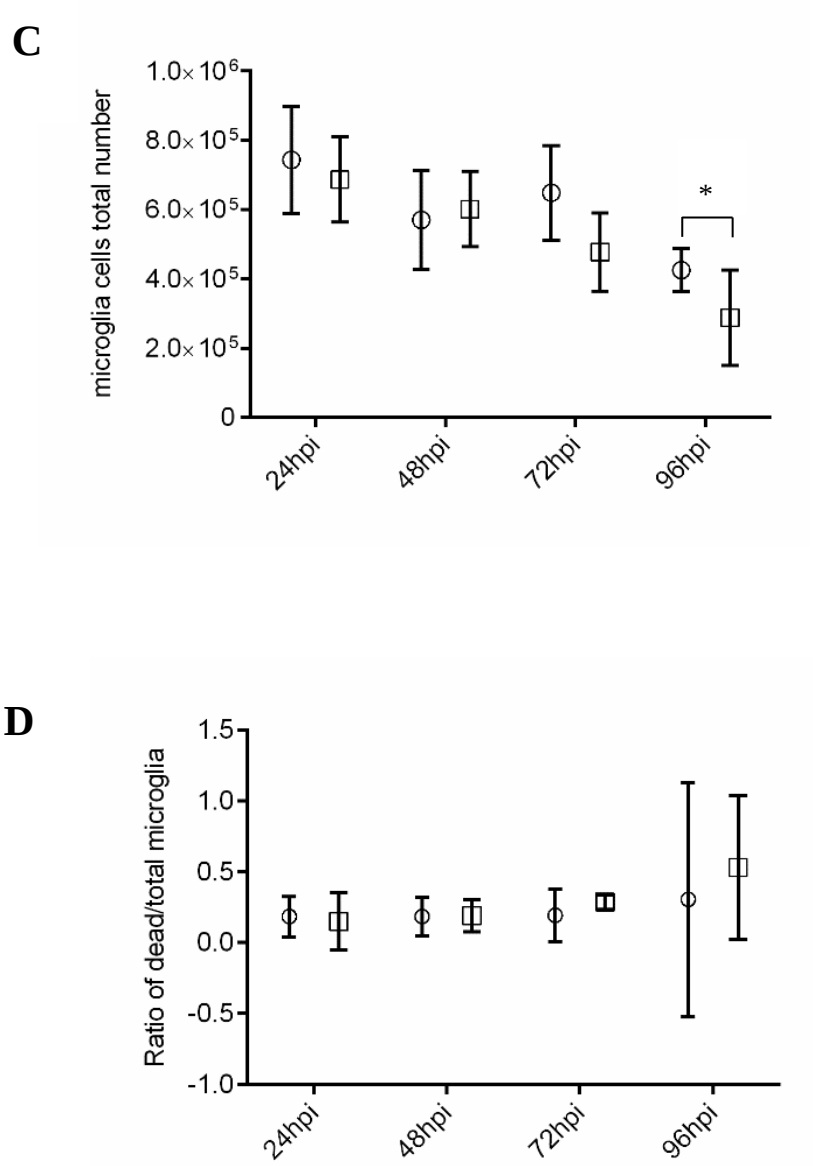

Figure 3.16. Live and dead cell number in HSV-1-infected microglia (MOI=0.01) over time. Cell counting by trypan blue exclusion staining of the number of live cells (**A**), the number of dead cells (**B**), the number of total cells (**C**) and the percentage of dead cells (**D**) in uninfected (circles) and HSV-1-infected (squares) microglia cells (MOI=0.01) at different time-points (24 h-96 h pi). Data are expressed as mean of cell counting + 95% CI. Each condition was assessed in triplicates in 3 independent experiments. (*) $p<0.05$; (***) $p<0.005$; (****) $p<0.001$ (multiple t-tests).

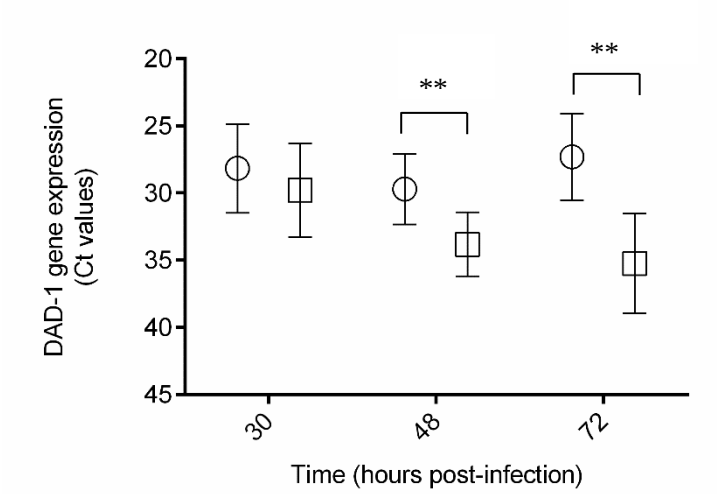

Figure 3.17. DAD-1 gene expression in HSV-1-infected microglial cells. HSV-1-infection was done at MOI=0.01. The values represent Ct values after qRT-PCR targeting DAD-1 from 1 µg of RNA extracts of uninfected (circles) or HSV-1-infected (MOI=0.01) (squares) microglial cells at 30, 48, 72 h pi. Data are expressed as the mean + 95% Confidence Interval (C.I) of 9 replicates from 3 independent experiments. (**) $p<0.005$ at 48 h pi and 72 h pi (multiple t-tests).

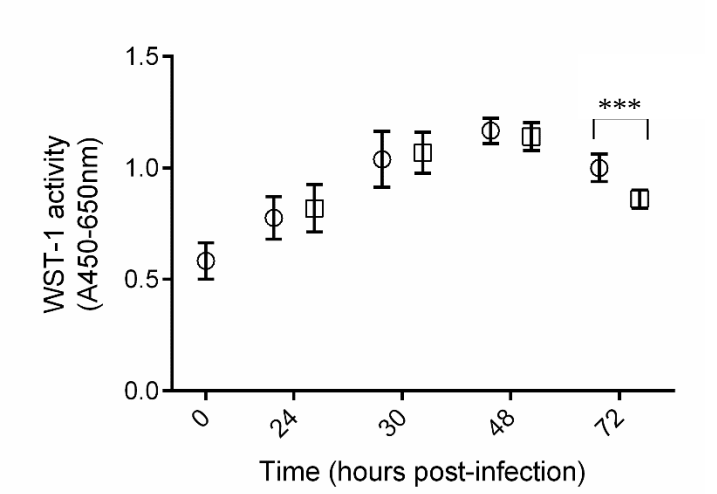

Figure 3.18. Mitochondrial activity in HSV-1-infected microglial cells. HSV-1 infection was done at MOI=0.01. The values represent WST-1 activity (Absorbance at 450 nm normalised by subtraction of the background (A650 nm) after addition of WST-1) of uninfected (circles) and HSV-1-infected microglial cells (squares) at different time-points (0-72 h pi). Data are expressed as mean + 95% CI of 30 replicates from 3 independent experiments. (***) $p<0.001$ (multiple t-tests).

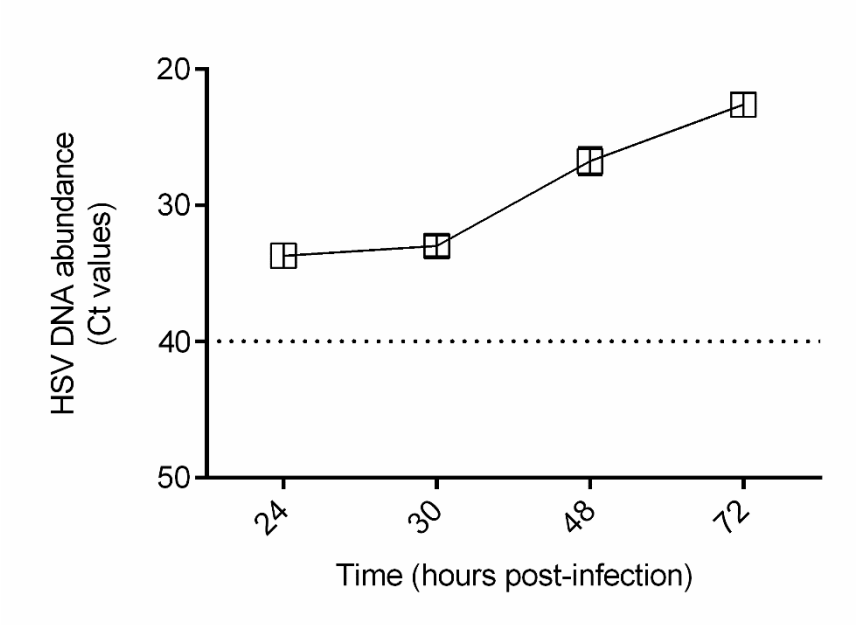

Figure 3.19. HSV DNA abundance in culture medium of HSV-1-infected microglial cells. HSV-1 infection was done at MOI=0.01. The values represent Ct values after HSV DNA qPCR from culture medium of HSV-1-infected microglia at 24, 30, 48, 72 h pi. Each point represents the mean + 95% CI of data from at least 3 independent experiments with triplicates used for each point in each experiment.

3.2.2.2. TNF and IFN-γ relative gene expression increase in microglia following HSV-1 infection

The relative gene expression of TNF was significantly increased in microglial cells at both 48 h and 72 h pi, while slightly increased at 24 h pi, following HSV-1 challenge (fig 3.20)

In these same cells after HSV-1 infection, a high increase in IFN-γ relative gene expression, was also observed at 48-96 h pi following a decrease at 24h pi (fig 3.21). No drastic change was seen for IL-1β or IL-6 relative gene expression at any of these time-points (fig 3.22 and 3.23).

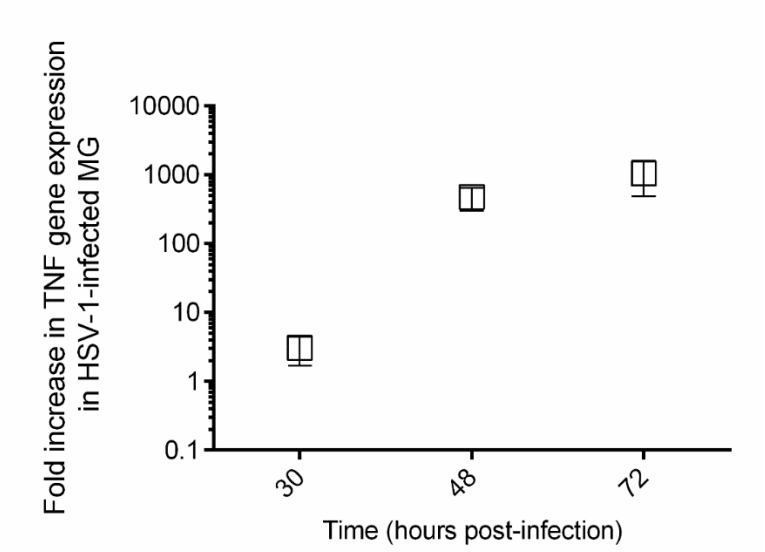

Figure 3.20. TNF relative gene expression in HSV-1-infected microglial cells. HSV-1 infection was done at MOI=0.01 in microglial cells. The data represent TNF relative gene expression expressed as mean +/- 95% CI of $2^{-\Delta\Delta Ct}$ values at 30 h, 48 h and 72 h post-infection. The scale is logarithmic. $2^{-\Delta\Delta Ct}$ values were obtained following qRT-PCR of TNF and DAD-1 genes. DAD-1 gene was used as reference (housekeeping) gene. From qRT-PCR Ct values of DAD-1 and TNF, ΔCt values [Ct (TNF)-Ct(DAD-1]) were obtained for both uninfected and HSV-1-infected cells. ΔΔCt values represented $[(\Delta Ct)_{HSV} - (\Delta Ct)_{uninfected}]$. Data were obtained from 3 independent experiments.

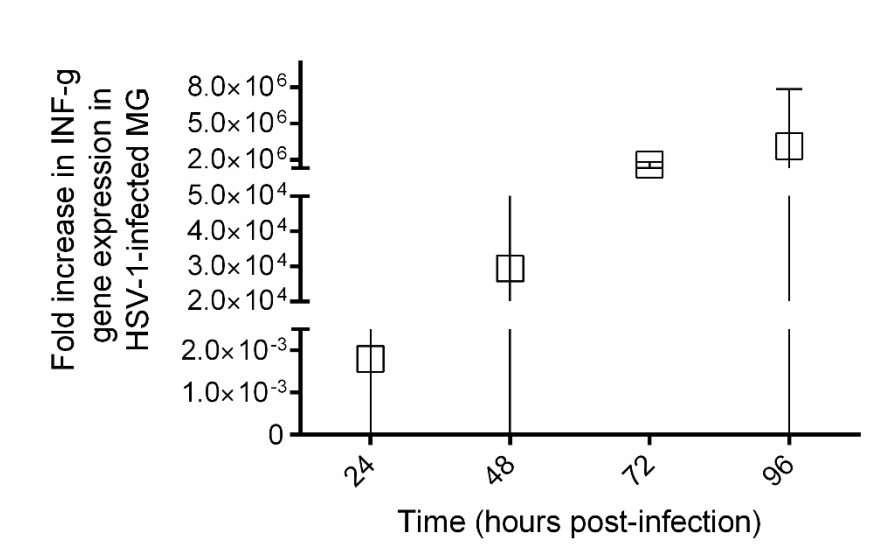

Figure 3.21. IFN-γ relative gene expression in HSV-1-infected microglial cells. HSV-1 infection was done at MOI=0.01 in microglial cells. The data represent INF-γ relative gene expression expressed as mean +/- 95% CI of $2^{-\Delta\Delta Ct}$ values at 30 h, 48 h and 72 h post-infection. $2^{-\Delta\Delta Ct}$ values were obtained following qRT-PCR of IFN-γ and DAD-1 genes. DAD-1 gene was used as reference (housekeeping) gene. From qRT-PCR Ct values of DAD-1 and IFN-γ, ΔCt values [Ct (IFN-γ)-Ct(DAD-1]) were obtained for both uninfected and HSV-1-infected cells. ΔΔCt values represented $[(\Delta Ct)_{HSV} - (\Delta Ct)_{uninfected}]$. Data were obtained from a single experiment.

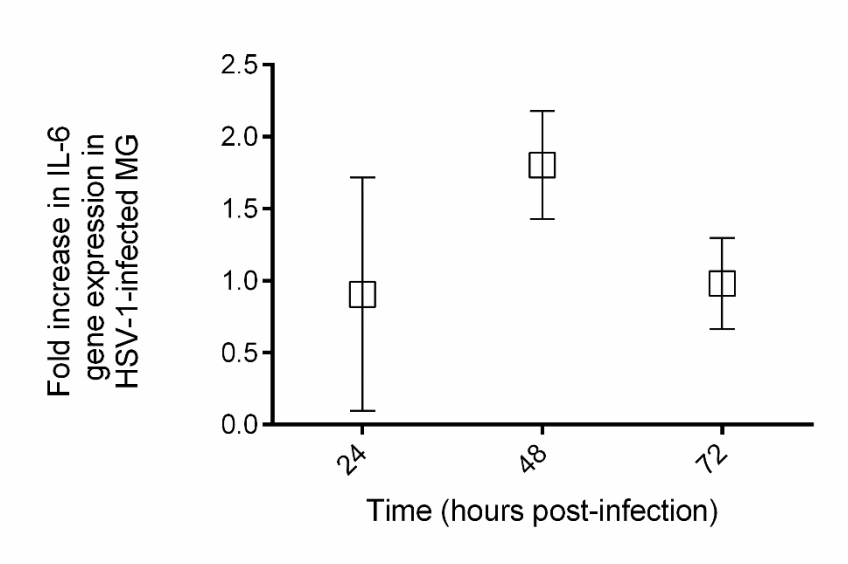

Figure 3.22. IL-6 relative gene expression in HSV-1-infected microglial cells. HSV-1 infection was done at MOI=0.01 in microglial cells. The data represent IL-6 relative gene expression expressed as mean +/- 95% CI of $2^{-\Delta\Delta Ct}$ values at 30 h, 48 h and 72 h post-infection. $2^{-\Delta\Delta Ct}$ values were obtained following qRT-PCR of IL-6 and DAD-1 genes. DAD-1 gene was used as reference (housekeeping) gene. From qRT-PCR Ct values of DAD-1 and IL-6, ΔCt values [Ct (IL-6)-Ct(DAD-1]) were obtained for both uninfected and HSV-1-infected cells. ΔΔCt values represented [$(\Delta Ct)_{HSV}$ - $(\Delta Ct)_{uninfected}$]. Data were obtained from a single experiment.

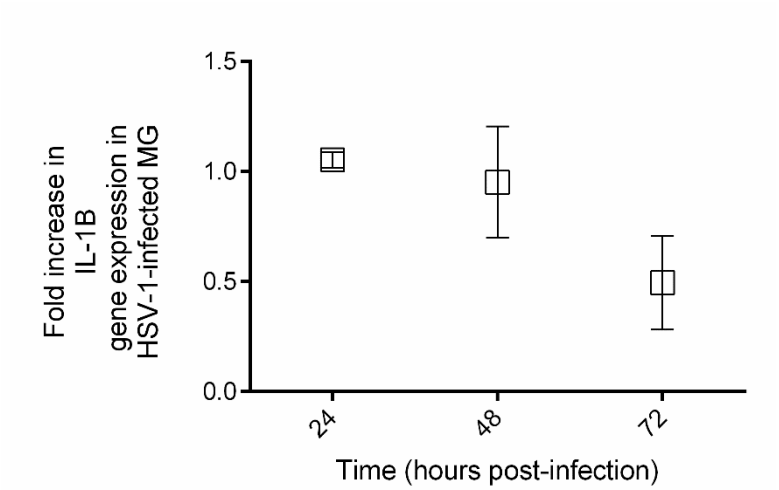

Figure 3.23. IL-1B relative gene expression in HSV-1-infected microglial cells. HSV-1 infection was done at MOI=0.01 in microglial cells. The data represent IL-1B relative gene expression expressed as mean +/- 95% CI of $2^{-\Delta\Delta Ct}$ values at 30 h, 48 h and 72 h post-infection. $2^{-\Delta\Delta Ct}$ values were obtained following qRT-PCR of IL-1B and DAD-1 genes. DAD-1 gene was used as reference (housekeeping) gene. From qRT-PCR Ct values of DAD-1 and IL-1B, ΔCt values [Ct (IL-1B)-Ct(DAD-1]) were obtained for both uninfected and HSV-1-infected cells.

ΔΔCt values represented [$(\Delta Ct)_{HSV}$ - $(\Delta Ct)_{uninfected}$]. Data were obtained from a single experiment.

3.2.2.3. An increase in secreted TNF is not detected by ELISA in microglia cell culture medium in response to HSV-1

Similar to what has been shown in neuroblastomas, there was no increase in TNF protein detected by ELISA in culture medium of HSV-1infected microglia compared to that of uninfected cells, at any time-points (24 h-96 h pi) (fig 3.24).

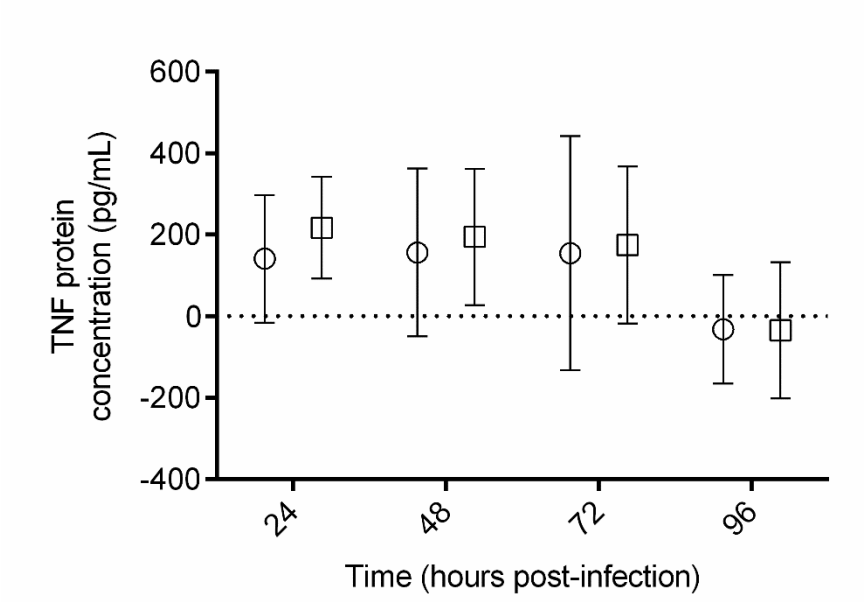

Figure 3.24. TNF protein concentration in culture medium of HSV-1-infected microglial cells. TNF concentration obtained by ELISA in culture medium of uninfected (circles) and HSV-1-infected microglia cells (squares) at -6, -1, 24, 48 and 72 h pi. TNF concentration was detected by spectrophotometer at 405 nm with correction at 650 nm. Values are expressed as mean of TNF concentration (pg/mL) + 95% CI. Each point is the mean of at least 6 replicates, from 3 different experiments. No statistical differences at any time-point (t-tests).

3.2.3. Comparisons of the dynamics of HSV-1 replication and HSV-1-associated cell viability loss in neuroblastoma and microglia cells

I wanted to compare the dynamics of HSV-1 infection in two different brain cells. Therefore I compared changes in viral load and cell viability among neuroblastoma ad microglial cells. Viral load was measured by HSV DNA by qPCR. Cell viability was measured using mitochondrial activity (via WST-1 assay). Cells were exposed to the same MOI (0.01).

The figure 3.25A compares two HSV DNA abundance over time from the culture medium of infected neuroblastoma (fig 3.7) and microglial cells (fig 3.19). Viral load in infected microglia cell culture medium was low at 24 h pi (Ct around 34) but was relatively high by 72 h pi (Ct around 23). The profile of HSV replication was different in neuroblastoma culture medium. The viral load appeared to plateau between 24 h and 72 h pi with a Ct value around 28 at 24 h pi and around 24 at 72 h pi. Hence, from 24 h to 72 h pi, culture medium HSV DNA abundance showed a faster rate of increase in infected microglia than neuroblastoma cells at this time-point (fig 3.25A). During this period, in average, HSV DNA abundance doubled every four hours in infected microglia culture medium while more than thirteen hours were needed in that of infected neuroblastoma cells (fig 3.25B). However, final viral load (at 72 h pi) was comparable between the two brain cell types.

The figure 3.26A compares the two mitochondrial activity for both infected neuroblastoma (fig 3.6) and microglial cells (fig 3.18). A steady decrease of mitochondrial activity among neuroblastoma cells can be observed following HSV-1-infection from 24 h to 72 h pi (fig 3.24A). The mitochondrial activity profile was different in microglial cells following HSV-1 infection (fig 3.26A). In microglia, there was an increase from 24 h to 48 h pi in WST-1 activity followed by a decrease from 48 h to 72 h pi. At 72 h pi, mitochondrial activity was estimated as null in infected neuroblastoma cells (fig 3.26A-B). In infected microglial cells,

mitochondrial activity had initially risen (48 h pi) and then fallen (72 h pi) to levels observed at 24 h pi (fig 3.26A-B).

During the period 24 to 72 h pi, HSV DNA replicates faster in microglia than in neuroblastomas cells. Mitochondrial activity, a proxy marker of cell viability, was steadily reduced in infected neuroblastoma cells and was essentially not detected at 72 h pi. Infected microglial cells showed a maintenance of mitochondrial activity at 72 h pi. Dynamics of HSV replication and cell viability were very different between HSV-1-infected microglia and neuroblastoma cells in the *in vitro* models used. Microglia cells could be described as more permissive to HSV-1 infection. They allowed viral replication rate while maintaining cell activity. Furthermore, infected neuroblastoma cells exhibited a higher viral load but reduced mitochondrial activity compared to infected microglial cells at 24 h pi.

A

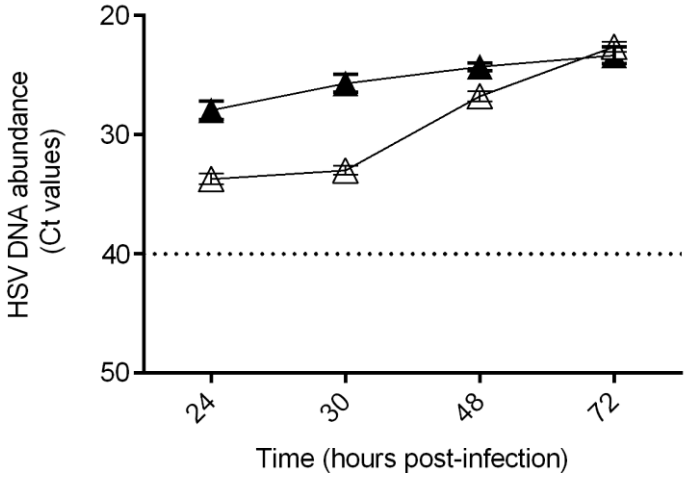

B

	Microglia	Neuroblastomas
slope of the linear trendline: HSV DNA Ct values= f(Time in hours)	-0,2418	-0,0742
Time (hours) for HSV DNA abundance to double in cell culture medium (from 24h to 72h pi)	4,13	13,48

Figure 3.25. Comparisons of dynamics of culture medium HSV DNA abundance between HSV-1-infected microglial and neuroblastoma cells. HSV-1 infection was done at MOI=0.01. **A. HSV DNA abundance in culture medium of infected microglial and neuroblastoma cells** The values represent Ct values after HSV DNA qPCR from culture medium of HSV-1-infected microglial (white triangles) or neuroblastoma (black triangles) cells at 24, 30, 48, 72 h pi. Each point represents the mean + 95% CI of data from at least 3 independent experiments with triplicates used for each point in each experiment. These data come from the figures 3.7 and 3.20. **B. Determination of the dynamics of HSV DNA abundance in culture medium of infected microglial and neuroblastoma cells using linear trend line and slope.** From each curve expressed in the figure 3.26A, a linear trendline was determined and a slope associated using the softwate "Excell" (Microsoft). From the slope

value, time (h) for HSV DNA abundance to double in cell culture medium from 24 to 72 h pi was calculated.

A

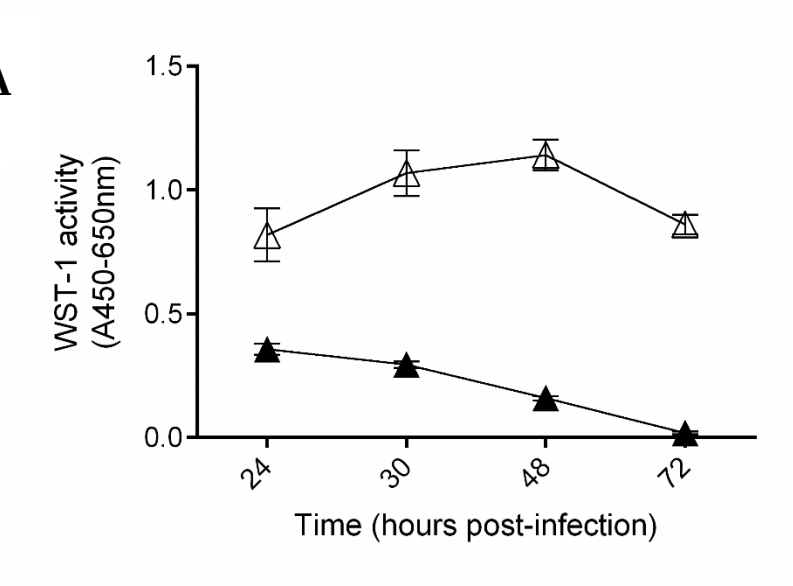

B

	Microglia	Neuroblastomas
slope of the linear trendline: WST-1 values= f(Time in hours)	-0,0006	-0,0069
Time (h) for WST-1 activity to be null	1162 (by considering a linear trendline)	74

Figure 3.26. Comparisons of dynamics of mitochondrial activity between HSV-1-infected microglial and neuroblastoma cells. HSV-1 infection was done at MOI=0.01. **A. Mitochondrial activity in infected microglial and neuroblastoma cells** The values represent mitochondrial activity measured by the WST-1 assay (A450 – A650 nm) in HSV-1-infected microglial (white triangles) or neuroblastoma (black triangles) cells at 24, 30, 48, 72 h pi. Data are expressed as mean + 95% CI of 30 replicates from 3 independent experiments. These data come from the figures 3.6 and 3.19. **B. Determination of the dynamics of**

mitochondrial activity in infected microglial and neuroblastoma cells using linear trend line and slope. From each curve expressed in the figure 3.27A, a linear trendline was determined and a slope associated using the softwate "Excell" (Microsoft). From the slope value, time (h) for WST-1 activity to be null was estimated.

3.2.4. HSV-1-infection in primary astrocytes

HSV-1 was associated with cell death and morphologic changes in primary astrocytes in a similar manner to that seen in neuroblastoma cells and microglia. The progression of HSV-1 infection (MOI=0.01) in primary astrocytes was observed under light microscope (fig 3.27). At 24 h post-infection (pi), infected astrocytes became less confluent and appeared more isolated (fig 3.27B) compared to the uninfected (fig 3.27A), demonstrating HSV-1-induced cell death. At this time-point, some infected astrocytes (but not the control uninfected cells) were already losing their normal shape (thin, very long, with occasional star-like ramifications) to become rounder, smaller and brighter. These phenomena became more pronounced over time. At 48 h pi, a higher proportion of infected cells looked small, round and bright (fig 3.27D) whereas 24 h later (72h pi), the monolayer of infected cells exhibited more gaps between cells, no "normal-shaped" astrocytes left and some giant, potentially multi-nuclei cells (syncytia-like structure) (fig 3.27F). There were no changes in the uninfected astrocyte monolayer over time (fig 3.27C and E). Cell counting showed that infection with HSV-1 was associated with a decrease in live astrocyte number along with an increase in the percentage of dead cells at 24 h, 48 h and 72 h pi (fig 3.28). There was also a decrease in DAD-1 gene expression in astrocytes following HSV-1 infection (fig 3.29). qRT-PCR targeting TNF in infected astrocytes was also performed. However, Ct values for this TNF target were routinely beyond the limits of detection of the PCR machine (data not shown), making an accurate detection of TNF expression following HSV-1 infection in astrocytes not possible.

A more in-depth study of HSV-1 infection in primary astrocytes (including an assessment of HSV-1 replication and new qRT-PCR targeting DAD-1) is discussed in chapter 7 in the context of co-culture with microglia.

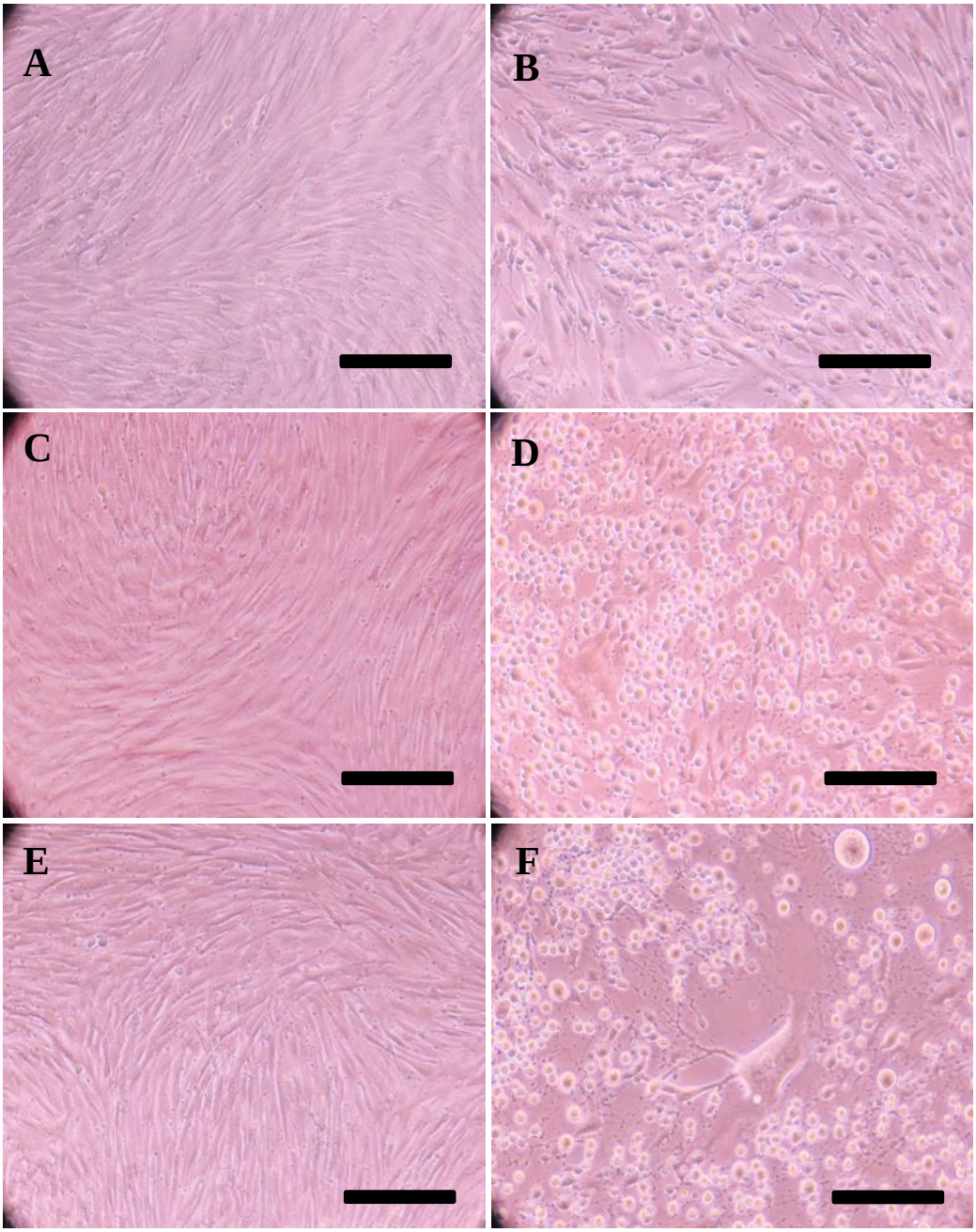

Figure 3.27. Microscopy pictures of HSV-1-infected primary astrocytes. HSV-1-infection was done at MOI=0.01. On the left panel, the uninfected astrocytes are represented at 24 h (**A**), 48 h (**C**) and 72 h (**E**) after time of infection for the infected cells. The monolayer of these uninfected cells is 100% confluent at all time-points. These uninfected cells exhibit the morphology of healthy primary astrocytes: they are thin, very long with some "star-like"-ramifications. (**B**), (**D**) and (**F**) represent HSV-1-infected astrocytes respectively at 24 h, 48 h and 72 h post-infection (h pi). Infected cells start to lose their confluence at 24 h pi with gaps in the monolayer and some round cells appearing (**B**). At 48 h pi (**D**) and 72 h pi (**F**), the infection has progressed with bigger gaps between cells and almost all cells seem round. At 72 h pi, a syncitia-like structure can also be observed. 10 x magnification. Scale bar: 50 µm.

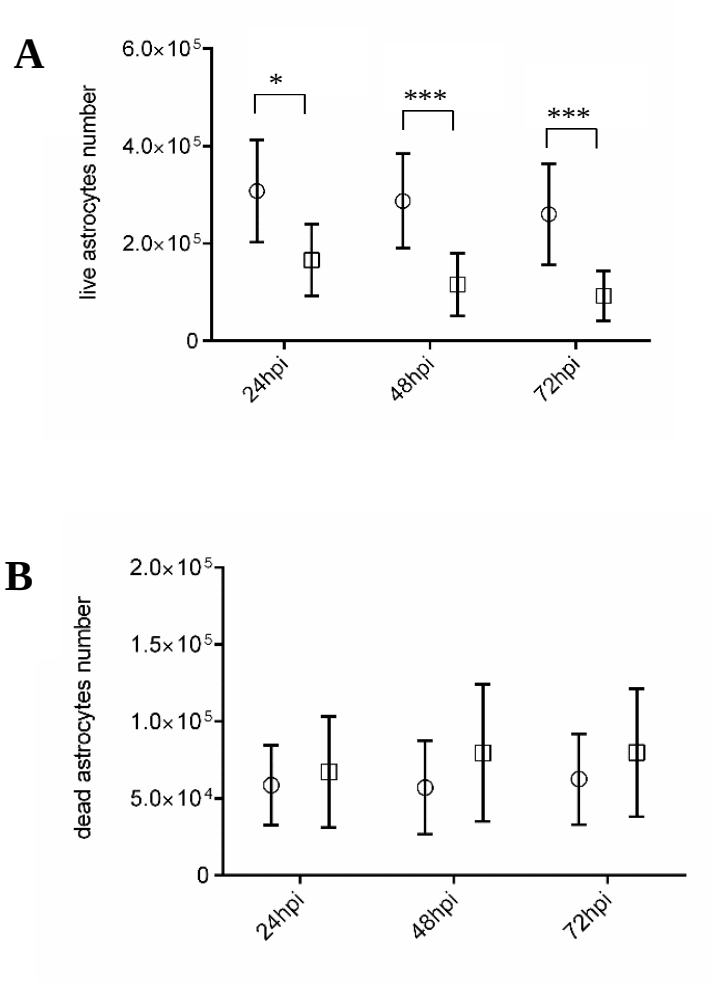

Figure 3.28. Figures 3.26B-C and legend on the next page.

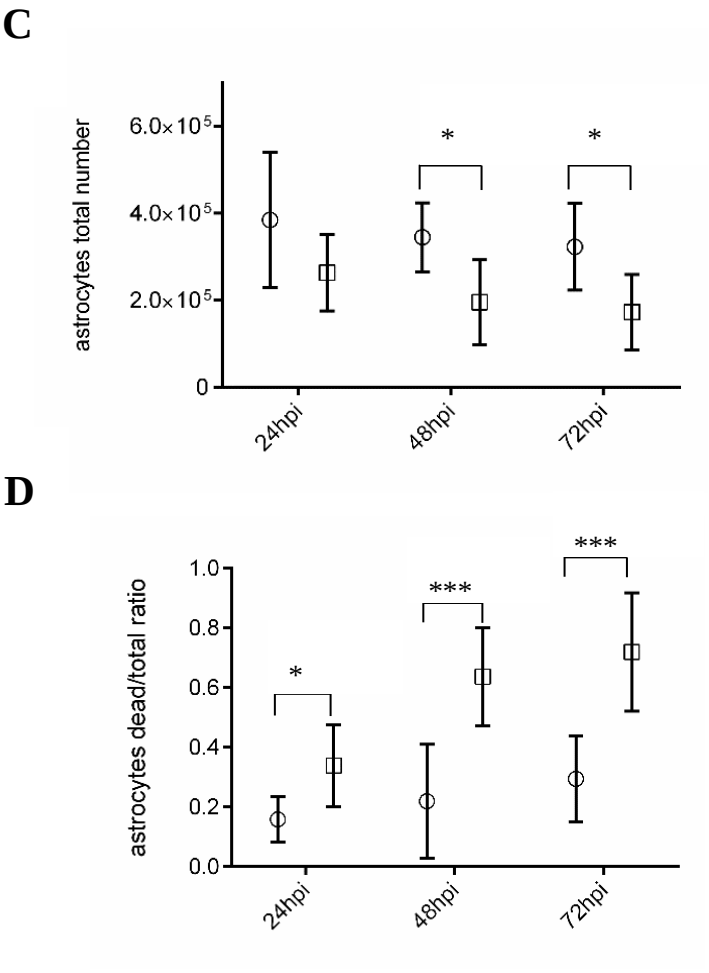

Figure 3.28. Live and dead cell number in HSV-1-infected astrocytes. HSV-1 infection was done at MOI=0.01. Cell counting by trypan blue exclusion staining of the number of live cells (**A**), the number of dead cells (**B**), the total number of cells (**C**) and the percentage of dead cells (**D**) was performed in uninfected (circles) or HSV-1-infected astrocytes (squares) at different time-points (24 h, 48 h, 72 h post-infection (pi)). Data are expressed as the mean of cell count + 95% CI. 3 independent experiments. (*) $p<0.05$; (***) $p<0.005$ (multiple t-tests).

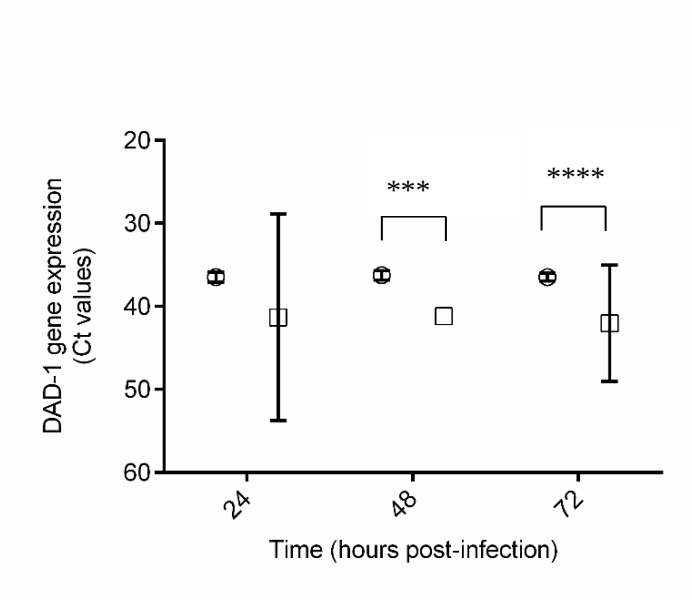

Figure 3.29. DAD-1 gene expression in HSV-1-infected astrocytes. HSV-1 infection was done at MOI=0.01. The values represent Ct values after qRT-PCR targeting DAD-1 from 1 µg of RNA extracts of uninfected (circles) or HSV-1-infected (squares) astrocytes at 24; 48 and 72 h post-infection (pi). Data are expressed as mean + 95% Confidence Interval (C.I) from one experiment. DAD-1 Ct values were in triplicate for uninfected. However, among infected samples, at every time-point, only one out of three replicates led to Ct values after qRT-PCR (missing values for the two others). Each replicate of the experiment was read twice by qPCR. (***) $p<0.005$; (****) $p<0.001$ (multiple t-tests).

3.3. Discussion

In this chapter, HSV-1 infection of three types of cells (neuroblastoma cells, microglia, primary astrocytes) have been characterised in terms of cell morphology and viability, viral replication and expression of TNF and/or INF-γ. Cell viability has been assessed by the analysis of attached cell areas on microscopy pictures by "ImageJ", cell counting using Trypan blue exclusion staining, qRT-PCR targeting the housekeeping gene DAD-1 and WST-1 assay measuring cell mitochondrial metabolism. Viral replication was measured by HSV DNA qPCR from culture medium of infected brain cells. Finally, TNF and INF-γ gene expression was assessed by qRT-PCR TNF protein levels were determined in cell culture medium by ELISA.

At the same MOI (0.01), in microscopy, it has been shown that HSV-1 was associated with both live cell loss and changes in morphology of neuroblastoma cells, microglia and primary astrocytes (fig3.2, 3.4, 3.12, 3.27). These morphologic changes resulted in a loss of their normal shape to a new phenotype of round and small cells. This may be due to the effect of HSV-1 on some plasma membrane proteins involved in cell adhesion and cell-cell junctions.

Attached cell area analysis on microscopy pictures (using "ImageJ"), cell counting by trypan blue exclusion, qRT-PCR targeting DAD-1 and WST-1 assay all confirmed quantitatively that HSV-1 was associated with a decrease in cell viability/mitochondrial activity in neuroblastoma, microglia and primary astrocytes (fig 3.3, 3.5-3.6, 3.14-3.18; 3.28-29). Crucially, with these measurement techniques, a decrease in live cells induced by HSV-1 infection was observed earlier in astrocytes (24 h pi) than in neuroblastomas (30 h-48 h pi) and microglia (48 h-72 h pi) suggesting that susceptibility to HSV-1 infection appears brain cell type-dependent. My observed decrease in mitochondrial activity (fig 3.6 and 3.18) in microglial and neuroblastoma cells following HSV-1-infection could be linked to another

study of my group. The latter showed that HSV-1 was linked to early and important selective mitochondrial damage in primary astrocytes[135].

HSV-1 was shown to be replicative (viral load increasing) in both neuroblastoma and microglial cells (fig 3.7 and fig 3.19). The two brain cell types exhibited different HSV-1 replication dynamics with a faster increase in microglia compared to neuroblastomas cells during the period 24h to 72h pi (fig 3.25). Nonetheless, viral loads at the final time point (72 h pi) were very similar. From 24 h to 72 h pi, mitochondrial metabolism, proxy marker of cell viability, was steadily reduced in infected neuroblastoma but not microglial cells (fig 3.26). This suggests that during this period (24-72 h pi), microglia cells were more permissive to HSV-1 than neuroblastoma cells, allowing viral replication with maintenance of cell activity. Furthermore, neuroblastoma cells were also impacted earlier by HSV-1 than microglia cells. At 48h pi, mitochondrial activity was already reduced in neuroblastoma cells (fig 3.6) but not in microglia (fig 3.18). Meanwhile, relative viral load was higher in infected neuroblastoma than in microglial cells (6 Ct difference) at 24h pi (fig 3.7 and 3.19). Therefore, dynamics of HSV-1 replication is different between microglial and neuroblastoma cells.

HSV DNA qPCR was performed in primary astrocytes in the context of co-culture with microglia (chapter 7). Virus load was again shown to increase in this astrocyte model.

In an *in vitro* study of Lokensgard and colleagues, it was shown HSV-1 syn 17+ was highly replicative in both neurons and astrocytes with viral titres peaking respectively at 48 h and 72 h pi as measured by 50% tissue culture infectious dose ($TCID_{50}$) assay[85]. However, HSV-1 syn 17+ was shown to replicate poorly in primary human foetal microglia with viral titres peaking only at 24 h pi. This differs to the results presented here for microglia, but could be explained by the fact they used primary human foetal microglia, a different HSV-1 strain and a different MOI.

In cerebrospinal fluid (CSF) samples from HSE, an increase in INF-γ and IL-6 levels were detected during the acute phase of illness (1st week) while an increase in TNF-α was observed during convalescence (weeks 2-6 of illness)[71]. Another study showed high CSF values of INF-γ at the time of admission and a maximum value of CSF IL-6 between 10^3-10^4 pg/ml were predictors of poor outcome[93]. Finally, in a mice *in vivo* model of HSE, valaciclovir combined with an anti-TNF was shown to be beneficial with a decrease in both brain inflammation and mortality[133]. Together, this data suggests that targeting TNF-α, INF-γ or IL-6, in combination with the standard treatment with aciclovir, may improve the outcome among HSE patients.

Numerous studies have shown microglia produce extensively pro-inflammatory cytokines such as TNF-α**,** INF-γ and IL-6 in response to HSV-1[142, 85, 106]. I assessed the gene expression of these cytokines in microglia after HSV-1 exposure. While IL-6 and IL-1B gene expression was relatively similar between HSV-1 infected and uninfected microglia (fig 3.22-3.23), significantly higher levels of TNF and INF-γ relative gene expression were observed for the infected cells at 48 h and 72 h pi (fig 3.20-21). TNF-α gene expression has been shown to be increased in murine microglia at 5 h pi and higher MOI (above MOI=1)[86]. TNF relative gene expression in HSV-1-infected neuroblastoma cells exhibited similar results, with a significant increase following infection at 30, 48 and 72 h pi (fig 3.8). In a single experiment, an increased INF-γ relative gene expression in neuroblastomas following HSV-1 infection was observed 39 h pi (data not shown).

No increase in TNF-α protein levels were not detected by ELISA analysis in culture medium of infected neuroblastomas or microglia compared to uninfected cells (fig 3.9 and 3.22). This is contradictory to another study which reports a drastic increase of TNF-α (up to 400 pg/ml) in cell culture medium of HSV-1-infected human foetal microglia compared to uninfected (24-72 h pi)[85]. This difference could be due to the use of foetal microglia, a different viral strain

and different MOIs or the fact that my HSE model represents the HSE acute phase in which viral load is high and CSF TNF protein levels low[71, 143].

My gene expression data indicates TNF transcription is increased following HSV infection. However, TNF ELISA did not detect an increase in "free" TNF in the cell culture medium. TNF protein production could still have increased inside the cells or at the cell membrane after HSV-1 challenge. As I saw an increase in TNF transcription, it was important to assess the impact of anti-TNF treatments in my HSE models. Hence, in chapter 6, the effect of the administration of a TNF inhibitor together with aciclovir in HSV-1-infected neuroblastoma and microglial cells is discussed.

The primary astrocytes I used exhibited a really low multiplication rate (2-3 weeks to become confluent after a 1/3 cell culture passage) and replication slowed further after ten passages. Subsequently, I did not have sufficient cells to do experiments such as ELISA test, qRT-PCR targeting INF-γ or WST-1 assay on them. Previous work from my research group indicates that HSV-1 was also associated with an increased TNF gene expression in primary astrocytes (unpublished data).

To summarise this chapter, I set up *in vitro* models of HSE using single culture of 3 different types of human brain cells infected by HSV-1. Interestingly, among them, I used Kelly neuroblastoma cells that had never been characterised following HSV-1 infection before this PhD. In this chapter, I showed that HSV-1 17+ was able to replicate and was associated with cell death and morphologic changes in this neuroblastoma cell model, and also in (transformed) microglia and primary astrocytes. A significant decrease in mitochondrial activity was observed in neuroblastoma and microglial cells following HSV-1-infection. Interestingly, I also showed that the expression of the pro-inflammatory genes TNF and INF-γ was increased following HSV-1 in both microglial and neuroblastoma cells. No change in

TNF protein levels in culture medium of these cells was observed. However, the ELISA tests I performed did not measure TNF production in cells.

In the next chapter (4), the effect of the antiviral drug aciclovir was assessed in these same HSV-1-infected brain cells.

Chapter 4 The effect of aciclovir on HSV-1-infection in human brain cells

4.1. Introduction

Before the advent of aciclovir as gold standard therapy used for HSE treatment, 70% of HSE (untreated) patients died while 97% of survivors did not return to normal function[49]. Aciclovir is an antiviral drug, converted by the enzyme thymidine kinase (TK) into a competitive inhibitor of DNA polymerase as a result blocking HSV genome replication. For HSE treatment, this drug is usually administrated at 10 mg/kg intravenously, every 8 h, for 2-3 weeks[49]. The administration of aciclovir in HSE patients has been shown to decrease both mortality and morbidity. In a Swedish prospective clinical study, among HSE patients treated by aciclovir, it was shown that 19% died and 56% returned to normal life 6 months after the onset of the disease[202]. In comparison, among HSE patients treated with vidarabine, another drug inhibiting HSV replication, 50% died and only 13% could return to normal life at the 6 months follow-up. Another study confirmed that aciclovir was a more efficient drug for HSE treatment than vidarabine[125]. Indeed, a reduced mortality (aciclovir:28% versus vidarabine: 54%) and an increase in the percentage of patients functioning normally at 6 months (aciclovir: 38% versus vidarabine: 14%) were observed again in HSE patients treated with aciclovir compared to the ones treated with vidarabine. Crucially, delays in aciclovir administration (beyond 48 h after hospital admission) were associated with worse prognosis[124]. Of note, a higher dose of aciclovir (15 mg/kg) was not associated with better outcome[144].

As previously discussed, in HSE patients treated with aciclovir, neurological sequelae are still very frequent. A study of long-term sequelae among HSE patients treated by aciclovir showed that 12% died within one month, 2% lived in a vegetative state, 17% experienced a severe disability, 21% a moderate disability and 48% a good recovery[53]. Among the long-term

survivors, 69% lived with memory impairment, and 20-35% experienced severe anxiety, impaired concentration, insomnia, irritability, fatigue, poor motivation, or emotional lability. This emphasizes the fact that although almost one in two patients have a good recovery, the majority of HSE patients experience long-term neurological sequelae. Interestingly, in mice affected by HSE, it was shown that aciclovir led to a reduction of the nervous system viral titres to undetectable levels. However, aciclovir had no effect on either brain inflammation or mortality[69]. Although aciclovir improves the outcome of HSE patients, this therapy exhibits important limitations. Around 10-20% of HSE patients treated with aciclovir still die and the majority exhibits long-term neurological sequelae. These limitations could be due to the fact that HSE pathogenesis seems to be due to direct viral damage and secondary damage due to the host immune responses to the virus[131, 91, 133, 93]. Aciclovir only targets HSV replication and has no direct effect on inflammation.

There is a lack of knowledge concerning the impact of aciclovir on HSV-1 infection of specific human brain cell types such as microglia or neurons/neuroblastoma cells. In this chapter, I studied the effect of aciclovir on HSV-1-infection of both microglial and neuroblastoma cells in separate sets of experiments. A standard concentration of 20 µM was used in all experiments with aciclovir treatment. This concentration was chosen following the data obtained from pharmokinetics studies on intravenous aciclovir. In a clinical study on postherpetic neuralgia treatment, after administering 10 mg/kg of aciclovir, the mean peak in plasma was 66.2 µM[145]. In a prospective study, it was shown that the average maximum plasma concentration of aciclovir was 8.2 mg/L in control (healthy) patients following intravenous administration of aciclovir at 5 mg/kg [146]. Hence, for a 10 mg/kg intravenous administration, we can suppose a plasma concentration of aciclovir around 16.2 mg/L that represents 72.8 µM. Hence, a maximum plasma concentration of aciclovir of 66.2-72.8 µM can be considered. In an article of King et al about aciclovir., it was stated that" 30% to 35% of the serum concentration of the drug is found in the brain humans"[147]. Therefore, the maximum brain aciclovir concentration

in HSE patients treated three time a day by 10 mg/kg of intravenous aciclovir should be around 19.9-25.5 µM. This is in adequacy with the concentration of 20 µM I used in my experiments.

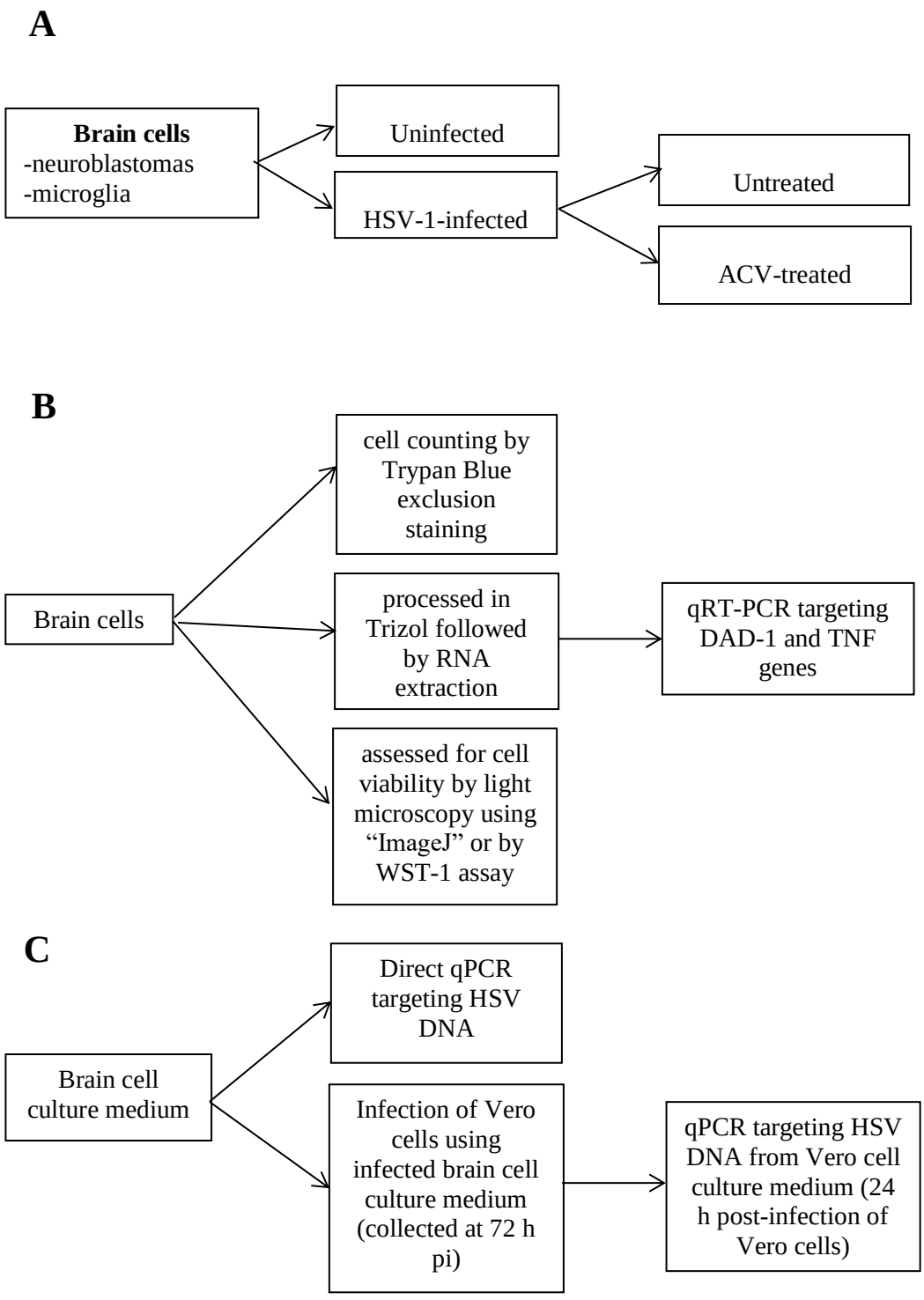

Figure 4.1. Experimental design for Chapter 4 "The effect of Aciclovir (ACV) on HSV-1-infection in human brain cells". (**A)** Brain cell populations used. **(B)** Techniques performed on brain cells following HSV-1-infection. **(C)** Techniques performed on brain cell culture medium following HSV-1-infection.

4.2. Results

4.2.1. The effect of Aciclovir on HSV-1-infection of neuroblastoma cells

4.2.1.1. Aciclovir is associated with a decrease in viral load and an increase in cell survival in HSV-1-infected neuroblastoma cells

In the previous chapter, it was shown that HSV-1 was replicative and led to morphological changes and extensive cell death in neuroblastoma cells. In this chapter, I have assessed if aciclovir, the antiviral drug, used clinically in HSE, could impact on cell viability and viral load in HSV-1-infected neuroblastoma cells. The treatment with aciclovir (20 µM) was done 24 h post-infection (pi).

Firstly, in light microscopy, an increase in cell survival could be observed in HSV-1-infected neuroblastomas treated with aciclovir compared to the infected untreated cells (fig 4.2-4.3). A lower proportion of gaps in the monolayer of infected cells treated with aciclovir was seen compared to the infected untreated cells both at 48 h and 72 h pi at 4 x-10 x magnification (fig 4.2C-E and fig 4.3C-E). No gaps were seen in uninfected neuroblastoma monolayers (fig 4.2A-B and fig 4.3A-B). By analysing 10 x magnification microscopy pictures using the software "ImageJ", a significant increase in the attached cell area could be observed in HSV-1-infected neuroblastomas following administration of aciclovir (20 µM) (fig 4.4).

The WST-1 assay measuring the mitochondrial metabolism at 48 h and 72 h pi (fig 4.6) quantitatively confirmed that aciclovir increased cell viability of HSV-1-infected neuroblastoma cells. However, no change in DAD-1 gene expression as measured by qRT-PCR in infected neuroblastoma cells was observed (fig 4.5).

Surprisingly, HSV DNA qPCR on culture medium of infected neuroblastomas showed no differences in HSV-1 load detection with or without aciclovir treatment (fig. 4.7). Next, the culture medium of infected neuroblastoma cells, untreated or treated with aciclovir, was used

to infect Vero cells. Following 24 h of Vero cell infection, a HSV DNA qPCR on Vero cell culture medium was performed (as explained by fig 4.1C). This qPCR showed a significant decrease in HSV DNA abundance (higher Ct values) in culture medium of Vero cells infected by the medium of HSV-1 infected neuroblastomas treated with aciclovir compared to the one infected by the medium of infected neuroblastomas untreated (fig 4.8). This suggests that aciclovir decreases the load of infective (active) viruses in culture medium. However, total load of HSV DNA (from active and inactive viral particles) remains the same during the *in vitro* infection of neuroblastoma cells following aciclovir administration.

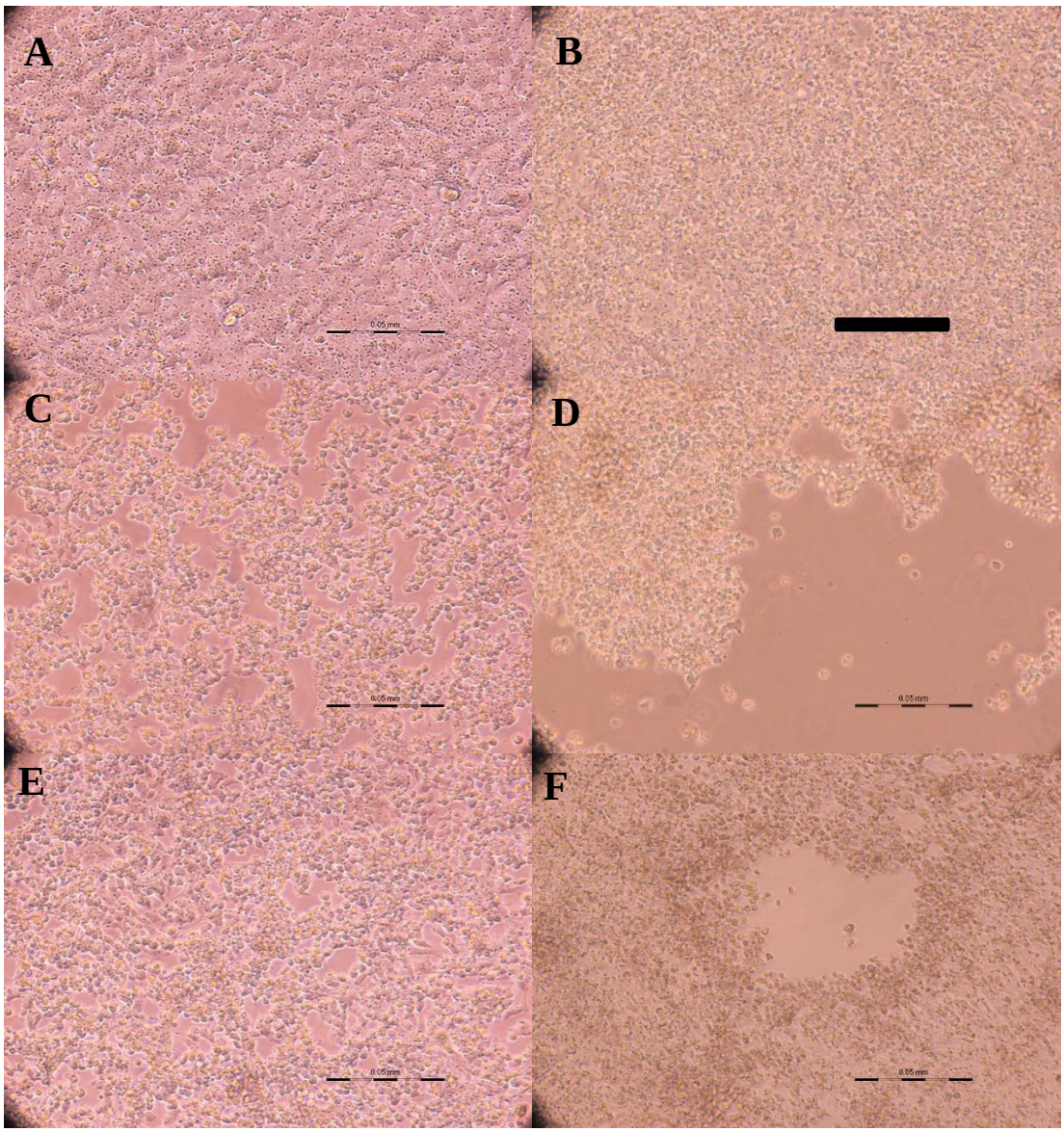

Figure 4.2. Microscopy pictures of HSV-1-infected neuroblastoma cells treated with aciclovir (10 x magnification). HSV-1 infection was performed at MOI=0.01. The treatment with aciclovir (20 µM) was done 24 h post-infection. The uninfected neuroblastoma cells are represented at 48 h (**A**) and 72 h (**B**) after infection of the HSV-1 infected counterparts. (**C**) and (**D**) show HSV-1-infected neuroblastoma cells (untreated) respectively at 48 h and 72 h pi. (**E**) and (**F**) show infected neuroblastoma cells treated with aciclovir at 48 h and 72 h pi respectively. By comparing (**C**) vs (**E**) and (**D**) vs (**F**), a lower proportion of gaps in the monolayer, signs of HSV-1-induced cell death, could be seen when infected cells are treated with aciclovir and at both time-points (**E** and **F**). These pictures are representative of at least 3 experiments. 10 x magnification. Scale bar: 50 µm.

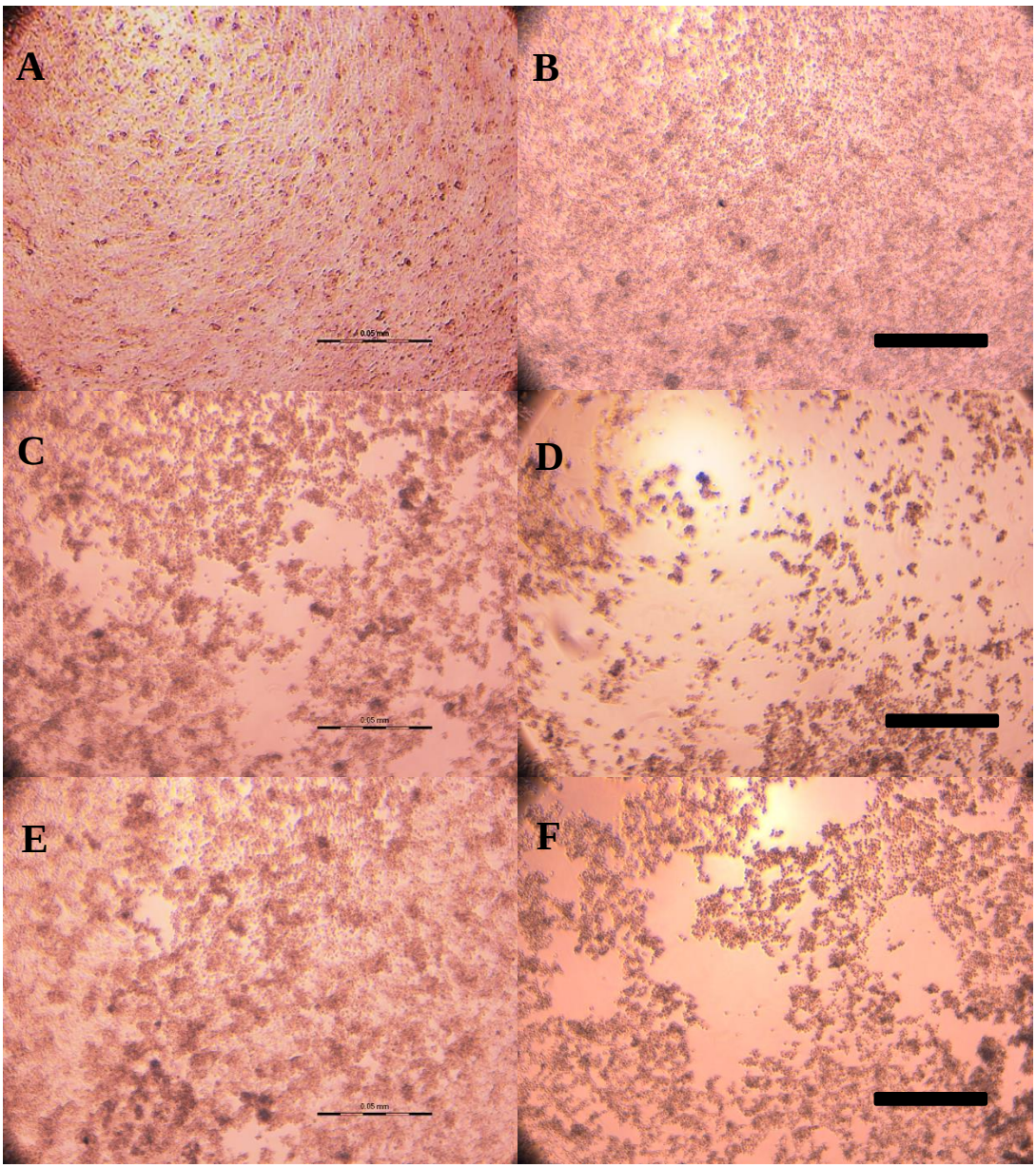

Figure 4.3. Microscopy pictures of HSV-1-infected neuroblastoma cells treated with aciclovir (4 x magnification). HSV-1 infection was performed at MOI=0.01. The treatment with aciclovir (20 µM) was done 24 h post-infection. The uninfected neuroblastoma cells are represented at 48 h (**A**) and 72 h (**B**) after infection of the HSV-1 infected counterparts. (**C**) and (**D**) show HSV-1-infected neuroblastoma cells (untreated) respectively at 48 h and 72 h pi. (**E**) and (**F**) show infected neuroblastoma cells treated with aciclovir at 48 h and 72 h pi respectively. By comparing (**C**) vs (**E**) and (**D**) vs (**F**), a lower proportion of gaps in the monolayer, signs of HSV-1-induced cell death, could be seen when infected cells are treated with aciclovir and at both time-points (**E and F**). 4 x magnification. Scale bar: 50 µm.

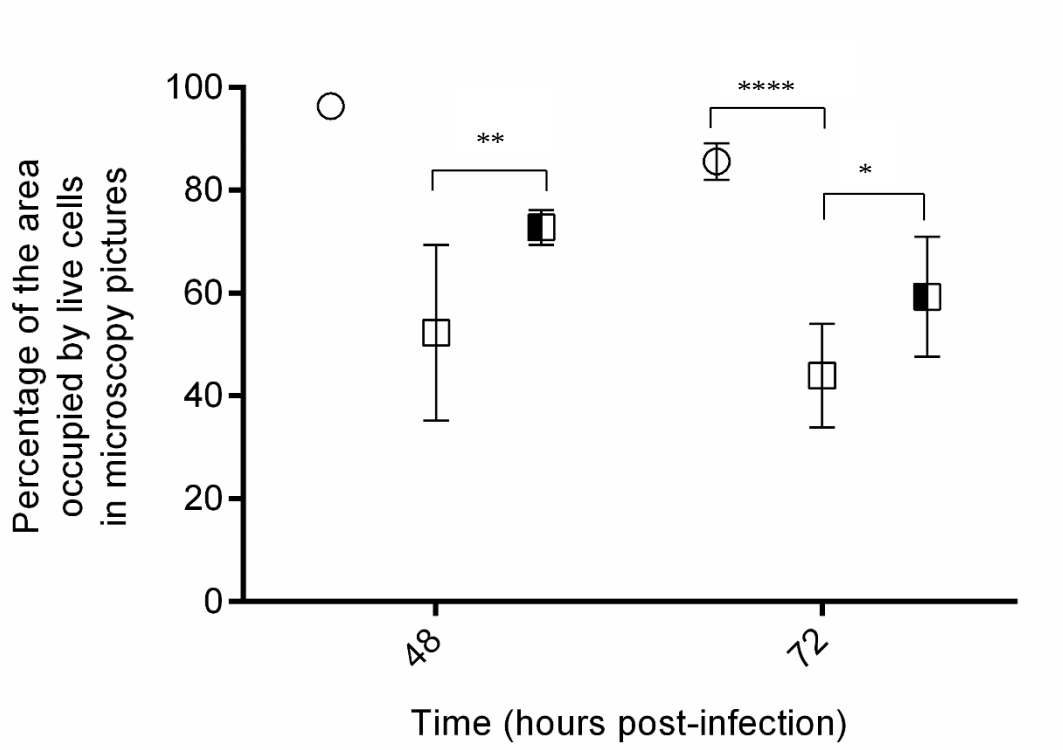

Figure 4.4. Influence of aciclovir treatment on the percentage of attached cell area in microscopy pictures of HSV-1-infected neuroblastoma cells. HSV-1-infection was done at MOI=0.01. Areas of attached neuroblastoma cells were measured by the software "ImageJ" from pictures taken at 48 h and 72 h post-infection of uninfected (circles) or infected (white squares) or aciclovir-treated infected (squares half-filled in black) neuroblastoma cells. Data are expressed as mean of the area of live cells + 95% CI and were obtained as described in the chapter 2 (Material and methods). At 48 h pi (24 h post-treatment), one picture for uninfected cells, three for infected untreated cells and three for infected cells treated with aciclovir (20 µM) were analysed. At 72 h pi (48 h post-treatment), nine pictures for uninfected cells, twenty-four for infected untreated cells and twenty-two pictures for infected cells treated with aciclovir were analysed. The pictures were representative of 3 independent experiments. ANOVA test statistically showed significant differences between the means of the different conditions at 72 h pi ($p<0.0001$). It could not be performed at 48 h pi as one group only includes one value. (*) $p<0.05$; (**) $p<0.01$; (****) $p<0.0001$ (multiple t-tests)

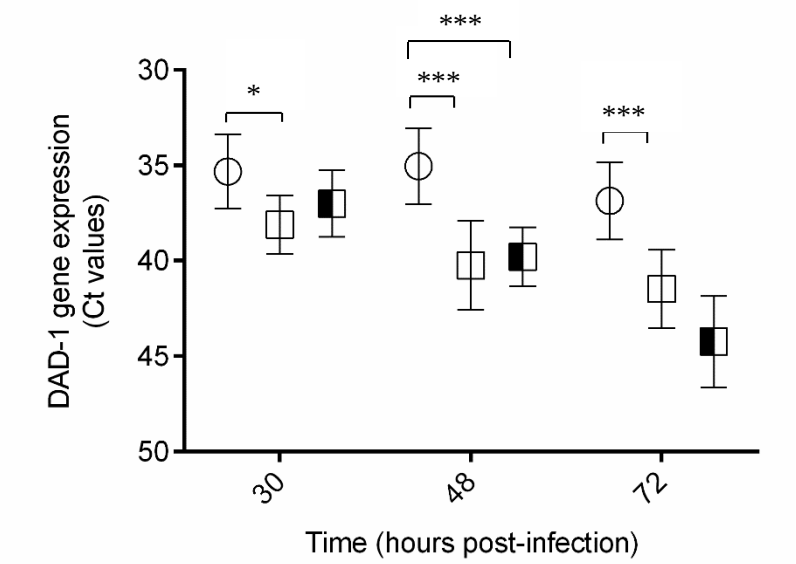

Figure 4.5. Influence of aciclovir on DAD-1 gene expression in HSV-1-infected neuroblastoma cells. HSV-1 infection was done at MOI=0.01. The treatment with aciclovir (20 µM) was done at 24 h pi. The values represent Ct values after qRT-PCR targeting DAD-1 from 1 µg of RNA extracts of uninfected (circles) or untreated infected (white squares) or aciclovir-treated infected (black half-filled squares) neuroblastoma cells at 30, 48, 72 h pi. Data are expressed as mean + 95% Confidence Interval (C.I) of 9 replicates from 3 independent experiments. ANOVA test statistically showed significant differences between the means of the different conditions at 48 h pi ($p<0.001$); 72 h pi ($p<0.0001$) but not at 30 h pi ($p>0.05$). (*) $p<0.05$; (**) $p<0.01$; (***) $p<0.005$ (multiple t-tests).

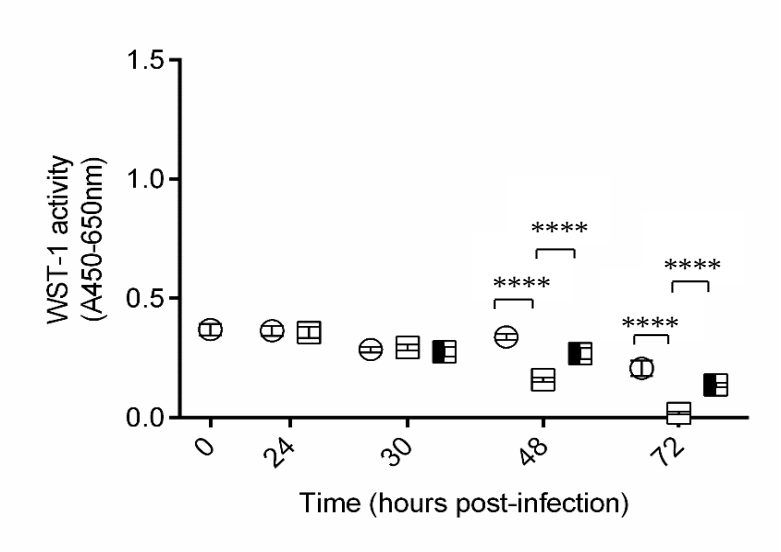

Figure 4.6. Influence of aciclovir on mitochondrial activity in HSV-1-infected neuroblastoma cells. HSV-1 infection was done at MOI=0.01. The treatment with aciclovir (20 µM) was done at 24 h pi. The values represent WST-1 activity (values of absorbance at

450 nm (A 450nm) normalised by subtraction of the background (A 650nm) after addition of WST-1). WST-1 assay has been performed in uninfected (circles), untreated infected (white squares) and aciclovir-treated infected (black half-filled squares) neuroblastomas at different time-points (0, 24, 30, 48, 72 h pi). Data are expressed as mean + 95% CI of 30 replicates from 3 independent experiments. ANOVA test statistically showed significant differences between the means of the different conditions at 48 h pi ($p<0.001$); 72 h pi ($p<0.0001$) but not at 30h pi ($p>0.05$). (****) $p<0.0001$ (multiple t-tests).

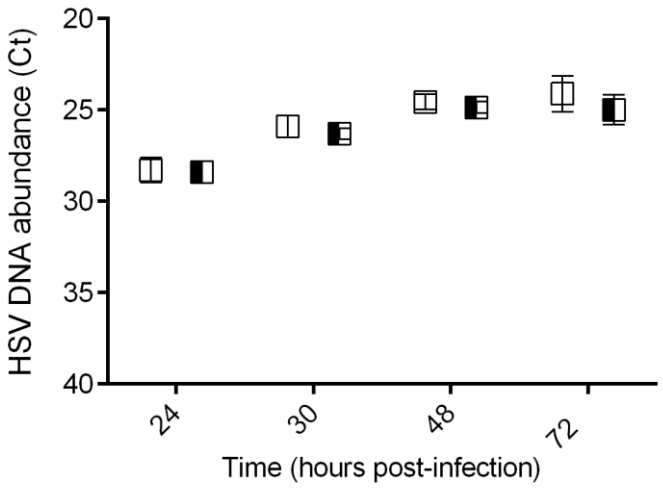

Figure 4.7. Influence of aciclovir on HSV DNA abundance in HSV-1-infected neuroblastoma cell culture medium. HSV-1 infection was done at MOI=0.01. The treatment with aciclovir (20 µM) was done at 24 h pi. The values represent Ct values after HSV DNA qPCR from culture medium HSV-1-infected (white squares) or aciclovir-treated infected (black half-filled squares) neuroblastoma cells at 24 (just before the treatment), 30, 48 and 72 h pi. Each point represents the mean + 95% CI of data from at least 3 independent experiments. Triplicates were used for each point-time in each experiment. Multiple t-tests were performed (no statistical difference ($p<0.05$) at any time-point).

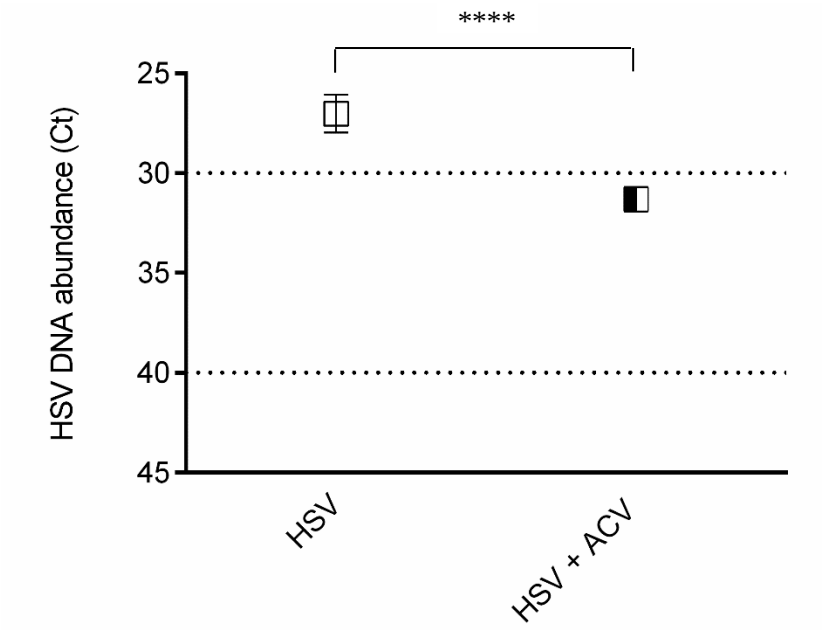

Figure 4.8. Influence of aciclovir on the viral load of active HSV-1 particles released in the culture medium of (infected) neuroblastoma cells. HSV-1 infection and treatment with aciclovir (20 µM) in neuroblastoma cells were done as described previously (i.e. figure 4.7). Then, the culture medium of infected untreated (white squares) or infected neuroblastoma cells treated with aciclovir (black half-filled squares) was taken off at 72 h pi and used to secondarily infect Vero cells. 24 h post-infection of Vero cells with neuroblastoma cell culture medium, a qPCR targeting HSV DNA was performed on Vero cell culture medium. The values represent Ct values after HSV DNA qPCR from Vero cell culture medium. Each point represents the mean + 95% CI of data from 2 independent experiments. Triplicates were used for each point-time in each experiment. (****) $p<0.0001$ (t-tests).

4.2.1.2. Aciclovir is associated with an increase in TNF relative gene expression in HSV-1-infected neuroblastoma cells

In the previous chapter, an increase in TNF relative gene expression had been observed in neuroblastoma cells following HSV-1-infection. Here, I assessed the impact of the drug aciclovir (20 µM), added at 24 h pi, on TNF relative gene expression. There was still an increase in TNF relative gene expression in HSV-1-infected neuroblastoma cells treated with aciclovir compared to the uninfected counterparts since all values of infected cells treated with aciclovir were still significantly superior to 1 (at least 30-40 times higher than uninfected for all time-points) (fig 4.9). Furthermore, the increase in TNF relative gene expression was significantly more elevated in HSV-1-infected-neuroblastoma cells treated with aciclovir compared to the infected untreated at 72 h pi.

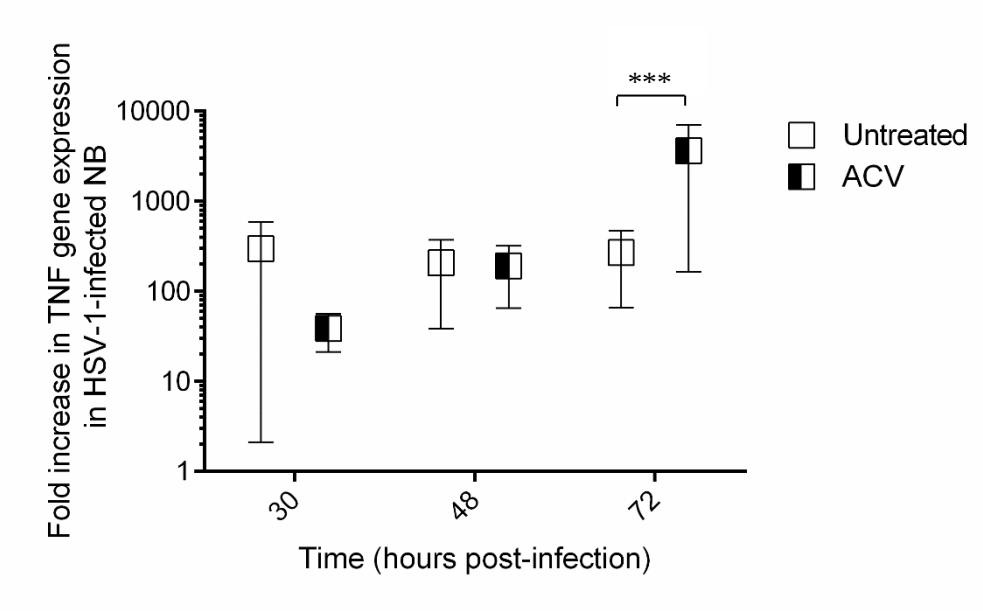

Figure 4.9. Influence of aciclovir on TNF relative gene expression in HSV-1-infected neuroblastoma cells. HSV-1 infection was done at MOI=0.01 in neuroblastoma cells. Aciclovir treatment (20 µM) was added at 24h pi. The data represent TNF relative gene expression expressed as mean +/- 95% CI of $2^{-\Delta\Delta Ct}$ values at 30 h, 48 h and 72 h post-infection (respectively 6h, 24h and 48h post-treatment). The scale is logarithmic. $2^{-\Delta\Delta Ct}$ values were obtained following qRT-PCR of TNF and DAD-1 genes. DAD-1 gene was used as reference (housekeeping) gene. From qRT-PCR Ct values of DAD-1 and TNF, ΔCt values [Ct (TNF)-Ct(DAD-1]) were obtained for both uninfected and HSV-1-infected cells. ΔΔCt values represented $[(\Delta Ct)_{HSV} - (\Delta Ct)_{uninfected}]$. Data were obtained from 3 independent experiments.(***): p<0,001 (multiple t-tests).

4.2.2. The effect of aciclovir on HSV-1-infection of microglial cells

4.2.2.1. Aciclovir is associated with an increase in cell survival and a decrease in viral replication in HSV-1-infected microglial cells

In the previous chapter, it was shown that HSV-1 was replicative and led to both morphologic changes and a decrease in cell viability in microglial cells. In this present chapter, I assessed if the antiviral drug aciclovir could influence both cell viability and viral load in HSV-1-infected microglial cells. Treatment with aciclovir (20 µM) in infected microglia was done at 24 h post-infection (h pi). An increase in microglial cell survival following HSV-1 infection was noticed, by visualisation using light microscopy, for infected cells treated with aciclovir compared to the infected untreated (fig 4.10). Indeed, infected microglial cells treated with aciclovir presented a lower proportion of gaps in the monolayer compared to the infected untreated cells both at 48 h and 72 h pi (fig 4.10 C-F). No signs of infection, such as gaps in the monolayer of cells, were seen for uninfected microglia cells (fig 4.10 A-B). By analysing 10 x magnification microscopy pictures using the software "ImageJ", an increase in the attached cell area could also be observed in HSV-1-infected microglial cells following administration of aciclovir (20 µM) (fig 4.11). Finally, both qRT-PCR targeting DAD-1 at 48 h and 72 h pi (fig 4.12) and WST-1 assay measuring the mitochondrial metabolism at 72 h pi (fig 4.13) quantitatively confirmed that aciclovir increased microglia cell mitochondrial activity during HSV infection.

At 48 h and 72 h pi, viral genome detection was significantly lower in culture medium of infected cells treated with aciclovir than in culture medium of infected untreated microglia cells (fig 4.14). This shows aciclovir inhibits HSV-1 replication in microglial cells

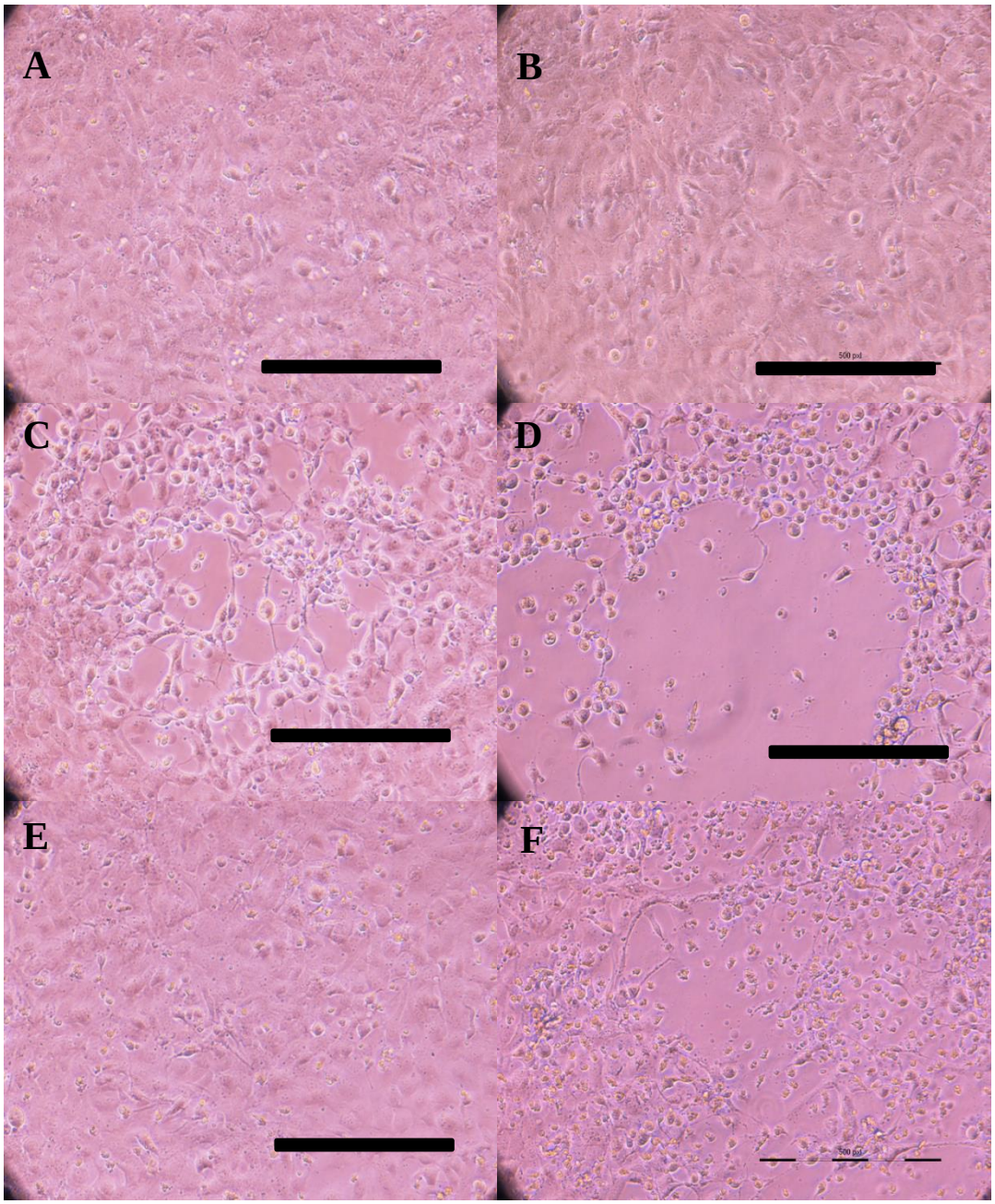

Figure 4.10. Microscopy pictures of HSV-1-infected microglial cells treated with aciclovir. HSV-1 infection was done at MOI=0.01. Treatment with aciclovir (20 µM) was done 24 h post-infection. The uninfected microglia cells are represented at 48 h (**A**) and 72 h (**B**) after infection of the HSV-1 infected counterparts. (**C**) and (**D**) show HSV-1-infected microglial cells (untreated) respectively at 48 h and 72 h pi. (**E**) and (**F**) show infected microglial treated with aciclovir at 48 h and 72 h pi respectively. By comparing (**C**) vs (**E**) and (**D**) vs (**F**), a lower proportion of gaps in the monolayer, signs of HSV-1-induced cell death, could be seen when infected cells are treated with aciclovir and at both time-points (**E and F**). These pictures are representative of 3 experiments. 10 x magnification. Scale bar: 50 µm.

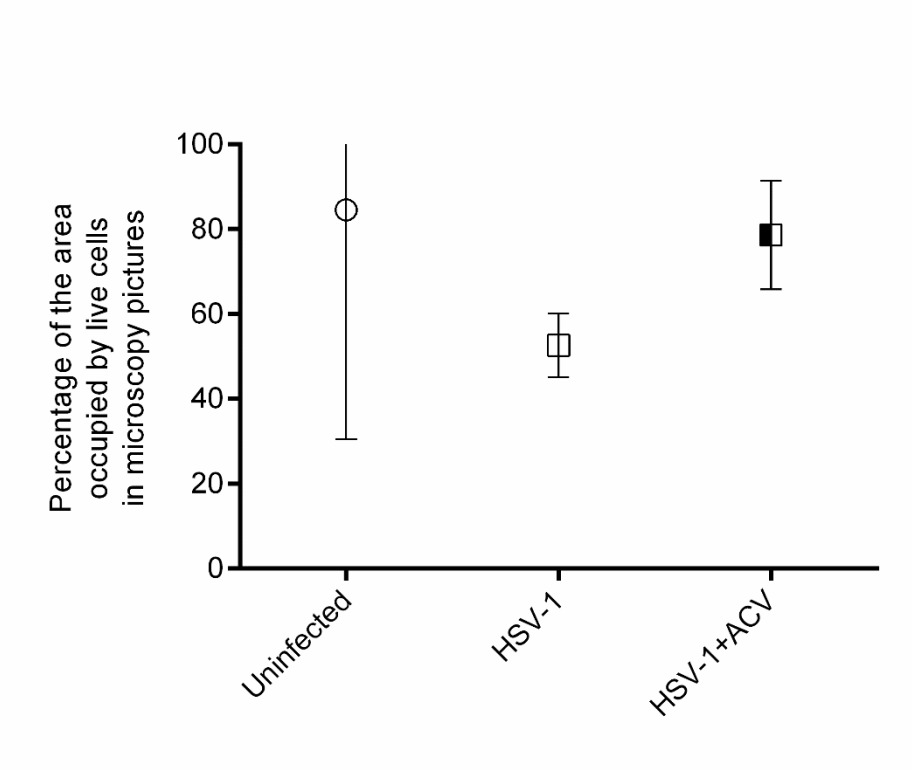

Figure 4.11. Influence of aciclovir on the percentage of attached cell area in microscopy pictures of HSV-1-infected microglial cells. HSV-1-infection was done at MOI=0.01. The treatment with aciclovir (20 µM) was done 24 h pi. Areas of live cells were measured by the software "ImageJ" from pictures taken at 72 h post-infection. HSV-1: HSV-1-infected microglial cells; HSV-1+ACV: HSV-1-infected microglial cells treated with aciclovir (20 µM). Two 4 x magnification microscope pictures for uninfected, four for HSV-1-infected and two for HSV-1-infected cells treated with aciclovir were analysed. Statistical analysis were not relevant due to a really low number of replicates.

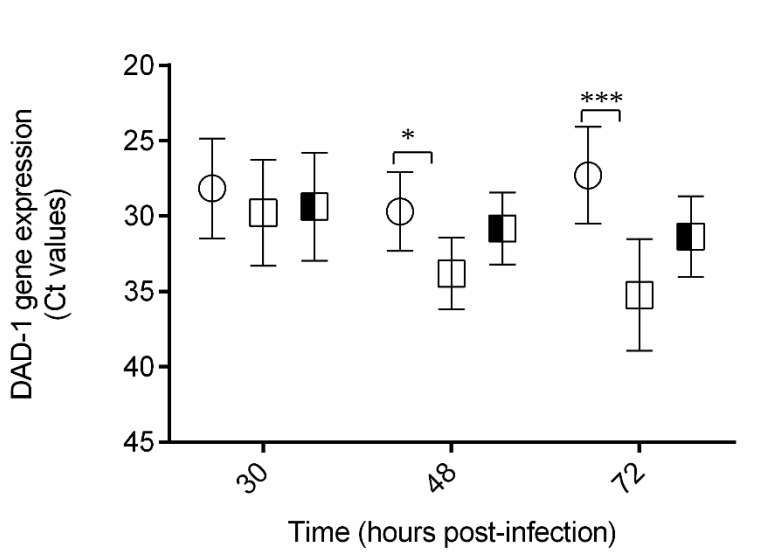

Figure 4.12. Influence of aciclovir on DAD-1 gene expression in HSV-1-infected microglial cells. HSV-1 infection was done at MOI=0.01. The treatment with aciclovir (20 μM) was done at 24 h pi. The values represent Ct values after qRT-PCR targeting DAD-1 from 1 μg of RNA extracts of uninfected (circles) or untreated infected (white squares) or aciclovir-treated infected (black half-filled squares) microglial cells at 30, 48, 72 h pi. Data are expressed as mean + 95% Confidence Interval (C.I) of 9 replicates from 3 independent experiments. ANOVA test statistically showed significant differences between the means of the different conditions at 72 h pi ($p<0.005$) but not at 30 h pi ($p>0.05$) or at 48h pi ($p>0.05$). (*) $p<0.05$; (***) $p<0.005$ (multiple t-tests).

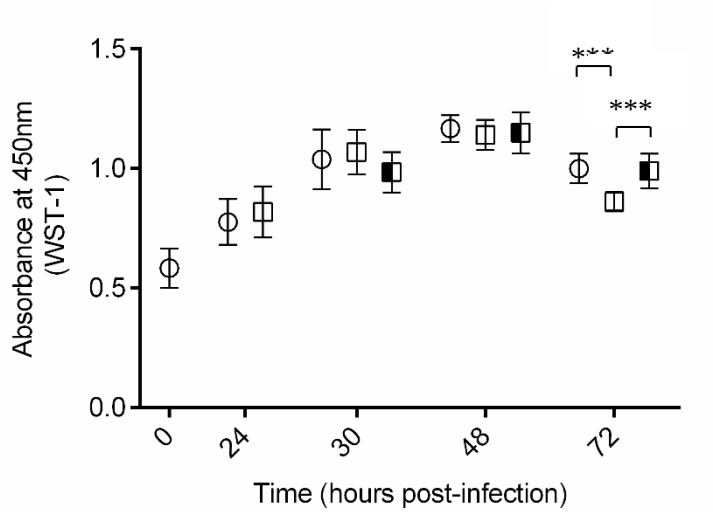

Figure 4.13. Influence of aciclovir on mitochondrial activity in HSV-1-infected microglia. HSV-1 infection was done at MOI=0.01. Treatment with aciclovir (20 μM) was done at 24 h pi. The values represent values of WST-1 activity (absorbance at 450 nm (A450 nm) normalised by subtraction of the background (A650 nm) after WST-1 addition). WST-1 assay was performed in uninfected (circles), untreated infected (white squares) and aciclovir-treated infected (black half-filled squares) microglia at different time-points (0, 24, 30, 48, 72 h pi).

Data are expressed as mean + 95% CI of 30 replicates from 3 independent experiments. ANOVA test statistically showed significant differences between the means of the different conditions at 72 h pi ($p<0.005$) but not at 30 h pi or at 48h pi. (***) $p<0.005$ (multiple t-tests).

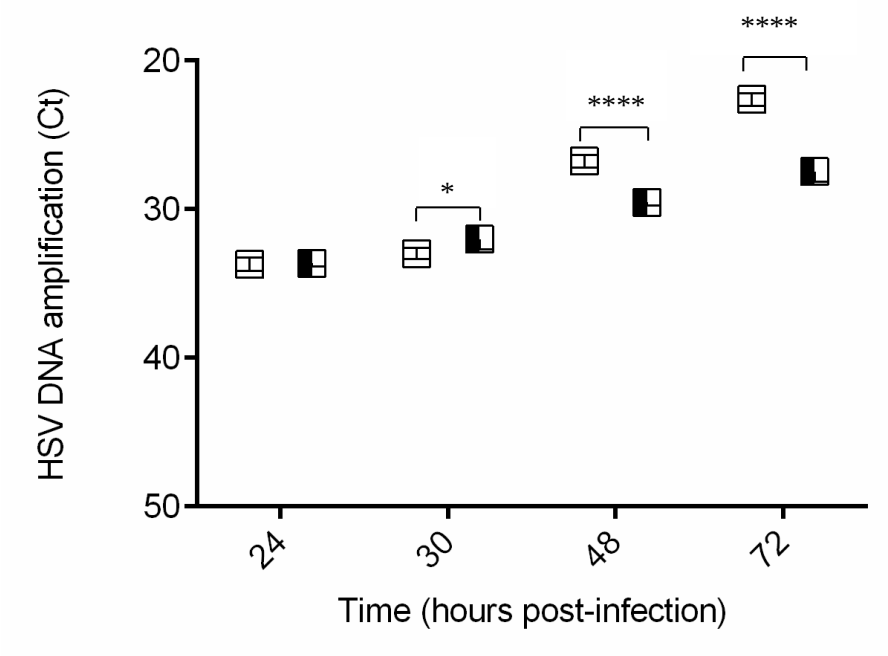

Figure 4.14. Influence of aciclovir on HSV DNA abundance in HSV-1-infected microglia culture medium. HSV-1 infection was done at MOI=0.01. Treatment with aciclovir (20 μM) was done at 24 h pi. The values represent Ct values after HSV DNA qPCR from culture medium of HSV-1-infected (white squares) or aciclovir-treated infected (black half-filled squares) microglia at 24 h (just before treatment), 30 h, 48 h and 72 h pi.. Each point represents the mean + 95% CI of data from at least 3 independent experiments. Triplicates were used for each point-time in each experiment. (*) $p<0.05$; (****) $p<0.0001$ (multiple t-tests).

4.2.2.2. Aciclovir is associated with a decrease in TNF relative gene expression following HSV-1 infection of microglial cells

In the previous chapter, HSV-1 was shown to induce an increase in TNF relative gene expression in microglial cells**.** Here, I assessed the effect of the drug aciclovir (20 µM), added at 24 h pi, on TNF relative gene expression in HSV-1-infected microglial cells. Interestingly, HSV-1 was still associated with a large increase in TNF relative gene expression in microglia at 48h and 72h pi in spite of the presence of aciclovir as observed with values much higher than one (fig 4.15). However, this increase was markedly lower in infected microglia cells treated with aciclovir compared to HSV-1-infected cells untreated, at 72 h pi (fig 4.15).

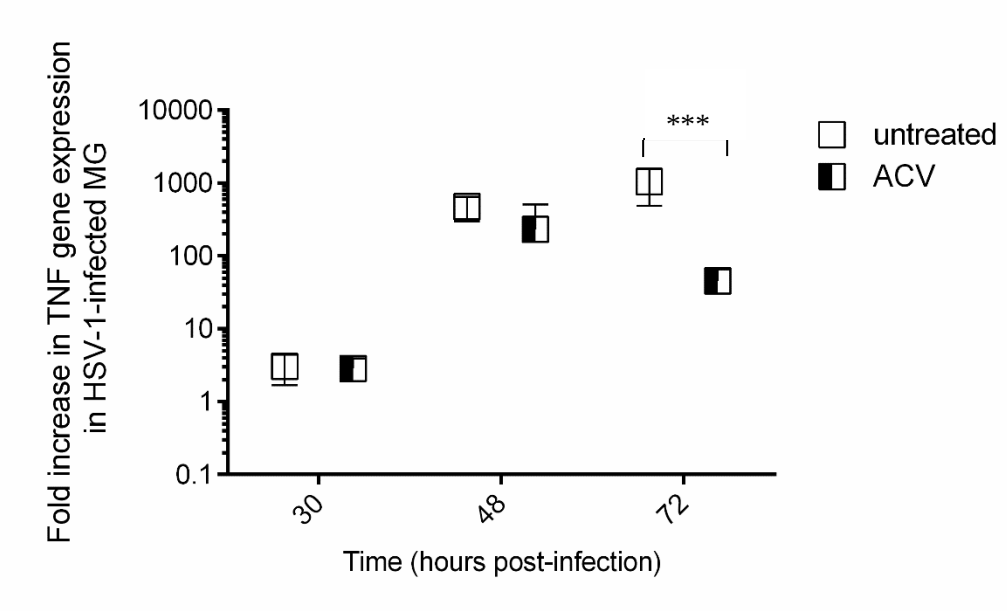

Figure 4.15. Influence of aciclovir on TNF relative gene expression in HSV-1-infected microglial cells. HSV-1 infection was done at MOI=0.01 in microglial cells. Aciclovir treatment (20 µM) was added at 24h pi. The data represent TNF relative gene expression expressed as mean +/- 95% CI of $2^{-\Delta\Delta Ct}$ values at 30 h, 48 h and 72 h post-infection (respectively 6 h, 24 h and 48 h post-treatment). The scale is logarithmic. $2^{-\Delta\Delta Ct}$ values were obtained following qRT-PCR of TNF and DAD-1 genes. DAD-1 gene was used as reference (housekeeping) gene. From qRT-PCR Ct values of DAD-1 and TNF, ΔCt values [Ct (TNF)-Ct(DAD-1]) were obtained for both uninfected and HSV-1-infected cells. ΔΔCt values represented $[(\Delta Ct)_{HSV} - (\Delta Ct)_{uninfected}]$. Data were obtained from 3 independent experiments.(***): p<0,001 (multiple t-tests).

4.3. Discussion

Aciclovir is the gold standard therapy used for HSE treatment, acting to inhibit HSV replication. It has significantly improved patient outcome and survival since it began to be clinically used for HSE in the 1980's [34, 107]. It has also been shown to be much more efficient than other antiviral drugs such as vidarabin[125, 202]. However, aciclovir is not an optimal therapy as 10-20% of patients treated with aciclovir die, and the majority of survivors experience long-term neurological sequelae[53, 34, 110].

Although the beneficial effect of aciclovir has been shown in HSE patients, less is known about the effect of aciclovir on specific human brain cell types, such as microglial cells or neurons, infected with HSV. In this chapter, I studied the effect of aciclovir on HSV-1-infected microglial cells and neuron-like cells (neuroblastomas). Cell survival, viral load in cell culture medium and TNF gene expression were assessed.

In HSV-1-infected neuroblastomas, aciclovir was associated with an increase in cell survival/mitochondrial metabolism as seen by (i) light microscopy and the analysis of attached cell area by the software "ImageJ" (fig 4.2-4.-4) and (ii) the WST-1 assay (fig 4.6) from 48 h to 72 h pi. Of note, aciclovir increased cell viability/mitochondrial metabolism following HSV-1-infection of neuroblastomas but not up to the levels of the uninfected cells. There were no differences in Ct values following qRT-PCR targeting DAD-1 between infected untreated and infected aciclovir-treated neuroblastomas (fig 4.5). This is not surprising as in qPCR a difference of only one cycle threshold, in the same conditions, means a two-fold change between them. As a result, slight differences in cell viability (below 2-fold change, for example, an increase or decrease in 10-80%) are not likely to be seen by comparing Ct values issued from qRT-PCR targeting DAD-1. Direct qPCR from culture medium of infected neuroblastoma cells did not show any differences in viral load between cells treated with aciclovir or untreated (fig 4.7). qPCR only detects HSV DNA, some of which may be partially

degraded, in some (damaged) viral particles, although detected by qPCR. Hence, it does not perfectly assess the ability of HSV-1 particles to be infective. The culture medium of infected neuroblastoma cells treated with aciclovir or untreated was then used to infect Vero cells. A second HSV DNA qPCR showed a decrease in viral load in culture medium of Vero cells infected by the culture medium of HSV-1 infected neuroblastoma cells treated with aciclovir compared to the ones infected by the culture medium of infected neuroblastoma cells untreated (fig 4.8). Hence, aciclovir was associated with a reduction of active HSV-1 viral load in infected neuroblastoma cells.

In HSV-1-infected microglia, aciclovir was also associated with an increase in cell survival/mitochondrial metabolism as seen by light microscopy followed by the analysis of attached cell areas by "ImageJ" (fig 4.10-11), WST-1 assay (fig 4.13) and qRT-PCR targeting DAD-1 (fig 4.12) at 48-72 h pi. Aciclovir was also associated with increased cell viability following HSV-1-infection of microglial cells. Unlike for neuroblastoma cells, direct HSV DNA qPCR from culture medium of infected microglia showed a significant decrease in HSV DNA abundance at 48 h and 72 h pi in cells treated with aciclovir (compared to untreated infected) (fig 4.14). Hence, aciclovir is responsible for HSV-1 load decrease in microglia.

Altogether, aciclovir has been shown to decrease viral load and increase cell survival in both HSV-1-infected neuroblastoma and microglial cells. This is in agreement with the fact that aciclovir is the antiviral therapy used for HSE treatment[125, 124, 202].

Interestingly, TNF relative gene expression was still increased in HSV-1-infected microglial and neuroblastoma cells compared to their uninfected counterparts (fig 4.9 and fig 4.15). However, the comparison of TNF relative gene expression between infected cells untreated and infected cells treated with aciclovir revealed differences between brain cell types. In neuroblastoma cells, aciclovir was associated with a significant increase in TNF relative gene expression in infected cells at 72h pi whereas in infected microglial cells, a decrease following

aciclovir treatment was observed at this same time-point. Aciclovir was associated with an increase in cell viability of both HSV-1-infected neuroblastoma and microglial cells. However, this was not associated with the same effect on TNF relative gene expression among these infected cells. This suggests TNF relative gene expression is not strongly associated with HSV-1-infected brain cell viability.

Of note, some of the techniques used appeared to have some limitations such as the qRT-PCR targeting DAD-1 as a proxy marker of cell viability and the direct HSV DNA qPCR on culture medium of infected brain cells to measure the impact of a drug on HSV replication. The qRT-PCR targeting DAD-1 was sensitive enough to detect differences in cell viability between uninfected and infected brain cells (chapter 3). However, for smaller differences requiring a higher sensitivity, like between two groups of infected cells (one treated with aciclovir, one untreated), it seems to be less precise. Thus, the qRT-PCR targeting DAD-1 was not sensitive enough to detect differences in cell viability between the untreated and aciclovir-treated HSV-1-infected neuroblastomas. Nevertheless WST-1 assay measuring mitochondrial activity, used by other researchers as a very accurate technic for cell viability[149] quantification was able to detect a difference also seen by attached cell area determination on microscopy pictures using the software "ImageJ". In the next chapters, WST-1 will be used as our selected method for cell viability measurement. Assessing HSV-1 load by direct HSV DNA qPCR from culture medium of brain cells showed significant differences between infected and uninfected cells (negative control) in the previous chapter. Nonetheless, comparing two groups of infected brain cells (one treated with aciclovir, one untreated) by the same technique was also less useful. Indeed, no differences were seen in this first direct qPCR on neuroblastoma cell culture medium between the untreated and the aciclovir-treated infected groups. But a second HSV DNA qPCR from Vero cell culture medium after infection of Vero cells using culture medium of infected neuroblastomas untreated or treated with aciclovir showed that aciclovir was also associated with a reduction of viral load of active HSV-1-particles in in neuroblastoma cells.

In the next chapters, this second infection in Vero cells followed by the secondary HSV DNA qPCR will also be performed when the first direct qPCR on culture medium of infected brain cells did not show significant differences between the different “infected” groups.

As discussed previously, aciclovir is a suboptimal treatment for HSE only targeting HSV replication. There is a growing body of evidence demonstrating HSE is the result of both HSV infection and detrimental immune responses[69, 71, 94, 93]. In this chapter, using a single dose of aciclovir, at 20 µM, markedly increased cell viability, but not as the same levels as seen in uninfected cells. Using anti-inflammatory drugs as adjunctive therapies to aciclovir for treatment of HSV-1-infected neuroblastomas and microglial cells may help to increase cell viability further. In the next chapter (chapter 5), I examined the effect of aciclovir combined with the anti-inflammatory drug dexamethasone on HSV-1-infected microglial and neuroblastoma cells.

Chapter 5 The effect of Dexamethasone on HSV-1 infection in human brain cells

5.1. Introduction

Dexamethasone and other glucocorticoids are drugs clinically used to treat a wide range of inflammatory conditions such as allergies, rheumatoid arthritis, ulcerative colitis and several skin diseases including psoriasis. Among CNS infections, glucocorticoids have been widely assessed in addition to antimicrobial therapy (cefotaxime) for treatment of patients with bacterial meningitis. Interestingly, adding dexamethasone early (first administration before or within the first hour following antimicrobial therapy administration; 10 mg every 6 h; at least 4 days) in addition to antibiotics has been associated with favourable outcome in an elderly population of patients suffering from acute bacterial meningitis and presenting high levels of immunosuppressive co-morbidity (including alcoholism, malignancy, diabetes mellitus, asplenia, HIV infection (positive status:1%))[150]. In an European clinical trial, a similar administration of early dexamethasone in adults with bacterial meningitis also led to more favourable outcome (higher Glasgow Coma Score) and a reduction in mortality at discharge but not one month or one year later (HIV status unknown)[151]. During the 1990's, administration of dexamethasone, 15 to 20 minutes prior to antimicrobial therapy in children with bacterial meningitis, quickly induced an improvement of cerebral perfusion pressure, a reduction in meningeal inflammation, and an overall better clinical condition and prognostic score (HIV status unknown)[152]. During the follow-up of this trial in Costa-Rica, a decrease in neurologic and audiologic sequelae in the population of children co-treated with dexamethasone was observed. However, a meta-analysis of individual data from five clinical trials stated that early administration of adjunctive dexamethasone in bacterial meningitis did not lead to a decrease in mortality or neurological disability but just to a slight reduction in hearing loss among survivors[153]. Of note, in this meta-analysis, the HIV positive status was

just above 40% among patients enrolled in both "steroid" and "placebo" groups. A randomised clinical trial on dexamethasone as adjunctive treatment in childhood bacterial meningitis in Malawi, showed that the administration of this steroid influenced neither mortality nor sequelae at final outcome[154]. In the latter study, HIV status was positive for 24% of patients in the "steroid" group and for 29% in the "placebo" group, and around 23-24% of patients in both groups were not HIV-tested. Finally, a systematic review of twenty-five clinical studies focusing on the impact of corticosteroids for acute bacterial meningitis concluded overall that corticosteroids significantly reduced hearing loss and neurological sequelae in high-income countries but not mortality rate in both low and high-income countries[155]. Nonetheless, corticosteroids seemed to induce a reduced mortality in patients affected by meningitis specifically caused by *Steptococcus pneumoniae* (but not by *Haemophilus influenza* or *Neisseria meningitis*). Hence, despite a large amount of clinical data, the beneficial impact of adjunctive steroids (mainly dexamethasone) in bacterial meningitis is still uncertain and remains an area for discussion. Nevertheless, these clinical studies revealed that (i) steroids never worsened the clinical state of patients, (ii) the beneficial impact could be dependent on the causative microbial agent and (iii) the positive effects of steroids in bacterial meningitis seem to be optimal during early administration (just before or until 1 h after antimicrobial therapy) in both adults and children. Furthermore, HIV status could affect the beneficial impact of adjunctive dexamethasone or corticosteroids on bacterial meningitis, thus HIV negative patients seem to benefit more from this treatment. *In vitro*, in a brain cell co-culture consisting of both astrocytes and microglia, lipopolysaccharide (LPS) challenge has been shown to induce an increase in microglia activation and a loss of astrocyte properties[156]. Crucially, in this experimental bacterial meningitis model, dexamethasone induced both a decrease in microglial activation and a restoration of astrocyte properties.

Herpes Simplex Encephalitis (HSE) pathogenesis is the result of both HSV infection and detrimental immune response as previously discussed[71, 94, 93, 131, 91, 133]. However, the gold

standard therapy to treat HSE is the intravenous administration of aciclovir targeting only viral replication[124]. Therefore, the use of anti-inflammatory drugs such as dexamethasone or other glucocorticoids as an adjuvant therapy to aciclovir in HSE could be a relevant approach to decrease both the detrimental immune response and overcome the current limitations of the antiviral therapy[157]. Nevertheless, only a few studies have assessed the effect of dexamethasone or other glucocorticoids to treat HSE.

In an *in vivo* model of HSE, it was shown that aciclovir combined to another glucorticoid drug, methylprednisolone, compared to the administration of aciclovir alone, reduced long-term Magnetic Resonance Imaging (MRI) abnormalities in the brains of mice[131].

In HSE patients, the administration of dexamethasone has been assessed combined with aciclovir in only a few small clinical studies. In one retrospective clinical study, a multiple logistic regression analysis revealed that the administration of glucocorticoids (initiation, dose and duration of treatment at the discretion of each clinician), used as adjuvant therapy to aciclovir, was one predictor of good outcome in HSE patients[158]. Another study on several HSE patients treated with aciclovir suggested that treatment with dexamethasone could induce a decrease in temporal lobe and total oedema volumes[132]. In a small retrospective study on children affected by HSE and all treated by aciclovir, the supplementary administration of glucocorticoids (prednisone or methylprednisolone; 2 mg/kg/day per oral; 2 weeks) started at the same time as acyclovir also led to better cognition, motor function and seizure control[129]. Finally, a case report also described the positive impact of short high-dose intravenous steroid therapy (1g of methylprednisolone per m^2 for 3 days) for a 16-month-old girl presenting HSE with clinical and radiologic deterioration despite aciclovir treatment[128].

Altogether, several small clinical and animal studies have shown a beneficial impact of the administration of glucocorticoids as adjuvant therapy to HSE[158, 132, 128, 129, 131]. However, despite these promising results, there is still a lack of clinical data to confirm glucocorticoids are

beneficient adjuvant therapies to aciclovir for HSE treatment. Unfortunately, one clinical trial which started in Germany in 2008, assessing the effect of dexamethasone as adjuvant therapy in HSE, stopped prematurately[159]. The trial seems to have ended because of poor recruitment, possibly due to clinical concerns of dexamethasone promoting HSV replication. A similar clinical trial, is currently led in the United-Kingdom (DexEnceph) and France (clinical trial references: ISRCTN11774734 and NCT03084783). The effect of Dexamethasone combined to aciclovir has been poorly assessed in *in vitro* models of HSE using HSV-1-infected human brain cells. To my knowledge, only one *in vitro* study assessed the impact of dexamethasone following HSV-1-infection in brain cells, using murine BV2 microglial cells[137]. This work showed that dexamethasone induced a reduction in protein secretion of the pro-inflammatory cytokines TNF-α and NO in these infected murine microglia cells, but the authors did not study the effect of this drug on viral replication, cell viability or cytokine gene expression level. In this chapter 5, I assessed the effect of dexamethasone in a human microglial cell line and Kelly neuroblastomas following HSV-1-infection at the level of cell viability, HSV-1 replication and TNF gene expression. The main aim was to see if the positive impact of dexamethasone as adjuvant therapy for HSE treatment seen in the few *in vivo* and small clinical studies, potentially partially due to oedema reduction, could also been observed in individual human brain cell lines infected by HSV-1.

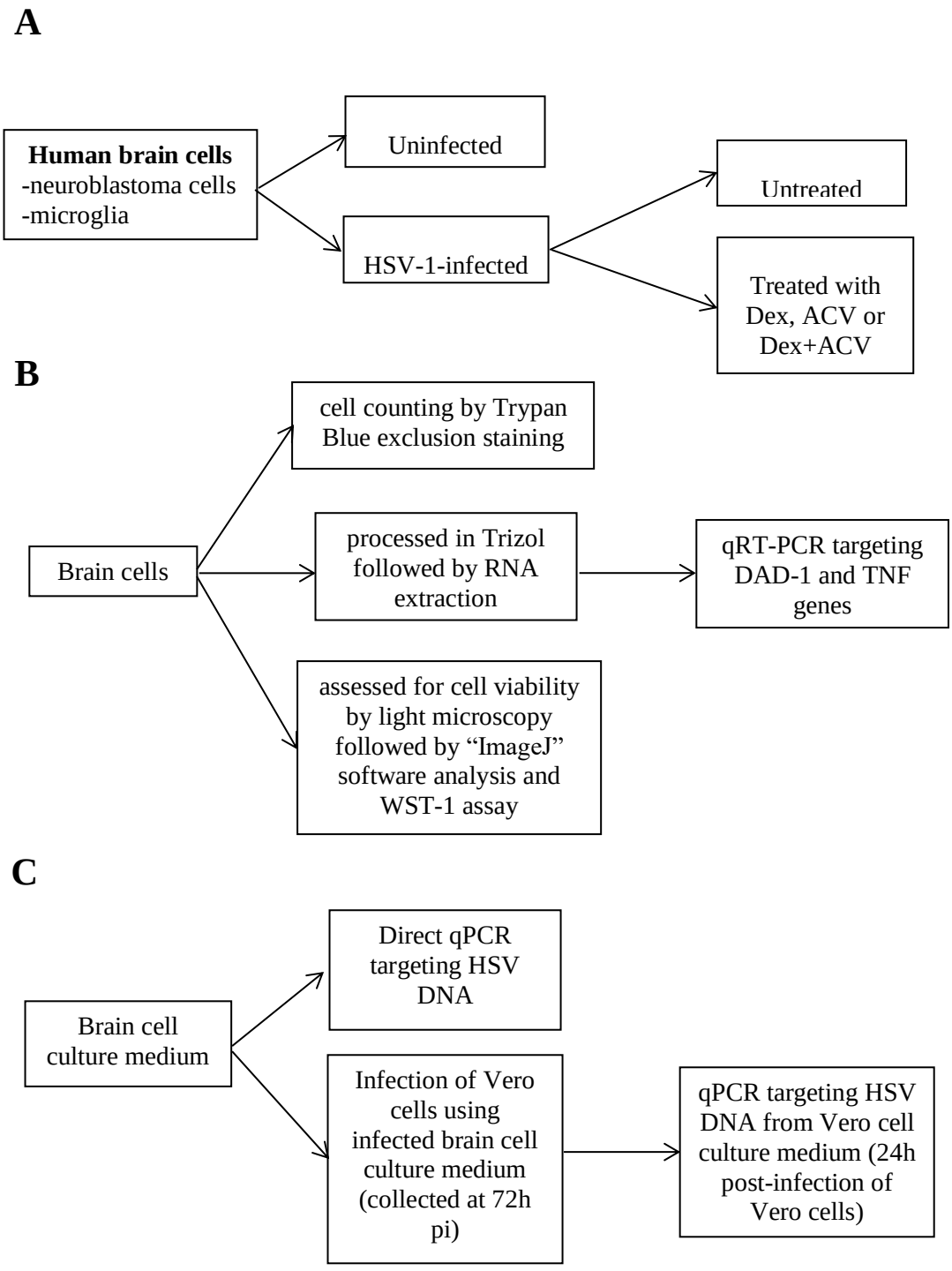

Figure 5.1. Experimental design for assessing the effect of sub-toxic doses of dexamethasone (dex) on HSV-1-infection in human brain cells. (**A)** Brain cell populations used. **(B)** Techniques performed on brain cells following HSV-1-infection. **(C)** Techniques performed on brain cell culture medium following HSV-1-infection.

5.2. Results

5.2.1. Toxic doses of dexamethasone in brain cells

5.2.1.1. Toxic doses of dexamethasone in neuroblastoma cells

Firstly, dexamethasone was shown to be toxic for (uninfected) neuroblastoma cells 24 h post-treatment at 500 µM (0.5 mM) as shown by a significant decrease in live cell counting by Trypan blue exclusion staining (fig 5.2). High dexamethasone concentrations (100-500 µM) were also associated with a decrease in live cell number in HSV-1-infected-neuroblastoma cells although not statistically significant ($p>0.05$).

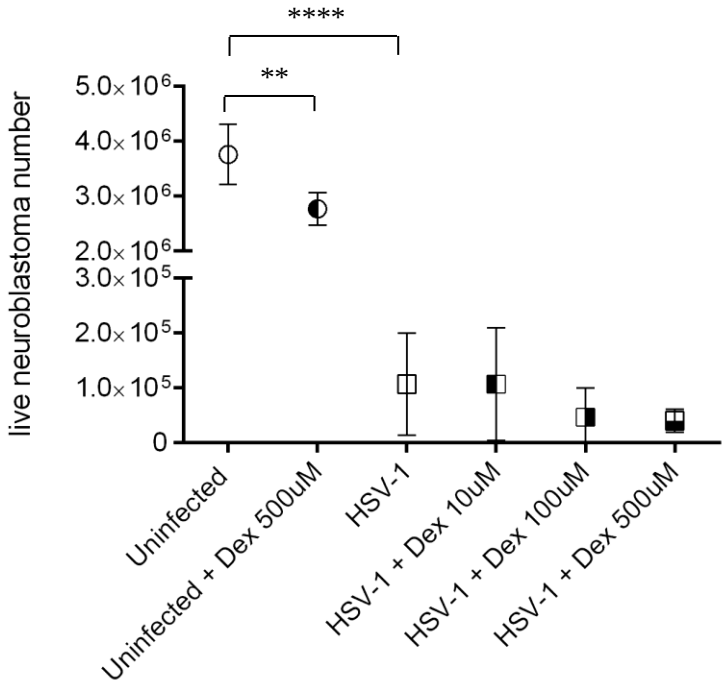

Figure 5.2. Live cell number in uninfected and HSV-1-infected neuroblastoma cells following treatment with high doses of dexamethasone. Uninfected neuroblastoma cells are represented by circles while HSV-1-infected ones are represented by squares. HSV-1 infection was done at MOI=0.001. (Dex) means Dexamethasone treatment has been done 24 h post-infection (h pi) at the concentration of 10, 100 or 500 µM as indicated. At 48 h pi (24 h post-treatment), live cells were counted using Trypan Blue exclusion staining. Data represent mean + 95% Confidence Interval (CI) of 6 replicates from 2 independent experiments. ANOVA test

statistically showed significant differences between the means of the different conditions ($p<0.0001$). (**) $p<0.01$, (**) $p<0.0001$ (t-tests).

5.2.1.2. Toxic doses of dexamethasone in microglial cells

Dexamethasone toxicity was also assessed in uninfected human microglia by observations in light microscopy (fig 5.3-5.5). As soon as 2 h post-treatment, 5 mM of dexamethasone induced visible toxicity characterized by extensive live cell loss as witnessed by an incomplete microglia cell monolayer (fig 5.3D). At this time, this toxic concentration also led to an obvious change in microglial cell morphology making "surviving" cells lose their normal shape (ovoid with ramifications) to become smaller, rounder and brighter. Pictures of microglia cells 24 h (fig 5.4D) and 48 h post-treatment (pt) (fig 5.5D) with 5 mM of dexamethasone also showed apparent changes in cell morphology and extensive decrease in live cell number with most cell debris seen at 48 h pt. Dexamethasone was also toxic in microgliam cells at 1 mM (fig 5.4C and 5.5C) but not at 0.5 mM (fig 5.4B and 5.5B) at 24 h and 48 h post-treatment as seen by the same HSV-1-induced cell damage (cell death and change in morphology). LD50, known as Lethal Dose 50%, is the dose for which a chemical induces 50% of cell death in a tissue. As demonstrated in figure 5.4, more than half of microglia cells were killed by 1 mM of dexamethasone (fig 5.4C) while no toxic effect on the cell monolayer could be seen with a concentration of 0.5 mM at 24 h post-treatment (fig 5.4B). This was similar at 48 h pt (fig 5.5). This suggests an LD50 of dexamethasone around 0.5-1 mM to consider in my experiments in microglial cells (48 h pt being the last time-point used in all my experiments). The dose of dexamethasone used in HSE clinical studies is around 40 mg/day[159]. This matches with a concentration of 2×10^{-2} mM in the bloodstream.

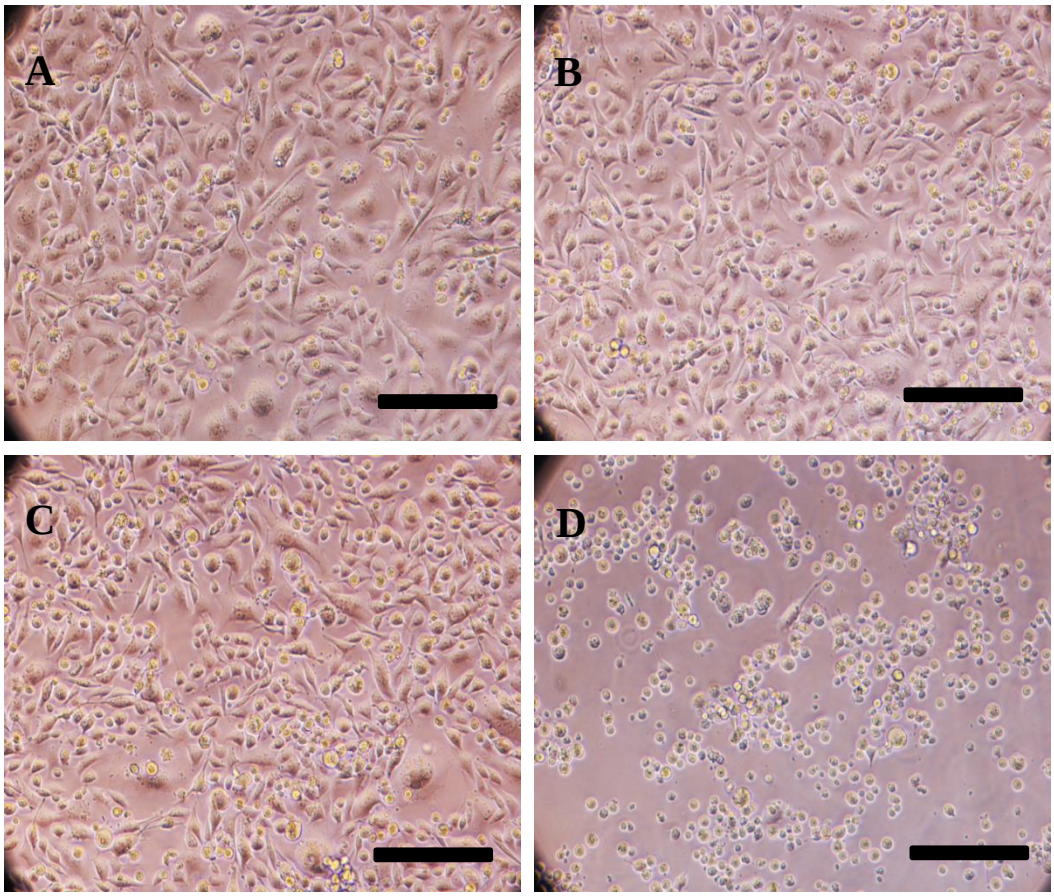

Figure 5.3. Microscopy pictures of HSV-1-infected microglial cells 2 h after high doses of dexamethasone. (A) Culture of (untreated) microglial cells 2 h after treatment of the dexamethasone-treated cells. Most of the cell**s** had the classic morphologic features of microglial cells with ovoid or fibroblast-like shape and ramifications. The confluence was around 70-80% and a few small round cells could be observed. **(B) Culture of microglial cells 2 h after treatment with 0.5 mM of Dexamethasone**. The picture is very similar to the untreated cells (A). **(C) Culture of microglia cells 2 h after treatment with 1 mM of Dexamethasone.** The picture is very similar to the untreated cells (A). **(D) Culture of microglial cells 2 h after treatment with 5 mM of Dexamethasone.** This treatment induced extensive live cell loss 2 h post-treatment as shown by the spaces between cells (20-30% confluence). Cells lost their classic microglia shape, almost all of them looked small and round. 10 x magnification. Scale bar: 50 µm.

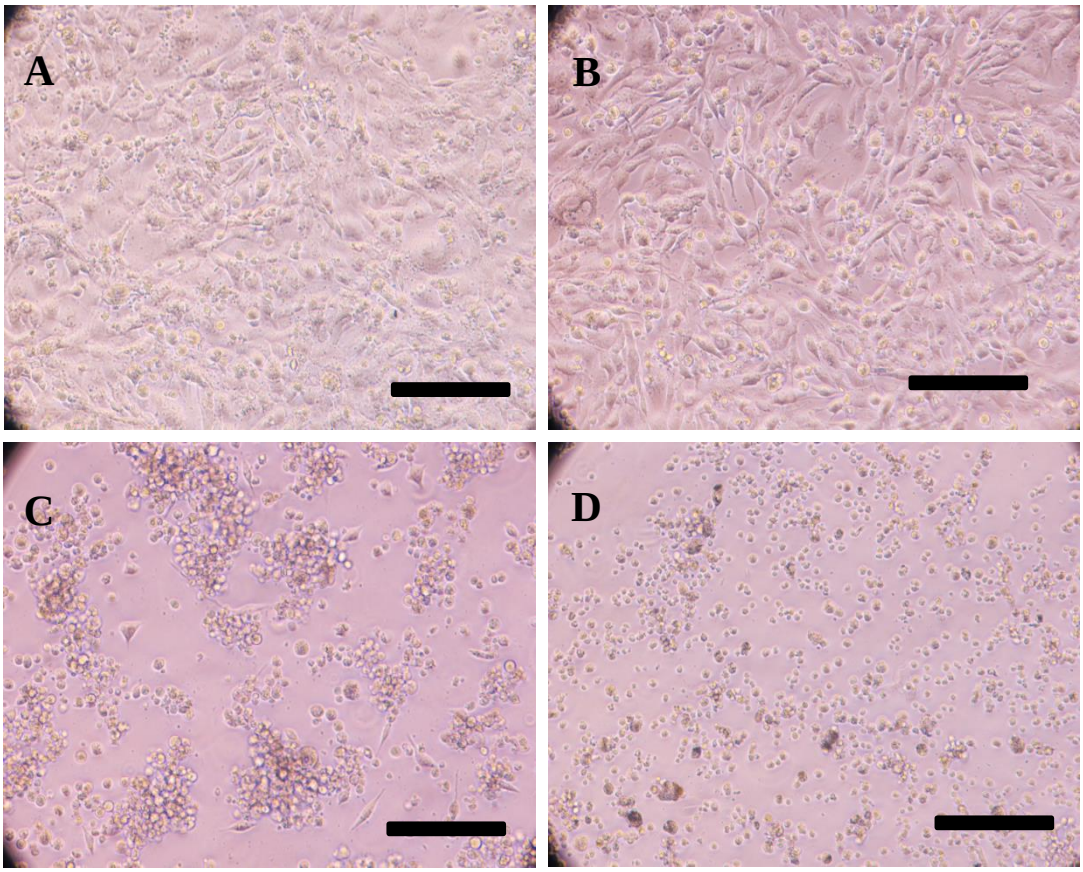

Figure 5.4. Microscopy pictures of HSV-1-infected microglial cells 24 h after high doses of dexamethasone. (A) Culture of (untreated) microglial cells 24 h after treatment of the treated ones. Most of the cell**s** had the classic morphologic features of microglial cells with ovoid or fibroblast-like shape and ramifications. The confluence was around 80% and a few small round cells could be observed. **(B) Culture of microglial cells 24 h after treatment with 0.5 mM of Dexamethasone**. The picture is very similar to the untreated cells (A). **(C) Culture of microglial cells 24 h after treatment with 1 mM of Dexamethasone.** This treatment induced extensive live cell loss as shown by the spaces between cells (20% confluence). Cells lost their classic microglia shape, almost all them looked small and round and formed clusters. **(D) Culture of microglia cells 24 h after treatment with 5 mM of Dexamethasone.** This treatment induced extensive live cell loss as shown by the spaces between cells (10-20% confluence). Cells lost their classic microglia shape, almost all of them looked small and round. 10 x magnification. Scale bar: 50 µm.

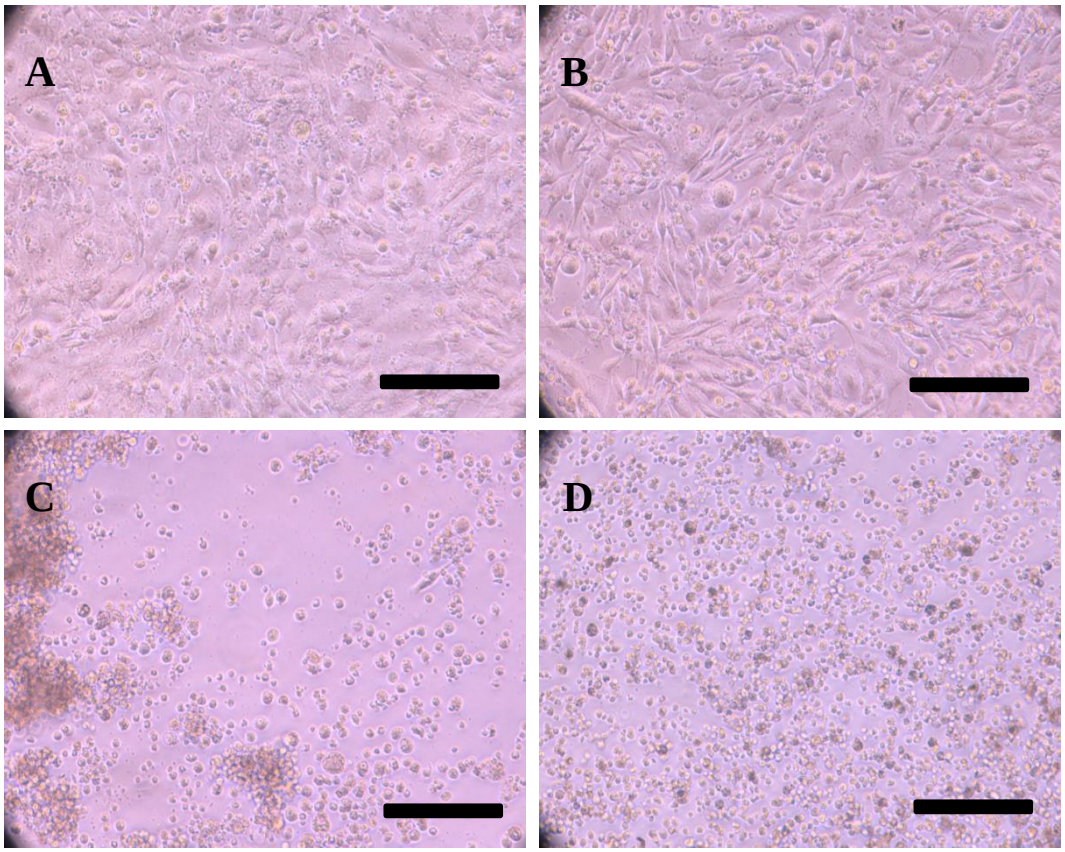

Figure 5.5. Microscopy pictures of HSV-1-infected microglial cells 48 h after high doses of dexamethasone. (A) Culture of (untreated) microglial cells 48 h after treatment of the treated ones. Most of the cells had the classic morphologic features of microglial cells with ovoid or fibroblast-like shape and ramifications. The confluency was around 80-90% and a few small round cells could be observed. **(B) Culture of microglial cells 48 h after treatment with 0.5 mM of Dexamethasone**. The picture is very similar to the untreated cells (A). **(C) Culture of microglial cells 48 h after treatment with 1 mM of Dexamethasone.** This treatment induced extensive live cell loss as shown by the spaces between cells (10% confluence). Cells lost their classic microglia shape, almost all of them looked small and round. There were a lot of cells floating and forming clusters. **(D) Culture of microglial cells 48 h after treatment with 5 mM of Dexamethasone**. The monolayer was completely different with only few cells attached compared to the one made by untreated (A). All cells lost their classic microglia shape, they all looked small and round. A lot of floating cells and debris could be observed.10 x magnification. Scale bar: 50 µm.

5.2.1.3. Toxic doses of dexamethasone in primary astrocytes

Dexamethasone toxicity was finally studied in (uninfected) primary astrocytes using light microscopy as well (fig 5.6-5.8). Similar to what was observed in microglial cells, at 2 h post-treatment (pt), 5 mM of dexamethasone was also toxic for astrocytes since it was associated with both an extensive decrease in live cells with big spaces between cells and a big proportion of cells losing their astrocyte classic morphology ("star-like" shape, thin, long with ramifications) to become smaller, rounder and brighter cells in light microscopy (fig 5.6D). At 24 h and 48 h pt, all astrocytes treated with 5 mM looked round and small with big spaces between cells indicating cell death (fig 5.7D and 5.8D). 1 mM but not 0.5 mM of dexamethasone was also toxic for astrocytes at 24 h and 48 h pt as witnessed by a visible decrease in live cells and morphologic changes in the cells (fig 5.7B-C and 5.8B-C). Crucially, more than half of the primary astrocytes were killed by 1 mM of Dexamethasone (fig 5.8C) while no toxic effect on the cell monolayer could be seen with a concentration of 0.5 mM at 48 h post-treatment (fig 5.8B). This also suggests a LD50 of dexamethasone around 0.5-1 mM to consider in my experiments in primary astrocytes (48h pt being the last time-point used for all my experiments).

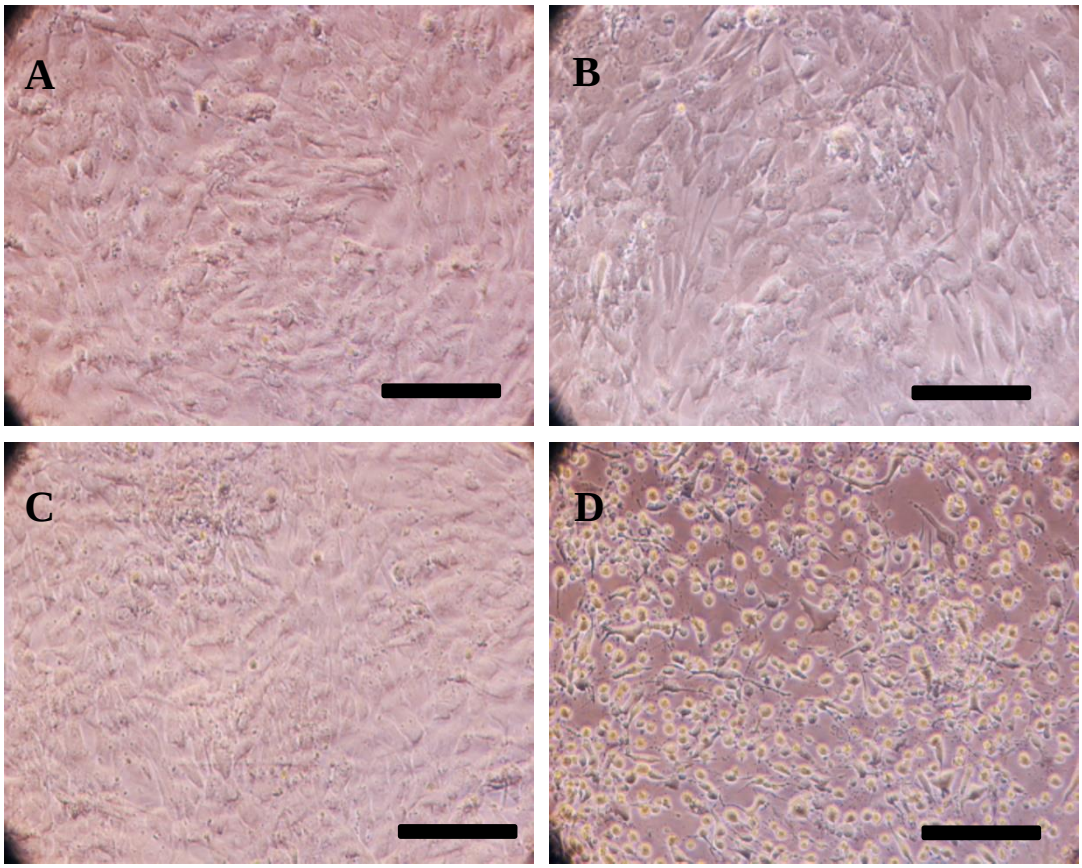

Figure 5.6. Microscopy pictures of HSV-1-infected astrocytes 2 h after high doses of dexamethasone. (A) Culture of (untreated) astrocytes 2 h after treatment of the treated ones. Most of the cells had the classic morphologic features of astrocytes: thin, long with a "star"-like shape and ramifications. The confluence was close to 100%. **(B) Culture of astrocytes 2 h after treatment with 0.5 mM of Dexamethasone**. The picture was very similar to the untreated cells (A). **(C) Culture of astrocytes cells 2 h after treatment with 1 mM of Dexamethasone.** The picture was very similar to the untreated cells (A). **(D) Culture of astrocytes 2 h after treatment with 5 mM of Dexamethasone.** This treatment induced extensive live cell loss as shown by the spaces between cells (30-40% confluency). Many cells lost their classic astrocyte shape, almost all of them looking small, round and bright in light microscopy. 10 x magnification. Scale bar: 50 µm.

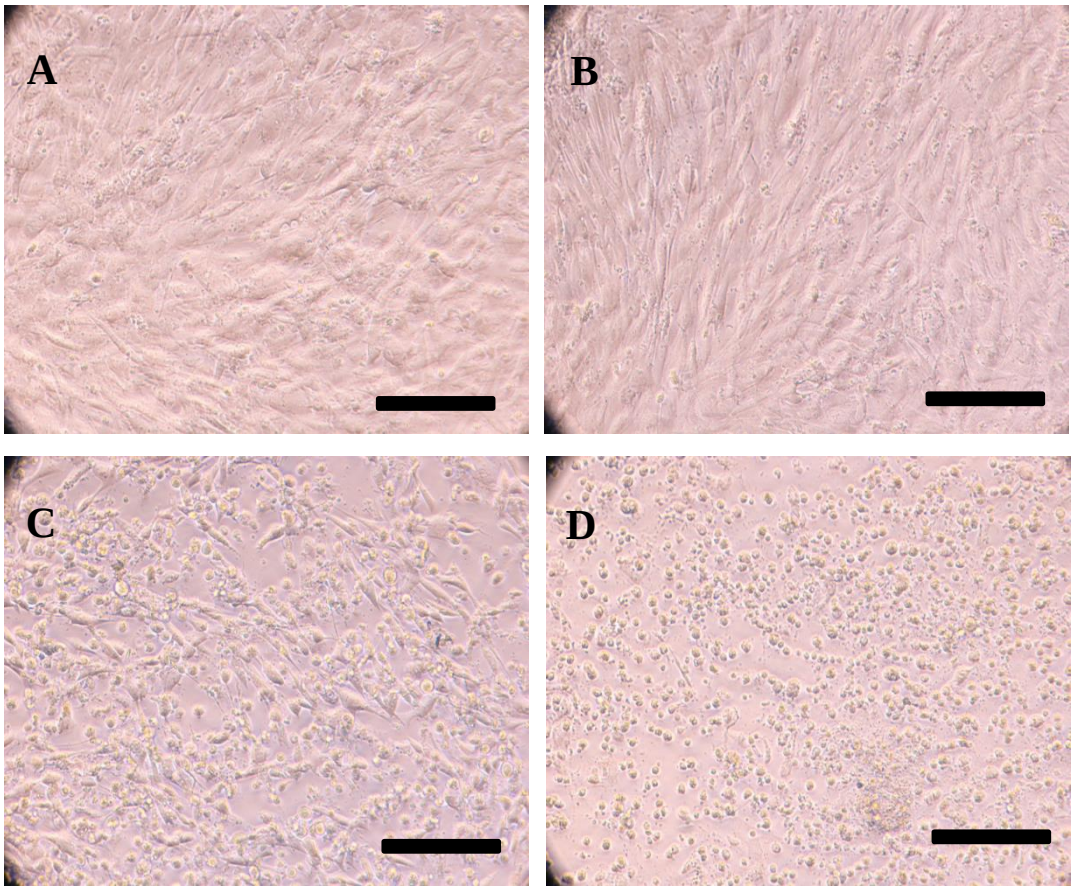

Figure 5.7. Microscopy pictures of HSV-1-infected astrocytes 24 h after high doses of dexamethasone. (A) Culture of (untreated) astrocytes 24 h after treatment of the treated ones. Most of the cell**s** had the classic morphologic features of astrocytes: thin, long with a "star"-like shape and ramifications. The confluency was close to 100%. **(B) Culture of astrocytes 24 h after treatment with 0.5 mM of Dexamethasone**. The picture was very similar to the untreated cells (A). **(C) Culture of astrocytes 24 h after treatment with 1 mM of Dexamethasone.** This treatment induced live cell loss as shown by gaps in the monolayer (60-70% confluence). A big proportion of the cells started to lose their astrocyte shape to become round and small. **(D) Culture of astrocytes 24 h after treatment with 5 mM of Dexamethasone.** This treatment induced extensive live cell loss as shown by the spaces between cells (around 40-50% confluency). Almost all cells looked small and round. 10 x magnification. Scale bar: 50 µm.

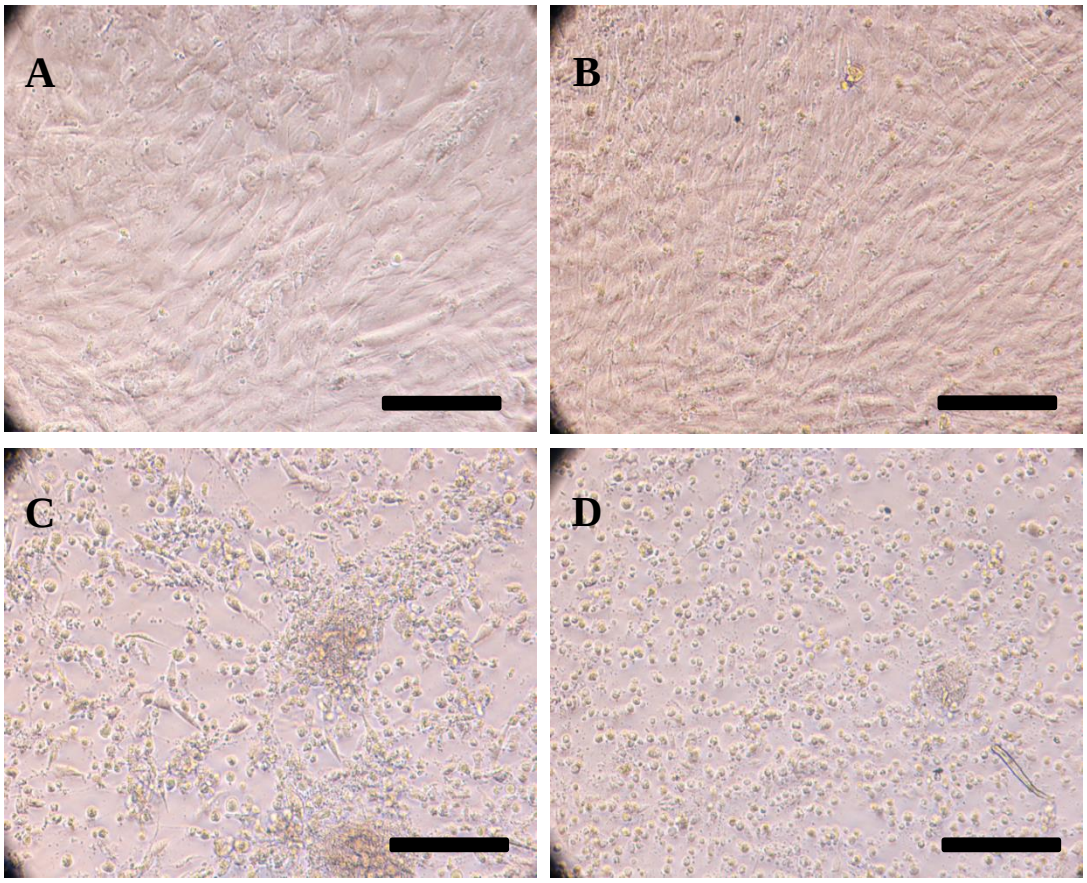

Figure 5.8. Microscopy pictures of HSV-1-infected astrocytes 48 h after high doses of dexamethasone. (A) Culture of (untreated) astrocytes 48 h after treatment of the treated ones. Most of the cells had classic morphologic features of astrocytes: thin, long with a "star"-like shape and ramifications. The confluence was close to 100%. **(B) Culture of astrocytes 48 h after treatment with 0.5 mM of Dexamethasone**. The picture was very similar to the untreated cells (A). **(C) Culture of astrocytes 48 h after treatment with 1 mM of Dexamethasone.** This treatment induced extensive live cell loss as shown by gaps in the monolayer (around 30% confluency). A big proportion of the cells lost their astrocyte shape to become round and small but there were still some astrocytes with classic morphology. **(D) Culture of astrocytes 48 h after treatment with 5 mM of Dexamethasone.** This treatment induced extensive live cell loss as shown by the spaces between cells (around 30% confluence). All cells looked small and round. 10 x magnification. Scale bar: 50 µm.

5.2.2. The effect of sub-toxic doses of dexamethasone combined to aciclovir on HSV-1-infection of neuroblastoma cells and microglia cells

5.2.2.1. Determination of the dose of dexamethasone to assess

As mentioned in previous sections above, in light microscopy, acute toxicity was seen in (uninfected) microglia and primary astrocytes from dexamethasone concentrations of 1 mM (but not 0.5 mM) and it was therefore concluded that the LD50 for dexamethasone should be in the range of 0.5-1 mM for both brain cell types. The same trend was also observed for HSV-1-infected-neuroblastoma cells. Indeed, by live cell counting, 0.5 mM (500 µM) dexamethasone was associated with a decrease slightly below 50% in live (uninfected) neuroblastoma number. Hence, the LD50 of dexamethasone in neuroblastomas is also higher than 0.5 mM and should also be around 0.5-1 mM. Interestingly, in the brain of patients suffering from glioblastomas and treated by dexamethasone, it was shown that the brain tissue concentration of dexamethasone which acts to potentially reduce oedema in this disease, is around one thousand times lower than the cytotoxic concentration determined in cell culture[156]. This suggests that it could be interesting to assess the biological effect of dexamethasone on HSV-1-infected brain cells combined with aciclovir using concentrations of dexamethasone around one thousand times lower than the previously determined LD50 (0.5-1 mM). Therefore, concentrations of around 0.5-1 µM were chosen. This is in agreement with the concentration used (0.5 µM) to demonstrate that dexamethasone administration was beneficial for microglia and astrocyte following LPS challenge in an *in vitro* model of bacterial meningitis[156]. As a result, the main concentration of dexamethasone assessed in the following experiments was 0.5 µM. The dose of dexamethasone used in HSE clinical studies is around 40 mg/day[159]. This matches with a concentration of 20 µM in the bloodstream (depending on the blood brain barrier permeability, only proportion of this 20 µM of dexamethasone will penetrate the brain parenchyma).

5.2.2.2. The effect of sub-toxic doses of dexamethasone combined with aciclovir in HSV-1-infected neuroblastoma cells

5.2.2.2.1. The effect of sub-toxic doses of dexamethasone combined with aciclovir on cell viability and viral replication in HSV-1-infected neuroblastoma cells

The effect of dexamethasone (0.5 µM), alone and combined with aciclovir (20 µM), was assessed on HSV-1-infected neuroblastoma cell viability. The cell viability levels were determined by light microscopy followed by analysis of microscopy pictures using the software "ImageJ", live cell counting after Trypan blue staining, WST-1 assay (measuring mitochondrial activity) and qRT-PCR targeting the housekeeping gene DAD-1. The treatment with dexamethasone and/or aciclovir was performed 24 h post-infection (pi).

In light microscopy, at 48 h post-treatment (pt) (72 h pi), more signs of infection (including live cell loss and debris) could be observed in infected cells untreated or treated with dexamethasone alone compared to infected neuroblastomas treated with aciclovir alone or combined with dexamethasone (fig 5.10). At 24 h pt, such a difference was not detectable since, at this earlier time-point, HSV-1 had only started to induce cell death sporadically and the monolayers of infected cells were all more than 90% confluent, independently of the treatment given (fig 5.9).

Analysing multiple microscope pictures at 4 x magnification using the software "ImageJ" also showed that the area of attached neuroblastomas was significantly bigger in HSV-1-infected neuroblastoma cells treated by aciclovir alone or combined with dexamethasone than in infected cells untreated at 48 h pt (fig 5.11) ($p<0.05$). The area of attached infected cells treated with dexamethasone alone was similar to that of infected cells untreated.

qRT-PCR targeting the housekeeping gene DAD-1 was sensitive enough to show differences in Ct values between uninfected and infected cells but not between infected neuroblastoma untreated, treated with dexamethasone, aciclovir or both (fig 5.12).

At 24 h and 48 h pt (48 h and 72 h pi), aciclovir alone or combined with dexamethasone, but not dexamethasone alone, was associated with an increase in mitochondrial activity in HSV-1-infected neuroblastoma cells as detected by the WST-1 assay (fig 5.13). However, dual therapy with aciclovir and dexamethasone did not lead to higher levels of mitochondrial activity than the administration of aciclovir alone. Of note, mitochondrial activity was also similar at 24 h and 48 h pt between infected neuroblastomas untreated and treated with dexamethasone emphasizing that dexamethasone was not detrimental for mitochondrial activity and cell viability in HSV-1-infected neuroblastoma cells.

Finally, a direct qPCR on HSV DNA from culture medium of infected neuroblastomas, did not show any differences in viral load between infected cells untreated or treated with aciclovir, dexamethasone or both (fig 5.14). As stated before, this technique does not perfectly reflect the amount of viruses remaining active or functional in culture medium. As a result, the culture medium of infected neuroblastomas untreated or treated with aciclovir, dexamethasone or both, was then used to infect Vero cells; at 24h after Vero cell infection, an HSV DNA qPCR on Vero cell culture medium was performed (fig 5.15). This secondary qPCR showed a decrease in HSV DNA abundance (higher Ct values) in culture medium of Vero cells infected by the medium of HSV-1 infected neuroblastoma cells treated with aciclovir alone or combined to dexamethasone, compared to those infected by the medium of infected neuroblastoma cells untreated or treated by dexamethasone alone (fig 5.15). As seen in the previous chapter, this confirms that aciclovir decreases viral load in HSV-1-infected neuroblastoma cells, but here it also shows that it is still the case in presence of dexamethasone.

Altogether, this shows dexamethasone (0.5 µM) has no positive effect on cell viability or viral load in HSV-1-infected neuroblastomas and suggests that the positive impact of aciclovir therapy combined to dexamethasone, very similar to the one caused by aciclovir alone, is only due to the inhibition of viral load by aciclovir. However, these experiments show that adding dexamethasone (0.5 µM) does not have a negative impact either, since it does not lead to an increase in live cell loss or higher viral load in HSV-1-infected neuroblastomas.

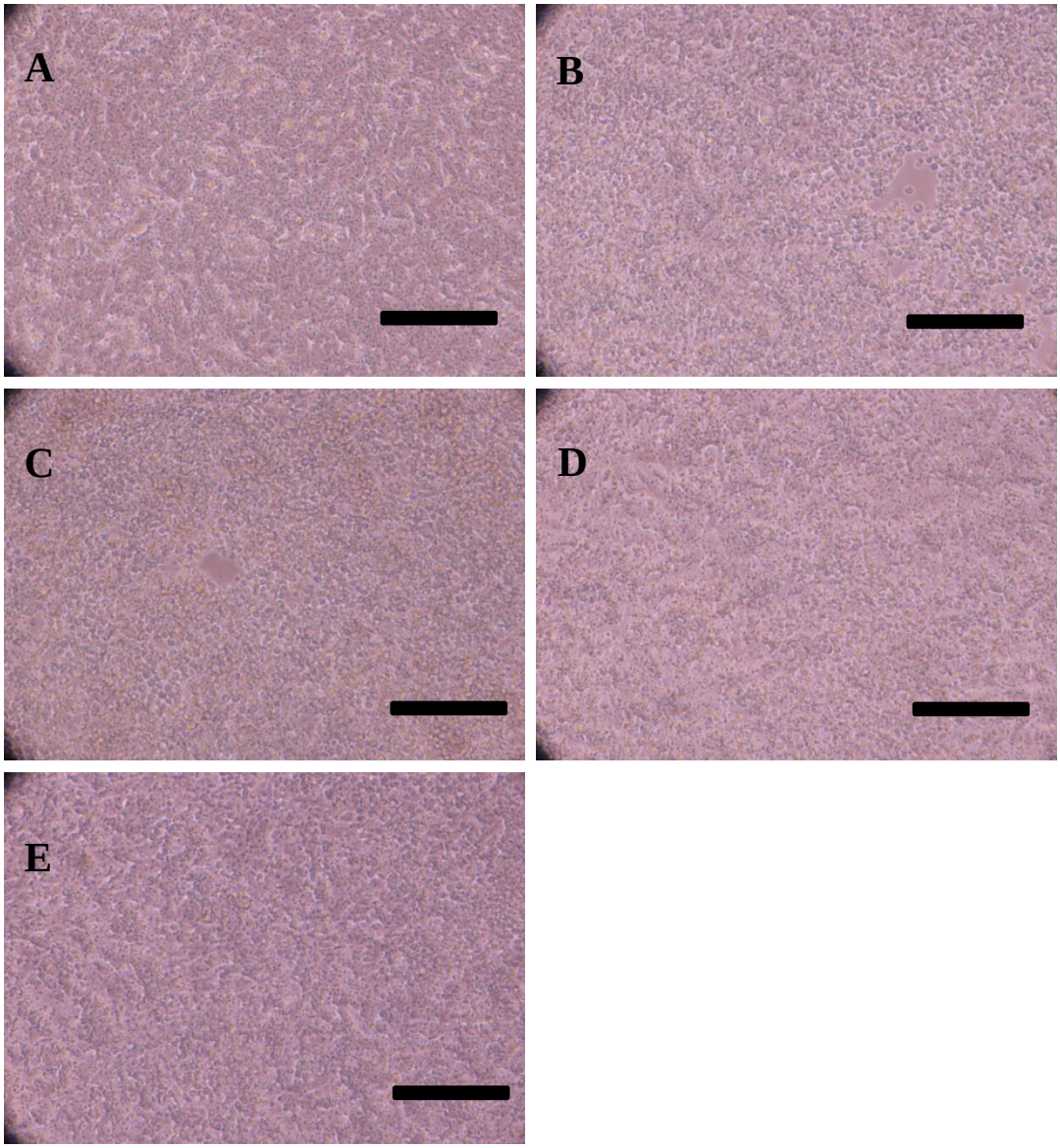

Figure 5.9. Microscopy pictures of HSV-1-infected neuroblastoma cells 48 h post-infection with a sub-toxic dose of dexamethasone (0.5 µM) alone or combined with aciclovir. HSV-1-infection was done at MOI=0.01. Treatment was done with dexamethasone (0.5 µM) and/or aciclovir (20 µM) at 24 h post-infection (pi). Pictures were taken at 48 h pi (24 h post-treatment). **(A) Uninfected neuroblastoma cells.** Most of the cells have classic morphologic features of neuroblastomas with a fibroblast-like shape. The confluence is around 100%. **(B) HSV-1-infected neuroblastoma cells untreated**. A round gap, a sign of viral-induced cell death, can be observed. Cells look also rounder and smaller than uninfected (A) **(C) HSV-1-infected neuroblastoma cells treated with Dexamethasone.** The picture is very similar to the one of infected untreated cells (B). Indeed, a gap in the monolayer and a change of cell morphology can also be observed. **(D) HSV-1-infected-neuroblastoma cells treated with aciclovir.** The picture is very similar to the one of uninfected cells (A). **(E) HSV-1-infected-neuroblastoma cells treated with aciclovir and dexamethasone.** The picture is very similar to the one of uninfected cells (A). 10 x magnification. Scale bar: 50 µm.

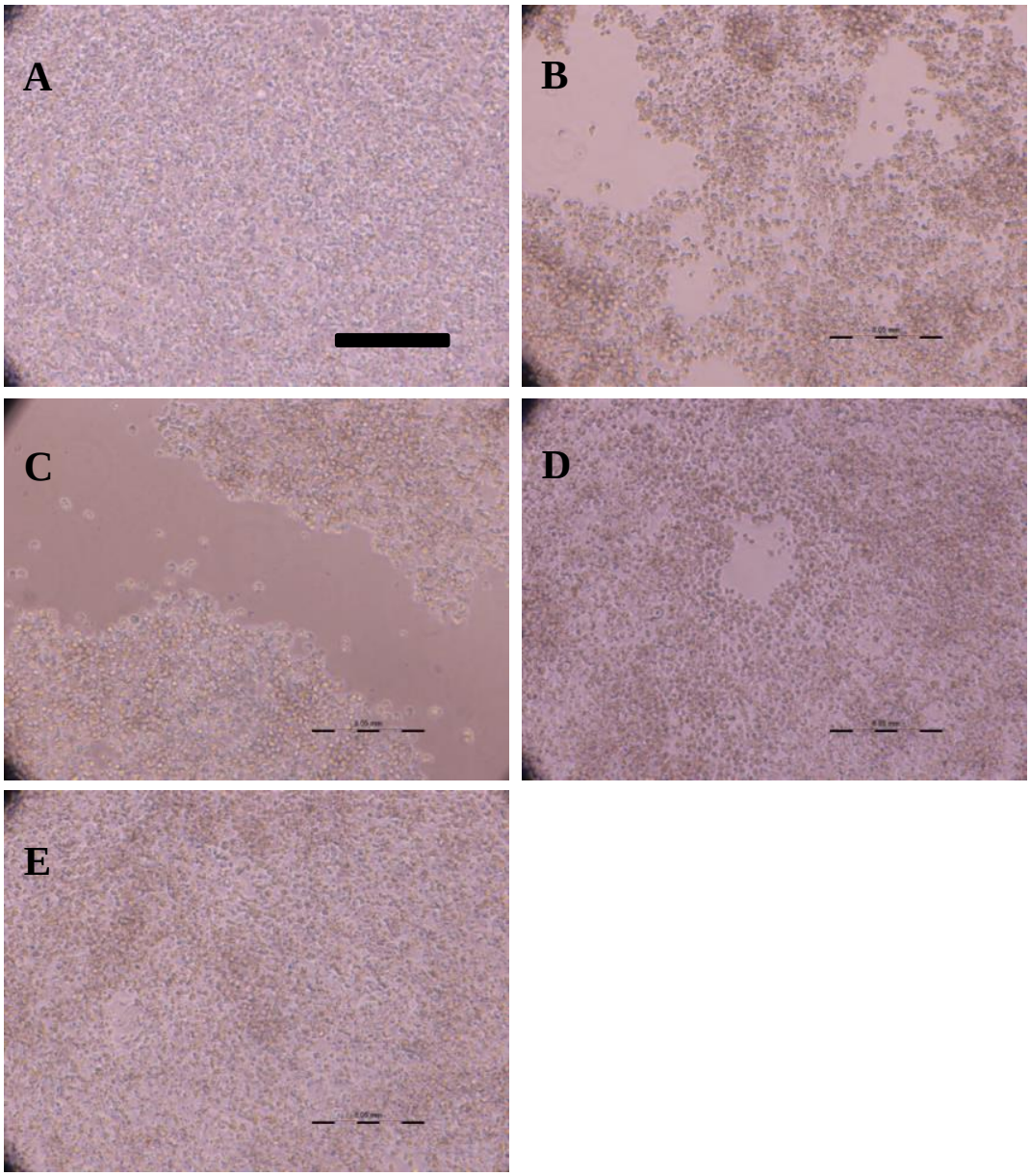

Figure 5.10. Microscopy pictures of HSV-1-infected neuroblastoma cells 72 h post-infection with a sub-toxic dose of dexamethasone (0.5 µM) alone or combined with aciclovir. HSV-1-infection was done at MOI=0.01. Treatment was done with dexamethasone (0.5 µM) and/or aciclovir (20 µM) at 24h post-infection (pi). Pictures were taken at 72 h pi (48 h post-treatment). **(A) Uninfected neuroblastoma cells.** Most of the cells look round now as they are overconfluent. **(B) HSV-1-infected neuroblastoma cells untreated**. There are big gaps in the monolayer now and, the confluence seems around 50%. **(C) HSV-1-infected neuroblastoma cells treated with dexamethasone.** The picture is very similar to the one of infected untreated cells (B). Indeed, a lot of cells are detached from the monolayer as we can see with the big gap (around 50% confluency). **(D) HSV-1-infected-neuroblastoma cells treated with aciclovir.** The monolayer presents signs of live cell loss with a central gap and more space between cells. However, the infection with aciclovir has induced less damage than for cells untreated (B) or treated with dexamethasone (C). Indeed, around 70-80% of cells are still present. **(E) HSV-1-infected-neuroblastoma cells treated with aciclovir and**

dexamethasone. The monolayer is still almost complete (around 90% confluent). 10 x magnification. Scale bar: 50 µm.

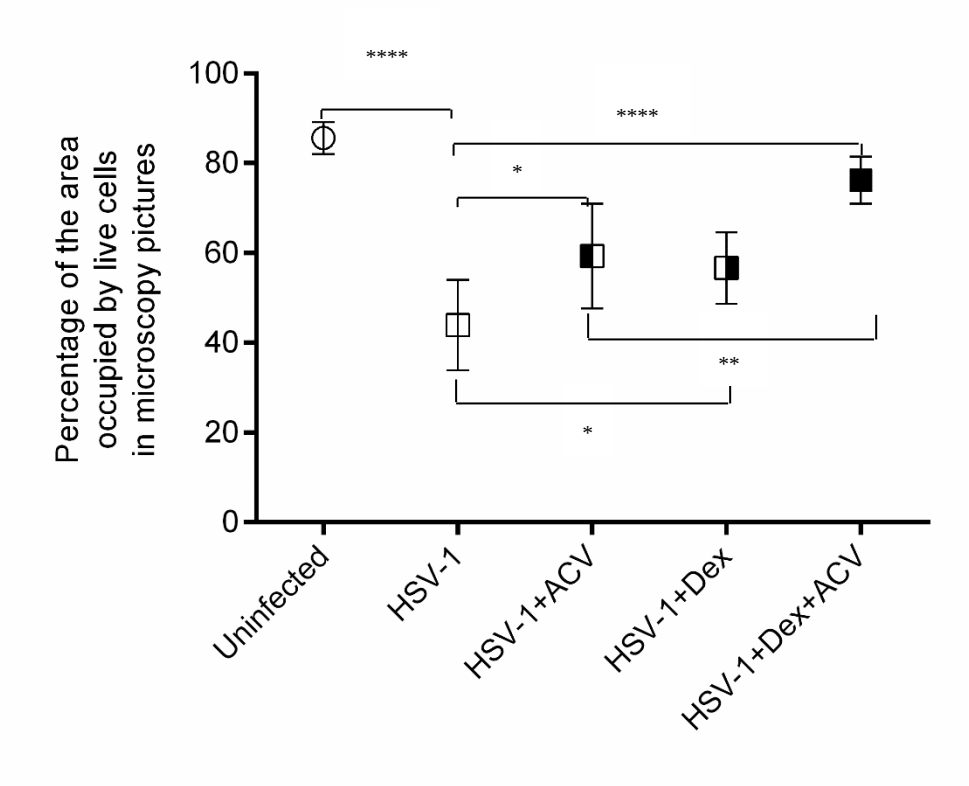

Figure 5.11. The effect of dexamethasone alone (0.5 µM) or combined with aciclovir on the attached cell area of microscopy pictures of HSV-1-infected neuroblastoma cells 72 h post-infection. HSV-1-infection was done at MOI=0.01. Treatment was done with dexamethasone (0.5 µM) and/or aciclovir (20 µM) 24 h post-infection (pi). Areas of attached cells were measured by the software "ImageJ" from pictures taken at 72 h post-infection (48 h post-treatment) of neuroblastoma cells uninfected (circles), infected untreated (white squares), infected treated with aciclovir (squares half-filled in black on the left side), infected treated with dexamethasone (squares half-filled in black on the right side) or infected treated with the combination "aciclovir+dexamethasone" (black squares). Data are expressed as mean of the area of live cells +95% CI and were obtained as described in the chapter 2. At 72 h pi (48 h post-treatment), nine pictures for uninfected cells, twenty-four for infected untreated cells, twenty-two pictures for infected cells treated with aciclovir, fourteen for infected cells treated with dexamethasone and thirteen for infected cells treated both aciclovir and dexamethasone were analysed. The pictures were representative of 3 independent experiments. ANOVA test statistically showed significant differences between the means of the different conditions ($p<0.0001$). (*) $p<0.05$; $p=0.01$; (****) $p<0.0001$ (t-tests).

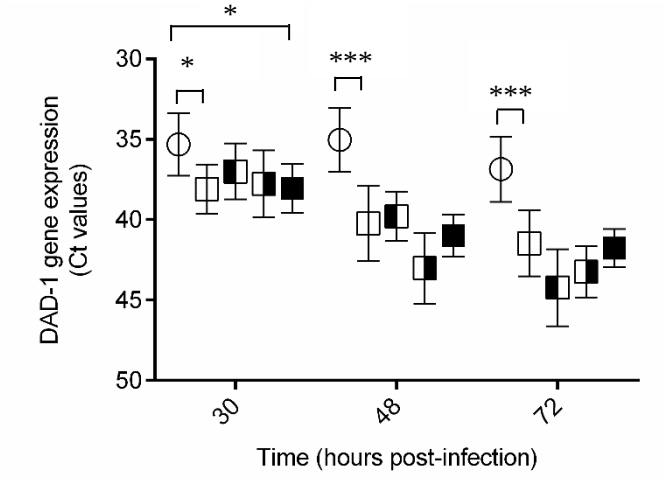

Figure 5.12. The effect of dexamethasone (0.5 µM) alone or combined with aciclovir on DAD-1 gene expression in HSV-1-infected neuroblastoma cells. HSV-1 infection was performed at MOI=0.01. The treatments with aciclovir (20 µM) and/or dexamethasone (0.5 µM) were done at 24 h pi. The values represent Ct values after qRT-PCR targeting DAD-1. qRT-PCR was performed using 1 µg of RNA extracts of uninfected (circles) or untreated infected (unfilled squares) or aciclovir-treated infected (squares half-filled in black on the left side) or dexamethasone-treated infected (squares half-filled in black on the right side) or "dexamethasone+aciclovir"-treated infected (black squares) neuroblastoma cells at 30, 48, 72 h pi. ANOVA test statistically showed significant differences between the means of the different conditions at 48 h pi ($p<0.0001$) and 72 h pi ($p<0.0001$) but not at 30 h pi ($p>0.05$). Data are expressed as mean + 95% Confidence Interval (C.I) of 9 replicates from 3 independent experiments. (*) $p<0.05$; (***) $p<0.005$ (multiple t-tests).

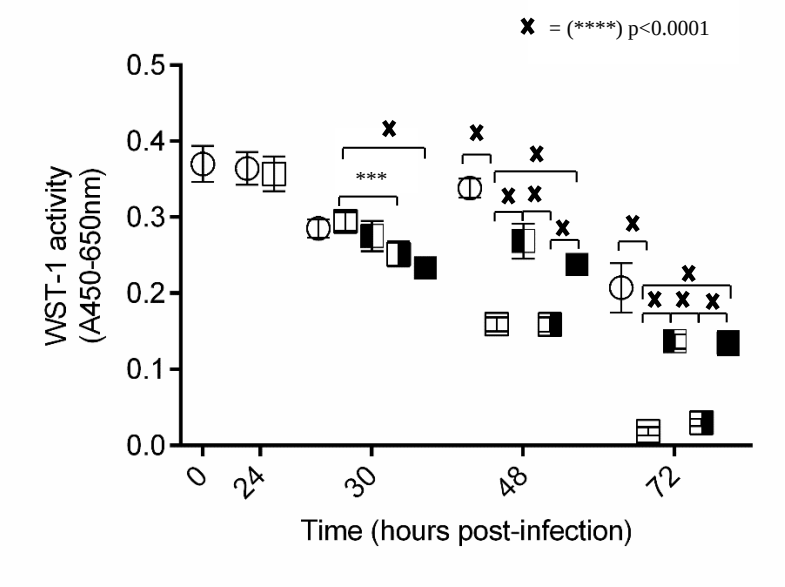

Figure 5.13. The effect of dexamethasone (0.5 µM) alone or combined with aciclovir on mitochondrial activity in HSV-1-infected neuroblastoma cells. HSV-1 infection was done

at MOI=0.01. The treatment with aciclovir (20 µM) and/or dexamethasone (0.5 µM) was done at 24 h pi. The values represent values of WST-1 activity (absorbance at 450 nm (A450nm) normalised by subtraction of the background (A650 nm)). WST-1 assay has been performed in uninfected (circles), untreated infected (unfilled squares) or aciclovir-treated infected (squares half-filled in black on the left side) or dexamethasone-treated infected (squares half-filled in black on the right side) or "dexamethasone+aciclovir"-treated infected (black squares) neuroblastoma cells at different time-points (0, 24, 30, 48, 72 h pi). Data are expressed as mean + 95% CI of 30 replicates from 3 independent experiments. ANOVA test showed statistical differences between the means of the different conditions for all time-points tested: 30 h, 48 h and 72 h pi ($p<0.0001$). (***): $p<0.005$; **X**= (****) $p<0.0001$ (multiple t-tests).

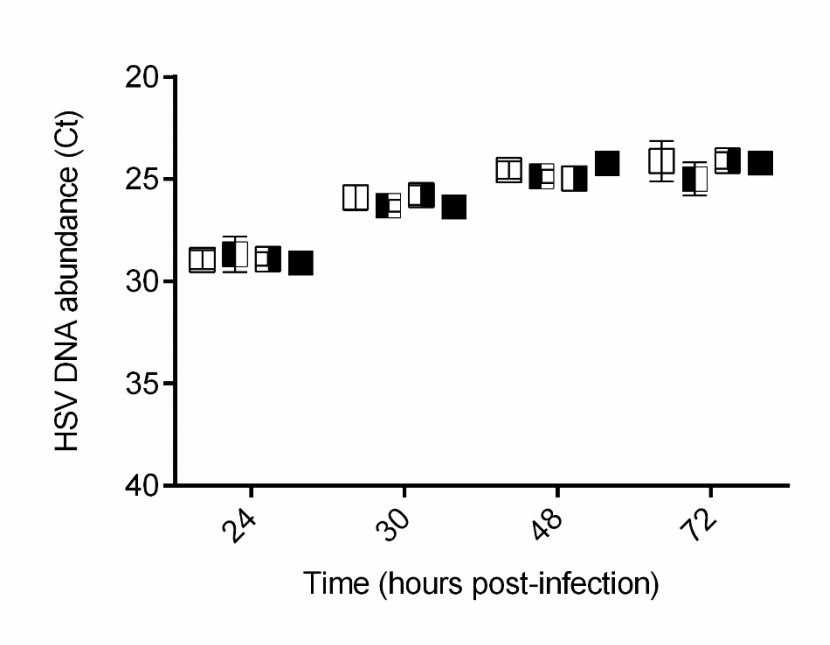

Figure 5.14. The effect of dexamethasone (0.5 µM) alone or combined with aciclovir on HSV DNA abundance in culture medium of HSV-1-infected neuroblastoma cells. HSV-1-infection was done at MOI=0.01. The treatments with aciclovir (20 µM) and/or dexamethasone (0.5 µM) were done at 24 h pi. The values represent Ct values after HSV DNA qPCR from culture medium of HSV-1-infected neuroblastoma cells: untreated (white), aciclovir-treated (half-filled in black on the left side), dexamethasone-treated (half-filled in black on the right side) or "dexamethasone+aciclovir"-treated (in black) at 24 (just before the treatment), 30, 48 h and 72 h pi. Each point represents the mean + 95% CI of data from at least 3 independent experiments. Triplicates were used for each point-time in each experiment. ANOVA test showed no statistical differences between the means of the different conditions at any time point.

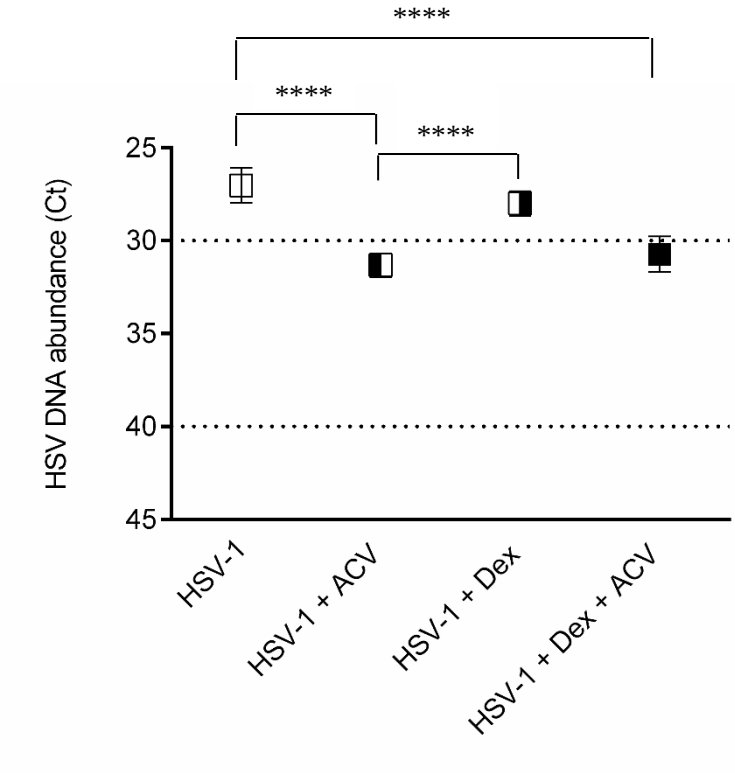

Figure 5.15. The effect of dexamethasone (0.5 µM) alone or combined with aciclovir on the viral load of active HSV-1 particles in the culture medium of infected neuroblastoma cells. HSV-1 infection was done at MOI=0.01 and treatment with aciclovir (20 µM) and/or dexamethasone (0.5 µM) in neuroblastoma cells were done as described previously (figure 5.14). Then, the culture medium of neuroblastoma cells infected untreated (white), treated with aciclovir (black squares half-filled on the left side), treated with dexamethasone (black squares half-filled on the right side) or treated with both aciclovir and dexamethasone (black squares) was taken at 72 h pi and used to secondarily infect Vero cells. 24 h post-infection of Vero cells with neuroblastoma culture medium, a qPCR targeting HSV DNA was performed on Vero cell culture medium. The values represent Ct values after HSV DNA qPCR from Vero cell culture medium. Each point represents the mean + 95% CI of data from 2 independent experiments. Triplicates were used for each point-time in each experiment. ANOVA test showed statistical differences between the means of the different conditions ($p<0.0001$). (****) $p<0.0001$ (t-tests).

5.2.2.2.2. The effect of sub-toxic doses of dexamethasone combined to aciclovir on TNF gene expression in HSV-1-infected neuroblastoma cells

In chapter 3, an increase in TNF relative gene expression was observed in neuroblastoma cells following HSV-1-infection. Furthermore, in chapter 4, treatment with aciclovir (20 µM) led to a further increase in TNF relative gene expression in infected neuroblastoma cells at 72nh pi. Here, I assessed the impact of the drug dexamethasone (0.5 µM), alone or combined with aciclovir (20 µM), on TNF relative gene expression in HSV-1-infected neuroblastoma cells. There was still a significant increase in TNF relative gene expression in HSV-1-infected neuroblastoma cells treated with dexamethasone co-treated with aciclovir or alone, compared to the uninfected counterparts as observed with all the values much higher than one (30-72 h pi) (fig 5.16). At 72 h pi, the infected cells untreated, treated with dexamethasone alone or combined with aciclovir presented similar TNF relative gene expression. Interestingly, aciclovir alone induced a more elevated TNF relative gene expression than all these other treatments.

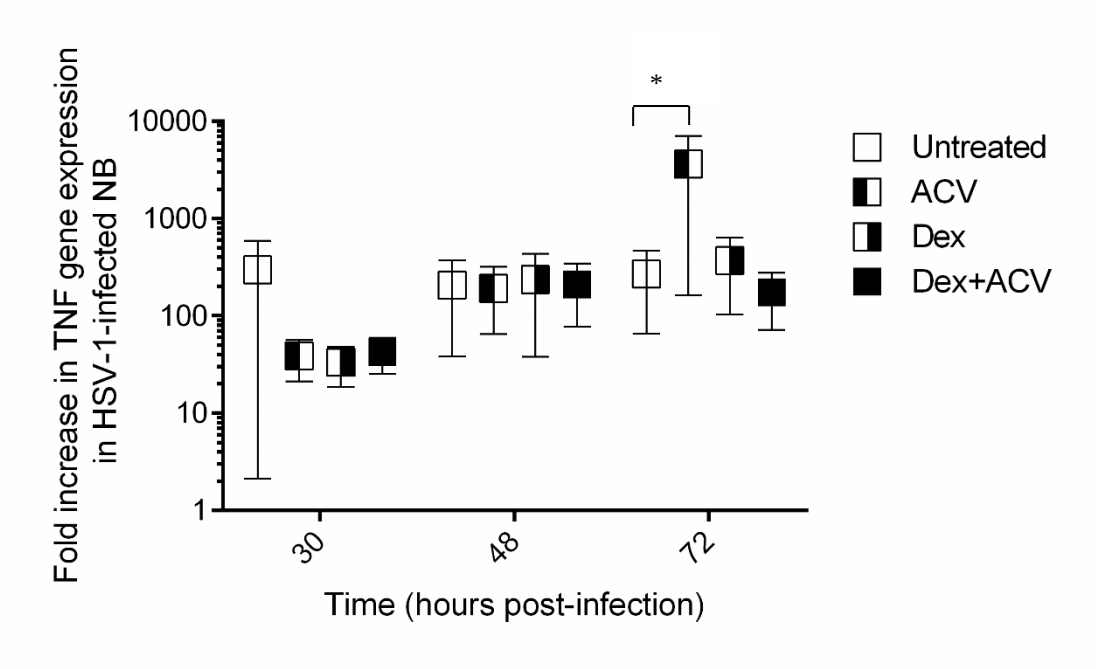

Figure 5.16. The effect of dexamethasone (0.5 µM) alone or combined with aciclovir on TNF relative gene expression in HSV-1-infected neuroblastoma cells. HSV-1 infection was done at MOI=0.01 in neuroblastoma cells. The treatments with aciclovir (20 µM); dexamethasone (0,5 µM) or both were added at 24 h pi. The data represent TNF relative gene expression expressed as mean +/- 95% CI of $2^{-\Delta\Delta Ct}$ values at 30 h, 48 h and 72 h post-infection (respectively 6 h, 24 h and 48 h post-treatment). The scale is logarithmic. $2^{-\Delta\Delta Ct}$ values were obtained following qRT-PCR of TNF and DAD-1 genes. DAD-1 gene was used as reference (housekeeping) gene. From qRT-PCR Ct values of DAD-1 and TNF, ΔCt values [Ct (TNF)-Ct(DAD-1]) were obtained for both uninfected and HSV-1-infected cells (untreated, treated with aciclovir, dexamethasone or both). For each condition (untreated, aciclovir, dexamethasone or both), ΔΔCt values represented $[(\Delta Ct)_{HSV+/-treatment} - (\Delta Ct)_{uninfected}]$. Data were obtained from 3 independent experiments. ANOVA test showed statistical differences between the means of the different conditions at 30 h ($p<0.05$) and 72 h pi ($p<0.001$) but not at 48 h pi ($p>0.05$). (*): $p<0,05$ (multiple t-tests).

5.2.2.3. The effect of sub-toxic doses of dexamethasone combined with aciclovir in HSV-1-infected microglial cells

5.2.2.3.1. The effect of sub-toxic doses of dexamethasone combined with aciclovir on cell viability and viral replication in HSV-1-infected microglia

The effect of 0.5 µM dexamethasone, alone and combined with aciclovir (20 µM) on cell viability of HSV-1-infected microglia cells by light microscopy, live cell counting, WST-1 assay measuring mitochondrial metabolism and qRT-PCR targeting the housekeeping gene DAD-1 was also assessed. Once again, the treatment with dexamethasone and/or aciclovir was done 24 h post-infection (pi).

By light microscopy (10 x magnification), 48h post-infection (pi) (24 h pt), no important differences in microglia cell viability and morphology could be seen between infected cells untreated or treated with aciclovir, dexamethasone or both (fig 5.17). However, at 72 h pi (48 h pt), at lower magnification (4 x), it was clear that aciclovir alone or combined with dexamethasone was similarly and significantly increasing HSV-1-infected microglia cell viability (fig 5.18). Despite a less clear effect, dexamethasone alone seemed to increase infected microglia cell viability at 48 h pt (72 h pi) (fig 5.18).

By qRT-PCR, at 48h post-treatment (72 h pi), it was shown that DAD-1 gene expression was more elevated in samples from infected microglial cells treated with aciclovir combined or not with dexamethasone than in untreated infected cells ($p=0.55$) (fig 5.19). The administration of aciclovir alone or combined to dexamethasone led to similar levels of DAD-1 gene expression. Furthermore, at this time, DAD-1 gene expression was not different between samples from infected microglial cells treated with dexamethasone alone or untreated.

The WST-1 assay, measuring mitochondrial metabolic activity, showed a similar profile at 72 h post-infection (48 h post-treatment) (fig 5.20). At this time point, the treatment with aciclovir

alone or combined with dexamethasone but not the administration of dexamethasone alone was associated with an increase in mitochondrial activity of microglial cells that was reduced following HSV-1-infection (fig 5.20). The levels of mitochondrial activity were very similar between infected cells treated with aciclovir alone or combined with dexamethasone. Of note, mitochondrial activity was also similar at this time-point between infected microglia cells untreated and treated with dexamethasone suggesting that dexamethasone was not detrimental for mitochondrial activity in HSV-1-infected microglila cells.

At the viral replication level, direct qPCR targeting HSV DNA on culture medium of infected microglial cells also presented the same dichotomy between cells treated with aciclovir or not (fig 5.21). Indeed, there was a significant and similar reduction of culture medium HSV DNA abundance among microglia cells infected and treated with aciclovir alone or combined with dexamethasone compared to the infected untreated or treated only by dexamethasone (fig 5.21).

Altogether, this shows that dexamethasone (0.5 µM) has no positive effect on cell viability or viral load in HSV-1-infected microglia cells. These data also suggest that the beneficial effects of aciclovir combined to dexamethasone in HSV-1-infected microglial cells on cell viability and viral load (decrease in viral load) observed during light microscopy, WST-1 assay, DAD-1 qRT-PCR and HSV-1 DNA qPCR, similar to the ones due to aciclovir alone, are due to the inhibition of HSV-1 replication by aciclovir. However, these experiments showed that the administration of dexamethasone (0.5 µM) does not have a negative impact since it does not lead to an increase in cell death or higher viral load in HSV-1-infected microglial cells.

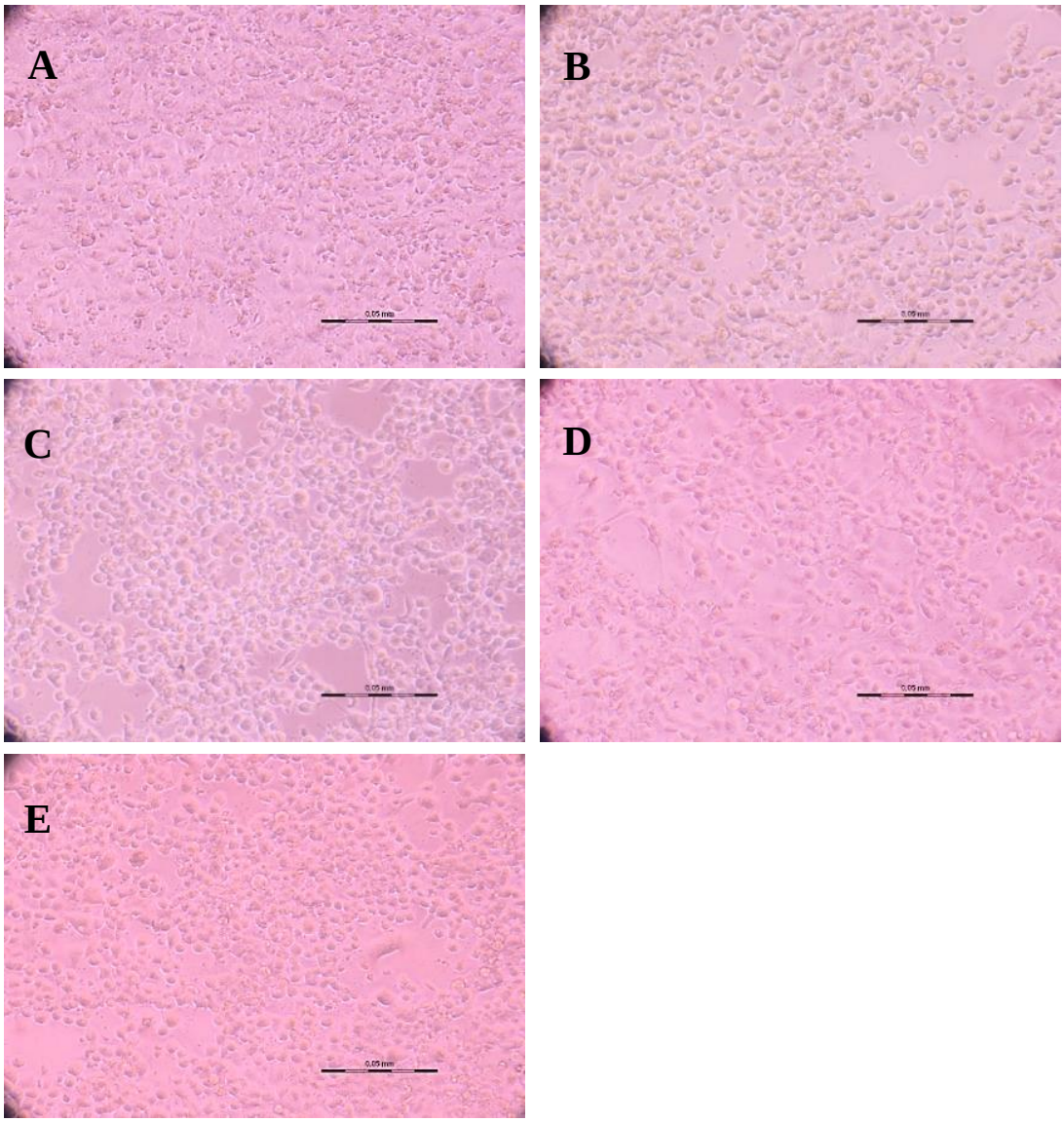

Figure 5.17. Microscopy pictures of HSV-1-infected microglial cells treated with a sub-toxic dose of dexamethasone (0.5 µM) alone or combined with aciclovir 48 h post-infection (24 h post-treatment). HSV-1-infection was done at MOI=0.01. Treatment was done with dexamethasone (0.5 µM) and/or aciclovir (20 µM) 24 h post-infection (pi). **(A) Uninfected microglial cells.** Most of the cells have the classic morphological features of microglial cells with ovoid or fibroblast-like shape and small ramifications. The confluency is around 90-100%. **(B) HSV-1-infected microglial cells untreated**. Big gaps, evidence of HSV-1-associated cell death, can be observed between cells (confluency around 60-70%) and a lot of cells are now round. **(C) HSV-1-infected microglial cells treated with dexamethasone.** The cell density is very similar to the one of infected untreated cells (B). **(D) HSV-1-infected-microglial cells treated with aciclovir.** The cell density is very similar to the one of infected untreated cells (B). **(E) HSV-1-infected-microglial cells treated with aciclovir and dexamethasone.** The cell density is very similar to the one of infected untreated cells (B). 10 x magnification.

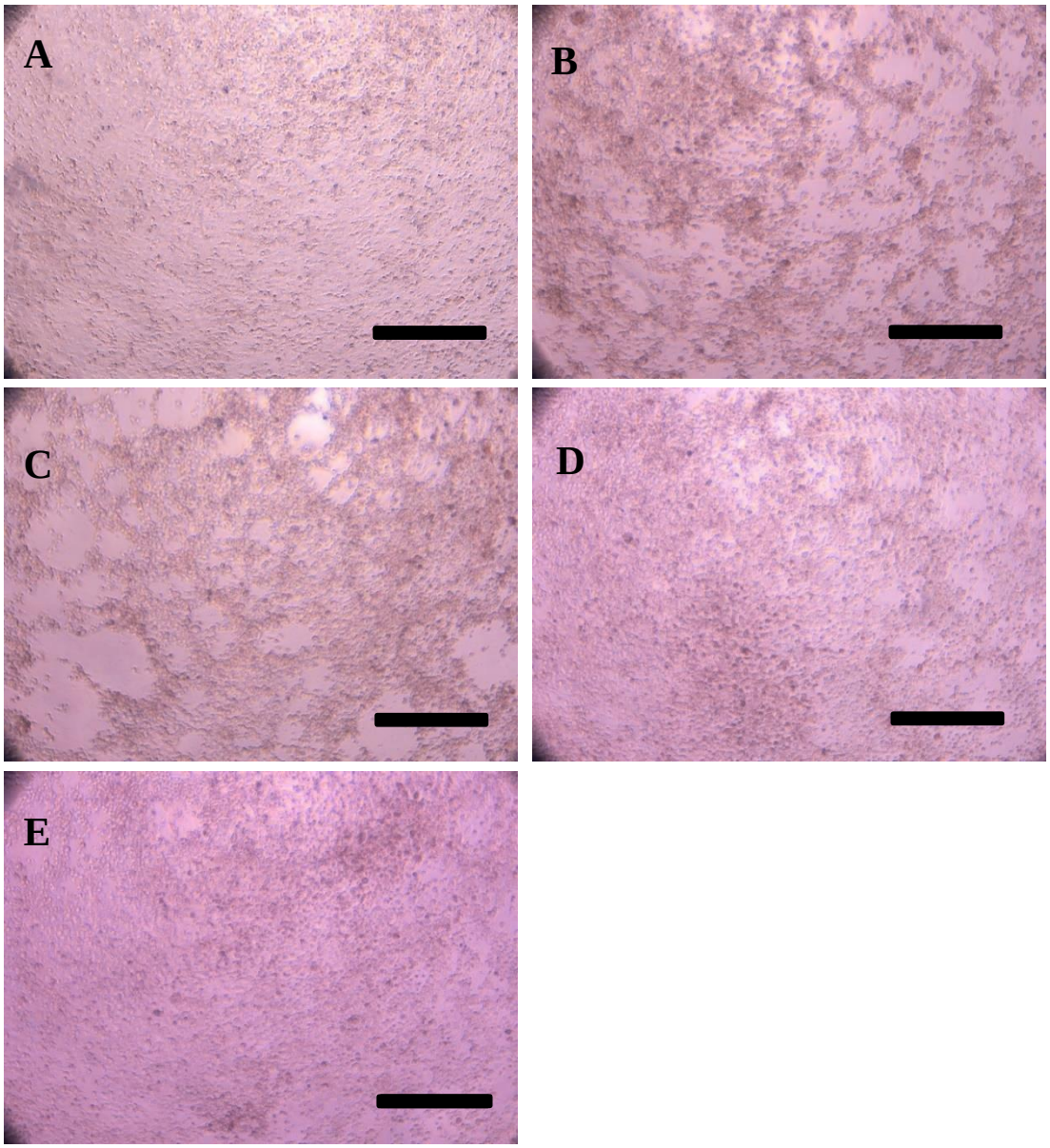

Figure 5.18. Microscopy pictures of HSV-1-infected microglia treated with a sub-toxic dose of dexamethasone (0.5 µM) alone or combined with aciclovir 72 h post-infection (48 h post-treatment). HSV-1-infection was done at MOI=0.01. Treatment was done with dexamethasone (0.5 µM) and/or aciclovir (20 µM) 24h post-infection (pi). **(A) Uninfected microglia.** The confluency is still around 90-100%. **(B) HSV-1-infected microglial cells untreated**. Many gaps have appeared between the cells, the confluency is now approximately 40-50%. **(C) HSV-1-infected microglial cells treated with Dexamethasone.** The confluency seems higher (60-70%) than in the picture (C). **(D) HSV-1-infected-microglia cells treated with aciclovir.** Only few gaps between cells can be seen (confluency seems around 80-90%). **(E) HSV-1-infected-microglial cells treated with aciclovir and dexamethasone.** The picture is similar to the one with aciclovir alone (D), with probably even less gaps between cells and slightly higher confluency. 4 x magnification. Scale bar: 125 µm.

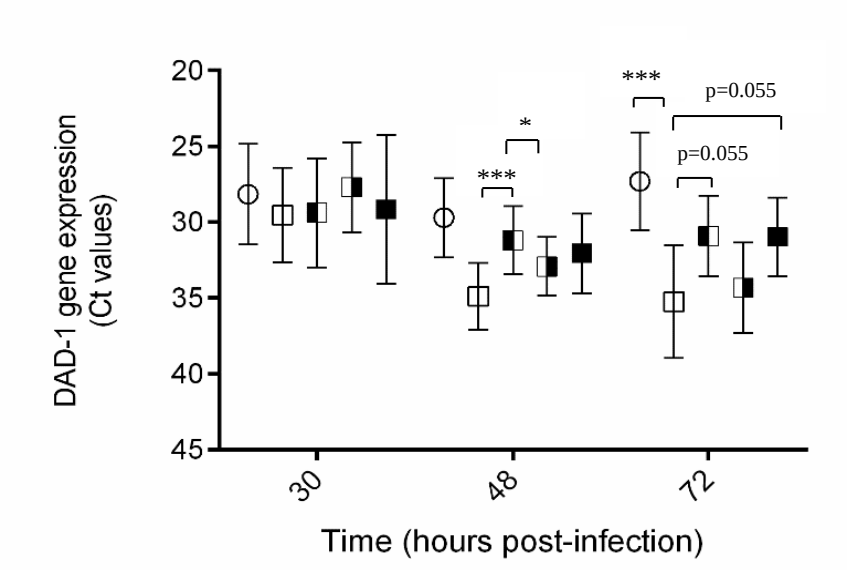

Figure 5.19. The effect of dexamethasone (0.5 µM) combined with aciclovir on DAD-1 gene expression in HSV-1-infected microglial cells. HSV-1 infection was done at MOI=0.01. The treatment with aciclovir (20 µM) and/or dexamethasone (0.5 µM) was done at 24 h pi. The values represent Ct values after qRT-PCR targeting DAD-1. qRT-PCR was performed from 1 µg of RNA extracts of uninfected (circles) or untreated infected (unfilled squares) or aciclovir-treated infected (squares half-filled in black on the left side) or dexamethasone-treated infected (squares half-filled in black on the right side) or "dexamethasone+aciclovir"-treated infected microglial cells at 30, 48, 72 h pi. Data are expressed as mean + 95% Confidence Interval (C.I) of 9 replicates from 3 independent experiments. ANOVA test showed statistical differences between the means of the different conditions at 48 h pi and 72 h pi ($p<0.005$) but not at 30 h pi ($p>0.05$). (*): $p<0,05$; (***) $p<0.005$ (multiple t-tests).

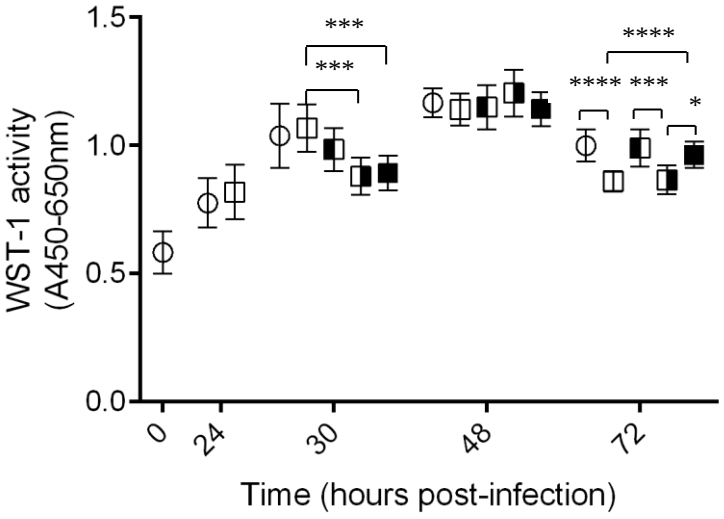

Figure 5.20. The effect of dexamethasone (0.5 µM) combined with aciclovir on mitochondrial activity in HSV-1-infected microglial cells. HSV-1-infection was done at MOI=0.01. The treatment with aciclovir (20 µM) and/or dexamethasone (0.5µM) was done at 24 h pi. The values represent values of WST-1 activity (absorbance at 450 nm (A450 nm) normalised by subtraction of the background (A650 nm)). WST-1 assay has been performed in uninfected (circles), untreated infected (unfilled squares) or aciclovir-treated infected (squares half-filled in black on the left side) or dexamethasone-treated infected (squares half-filled in black on the right side) or "dexamethasone+aciclovir"-treated infected (black squares) microglial cells at different time-points (0, 24, 30, 48 and 72h pi). Data are expressed as mean + 95% CI of 30 replicates from 3 independent experiments. ANOVA test showed statistical differences between the means of the different conditions at 30 h and 72 h pi ($p<0.001$) but not at 48 h pi ($p>0.05$). (*) $p<0.05$, (***) $p<0.005$, (****) $p<0.0001$ (multiple t-tests).

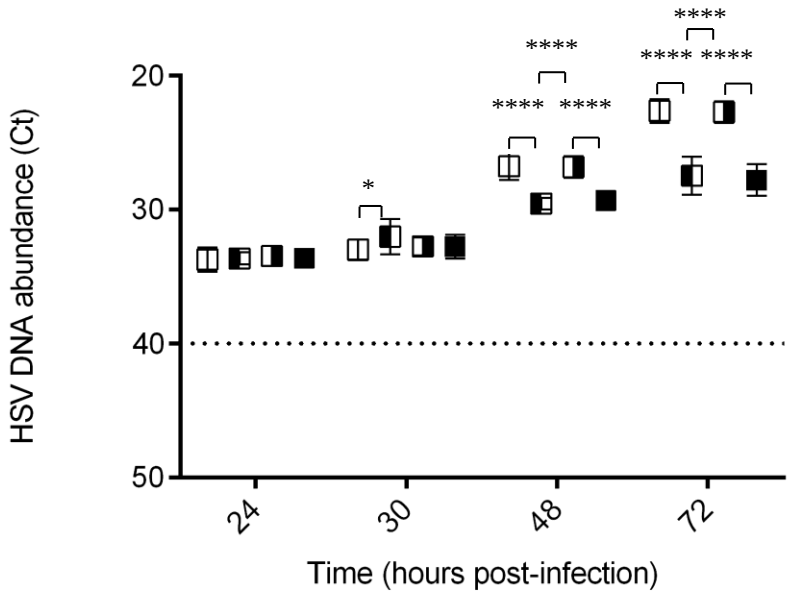

Figure 5.21. The effect of dexamethasone (0.5 µM) combined with aciclovir on HSV DNA abundance in culture medium of HSV-1-infected microglial cells. HSV-1-infection was done at MOI=0.01. The treatment with aciclovir (20uM) and/or dexamethasone was done at 24 h pi. The values represent Ct values after HSV DNA qPCR from culture medium of HSV-1-infected (white) or aciclovir-treated infected (squares half-filled in black on the left side) or dexamethasone-treated infected (squares half-filled in black on the right side) or "dexamethasone+aciclovir"-treated infected (black squares) microglial cells at 24 (just before the treatment), 30, 48 and 72 h pi. Each point represents the mean + 95% CI of data from at least 3 independent experiments. Triplicates were used for each point-time in each experiment. ANOVA test showed statistical differences between the means of the different conditions at 30 h ($p<0.05$), 48 h ($p<0.0001$) and 72 h pi ($p<0.0001$) but not at 24 h pi ($p>0.05$). (*): $p<0.05$; (****): $p<0.0001$ (multiple t-tests).

5.2.2.3.2. The effect of sub-toxic doses of dexamethasone combined with aciclovir on TNF relative gene expression in HSV-1-infected microglia cells

In chapter 3, an increase in TNF relative gene expression was observed in microglial cells following HSV-1-infection and in chapter 4, I could see that the treatment with aciclovir (20 µM) decreased TNF relative gene expression in infected microglia at 72 h pi. Here, I assessed the impact of the drug dexamethasone (0.5 µM) alone or combined with aciclovir (20uM) on TNF relative gene expression in these HSV-1-infected microglial cells.

At 48 h-72 h pi (24 h-48h post-treatment), there was still an increase in TNF relative gene expression in HSV-1-infected microglia treated with dexamethasone co-treated or not with aciclovir compared to the uninfected counterparts as observed with all the values much higher than one (fig 5.22). At 72 h pi, a significant decrease in TNF relative gene expression could be observed in HSV-1-infected microglial cells when treated with aciclovir alone or combined with dexamethasone compared to untreated. This was not the case for dexamethasone alone.

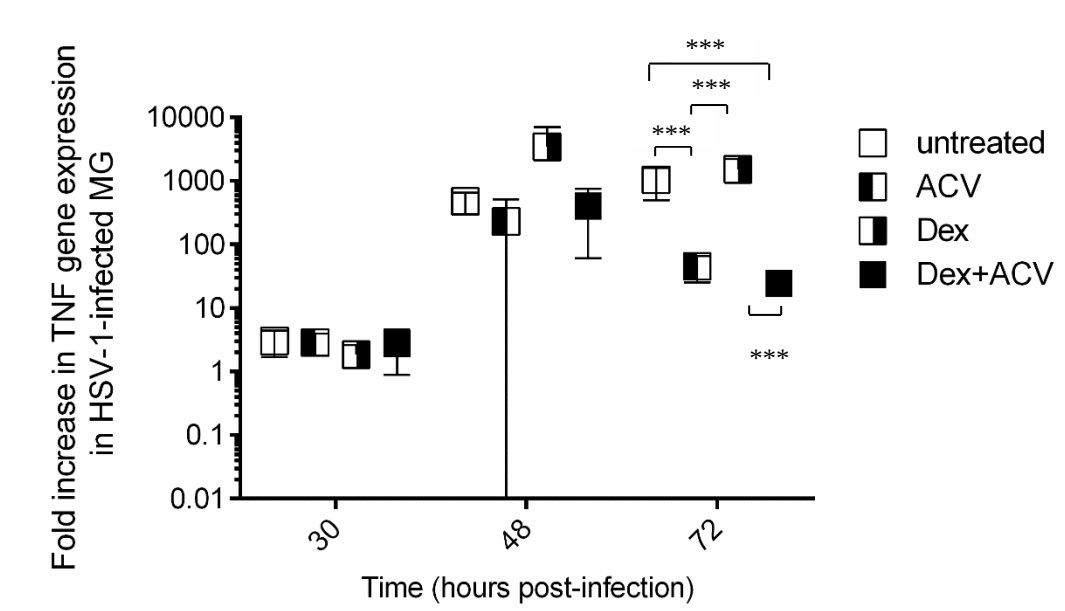

Figure 5.22. The effect of dexamethasone (0.5 µM) combined with aciclovir on TNF relative gene expression in HSV-1-infected microglial cells. HSV-1 infection was done at MOI=0.01 in microglial cells. The treatments with aciclovir (20 µM); dexamethasone (0,5 µM) or both were added at 24 h pi. The data represent TNF relative gene expression expressed as mean +/- 95% CI of $2^{-\Delta\Delta Ct}$ values at 30 h, 48 h and 72 h post-infection (respectively 6 h, 24 h and 48 h post-treatment). The scale is logarithmic. $2^{-\Delta\Delta Ct}$ values were obtained following qRT-PCR of TNF and DAD-1 genes. DAD-1 gene was used as reference (housekeeping) gene. From qRT-PCR Ct values of DAD-1 and TNF, ΔCt values [Ct (TNF)-Ct(DAD-1]) were obtained for both uninfected and HSV-1-infected cells (untreated, treated with aciclovir, dexamethasone or both). For each condition (untreated, aciclovir, dexamethasone or both), ΔΔCt values represented $[(\Delta Ct)_{HSV+/-treatment} - (\Delta Ct)_{uninfected}]$. Data were obtained from 3 independent experiments. ANOVA test showed statistical differences at 72h pi ($p<0.0001$) but not at 30 h ($p>0.05$) and 48 h pi ($p>0.05$) between the means of the different conditions. (***): $p<0,001$ (multiple t-tests).

5.3. Discussion

Herpes Simplex Encephalitis (HSE) pathogenesis is due to both HSV replication and subsequent detrimental immune responses[71, 94, 93, 131, 91, 133]. However, the therapy that is clinically used is the antiviral aciclovir. Hence, combining an anti-inflammatory drug with aciclovir may improve HSE patient outcome. Several clinical studies on HSE patients have already shown that some immunosuppressive drugs belonging to the glucocorticoids, including dexamethasone, were predictors of good outcome and reduced oedema in adults and decreased morbidity in children[158, 132, 160]. However, more data especially from bigger clinical studies, are needed to validate the positive impact of dexamethasone as HSE adjuvant therapy. Before this PhD project, there were no *in vitro* data detailing the effect of dexamethasone on specific HSV-1-infected-human brain cell type such as human neuron-like cells (neuroblastomas) or microglia cells. Therefore, it was of main interest to assess the effect of dexamethasone combined to aciclovir on cell survival and viral load in HSV-1-infected neuroblastoma and microglial cells.

Firstly, dexamethasone toxicity was studied by light microscopy and the LD50, Lethal Dose 50% (dose for which a chemical induces 50% of cell death in a tissue) was valued at 0.5-1 mM in neuroblastoma cells, microglia and primary astrocytes (fig 5.2-5.8). Hence, below 0.5 mM, dexamethasone was not seen as toxic for these brain cells. One study has concluded that the brain tissue concentration of dexamethasone used to effectively treat patients suffering from glioblastomas was one thousand time lower than the LD50 from *in vitro* studies[161]. Another study investigating an *in vitro* model of bacterial meningitis, showed that a concentration of dexamethasone of 0.5 µM had a beneficial effect on a LPS-challenged co-culture of microglia and astrocytes[156]. Altogether, a 0.5 µM concentration of dexamethasone appeared to be the most relevant dose to use for assessing the effect of this drug, combined with aciclovir, in HSV-1-infected brain neuroblastoma and microglial cells. The dose of dexamethasone used in

HSE clinical studies is around 40 mg/day[159]. This matches with a concentration of 20 µM in the bloodstream (depending on the blood brain barrier permeability, only proportion of this 20 µM of dexamethasone will penetrate the brain parenchyma).

In light microscopy, an apparent increase in infected neuroblastoma (at 48 h and 72 h pi) and microglial cell (at 72 h pi) viability could be observed after treatment with aciclovir alone or combined with dexamethasone (0.5 µM) (but not with dexamethasone alone) (fig 5.9-10 and fig 5.18). Crucially, dexamethasone alone (0.5 µM) was not detrimental and did not induce more visible cell damage in infected microglial (at 72 h pi) and neuroblastoma cells (at 48 h and 72h pi) (fig 5.9-10 and fig 5.18).

Dexamethasone (0.5 µM) alone had no impact in mitochondrial activity, proxy marker of cell viability, following HSV-1-infection, both in neuroblastoma and microglial cells as observed using WST-1-assays (fig 5.13 and fig 5.20). Nevertheless, dexamethasone (0.5 µM) combined with aciclovir (20 µM) was associated with an increase in mitochondrial metabolism similar to that induced by aciclovir alone both in HSV-1-infected neuroblastomas at 48 h and 72 h post-infection (pi) (24 h and 48 h pt) and in infected microglia cells at 72 h pi (48 h pt) ($p<0.0001$).

In HSV-1-infected neuroblastoma cells, these WST-1 results were confirmed by another quantitative technique assessing cell viability at 72 h pi (48 h pt) using the software "ImageJ" to measure the area of attached cells from microscopy pictures (fig 5.11). Indeed, bigger attached cell areas were significantly measured at 72 h pi (48 h pt) for infected neuroblastoma cells treated with aciclovir alone or combined to dexamethasone but not for infected cells untreated or treated with dexamethasone alone ($p<0.05$). The issue of sensibility of qRT-PCR targeting DAD-1 had already been raised in the previous chapter and here again, no differences could be seen in DAD-1 Ct values between HSV-1-infected neuroblastoma cells untreated or treated with dexamethasone, aciclovir or both (fig 5.12).

In HSV-1-infected microglial cells, the WST-1 results showing a microglia cell viability increase due to the treatments "aciclovir/dexamethasone" or aciclovir alone 72 h after HSV-1-infection (48 h pt) was confirmed by qRT-PCR targeting DAD-1 ($p=0.055$) despite the low sensitivity of this technique (fig 5.19). Unfortunately, there were not enough 4 x magnification microscope pictures of quality to use the software "ImageJ" for quantification of attached microglia cell areas.

In an *in vivo* mice model of HSE, a decrease in brain inflammation was observed following dexamethasone administration[137]. Another mice *in vivo* study showed a decrease in MRI brain abnormalities of HSE affected mice with the dual treatment aciclovir and the glucocorticoid methylprednisolone compared to aciclovir therapy alone[131]. Moreover, few small clinical and animal studies reported a beneficial impact of the administration of glucocorticoids as adjuvant therapy to HSE[158, 132, 128, 129, 131]. The administration of the glucocorticoid dexamethasone in my *in vitro* models of HSE in single culture did not show such beneficial effects on brain cell viability although not detrimental either. More complex HSE *in vitro* models associating different brain cells, a longer time of infection (using lower MOI) would be interesting to be closer to *in vivo* conditions and reassess dexamethasone effect.

Following HSV-1-infection in primary astrocytes, changes in mitochondrial activity coded by mitochondrial genes have been shown early and prior to nuclear gene expression-coded modifications and cell death[63]. In astrocytes, this may suggest overall that HSV-1 firstly leads to changes in mitochondria activity that could be detected by WST-1 assay and afterwards other metabolic changes causing cell death that can be detected by microscopy or qRT-PCR targeting DAD-1. This may also be the case for neuroblastoma cells as WST-1 assay demonstrated an increase in neuroblastoma mitochondrial activity as early as 48 h pi (24 h pt) while cell viability loss could not be properly seen before 72 h pi (48 h pt) by light microscopy analysis.

At the level of HSV load, it was also shown that aciclovir and aciclovir combined with dexamethasone but not dexamethasone alone were associated with a decrease in viral load in HSV-1-infected neuroblastoma and microglial cells (fig 5.15 and 5.21 respectively). This suggests that the combination aciclovir/dexamethasone has an inhibitory effect on HSV-1 load only driven by the action of aciclovir. Crucially, dexamethasone alone did not induce any exacerbation of HSV-1 load either brain cell types. This is in agreement with a study of Thompson *et al*., demonstrating that dexamethasone did not exacerbate HSV-1 replication and dissemination in HSE-affected rat (infection into the cervical vagus nerve with 10^5 plaque-forming units (pfu)) brain both when administered alone or combined with aciclovir[162].

Altogether, the results of this chapter revealed that (i) the combination aciclovir/dexamethasone had a positive impact on cell survival of HSV-1-infected neuroblastoma and microglial cells probably only due to the inhibitory effect of aciclovir on viral load and that (ii) the addition of dexamethasone did not lead to any negative impact on either brain cell viability or viral load in these models. The latter point is clinically interesting as the addition of dexamethasone or other anti-inflammatory drugs for treatment of viruses-infected brain cells is quite controversial. Indeed, there is a fear by some clinicians that the administration of such anti-inflammatory drugs would exacerbate viral replication and hence brain cell damage.

Interestingly, it has also been shown that dexamethasone alone, or combined with aciclovir, maintained high levels of TNF relative gene expression in HSV-1-infected microglia and neuoblastoma cells compared to the basal level in uninfected (untreated) cells (fig 5.16 and fig 5.22). However, the comparison of TNF relative gene expression between infected cells untreated and infected cells treated with dexamethasone, aciclovir or both revealed differences between brain cell types.

In HSV-1-infected neuroblastoma cells, dexamethasone alone, or combined with aciclovir did not lead to any significant difference in TNF relative gene expression compared to the (infected) untreated at 48-72 h pi (24-48 h pt) (fig 5.16). However, aciclovir alone was associated, at 72 h pi (48 h post-treatment), with a significant increase in TNF relative gene expression in infected neuroblastoma cells. Both aciclovir and aciclovir combined to dexamethasone increased cell viability, and in a similar way, following HSV-1 infection. However, they differently influenced TNF relative gene expression. This suggests that TNF relative gene expression does not seem to be a useful predictor of HSV-1-infected neuroblastoma cell viability/death in my *in vitro* model.

In microglial cells, aciclovir alone and combined to dexamethasone was associated with a decrease in TNF relative gene expression in infected cells compared to infected cells untreated at 72 h pi (fig 5.22). At this same time-point, dexamethasone alone seemed to induce a slight but not significant increase in TNF relative gene expression in infected microglia cells. Of note, another *in vitro* study using HSV-1-infected murine microglial cells showed that dexamethasone induced a decrease in TNF-α protein release in HSV-1-infected BV2 microglia cell supernatant[137]. This difference with my results may be explained either by the fact human microglial cells were not used in this study or because a decrease in protein release could lead to a feedback-loop increasing TNF gene expression.

To conclude, dexamethasone has no additive benefit with aciclovir in my model. Crucially, it is not harmful in either HSV-1-infected neuroblastoma or microglial cells both in terms of cell viability and HSV-1 load. The latter point may be another argument for clinicians to be less worried about administrating dexamethasone in combination with aciclovir in HSE patients. However, its action has still to be tested in more complex systems, closer to *in vivo* conditions of brains affected by HSE. Such systems could consist of several HSV-1-infected brain cells

simultaneously and include peripheral immune cells such as peripheral macrophages and T-cell.

In the next chapter, another candidate as adjuvant therapy to aciclovir in HSE, the anti-TNF Infliximab, was assessed in HSV-1-infected neuroblastoma and microglial cells.

Chapter 6 The effect of Infliximab on HSV-1 infection in human brain cells

6.1. Introduction

Herpes Simplex Encephalitis (HSE) is a lethal disease characterised by brain inflammation due to both HSV-induce damage and subsequent detrimental immune responses[71, 94, 131, 93, 130]. The gold standard therapy is the antiviral drug aciclovir. Aciclovir only targets viral replication and has limitations as a treatment as demonstrated by the fatal outcome in 8-20% of HSE patients and a high percentage of neurological sequelae among survivors[163, 127, 53, 39]. A few small clinical studies and *in vivo*/*in vitro* works have suggested that the use of anti-inflammatory drugs, especially glucocorticoids, as adjuvant therapy to aciclovir in HSE could be potentially beneficial for patients[132, 115, 130, 131, 133]. This effect could possibly be due to their inhibitory action on this detrimental immune response[132, 115, 130, 131, 133]. However, this effect has not been confirmed in clinical trials or verified in *in vitro* models of HSE using different human brain cell types such as neuroblastoma or microglial cells. In the previous chapter, I have assessed the effect of the glucocorticoid drug dexamethasone combined with aciclovir on cell viability, viral replication, TNF gene expression and mitochondrial activity in these HSV-1-infected brain cells. I found that adding dexamethasone to aciclovir did not have any impact on cell survival, mitochondrial activity or viral replication in both HSV-1-infected neuroblastoma and microglial cells.

TNF-α protein levels have been found to be elevated in the cerebrospinal fluid (CSF) of HSE patients[71]. High CSF TNF levels are observed during the convalescence stage of illness. These findings suggest a detrimental immune response may persist after the acute phase and contributes to neurological sequelae. Furthermore, in chapter 3, I saw a significant increase in TNF relative gene expression but not in TNF protein extra-cellular production at 24 h-72 h

post-infection (pi) in human microglial and neuroblastoma cells following HSV-1 infection at MOI=0.01. However, an *in vitro* study of Lokensgard *et al.* using a higher MOI (MOI=1) showed that a high concentration of TNF proteins was released by purified human foetal microglia, but not by astrocytes or neurons 24 h-72 h after HSV-1-infection[85]. In this same study, HSV-1 was also associated with a significant increase in TNF mRNA expression (observed by RNase protein assay) in human foetal microglia from 3 to 24 h post-infection (pi) and peaking and 8 h pi. Lokensgard *et al.* also showed, in another study, by real-time qPCR a 600-fold increase in TNF gene expression following HSV-1 infection in murine microglia cells at 5 h pi and at MOI=2[86]. These two studies used different microglial cells (murine and human foetal), a higher MOI and earlier time-points than the ones I have used in my experiments making direct comparisons difficult. However, in common, with my experiments, they all showed an increase in TNF gene expression following HSV-1-infection of microglial cells. Altogether, TNF expression could be associated with a HSV-1-induced pro-inflammatory response especially in microglia. It may represent a target for an adjuvant therapy to use combined with aciclovir to improve HSE treatment. Crucially, a murine *in vivo* study showed that combining the antiviral valacyclovir and the anti-TNF etanercept, significantly increased mice survival after HSV-1 infection compared to untreated counterparts or mice treated with only one of these two drugs [133].

TNF combined with aciclovir has never been studied in clinical or *in vitro* studies using human brain cells. In this new chapter, an anti-inflammatory drug from the TNF inhibitors family, infliximab, was assessed as adjuvant therapy to aciclovir in *in vitro* models of HSE. TNF inhibitors such as infliximab (but also etanercept, adalimumab and certolizumab) are used to treat a wide range of inflammatory conditions. These inflammatory conditions include rheumatoid arthritis, psoriasis, ankylosing spondylitis, Crohn's disease, ulcerative colitis etc. Of note, a few clinical case reports have suggested HSE could sometimes be induced by TNF inhibitor treatments in patients suffering from rheumatologic disorders[164 165]. This may be due

to a potential effect of TNF inhibitors on reactivating HSV from latency within nerves. However, using TNF inhibitors to treat HSE once inflammation has already affected the brain could result in different observations and may be beneficial.

Infliximab targets not only soluble TNFα but also transmembrane TNFα. As a result, transmembrane TNF, which was not measured by the ELISA tests performed in the chapter 3, may be increased within the membrane of neuroblastoma and microglial cells following HSV-1-infection..

The main goal of chapter 6 is to determine if infliximab alone or combined with aciclovir has an impact on cell survival, mitochondrial metabolism, viral load and TNF gene expression in both HSV-1-infected-microglial and neuroblastoma cells compared to infected cells treated by aciclovir alone or untreated.

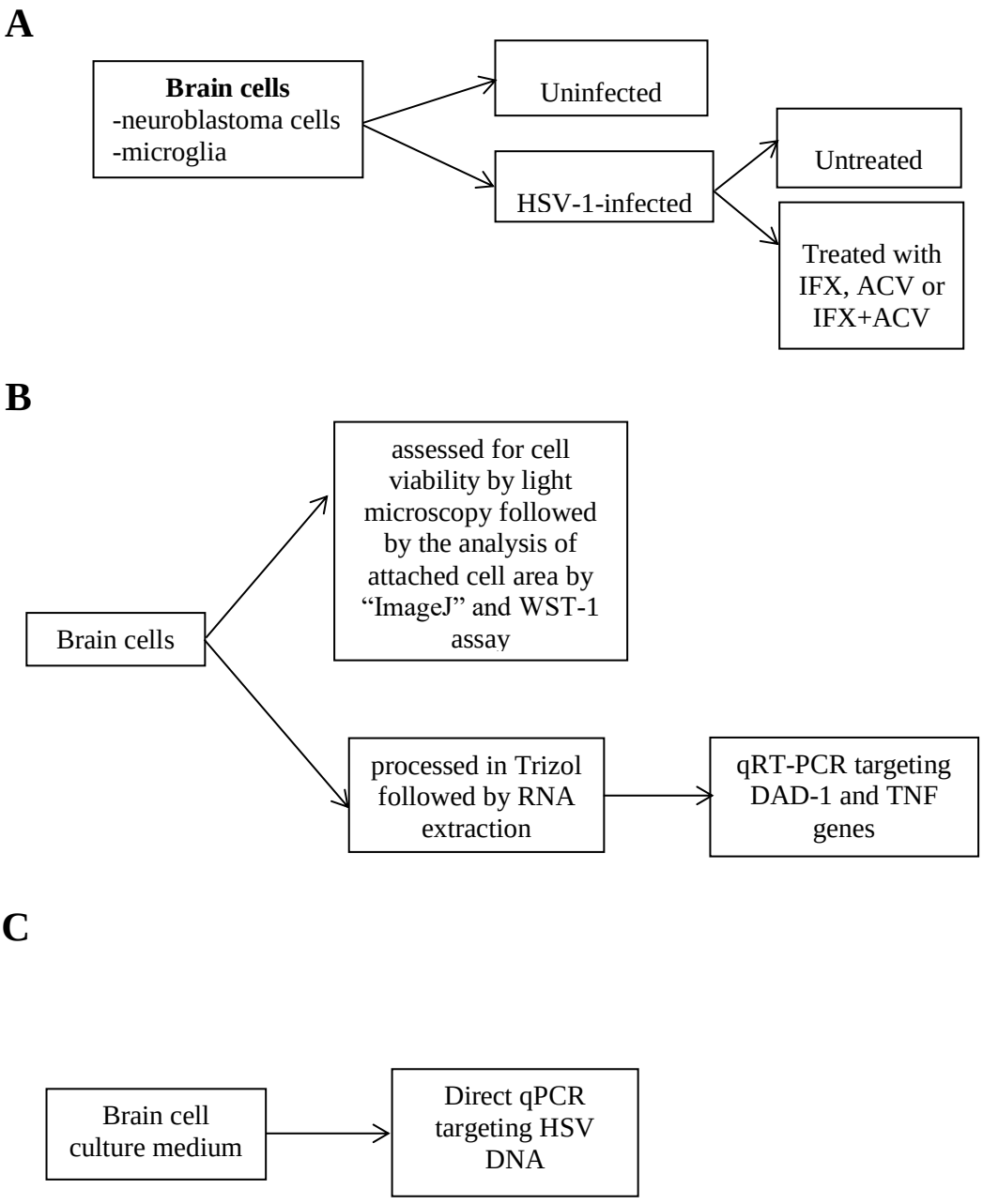

Figure 6.1. Experimental design for assessing the effect of Infliximab (IFX) alone or combined to aciclovir (ACV) in HSV-1-infected human neuroblastoma and microglial cells. (**A)** Brain cell populations used. **(B)** Techniques performed on brain cells following HSV-1-infection. **(C)** Technique performed on brain cell culture medium following HSV-1-infection.

6.2. Results

6.2.1. Effect of infliximab combined to aciclovir in HSV-1-infected neuroblastoma cells

6.2.1.1. Infliximab alone (from 0.5 mg/ml) partially rescues HSV-1-infected neuroblastoma cells

Firstly, the effect of infliximab alone at a wide range of concentrations (0.01 to 1 mg/ml) was assessed in HSV-1-infected neuroblastoma cells by light microscopy. From 0.01 mg/ml (data not shown) to 0.1 mg/ml (fig 6.2C), there was no improvement in infected cell survival in comparison to infected cells untreated at 48 h post-treatment (48 h pt). However, infliximab at 0.5 mg/ml (fig 6.2D) and 1 mg/ml (fig 6.2E) was associated with a rise of HSV-1-infected-neuroblastoma viability as shown by the visible increase in the proportion of live cell still attached at this same time-point. Since similar beneficial effects were seen for infliximab at both concentrations, it was decided to continue experiments using the lowest concentration (0.5 mg/ml). In uninfected cells, no signs of toxicity could be observed at any concentrations of infliximab tested (up to 1 mg/ml) (data not shown).

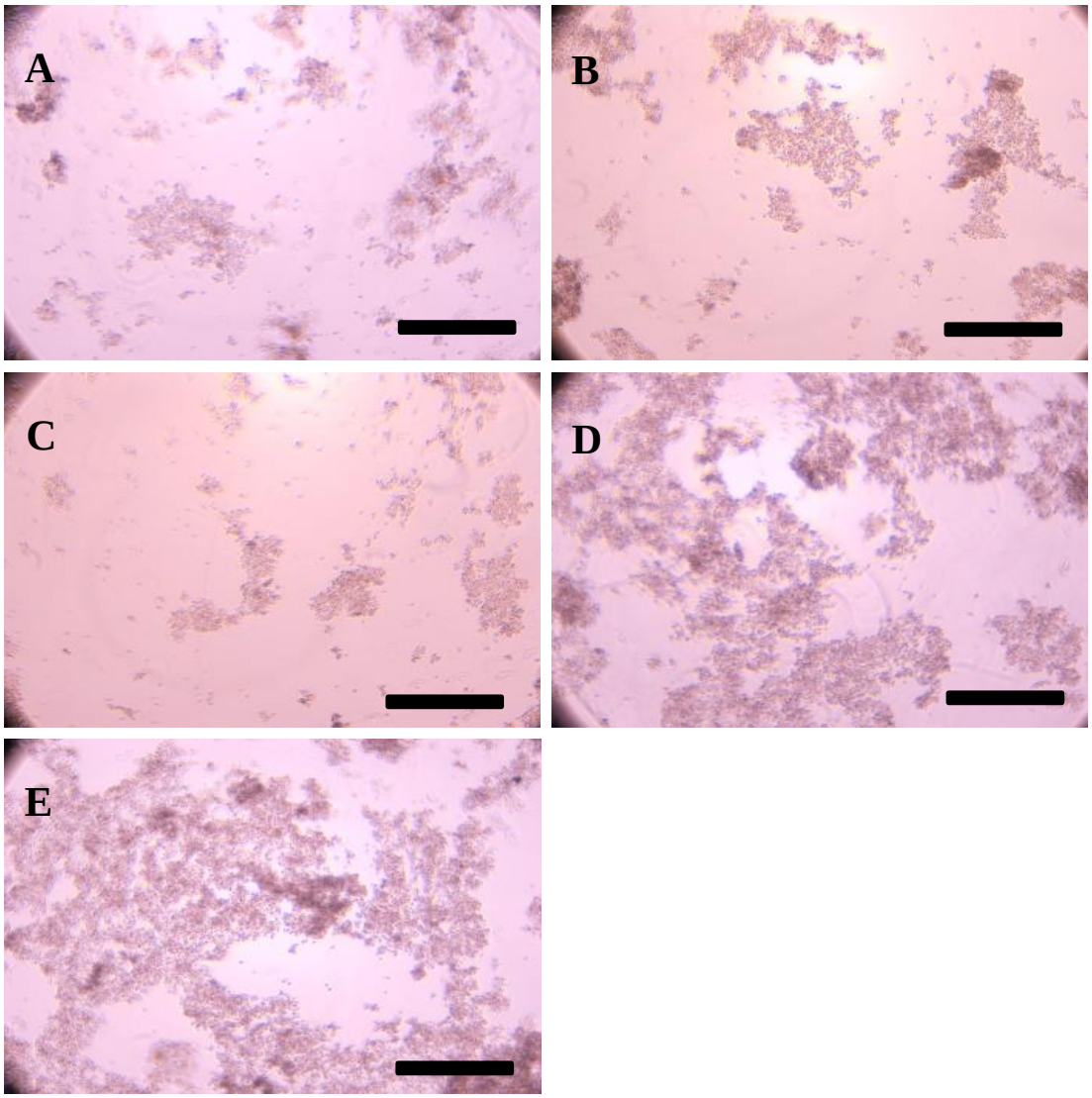

Figure 6.2. Microscopy observations of HSV-1-infected neuroblastoma cells treated with various doses of infliximab at 72 h post-infection (48 h post-treatment). HSV-1-infection was done at MOI=0.01. Treatment with infliximab was performed at different concentrations (0.05-1 mg/ml) 24 h post-infection (pi). Pictures were taken at 72 h pi (48 h pt) and are representative of multiple replicates for each condition. **(A) HSV-1-infected neuroblastoma cells untreated.** Extensive live cell loss has happened, only few live cells are still attached (around 10%). **(B) HSV-1-infected neuroblastoma cells treated with infliximab at 0.05 mg/ml**. Extensive live cell loss has happened, only few live cells are still attached (around 10%). **(C) HSV-1-infected neuroblastoma cells treated with infliximab at 0.1 mg/ml**. Extensive live cell loss has happened, only few live cells are still attached (around 10%). **(D) HSV-1-infected neuroblastoma cells treated with infliximab at 0.5 mg/ml**. More cells survived (around 40%) compared to those in pictures (A-C). **(E) HSV-1-infected neuroblastoma cells treated with infliximab at 1 mg/ml**. More cells survived (around 50%) compared to those in pictures (A-C). 4 x magnification. Scale bar: 125 µm.

6.2.1.2. Effect of infliximab alone and combined with aciclovir on TNF gene expression in HSV-1-infected neuroblastoma cells

In chapter 3, an increase in TNF relative gene expression was observed in neuroblastoma cells following HSV-1-infection. In chapter 4, treatment with aciclovir (20 µM) increased TNF relative gene expression in infected neuroblastoma cells beyond that seen in HSV-1-infected cells alone (72 h pi). Here, I have assessed the impact of the anti-TNF drug infliximab (0.5 mg/ml) alone or combined with aciclovir (20 µM) on TNF relative gene expression in HSV-1-infected neuroblastoma cells. TNF relative gene expression is based on the TNF absolute gene expression (data non shown) normalised by DAD-1 absolute gene expression (fig 6.3). Of note, there was still an increase in TNF relative gene expression in HSV-1-infected neuroblastoma cells treated with infliximab co-treated or not with aciclovir compared to the uninfected counterparts as observed with all the values much higher than one (30-72 h pi) (fig 6.4).

This increase in TNF relative gene expression compared to uninfected was quite similar between HSV-1-infected neuroblastoma cells untreated, treated with infliximab, aciclovir or both at 30 h pi (6 h pt) and 48 h pi (24 h pt). At 72 h pi, in infected neuroblastoma cells, aciclovir led to a higher increase in TNF relative gene expression compared to the other treatments ($p<0.05$).

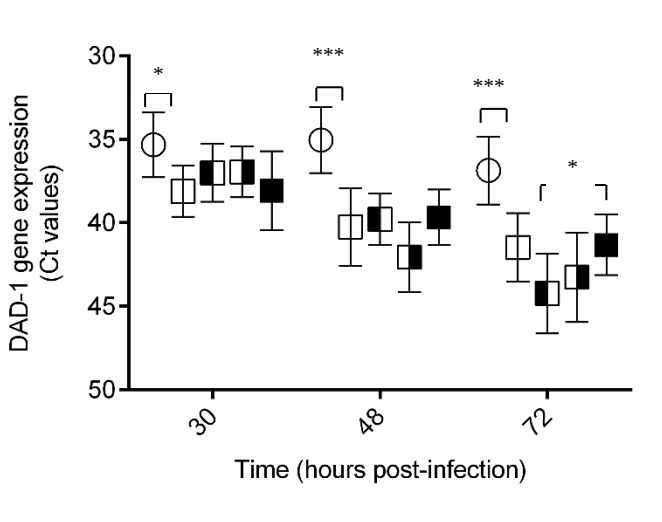

Figure 6.3. The effect of infliximab alone and combined with aciclovir on DAD-1 absolute gene expression in HSV-1-infected neuroblastoma cells. HSV-1 infection was done at MOI=0.01. Treatment with aciclovir (20 µM) and/or infliximab (0.5 mg/ml) was done at 24 h pi. Absolute DAD-1 gene expression in uninfected (circles) or infected untreated (unfilled squares) or aciclovir-treated infected (squares half-filled in black on the left side) or infliximab-treated infected (squares half-filled in black on the right side) or "infliximab+aciclovir"-treated infected (black squares) neuroblastoma cells at 30, 48 and 72 h pi. Data are expressed as the mean of qRT-PCR DAD-1 Ct values + 95% CI and were obtained from 3 independent experiments, each condition being assessed in triplicate. ANOVA test statistically showed differences between the means of the different conditions at 48h ($p<0.0001$) and 72h pi ($p<0.0001$) but not at 30 h ($p>0.05$). (*) $p<0.05$; (***) $p<0.005$ (multiple t-tests).

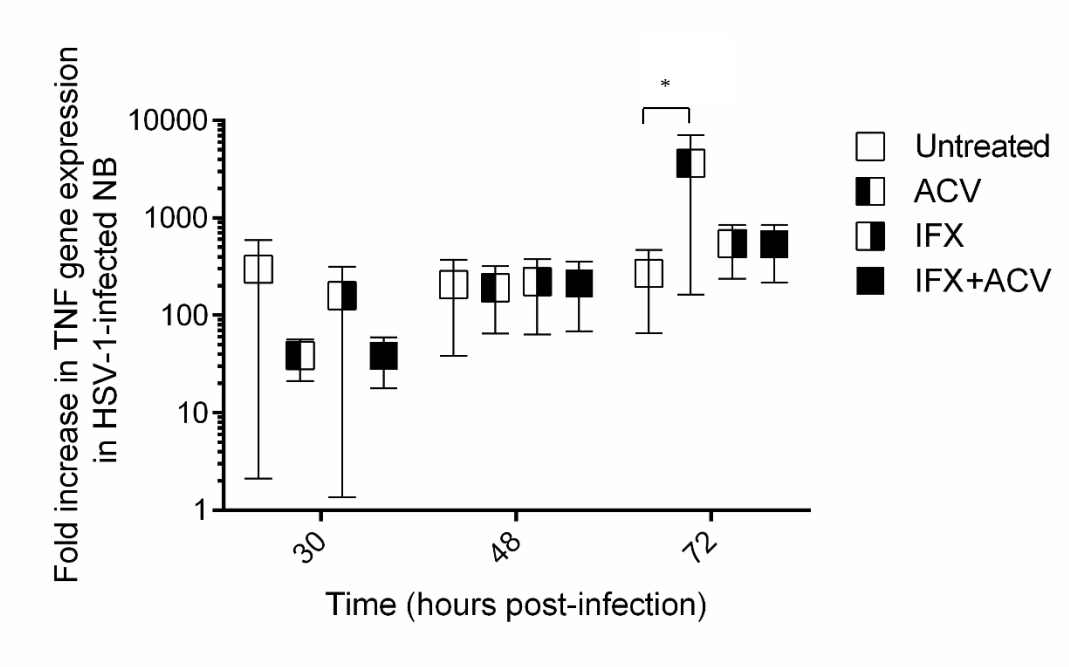

Figure 6.4. The effect of infliximab (0.5 mg/ml) alone or combined with aciclovir on TNF relative gene expression in HSV-1-infected neuroblastoma cells. HSV-1 infection was done at MOI=0.01 in neuroblastoma cells. The treatments with aciclovir (20 µM); infliximab (0,5 mg/ml) or both were added at 24 h pi. The data represent TNF relative gene expression expressed as mean +/- 95% CI of $2^{-\Delta\Delta Ct}$ values at 30 h, 48 h and 72 h post-infection (respectively 6 h, 24 h and 48 h post-treatment). The scale is logarithmic. $2^{-\Delta\Delta Ct}$ values were obtained following qRT-PCR of TNF and DAD-1 genes. DAD-1 gene was used as reference (housekeeping) gene. From qRT-PCR Ct values of DAD-1 and TNF, ΔCt values [Ct (TNF)-Ct(DAD-1]) were obtained for both uninfected and HSV-1-infected cells (untreated, treated with aciclovir, infliximab or both). For each condition (untreated, aciclovir, infliximab or both), ΔΔCt values represented $[(\Delta Ct)_{HSV+/-treatment} - (\Delta Ct)_{uninfected}]$. ANOVA test statistically showed significant differences between the means of the different conditions at 72 h pi ($p<0.005$) but not at 30 h ($p>0.05$) and 48 h pi ($p>0.05$). Data were obtained from 3 independent experiments. (*): $p<0,05$ (multiple t-tests).

6.2.1.3. Effect of infliximab alone and combined with aciclovir on cell viability, mitochondrial metabolism and viral replication in HSV-1-infected neuroblastoma cells

Microscopy studies confirmed that infliximab at 0.5 mg/ml alone led to an increased cell survival of HSV-1-infected neuroblastoma cells both at 48 h and 72 h post-infection (24 h and 48 h post-treatment (pt)) (fig 6.5 and 6.6). The same beneficial effect was also noticed with aciclovir (20 µM) alone at both time-points confirming the results of the chapter 4. However, at 72 h pi, treatment with aciclovir increased infected cell survival at a higher level than infliximab therapy alone (fig 6.6). Following HSV-1-infection, a higher proportion of cells with uninfected neuroblastoma cell features, such as fibroblast-like morphology, could be observed in presence of infliximab and/or aciclovir but not in the untreated infected populations at 48 h pi (fig 6.5). Finally, the impact of infliximab combined with aciclovir on HSV-1-infected neuroblastoma cells appeared similar to that of aciclovir alone. Co-treatment led to (i) an increase in infected neuroblastoma viability similar to that observed after aciclovir monotherapy at 48 h and 72 h pi; and (ii) a partial preservation of fibroblast-like morphology in the infected cells at 48 h pi (fig 6.5 and 6.6).

Analysing multiple microscopy pictures at 4 x magnification using the software "ImageJ" also showed that the attached cell area was significantly bigger in infected cells treated by aciclovir, infliximab or both than in infected cells untreated at 48 h pi (fig 6.7) ($p<0.05$ or $p<0.01$). At 72 h pi, only HSV-1-infected neuroblastomas treated with aciclovir alone or combined with infliximab, but not infected cells treated with infliximab alone (although the same trend was also observed), presented significantly bigger areas of attached cells compared to infected untreated cells following statistical analysis (fig6.7) ($p<0.05$).

At 48-72 h pi, treatment with aciclovir, infliximab or combination of both, was shown to significantly increase mitochondrial activity of HSV-1-infected neuroblastoma cells, as demonstrated by the WST-1 assay (fig 6.8). However, this was much more significant with

aciclovir alone or combined with infliximab than with infliximab monotherapy ($p<0.0001$). Furthermore, dual therapy did not lead to a higher WST-1 activity than aciclovir alone, but a similar one.

Surprisingly, a direct HSV DNA qPCR from culture medium of infected neuroblastoma cells showed that infliximab alone or combined to aciclovir but not aciclovir alone was associated with a significant decrease in HSV DNA abundance (6-48 h pt) (fig 6.9) ($p<0.001$ or $p<0.0001$). The decrease in viral load was similar between cells treated with infliximab alone or combined with aciclovir.

Altogether, this suggests that infliximab increases cell viability and mitochondrial metabolism following HSV-1-infection, possibly by reducing viral load. However, although its antiviral effect seems to be more rapid than aciclovir in this brain cell type, aciclovir led to a much higher levels of mitochondrial activity and to a higher survival of HSV-1-infected neuroblastoma cells compared to the effect of infliximab alone. Finally, the combination "aciclovir/infliximab" led to similar effects than aciclovir alone on cell survival and mitochondrial metabolism (fig 6.5-6.8).

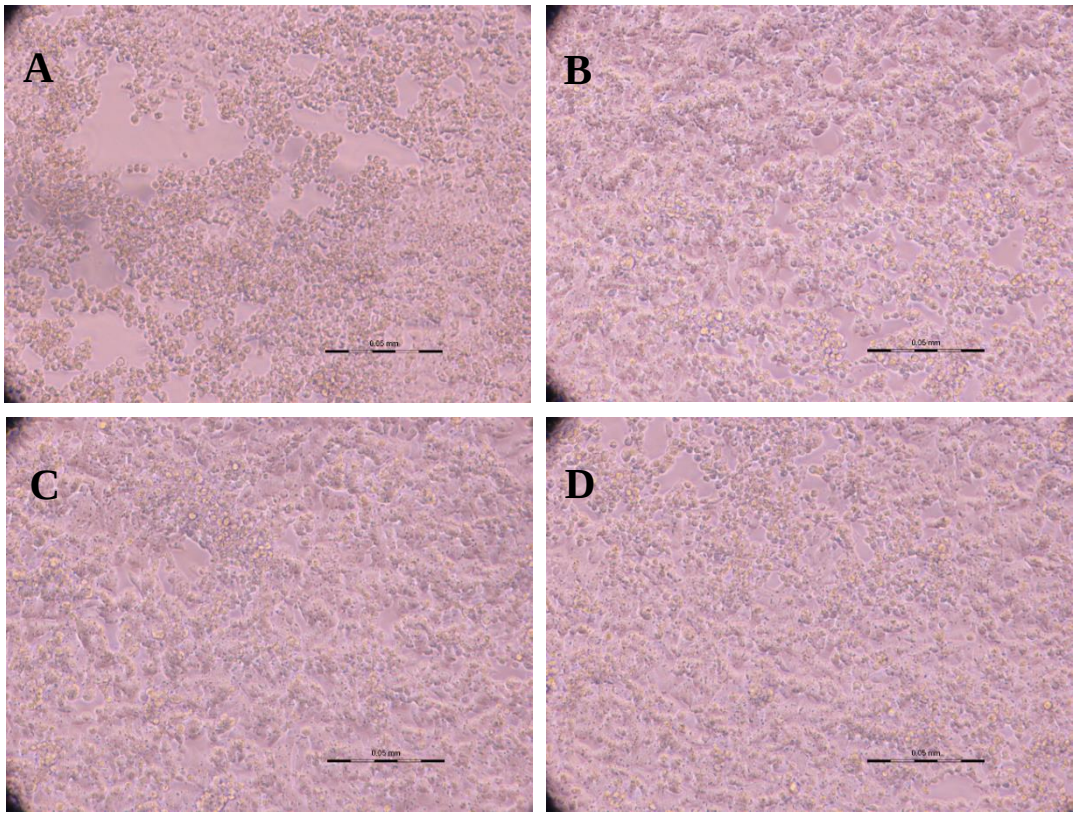

Figure 6.5. Microscopy pictures of HSV-1-infected neuroblastoma cells treated with infliximab (0.5 mg/ml) alone or combined with aciclovir at 48 h post-infection (24 h post-treatment). HSV-1-infection was done at MOI=0.01. Treatment was done with infliximab (0.5 mg/ml), aciclovir (20 µM) and infliximab combined with aciclovir 24 h post-infection (pi). Pictures were taken 48 h pi (24 h post-treatment). **(A) HSV-1-infected neuroblastoma cells untreated.** Big gaps have appeared in the monolayer (around 60% confluent) and all cells look round. **(B) HSV-1-infected neuroblastoma cells treated with infliximab**. Only a few small gaps have appeared (around 80% confluent) and a lot of the cells still have typical neuroblastoma morphologic features. **(C) HSV-1-infected neuroblastoma cells treated with aciclovir.** Similar to picture (B). **(D) HSV-1-infected neuroblastoma cells treated with infliximab and aciclovir** Similar to pictures (B-C). 10 x magnification. Scale bar: 50 µm.

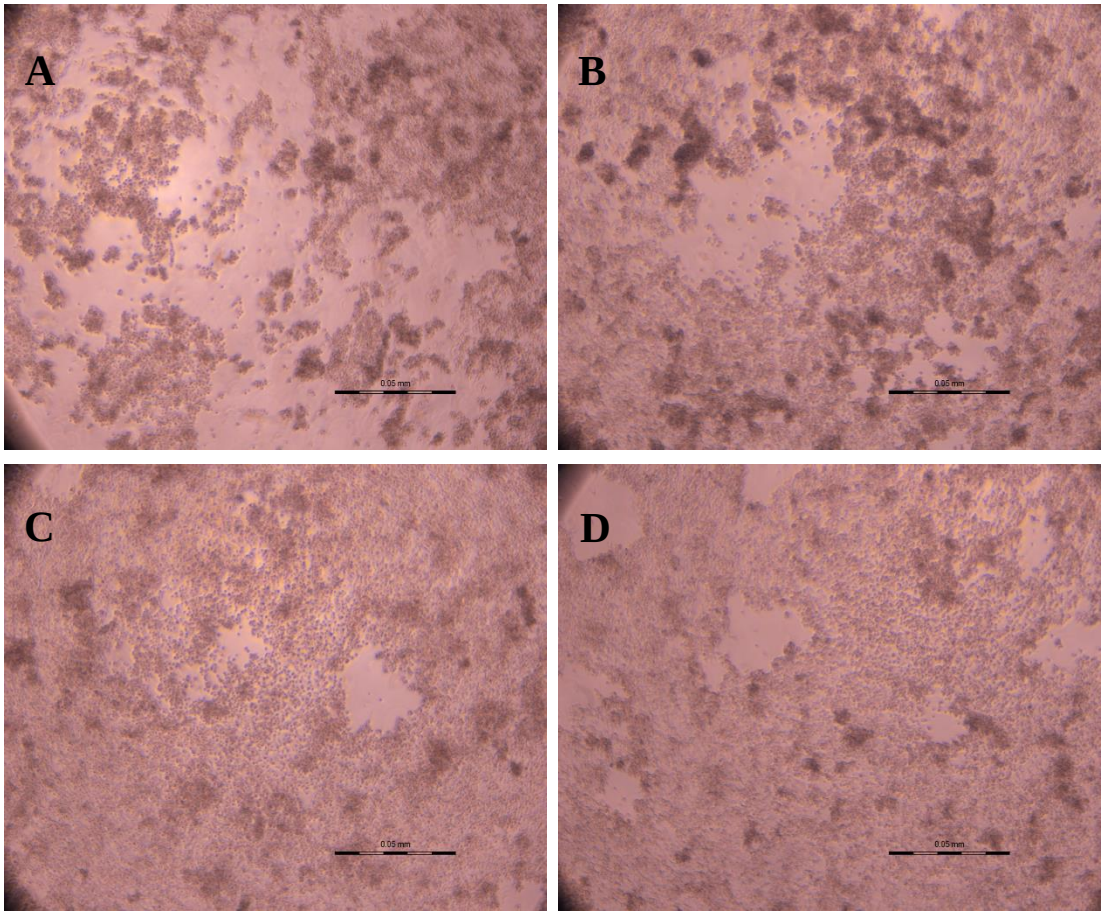

Figure 6.6. Microscopy pictures of HSV-1-infected neuroblastoma cells treated with infliximab (0.5 mg/ml) alone or combined with aciclovir at 72 h post-infection (48 h post-treatment). HSV-1-infection was done at MOI=0.01. Treatment was done with infliximab (0.5 mg/ml), aciclovir (20 µM) and infliximab combined with aciclovir 24 h post-infection (pi). Pictures were taken 72 h post-infection (48 h post-treatment). **(A) HSV-1-infected neuroblastoma cells untreated.** The majority of cells have died and detached (around 20-30% confluency). All cells look round. **(B) HSV-1-infected neuroblastoma cells treated with infliximab**. More cells survived compared to those in picture (A) (around 50-60% confluency). All cells look round. **(C) HSV-1-infected neuroblastoma cells treated with aciclovir.** All cells look round but the majority of cells are still alive (around 90% confluency). **(D) HSV-1-infected neuroblastoma cells treated with infliximab and aciclovir.** All cells look round but the majority of cells are still alive (around 80% confluency). 4 x magnification. Scale bar: 50 µm.

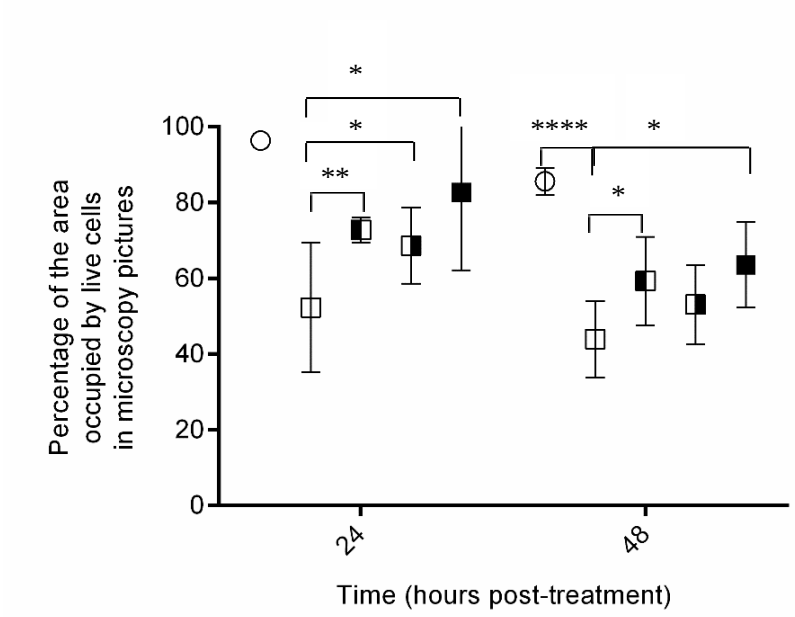

Figure 6.7. The effect of infliximab alone (0.5mg/ml) or combined with aciclovir on attached cell area of HSV-1-infected neuroblastoma cell microscopy pictures at 72 h post-infection (48 h post-treatment). HSV-1-infection was done at MOI=0.01. Treatment was done with infliximab (0.5 mg/ml), aciclovir (20 µM) and infliximab combined with aciclovir 24h post-infection (pi). Areas of attached cells were measured by the software ImageJ from pictures taken at 48 h and 72 h post-infection (24 h and 48 h pt respectively) of neuroblastoma cells uninfected (circles), infected untreated (white squares), infected treated with aciclovir (squares half-filled in black on the left side), infected treated with infliximab (squares half-filled in black on the right side) or infected treated with the combination "aciclovir+infliximab" (black squares). Data are expressed as mean of the area of live cells +95% CI and were obtained as described in the chapter 2 (Materials and Methods). At 48 h pi (24 h post-treatment), one picture for uninfected cells, three for infected untreated cells, three for infected cells treated with aciclovir, three for infected cells treated with infliximab and three for infected cells treated with both aciclovir and infliximab were analysed. At 72 h pi (48 h post-treatment), nine pictures for uninfected cells, twenty-four for infected untreated cells, twenty-two pictures for infected cells treated with aciclovir, twenty-one pictures for infected cells treated with infliximab and nineteen pictures for infected cells treated with both aciclovir and infliximab were analysed. The pictures were representative of 3 independent experiments. ANOVA test statistically showed significant differences between the means of the different conditions at 72 h pi (48 h pt)($p<0.001$). (*) $p<0.05$; (**) $p<0.01$, (***) $p<0.005$, (****) $p<0.0001$ (multiple t-tests).

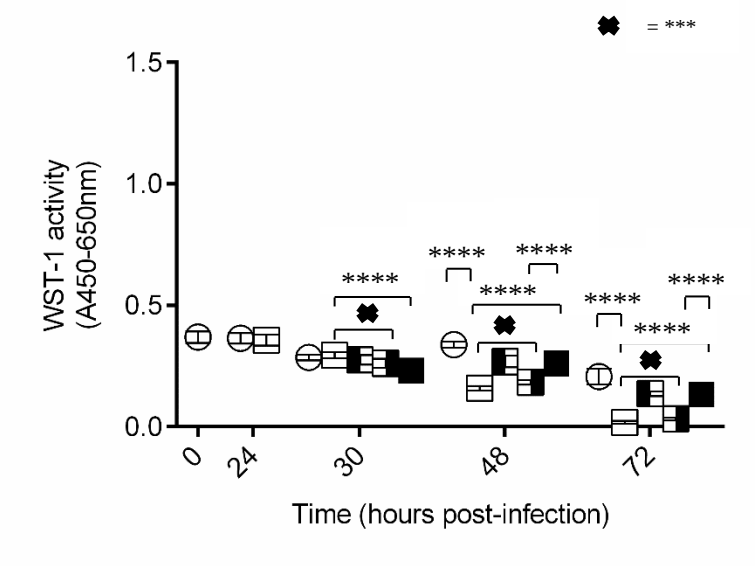

Figure 6.8. The effect of infliximab (0.5 mg/ml) alone and combined with aciclovir on the mitochondrial metabolism (WST-1 assay) of HSV-1-infected neuroblastoma cells. HSV-1 infection was done at MOI=0.01. The treatment with aciclovir (20 µM), infliximab (0.5 mg/ml) or both was done at 24 h pi. The values represent WST-1 activity (absorbance at 450 nm (A450 nm) normalised by subtraction of the background (A650 nm) after WST-1 addition). WST-1 assay has been performed in uninfected (circles), untreated infected (unfilled squares) or aciclovir-treated infected (squares half-filled in black on the left side) or infliximab-treated infected (squares half-filled in black on the right side) or "infliximab+aciclovir"-treated infected (black squares) neuroblastoma cells at different time-points (0, 24, 30, 48, 72 h pi). Data are expressed as the mean + 95% CI of 30 replicates from 3 independent experiments. ANOVA test showed statistical differences between the means of the different conditions for all time-points tested: 30 h, 48 h and 72 h pi ($p<0.0001$). **X**= (***) $p<0.005$; (****) $p<0.001$ (multiple t-tests).

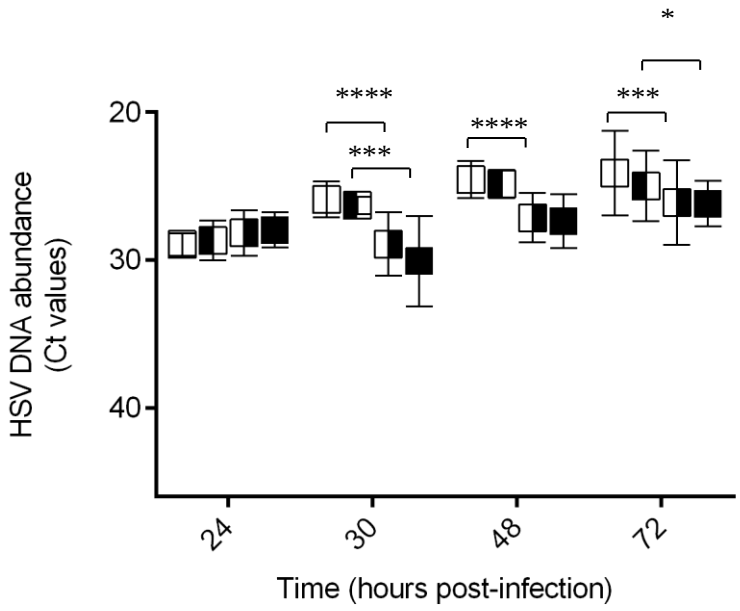

Figure 6.9. The effect of infliximab (0.5 mg/ml) alone and combined with aciclovir on HSV DNA abundance in HSV-1-infected neuroblastoma cell culture medium. HSV-1-infection was done at MOI=0.01. The treatment with aciclovir (20 µM), infliximab (0.5 mg/ml) or both was done at 24 h pi. The values represent Ct values after HSV DNA qPCR from culture medium of HSV-1-infected (white) or aciclovir-treated infected (squares half-filled in black on the left side) or infliximab-treated infected (squares half-filled in black on the right side) or "infliximab+aciclovir"-treated infected neuroblastoma cells at 24 (just before the treatment), 30, 48 and 72 h pi (0, 6, 24 and 48 h post-treatment respectively). Each point represents the mean + 95% CI of data from at least 3 independent experiments. Triplicates were used for each time-point in each experiment. ANOVA test showed statistical differences between the means of the different conditions at 30 h ($p<0,0001$), 48 h pi ($p<0,0001$) and 72 h pi ($p<0.005$) but not at 24 h pi ($p>0.05$). (*) $p<0.05$, (***) $p<0.005$, (****) $p<0.0001$ (multiple t-tests).

6.2.2. Effect of infliximab combined to aciclovir in HSV-1-infected microglial cells

6.2.2.1. Effect of infliximab alone and combined with aciclovir on TNF gene expression in HSV-1-infected microglial cells

In chapter 3, an increase in TNF relative gene expression was observed in microglial cells following HSV-1-infection and in chapter 4, I could observe that treatment with aciclovir (20 µM) decreased TNF relative gene expression in infected microglia at 72 h pi. Here, I assessed the impact of the drug infliximab (0.5 mg/ml) alone or combined with aciclovir (20 µM) on TNF relative gene expression in HSV-1-infected microglial cells. TNF relative gene expression is based on TNF absolute gene expression (data non shown) normalised by DAD-1 absolute gene expression (fig 6.10)

At 48 h and 72 h pi, there was an increase in TNF relative gene expression in HSV-1-infected microglial cells treated with aciclovir, infliximab alone, or combined with aciclovir compared to the uninfected counterparts as observed with all the values superior to one (fig 6.11). At 72 h pi (48 h pt), aciclovir alone ($p<0.005$) and combined with infliximab ($p<0.005$) were associated with a reduced TNF relative gene expression in infected cells while infliximab alone was associated with a slight but not significant increase (fig 6.11).

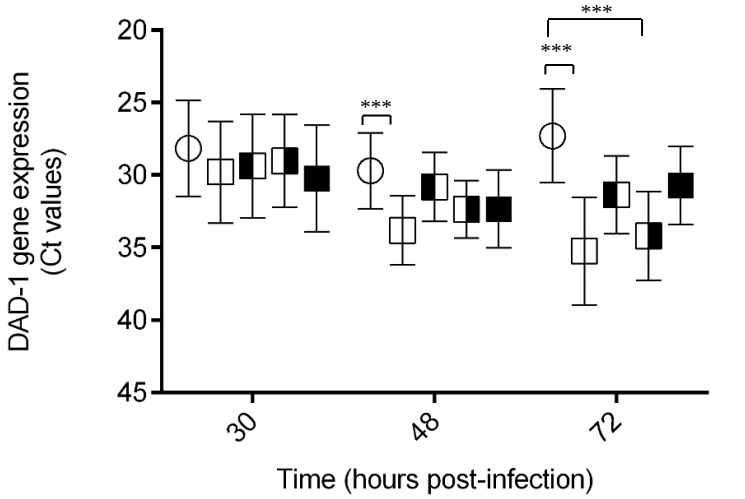

Figure 6.10. The effect of infliximab alone (0.5 mg/ml) and combined with aciclovir on DAD-1 absolute gene expression in HSV-1-infected microglial cells. HSV-1 infection was done at MOI=0.01. Treatment with aciclovir (20 µM) and/or infliximab (0.5 mg/ml) was done at 24 h pi. Absolute DAD-1 gene expression in uninfected (circles) or infected untreated (unfilled squares) or aciclovir-treated infected (squares half-filled in black on the left side) or infliximab-treated infected (squares half-filled in black on the right side) or "infliximab+aciclovir"-treated infected (black squares) microglial cells at 30, 48 and 72 h pi. Data are expressed as the mean of qRT-PCR DAD-1 Ct values + 95% CI and were obtained from 3 independent experiments, each condition being assessed in triplicate. ANOVA test statistically showed significant differences between the means of the different conditions at 48 h and 72 h pi ($p<0.005$) but not at 30 h ($p>0.05$). (***) $p<0.005$ (multiple t-tests).

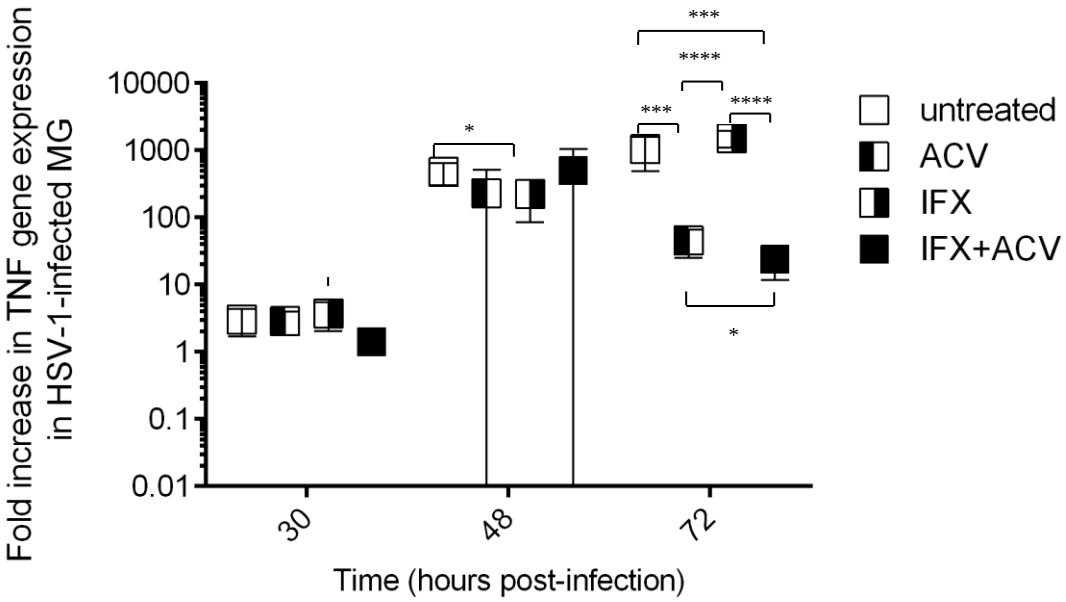

Figure 6.11. The effect of infliximab (0.5 mg/ml) alone and combined with aciclovir on TNF relative gene expression in HSV-1-infected microglial cells. HSV-1 infection was done at MOI=0.01 in microglial cells. The treatments with aciclovir (20 µM); infliximab (0,5 mg/ml) or both were added at 24 h pi. The data represent TNF relative gene expression expressed as mean +/- 95% CI of $2^{-\Delta\Delta Ct}$ values at 30 h, 48 h and 72 h post-infection (respectively 6 h, 24 h and 48 h post-treatment). The scale is logarithmic. $2^{-\Delta\Delta Ct}$ values were obtained following qRT-PCR of TNF and DAD-1 genes. DAD-1 gene was used as reference (housekeeping) gene. From qRT-PCR Ct values of DAD-1 and TNF, ΔCt values [Ct (TNF)-Ct(DAD-1]) were obtained for both uninfected and HSV-1-infected cells (untreated, treated with aciclovir, infliximab or both). For each condition (untreated, aciclovir, infliximab or both), ΔΔCt values represented $[(\Delta Ct)_{HSV+/-treatment} - (\Delta Ct)_{uninfected}]$. ANOVA test showed statistical differences at 72h pi ($p<0.0001$) but not at 30 h ($p>0.05$) and 48 h pi ($p>0.05$) between the means of the different conditions. Data were obtained from 3 independent experiments. (*): $p<0.05$;(**): $p<0.005$; (***): $p<0.0001$ (multiple t-tests).

6.2.2.2. Effect of infliximab alone or combined with aciclovir on cell viability, mitochondrial activity and viral replication in HSV-1-infected microglial cells

The dose of infliximab used to treat HSV-1 infected microglial cells was 0.5 mg/ml as done in neuroblastoma cells. By light microscopy, like for neuroblastoma cells, it was shown that infliximab, aciclovir (20 µM) and infliximab combined with aciclovir increased HSV-1-infected microglial cell viability at both 48 and 72 h post-infection (pi) (24 and 48 h post-treatment (pt)) (fig 6.12-13). Indeed, all these treatments led to more live infected cells attached to the plate compared to the infected cells untreated. This trend was confirmed by the analysis of attached cell area performed by using the software "ImageJ" on several 4 x magnification microscopy pictures for each conditions (fig 6.14). It was shown that the area of live microglia cells per picture was approximately 84.5% for uninfected, 52.6% for infected untreated, 78.7% for infected cells treated with aciclovir, 66.2% for infected cells treated with infliximab and 78.2% for infected cells treated with both infliximab and aciclovir.

WST-1 assays demonstrated that the decrease in mitochondrial activity in microglia cells following HSV-1 infection and observed at 72 h post-infection (48 h post treatment) could be significantly increased by aciclovir ($p<0.005$) and infliximab ($p<0.05$) (fig 6.15). The same trend was observed with the combination of both therapies, but this was not statistically significant ($p=0.076$) (fig 6.15).

Direct HSV DNA qPCR from culture medium of HSV-1-infected microglial cells untreated or treated showed that infliximab alone or combined to aciclovir but not aciclovir alone was associated with a significant decrease in viral genome detection at 30 h post-infection (pi) (6h post-treatment (pt)) (fig6.16) ($p<0.0001$). At 48 h and 72 h pi, the administration of infliximab, aciclovir and both led to a decrease in HSV-1 DNA abundance compared to infected cells untreated ($p<0.0001$). Interestingly, at 48 h and 72 h pi (24 h and 48 h pt) the most important decrease in viral load was observed for the co-treatment infliximab/aciclovir ($p<0.005$ or

$p<0.0001$). Of note, at 72 h pi (48 h pt), viral load was lower in culture medium of infected microglia cells treated with aciclovir alone compared to that in culture medium of cells treated with infliximab alone ($p<0.0001$). This suggests that the potential antiviral effect of infliximab in microglial cells is faster to act, but shorter-lived than that due to aciclovir.

As in the case for neuroblastoma cells, infliximab alone has been shown to increase both cell survival and mitochondrial metabolism and decrease culture medium viral load following HSV-1-infection of microglia cells. However, the effect of infliximab combined with aciclovir was not superior to the effect of aciclovir alone at the level of cell survival and mitochondrial metabolism in HSV-1-infected microglial cells.

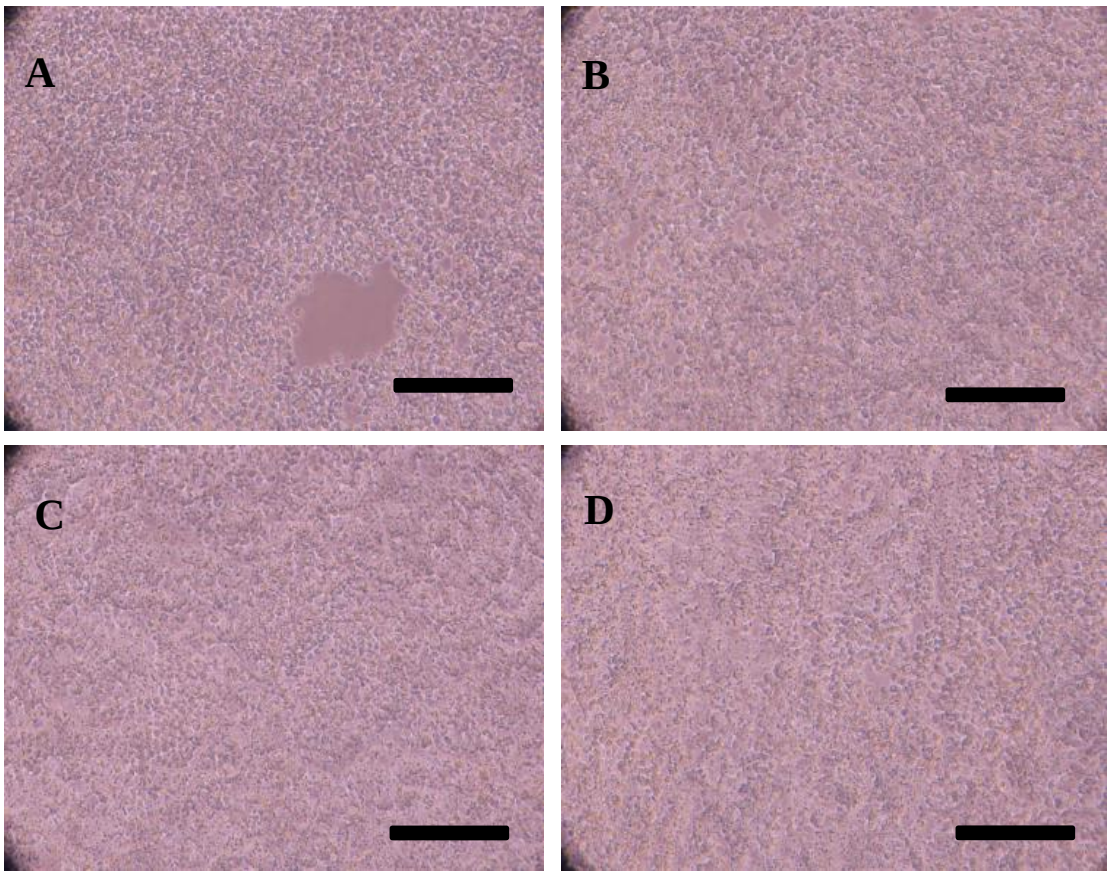

Figure 6.12. Microscopy pictures of HSV-1-infected microglial cells treated with infliximab (0.5 mg/ml) alone or combined with aciclovir at 48 h post-infection (24 h post-treatment). HSV-1-infection was done at MOI=0.01. Treatment was done with infliximab (0.5 mg/ml), aciclovir (20 µM) and infliximab combined to aciclovir 24 h post-infection (pi). Pictures were taken 48 h post-infection (24 h post-treatment). **(A) HSV-1-infected microglial cells untreated.** One big gap has appeared in the monolayer and all cells look round. **(B) HSV-1-infected microglial cells treated with infliximab**. No big gaps can be observed but most of the cells have become round. **(C) HSV-1-infected microglial cells treated with aciclovir.** Cells look similar to picture (B). **(D) HSV-1-infected microglial cells treated with infliximab and aciclovir.** Cells look similar to pictures (B-C). 10 x magnification. Scale bar: 50 µm.

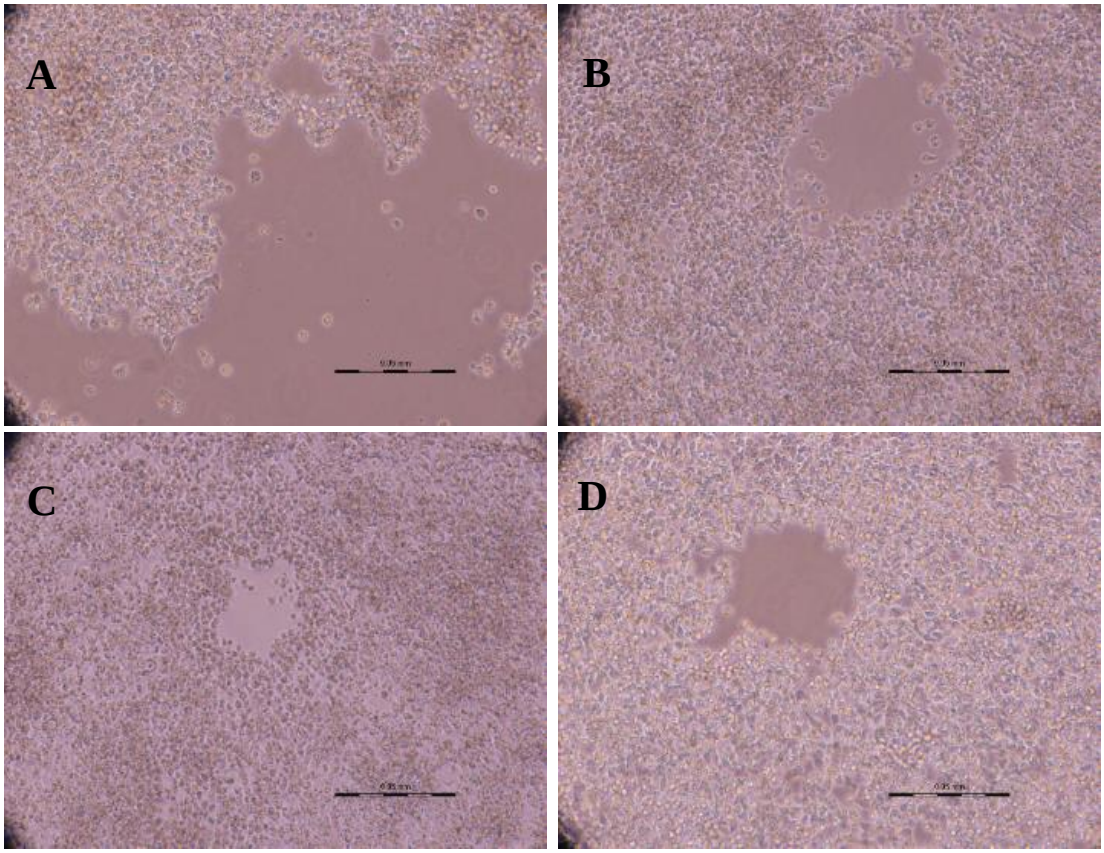

Figure 6.13. Microscopy pictures of HSV-1-infected microglial cells treated with infliximab (0.5 mg/ml) alone or combined with aciclovir at 72 h post-infection (48 h post-treatment). HSV-1-infection was done at MOI=0.01. Treatment was done with infliximab (0.5 mg/ml), aciclovir (20uM) and infliximab combined with aciclovir 24 h post-infection (pi). Pictures were taken 72 h pi (48 h post-treatment). **(A) HSV-1-infected microglial cells untreated.** Big gaps have appeared in the monolayer (around 30-40% confluent) and all cells look round. **(B) HSV-1-infected microglial cells treated with infliximab**. All cells look round but no extensive cell death could be observed (around 80-90% confluent). **(C) HSV-1-infected microglial cells treated with aciclovir.** Similar to picture (B). **(D) HSV-1-infected microglial cells treated with infliximab and aciclovir.** Almost all cells are still attached. There are still an important proportion of cells with microglia cell morphologic features. 10 x magnification. Scale bar: 50 µm.

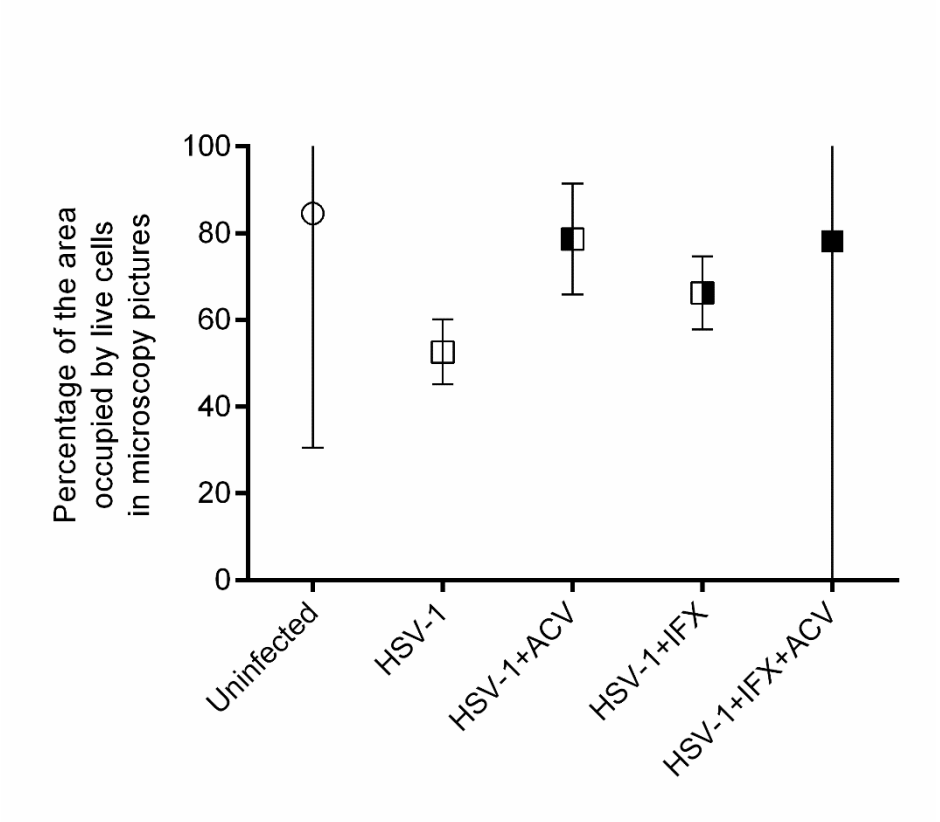

Figure 6.14. The effect of infliximab alone (0.5 mg/ml) or combined with aciclovir on attached cell area of HSV-1-infected microglial cells microscopy pictures at 72h post-infection (48h post-treatment). HSV-1-infection was done at MOI=0.01. Treatment was done with infliximab (0.5 mg/ml), aciclovir (20 μM) and infliximab combined with aciclovir 24 h post-infection (pi). Areas of attached cells were measured by the software "ImageJ" from pictures taken at 72 h post-infection (48 h post-treatment). Two 4 x magnification pictures for uninfected, four for HSV-1 infected, two for HSV-1-infected cells treated with aciclovir, four for HSV-1-infected cells treated with infliximab and two for HSV-1-infected cells treated with infliximab and aciclovir were analysed. Statistical analysis were not performed due to too few replicates.

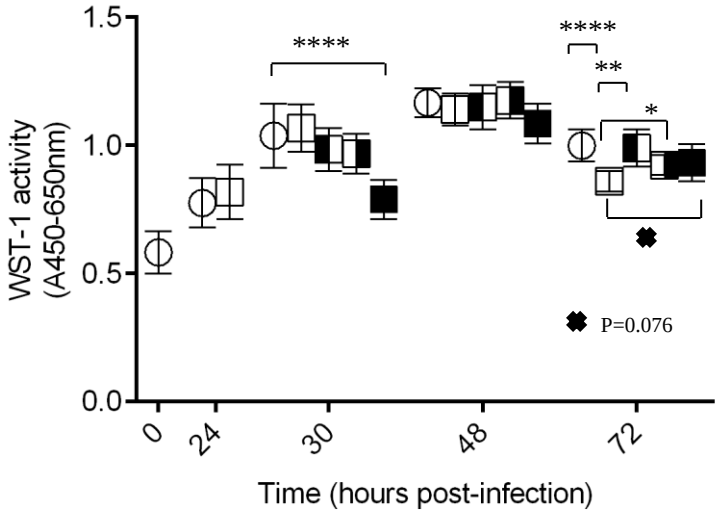

Figure 6.15. The effect of infliximab alone (0.5 mg/ml) and combined with aciclovir on the mitochondrial metabolism of HSV-1-infected microglial cells at 72 h post-infection (48 h pt). HSV-1 infection was done at MOI=0.01. Treatment with aciclovir (20 µM), infliximab (0.5 mg/ml) or both was done at 24h pi. Values represent absorbance measurements at 450 nm (A450 nm) normalised by subtraction of the background (A650 nm). The WST-1 assay was performed in uninfected (circles), untreated infected (unfilled squares) or aciclovir-treated infected (squares half-filled in black on the left side) or infliximab-treated infected (squares half-filled in black on the right side) or "infliximab+aciclovir"-treated infected (black squares) microglial cells at different time-points (0, 24, 30, 48 and 72 h pi). Data are expressed as the mean + 95% CI of 30 replicates from 3 independent experiments. ANOVA test showed statistical differences between the means of the different conditions at 30 h ($p<0.0001$) and 72 h pi ($p<0.005$) but not at 48h pi ($p>0.05$). **X**=0.076, (*) p=0.05, (***) $p<0.005$; (****) $p<0.001$ (multiple t-tests performed at all time points but 0 h pi).

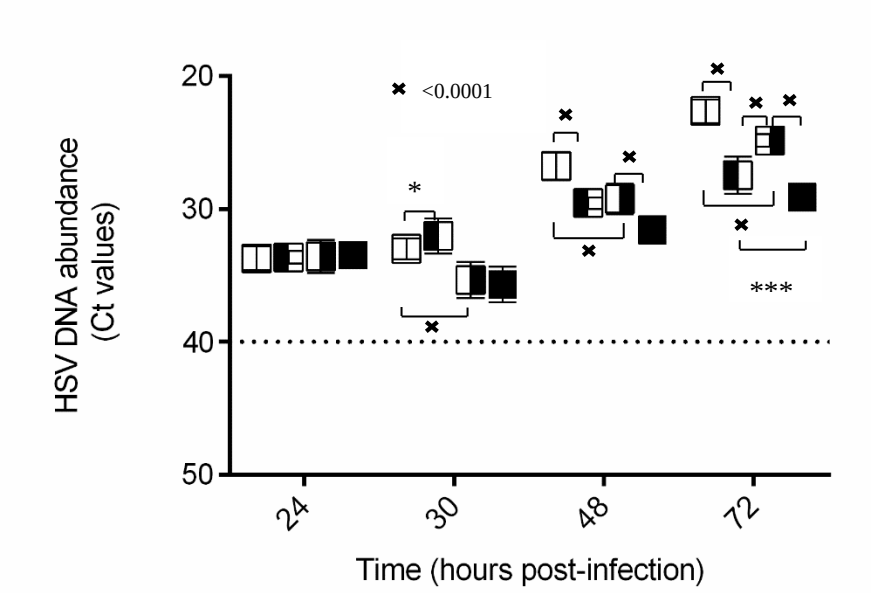

Figure 6.16. The effect of infliximab (0.5 mg/ml) alone and combined with aciclovir on HSV DNA abundance in HSV-1-infected microglial culture medium. HSV-1-infection was done at MOI=0.01. Treatment with aciclovir (20 µM), infliximab (0.5 mg/ml) or both was done at 24 h pi. The values represent Ct values after HSV DNA qPCR was performed on culture medium of HSV-1-infected (white) or aciclovir-treated infected (squares half-filled in black on the left side) or infliximab-treated infected (squares half-filled in black on the right side) or "infliximab+aciclovir"-treated infected microglial cells at 24 (just before the treatment), 30, 48 and 72 h pi (0, 6, 24 and 48 h post-treatment respectively). Each point represents the mean + 95% CI of data from at least 3 independent experiments. Triplicates were used for each point-time in each experiment. ANOVA test showed statistical differences between the means of the different conditions at 30 h, 48 h and 72 h pi ($p<0.001$) but not at 24 h pi. (*) $p<0.01$, (***) $p<0.005$ **X**=(****) $p<0.0001$ (multiple t-tests).

6.3. Discussion

The limitations of aciclovir for treatment of HSE patients clearly emphasize the need of discovering new adjunctive therapies. In chapter 4, aciclovir (20 µM) limitations were noticed *in vitro* during treatment of both HSV-1-infected neuroblastoma and microglial cells as this antiviral only partially rescued cell viability and mitochondrial activity both dampened by HSV-1. As previously mentioned for HSE clinical and *in vivo* studies, it is thought that this suboptimal therapeutic action of aciclovir is the consequence of its limited activity. Indeed, it only targets HSV replication but the not immune response. As a result, using an adjunctive therapy targeting the pro-inflammatory response to HSV-1 could improve treatment efficiency.

Interestingly, in chapter 3, in both infected microglial and neuroblastoma cells, HSV-1 led to a significant increase in expression of the pro-inflammatory gene TNF as observed at 24 h-72 h pi (confirmed by other studies as discussed previously). Furthermore, an increase in CSF TNF levels during HSE convalescence stage was clinically observed by Aurelius et al.[71]. In an *in vivo* study, an improvement of the outcome of HSE mice treated with valacyclovir (oral acyclovir) was observed following the administration of the anti-TNF etanercept[133]. Hence, the hypothesis of this chapter was that infliximab, TNF inhibitor, as adjuvant therapy to aciclovir could improve cell viability in HSV-1-infected neuroblastoma and microglial cells by its anti-inflammatory action on TNF.

Microscopy study showed that the concentration of 0.5 mg/ml was the most suitable to use for treatment of HSV-1-infected neuroblastomas (fig 6.2). This concentration was used in all other experiments in this chapter. As in previous chapters, the concentration of aciclovir used in all the experiments was 20 µM.

Firstly, in my experiments, infliximab alone was shown to increase cell survival and mitochondrial metabolism in HSV-1-infected neuroblastomas and microglia cells as observed by the analysis of attached cell area performed with the software "imageJ" on microscopy pictures and by WST-1 assay at 48 h and/or 72 h post-infection (h pi) (24 h and 48 h post-treatment (h pt)) (fig 6.7- 6.8 and fig 6.14-6.15). Surprisingly, viral load was quickly and drastically decreased by infliximab alone in both infected microglia cell and neuroblastomas culture medium as early as 6 h pt (30 h pi) (fig 6.9 and 6.16). Viral load was still significantly lower in infected neuroblastoma and microglial cells treated with infliximab than in the untreated cells at 48 h and 72 h pi (24 h and 48 h pt). Interestingly, in both infected brain cell types, at 30 h pi (6 h pt), infliximab but not aciclovir was associated with a reduced viral load whereas at 72 h pi (48 h pt), aciclovir led to a similar (in neuroblastoma cells) or higher (in microglial cells) decrease in HSV DNA abundance compared to infliximab. This may suggest that infliximab (0.5 mg/ml) has an anti-HSV-1 effect, potentially shorter than aciclovir (20 µM) treatment.

Crucially, this is the first time that infliximab has been associated with an anti-HSV-1 action. Interestingly, another anti-TNF, etanercept, used alone, was already shown to act as an antiviral against Japanese encephalitis virus in brain cells[134]. In this latter study, etanercept alone was shown to lead to a decrease in mouse mortality and brain inflammation.

In culture medium of both infected microglial and neuroblastoma cells, the combination of both drugs was the treatment with the lowest viral DNA load at 48 h and 72 h pi (24 h and 48 h pt) (fig 6.16, fig 6.9). However, the combined treatment of infliximab and aciclovir did not appear to lead to a better outcome than aciclovir alone in HSV-1-infected neuroblastoma and microglial cells; both drugs induced similar cell survival and mitochondrial activity profiles (fig 6.7-6.8 and fig 6.14-6.15). Interestingly, before increasing mitochondrial activity at 48 h and/or 72 h pi (24 h and/or 72 h pt) in HSV-1-infected neuroblastoma and microglial cells, it

seems infliximab was associated with an initial decrease in mitochondrial activity observed at 6 h pt (30 h pi). Several papers have reported that infliximab is able to induce apoptosis in several cell types such as immune cells (i.e macrophages and monocytes)[166, 167]. Therefore, perhaps infliximab induces early apoptosis in a proportion of cells before its antiviral effects manifests in HSV-1-infected cells.

Infliximab alone or combined with aciclovir influenced TNF relative gene expression in HSV-1-infected brain cells in a different way in the different cell types. Overall, TNF relative gene expression is still higher in infected neuroblastoma and microglial cells regardless of the treatment (infliximab, aciclovir or both) than in their uninfected counterparts (fig 6.4 and 6.11). In infected neuroblastoma cells, TNF relative gene expression was even more increased by aciclovir alone than by any other treatments ($p<0.05$) at 72 h pi (48 h pt) (fig 6.4). The gene expression profile was different in HSV-1-infected microglia at 72 h pi; with a slight but not significant increase in TNF relative gene expression after treatment with infliximab alone, but a significant decrease with aciclovir alone or combined to infliximab (fig 6.11). Similarly to the conclusions of the chapter 5, TNF relative gene expression does not correlate with survival of HSV-1-infected neuroblastomas or microglial cells.

Altogether this suggests that infliximab alone is (0.5 mg/ml) similar to aciclovir (20 µM) in infected microglial and neuroblastoma cells works as an anti-HSV-1 agent, maintaining cell survival and mitochondrial activity while reducing viral load. However, infliximab does not lead to higher levels of cell survival and mitochondrial activity than aciclovir in HSV-1 infected neuroblastoma and microglial cells. The combination aciclovir/infliximab does not even induce a significant increase in mitochondrial activity in HSV-1-infected microglia cells. (compared to untreated infected cells) Hence, one dose of infliximab does not seem to be a good adjuvant therapy in individual culture of these HSV-1-infected brain cells as its combination with aciclovir does not lead to significant improvement of cell survival or

mitochondrial metabolism compared to aciclovir alone. Nonetheless, the dual therapy aciclovir/infliximab were associated with lower viral load than aciclovir alone in both microglial and neuroblastoma cells. Hence, administering repeated doses of infliximab (0.5 mg/ml) in these models may be interesting to improve its efficiency, as its inhibitory effect on HSV-1 replication appears to be quick and weaken over time compared to aciclovir.

Infliximab is commonly used as an anti-inflammatory drug. For example, it is to treat Inflammatory Bowel Disease (I.B.D), reducing disease activity and improving patient quality of life. The biological action of infliximab in I.B.D. has been recently reviewed and shown to be involved in: (i) downregulating inflammatory cytokines, (ii) inducing apoptosis of activated lymphocytes, (iii) downregulating Th1, (iv) inducing Treg and regulatory macrophages, (v) inhibiting NF-kB and (vi) promoting MAPK signalling[168]. In an *in vivo* model of HSE, combining another TNF inhibitor, etanercept, to the antiviral therapy valaciclovir induced an increased life expectancy in mice, together with a reduced brain inflammation compared to valaciclovir alone [133]. Crucially, there were no significant differences in brain viral load between HSV-1-infected-mice treated with valaciclovir alone or combined to etanercept. This suggested that the life expectancy of infected mice treated with both valaciclovir and etanercept was higher than that of infected mice treated by the valacyclovir alone because of the anti-inflammatory action of this anti-TNF etanercept.

My *in vitro* models do not exceed 3 days. They may be a representation of acute HSE in which viral load is high and CSF TNF levels are not yet elevated[143], [71]. Hence, the increase in cell survival and mitochondrial metabolism observed following administration of infliximab alone (24 h-48 h post-treatment) in infected neuroblastoma and microglial cells could also be the result of an inhibitory action of infliximab on other pro-inflammatory cytokines or just the consequence of its quick anti-HSV-1 action. More studies are needed for a better understanding of the effect of infliximab in HSV-1-infected brain cells.

Finally, infliximab is usually administrated to patients suffering from inflammatory diseases. The human host is complex, and infliximab likely impacts, at the cellular level on a wide range of host cells simultaneously, including various immune cells. In this chapter, I have studied its impact only in one brain cell type at the time. In the next chapter, I have optimised new *in vitro* HSE models using a co-culture of human brain cells to begin to more closely model the *in vivo* response.

Chapter 7 Co-culture of HSV-1-infected human brain cells

7.1. Introduction

In the previous chapters, the effects of administering aciclovir (chapter 4), dexamethasone alone and combined to aciclovir (chapter 5), infliximab alone and combined with aciclovir (chapter 6) have been studied in HSV-1-infected neuroblastoma and microglial cells separately. These effects have been assessed at the level of cell viability, TNF gene expression and viral load. The data obtained offered a better understanding of HSV-1 infection in each human brain cell type. They also provided insight into the relevance of anti-inflammatory drugs as adjunctive therapies in combination with aciclovir in human brain cells following HSV-1infection.

HSV Encephalitis (HSE) is the result of HSV-1 infection and subsequent immune response in the brain tissue that contains multiple cell types, such as neurons, microglia cells, astrocytes, oligodendrocytes[45, 49, 169, 37, 85 ,170]. Each brain cell type leads to a specific response to the virus and these brain cell types also interact with each other adding another degree of complexity[140, 171, 90, 68].

In HSE, microglia cells, resident brain macrophages, are a key cell type involved in HSV-1 brain infection, although their role is still not completely clear. Activated microglia and gliosis are histopathological features in HSE brain tissue[35, 143]. Some studies showed microglial cells to be protective in HSE[136, 87]. Chucair-Elliott *et al.* demonstrated *in vitro* with murine cells that microglia protected neuronal loss following HSV-1-infection of neural progenitor cells (NPC)[136]. In a HSE mouse model, microglia were shown essential to counter HSV-1-induced brain lateral ventricle enlargement and encephalitis[87]. However, another study demonstrated that the presence of microglia was associated with neural oxidative damage and toxicity via TLR2 activation[99]. Hence, there is a need to better understand the role of microglia cells and

their interaction with other brain cell types during HSV-1 infection. To study such interactions, I developed more complex HSV-1-infection *in vitro* models using microglia in co-culture.

Several studies have used brain cell co-cultures. In an *in vitro* model of bacterial meningitis, astrocytes (95%) and microglia cells (5%) were co-cultured together in the same compartment before LPS challenge[156]. Another mixed co-culture of astrocytes/microglia cells was used to assess the effect of astrocytes on microglia cell activation[172]. Co-cultures of astrocytes/neurons and microglia/neurons were also performed using coverslips in a thiamine deficiency study[141]. Only two studies, previously mentioned, using co-cultures in *in vitro* models of HSE have been published, both used murine cells. In the first one, 30,000 neural progenitor cells (NPC) were co-cultured with 200,000 microglia cells in the same well and microglia cells were shown to prevent neuronal loss upon differentiation following HSV-1 infection of NPC[136]. In the second one, microglia co-cultured at the ratios 1/5 or 1/10 with mixed neural cultures (85-90% neurons, 10-15% astrocytes and less than 2% of microglia cells) were demonstrated to cause oxidative stress and neuronal damage[99]. To my knowledge, there are no studies of HSV-1-infection using a co-culture of human microglia with another human brain cell type. Further *in vitro* studies using human brain cells need to investigate the role of microglia on HSV-1 infection of other brain cells.

In this chapter, two new HSV-1-infection *in vitro* systems using human brain cells co-cultured with microglia have been set up and preliminary works have been performed in them. To assess the remote effect of microglia, cell types were cultured in different compartments separated via pore-containing inserts. These inserts allowed exchange of fluid, small molecules and viruses through the pores (diameter: 0.4 µm) (description in chapter 2 “Material and Methods”). In the first model, the co-culture consisted of HSV-1-infected neuroblastomas in the bottom compartment and microglia in the top one. In the second model, HSV-1-infected primary astrocytes were in the bottom compartment and microglia in the top. In each model,

HSV-1-infection was performed at MOI=0.01 in neuroblastoma cells or astrocytes. The effects of the microglia co-culture on HSV-1-infected neuroblastoma cells or astrocytes were observed at 24, 48 and 72h pi.

The goals of this chapter were to set up these co-culture models and study the remote influence of microglia co-culture (assuming soluble factors are released by microglia in my model), on HSV-1-infection of primary astrocytes or neuroblastomas by observing cell viability and viral load.

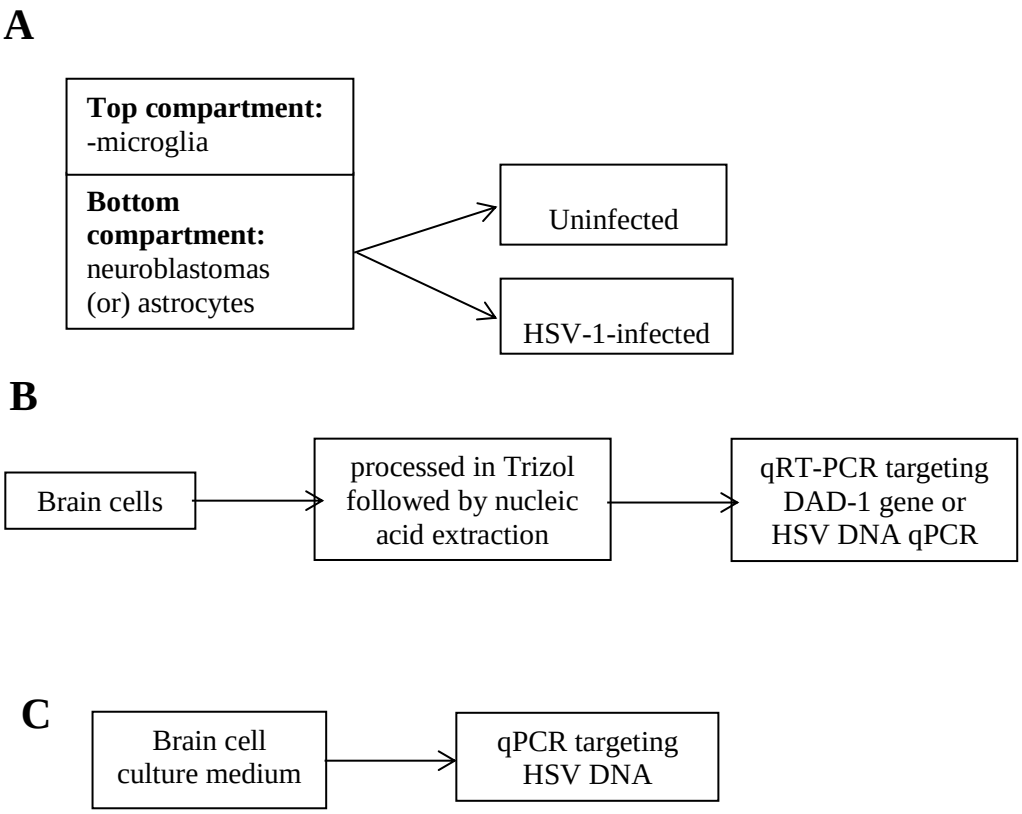

Figure 7.1. Experimental design for assessing the effect of microglia on HSV-1-infection of neuroblastoma cells and primary astrocytes. (**A)** Brain cell populations used. **(B)** Techniques performed on brain cells following HSV-1-infection. **(C)** Techniques performed on brain cell culture medium following HSV-1-infection.

7.2. Results

7.2.1. HSV-1-infection of neuroblastoma cells co-cultured with microglial cells

Here, I assessed the effect of microglia on HSV-1-infected neuroblastoma cells. By light microscopy, an increase in live neuroblastoma cell density could be observed when neuroblastomas were co-cultured with microglial cells at multiple time-points (fig 7.2-4). The increase in infected neuroblastoma cell density when co-cultured with microglia was consistently observed in several 10 x magnification microscope pictures at both 48 h and 72 h pi (fig 7.3-4). Further examples of the higher cell density due to microglia co-culture are shown in the figures 7.5 and 6. The analysis of attached cell area via the software "ImageJ" was only performed using 4 x magnification microscope pictures for technical reasons involving picture brightness. At 72 h pi, 4 x magnification microscope pictures also showed an increase in infected neuroblastoma cell survival when co-cultured with microglial cells (fig 7.7). Although showing the same trend, the analysis of attached neuroblastoma cell area by "ImageJ" was done with too few pictures at 4 x magnification for statistical significance (fig 7.8).

At 72 h pi, DAD-1 gene abundance was significantly higher among infected neuroblastoma cells co-cultured with microglia compared to the neuroblastoma cells cultured alone (fig 7.9A). The analysis of DAD-1 ΔCt values ((DAD-1 Ct) infected – (DAD-1 Ct) uninfected) also showed that DAD-1 gene expression was higher during HSV-1-infection of neuroblastoma cells when co-cultured with microglial cells (lower ΔCt value) (fig 7.9B).

The co-culture with microglial cells did not induce any change in HSV DNA abundance in neuroblastoma cell culture medium (24 h-72 h pi) (fig 7.10). However, the presence of microglia induced a significant decrease in HSV DNA abundance within neuroblastoma cells at 72 h pi (fig 7.11).

HSV DNA qPCR in microglia cell culture medium (insert-top compartment) showed an increase in HSV DNA abundance over time (6-72 h pi) when co-cultured with HSV-1-infected neuroblastoma cells (fig 7.12). Finally, qPCR from nucleic extract of microglia cells co-cultured with infected neuroblastoma cells showed very low levels of HSV DNA amplification (72h pi) (data not shown).

Overall, under these experimental conditions, the presence of microglial cells in co-culture appears to protect HSV-1-infected neuroblastoma cells.

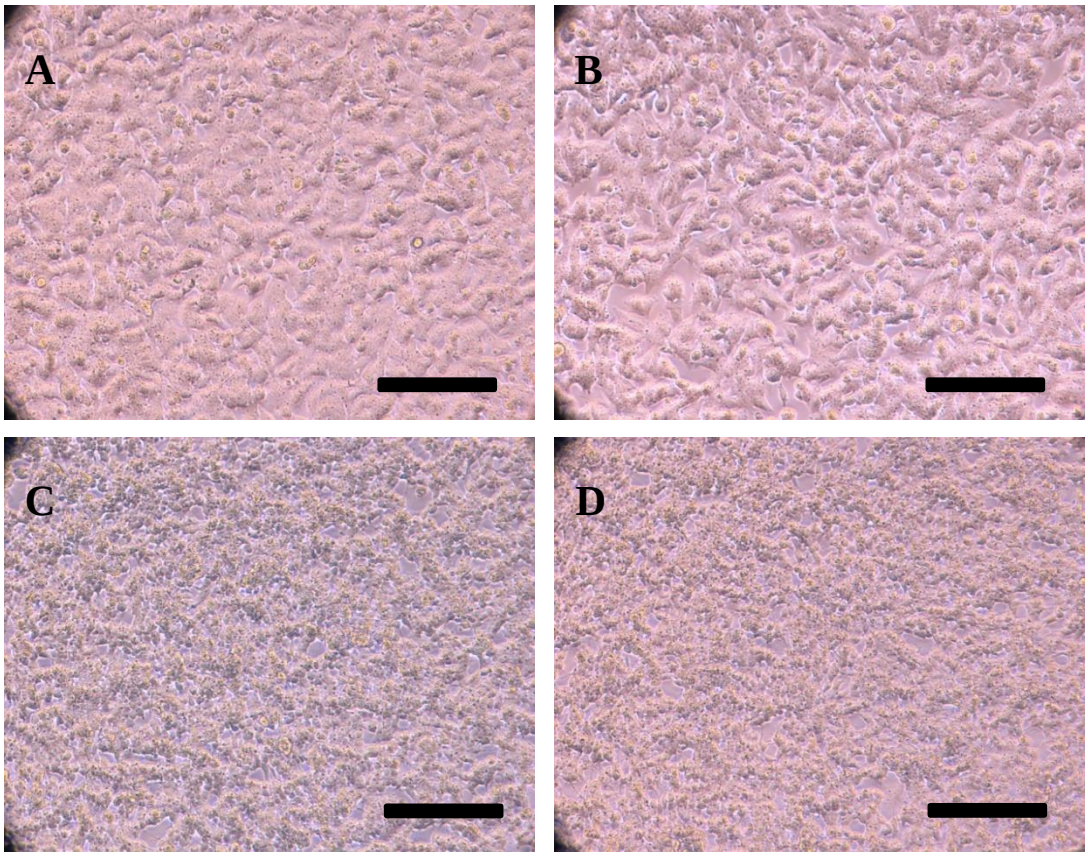

Figure 7.2. Microscopy pictures of HSV-1-infected neuroblastoma cells co-cultured with microglia at 24h post-infection. HSV-1-infection was done in neuroblastoma cells at MOI=0.01. Pictures of neuroblastoma cells were taken 24 h pi by light microscopy. **A.** Uninfected neuroblastoma cells. Cells are 100% confluent, big and exhibit fibroblast-like morphology. **B.** HSV-1-infected neuroblastoma cells. There are more spaces between cells and few round cells can be observed. **C.** Uninfected neuroblastoma cells co-cultured with 300,00 microglia cells. Cells are 100% confluent but they look smaller and rounder than in (C). **D.** HSV-1-infected neuroblastoma cells co-cultured with 300,000 microglial cells. The picture is similar as the one in C. 10 x magnification. Scale bar: 50 µm.

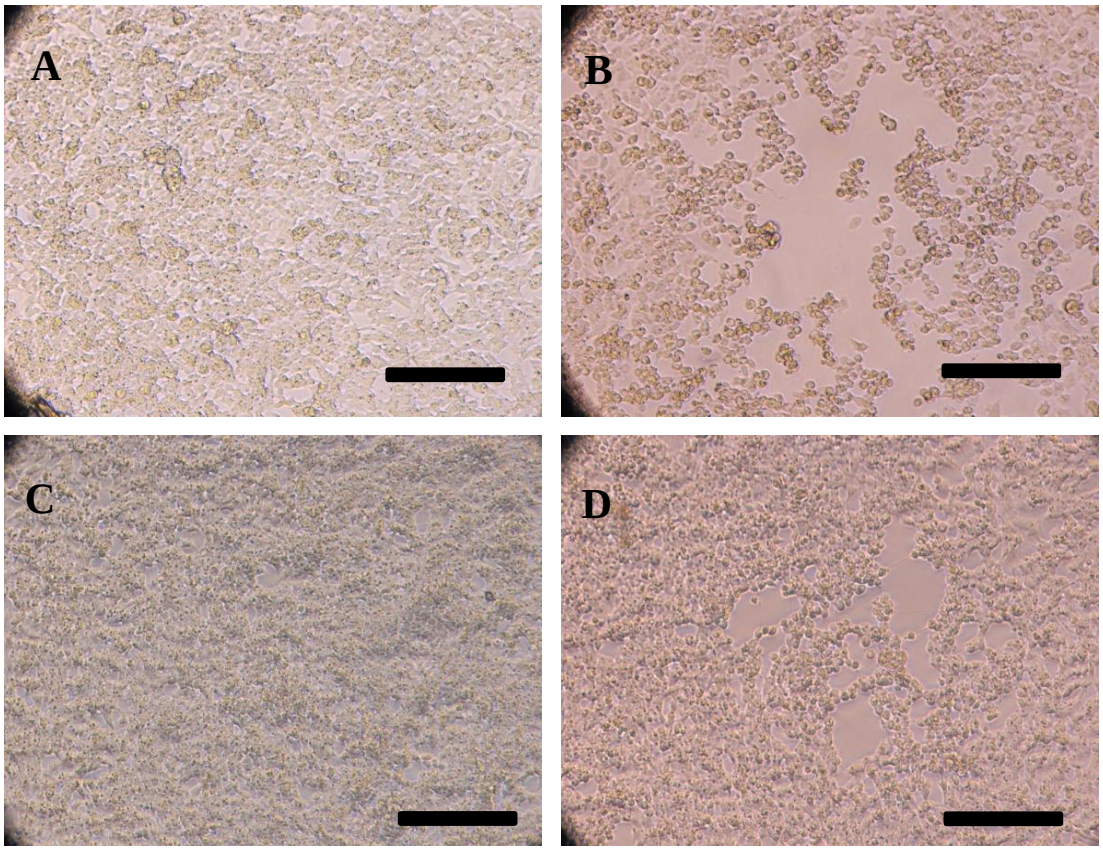

Figure 7.3. Microscopy pictures of HSV-1-infected neuroblastoma cells co-cultured with microglia at 48h post-infection. HSV-1-infection was done in neuroblastoma cells at MOI=0.01. Pictures of neuroblastoma cells were taken 48h pi by light microscopy. **A.** Uninfected neuroblastoma cells. Cells are around 90% confluent. **B.** HSV-1-infected neuroblastoma cells. There are big spaces and gaps between cells (around 50% confluent). **C.** Uninfected neuroblastoma cells co-cultured with 300,000 microglia cells. Cells are 100% confluent, darker and more numerous than in (C). **D.** HSV-1-infected neuroblastoma cells co-cultured with $3x10^5$ microglia cells. Gaps have appeared in the monolayer (around 80% confluent). 10x magnification. Scale bar: 50 µm.

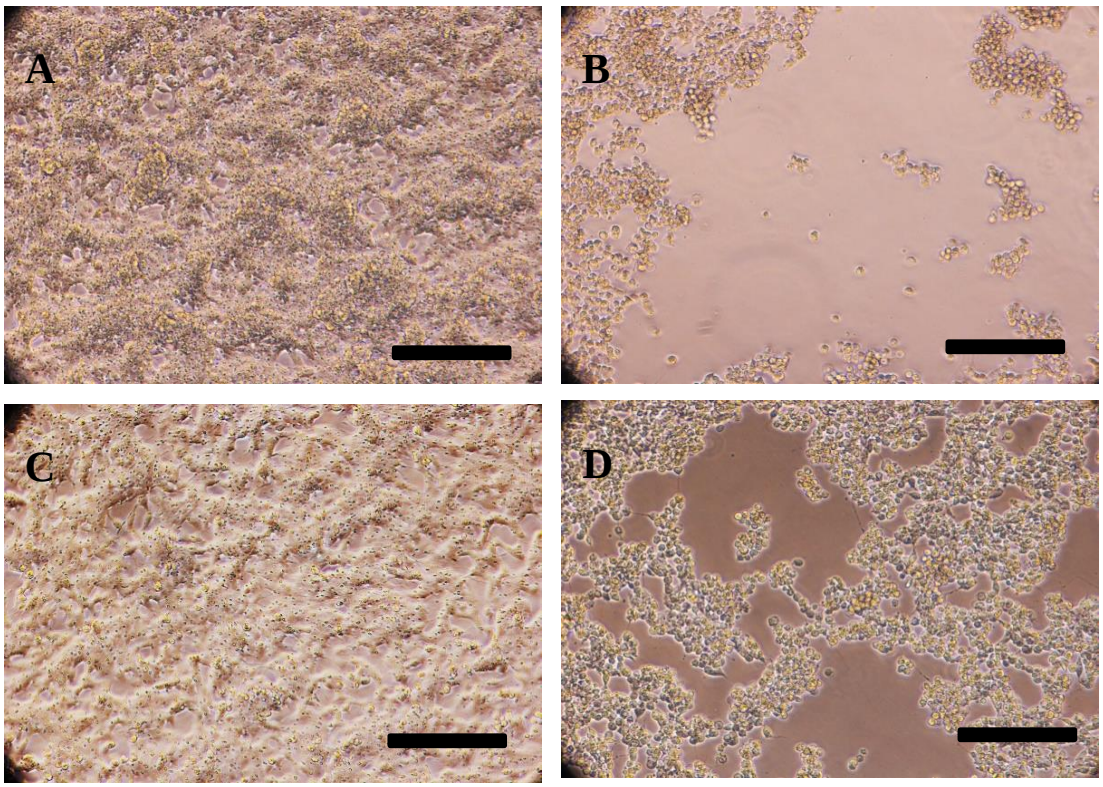

Figure 7.4. Microscopy pictures of HSV-1-infected neuroblastoma cells co-cultured with microglia at 72 h post-infection. HSV-1-infection was done in neuroblastoma cells at MOI=0.01. Pictures of neuroblastoma cells were taken 72h pi by light microscopy. **A.** Uninfected neuroblastoma cells. Few small gaps in the monolayer can be observed (around 90% confluent). In some parts, cell density seems really important with cells on top of each other **B.** HSV-1-infected neuroblastoma cells. Only few cells are still attached (around 15-20% confluent). **C.** Uninfected neuroblastoma cells co-cultured with 300,000 microglial cells. The picture is similar to picture (A). **D.** HSV-1-infected neuroblastoma cells co-cultured with 300,000 microglial cells. Cell density has dropped with a confluency around 30-40%. 10 x magnification. Scale bar: 50 µm.

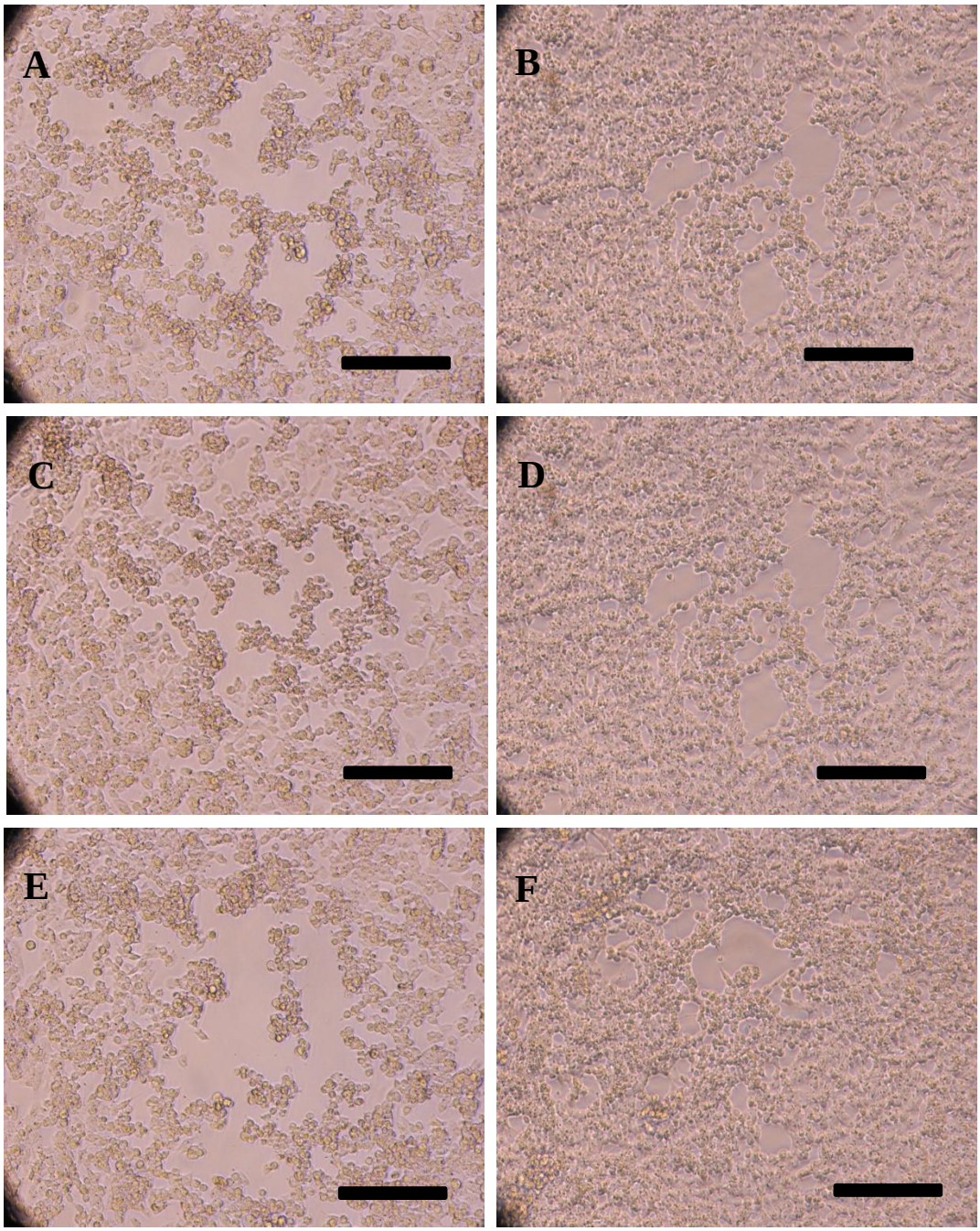

Figure 7.5. Supplementary microscopy pictures of HSV-1-infected neuroblastoma cells co-cultured with microglia at 48 h post-infection. HSV-1-infection was done in neuroblastoma cells at MOI=0.01. Pictures of neuroblastoma cells were taken 48h pi by light microscopy. **A, C, E**. HSV-1-infected neuroblastoma cells. There are big spaces and gaps between cells (around 50% confluent). **B, D, F.** HSV-1-infected neuroblastoma cells co-cultured with $3x10^5$ microglial cells. Gaps have appeared in the monolayer (around 80% confluent) but the monolayers are more dense than that of infected cells cultured alone. 10 x magnification. Scale bar: 50 µm.

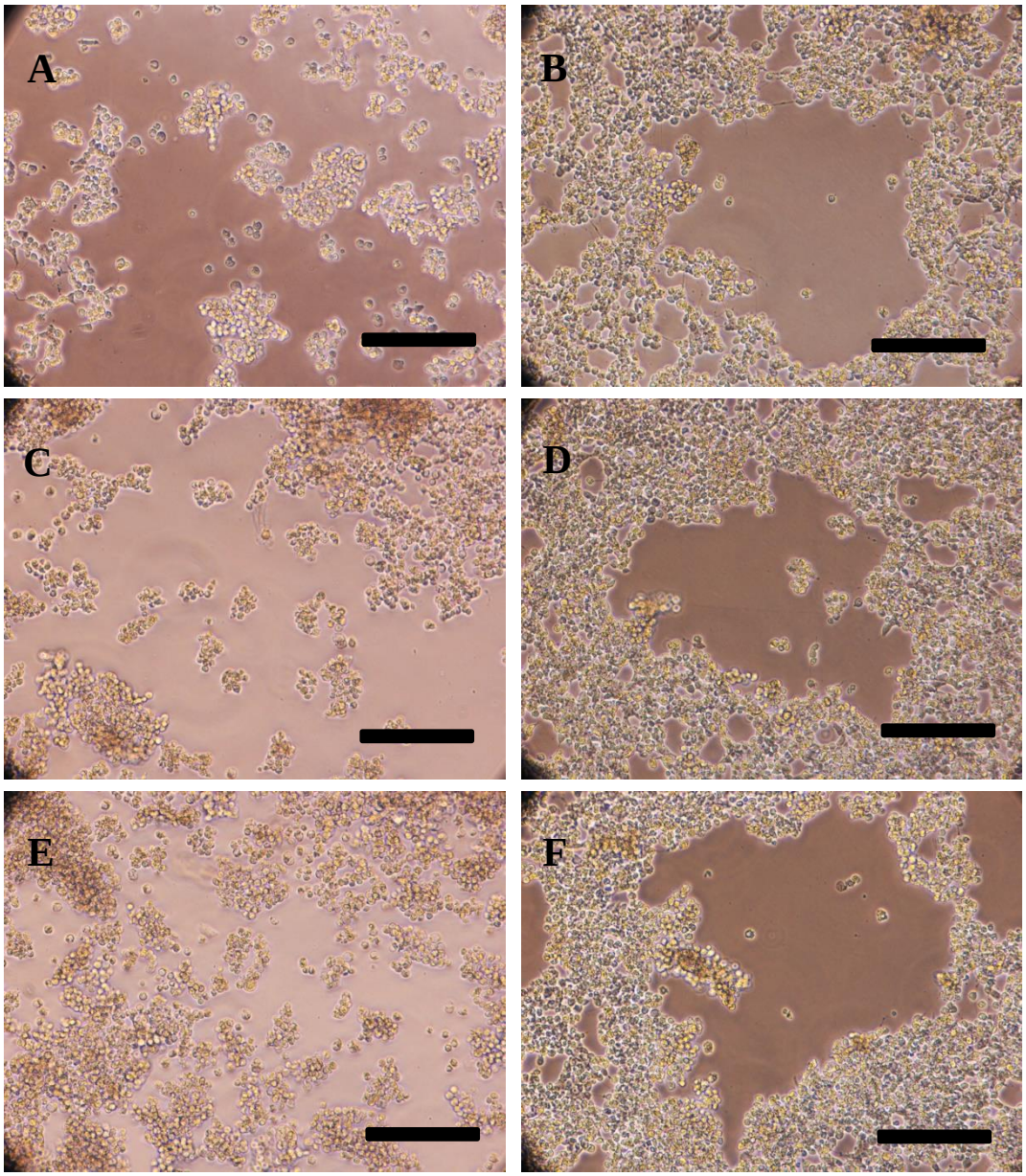

Figure 7.6. Supplementary microscopy pictures of HSV-1-infected neuroblastoma cells co-cultured with microglia at 72 h post-infection. HSV-1-infection was done in neuroblastoma cells at MOI=0.01. Pictures of neuroblastoma cells were taken 72 h pi by light microscopy. **A, C, E.** HSV-1-infected neuroblastoma cells. Only few cells are still attached (around 20% confluent) and a lot of cell debris are floating. **B, D, F.** HSV-1-infected neuroblastoma cells co-cultured with 300,000 microglia cells. Cell density has dropped with a confluency around 30-40%. 10 x magnification. Scale bar: 50 µm.

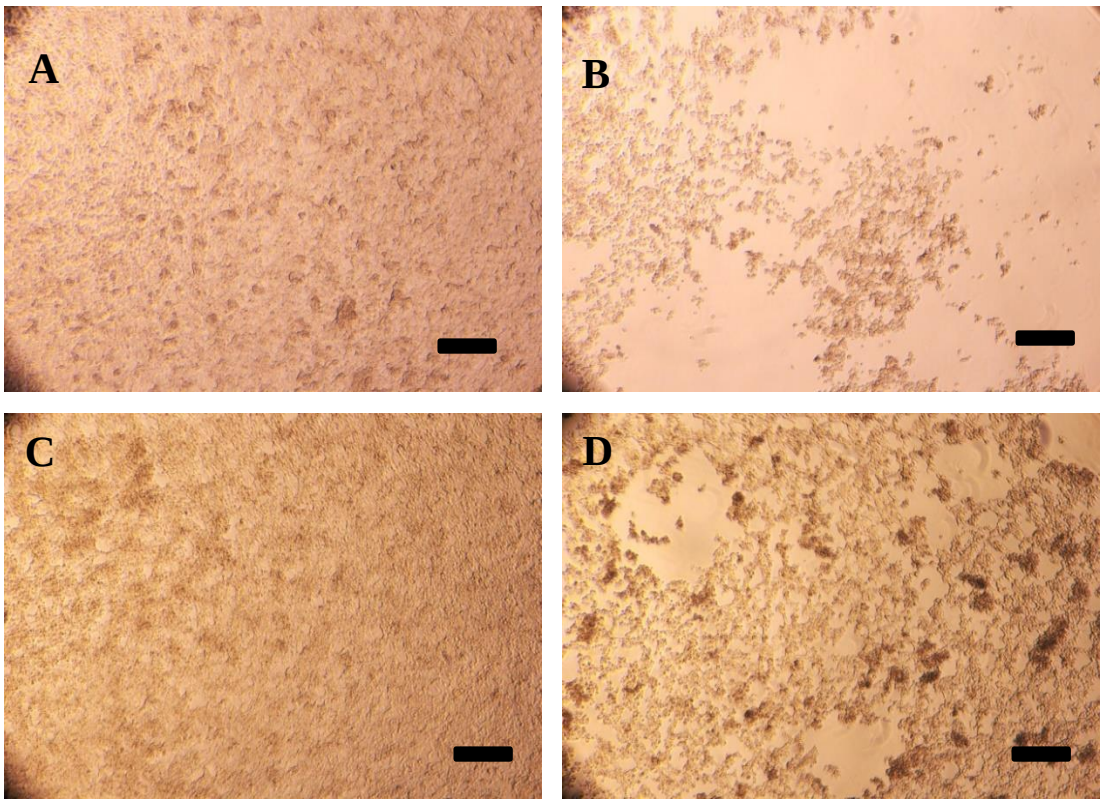

Figure 7.7. Microscopy pictures of HSV-1-infected neuroblastoma cells co-cultured with microglia at 72h post-infection (4x magnification). HSV-1-infection was done in neuroblastoma cells at MOI=0.01. Pictures of neuroblastoma cells were taken 72h pi by light microscopy. **A.** Uninfected neuroblastoma cells. Few small gaps in the monolayer can be observed (around 90% confluent). **B.** HSV-1-infected neuroblastoma cells. Only few cells are still attached (around 15-20% confluent). **C.** Uninfected neuroblastoma cells co-cultured with 300,000 microglial cells. Cell density seem even higher than in (A). **D.** HSV-1-infected neuroblastoma cells co-cultured with 300,000 microglial cells. Cell density has dropped with a confluency around 50%. 4 x magnification. Scale bar: 50 µm.

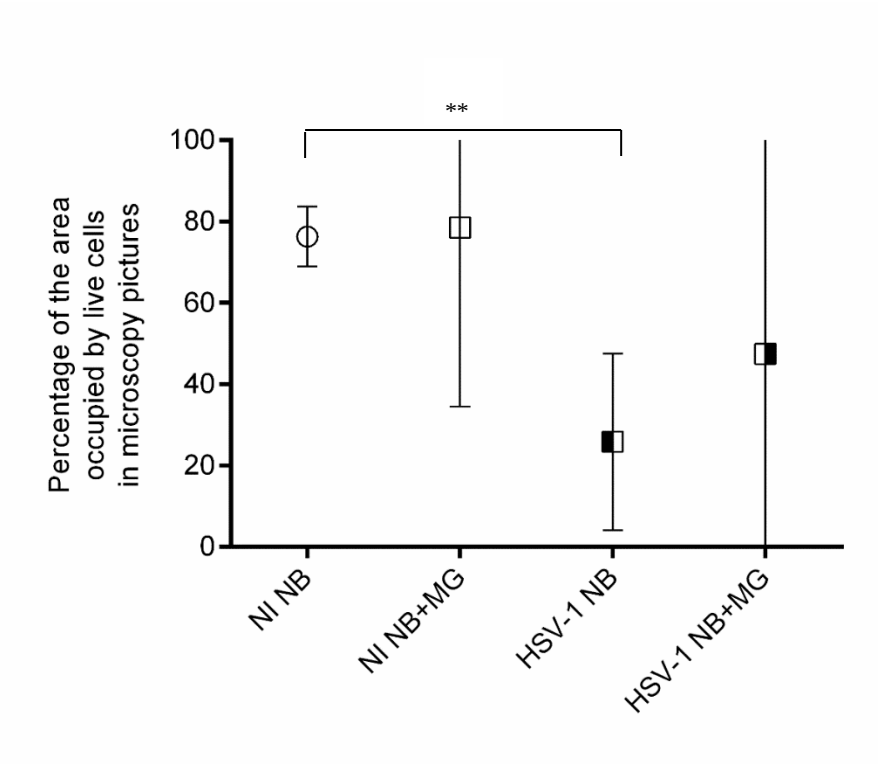

Figure 7.8. The effect of microglia culture on attached cell area on microscopy pictures of HSV-1-infected neuroblastoma cells at 72 h post-infection. NI NB: Uninfected neuroblastoma cells; NI NB+MG: Uninfected neuroblastoma cells co-cultured with microglia; HSV-1 NB: HSV-1-infected neuroblastoma cells; HSV-1 NB+MG: HSV-1-infected neuroblastoma cells co-cultured with microglia. HSV-1-infection was done at MOI=0.01 in neuroblastomas. Areas of live neuroblastoma cells were measured by the software "ImageJ" from 4 x magnification pictures taken at 72 h post-infection. Data are expressed as mean of the area of live cells +95% CI and were obtained as described in the chapter 2 (Materials and Methods). Three pictures for NI NB, two pictures for NI NB+MG, five for HSV-1 NB and three for HSV-1 NB+MG were analysed. These pictures come from a single experiment. ANOVA statistically showed significant differences between the means of the different conditions ($p<0.005$). (**) $p<0.005$ (t-test).

A

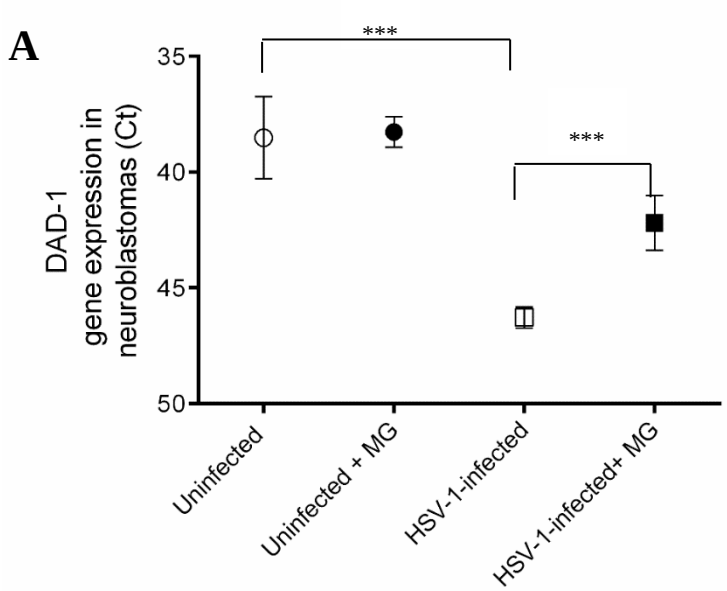

B

	(DAD-1 Ct)infected - (DAD-1 Ct) uninfected
NB	7,76
NB+MG	3,92

Figure 7.9. The effect of microglia co-culture on DAD-1 gene expression in HSV-1-infected neuroblastoma cells. A. DAD-1 gene expression in neuroblastoma cells (Ct values) co-cultured or not with microglial cells. HSV-1-infection was done in neuroblastoma cells at MOI=0.01 and DAD-1 gene expression was measured at 72h pi. The values represent Ct values after qRT-PCR targeting DAD-1 in uninfected (circle) or HSV-1-infected (squares) neuroblastoma cells co-cultured with microglial cells (filled in black) or not (filled in white). Each point represents the mean + 95% CI of data from one experiment. Triplicates were used for each point-time. ANOVA statistically showed significant differences between the means of the different conditions ($p<0.0001$). (**) $p<0.005$ (t-test). (***) $p<0.005$ (multiple t-tests). **B.** DAD-1 ΔCt values in infected neuroblastomas co-cultured or not with microglial cells. NB: Infected Neuroblastoma cells cultured alone; NB+MG: Infected Neuroblastoma cells co-cultured with microglial cells. The data in this table represents the delta Ct values of the gene DAD-1 in Infected neuroblastoma cells culture alone (NB) and in infected neuroblastoma cells co-cultured with microglia. The results were obtained by calculating "DAD-1 Ct (infected) - DAD Ct (uninfected)" from the figure A for both conditions.

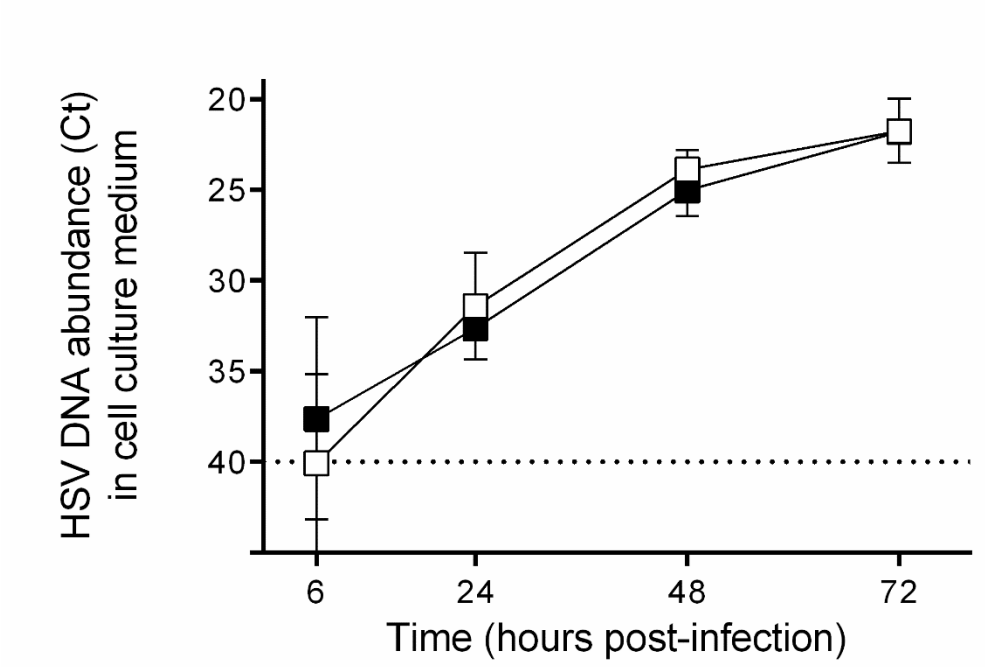

Figure 7.10. Influence of microglia co-culture on HSV DNA abundance in neuroblastoma cell culture medium following HSV-1 infection in neuroblastoma cells. HSV-1-infection was done in neuroblastomas at MOI=0.01. HSV DNA abundance was measured in neuroblastoma culture medium at 6, 24, 48, and 72 h pi. The values represent Ct values after HSV DNA qPCR from culture medium of HSV-1-infected neuroblastomas co-cultured with microglia (filled in black) or not (in white). Each point represents the mean + 95% CI of data from one experiment. Triplicates were used for each time-point. Multiple t-tests were performed (no statistical difference at any time-point).

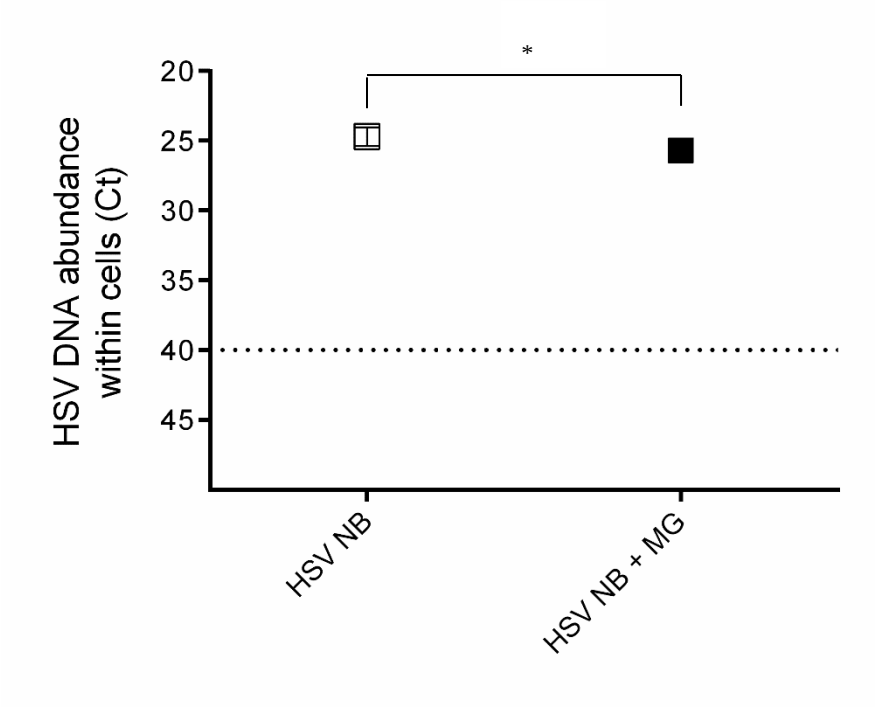

Figure 7.11. Influence of microglia co-culture on HSV DNA abundance within neuroblastoma cells following HSV-1-infection in neuroblastoma cells. HSV NB: HSV-1-infected neuroblastomas, HSV NB + MG: HSV-1-infected neuroblastomas co-cultured with microglia. HSV-1-infection was done in neuroblastomas at MOI=0.01. HSV DNA abundance was measured within neuroblastomas at 72 h pi following nucleic acid extraction. The values represent Ct values after HSV DNA qPCR following nucleic extraction from HSV-1-infected neuroblastomas, co-cultured with microglia (in black) or not (in white). Each point represents the mean + 95% CI of data from one experiment. Triplicates were used for each point-time in each experiment. (*) $p<0.05$ (t-test).

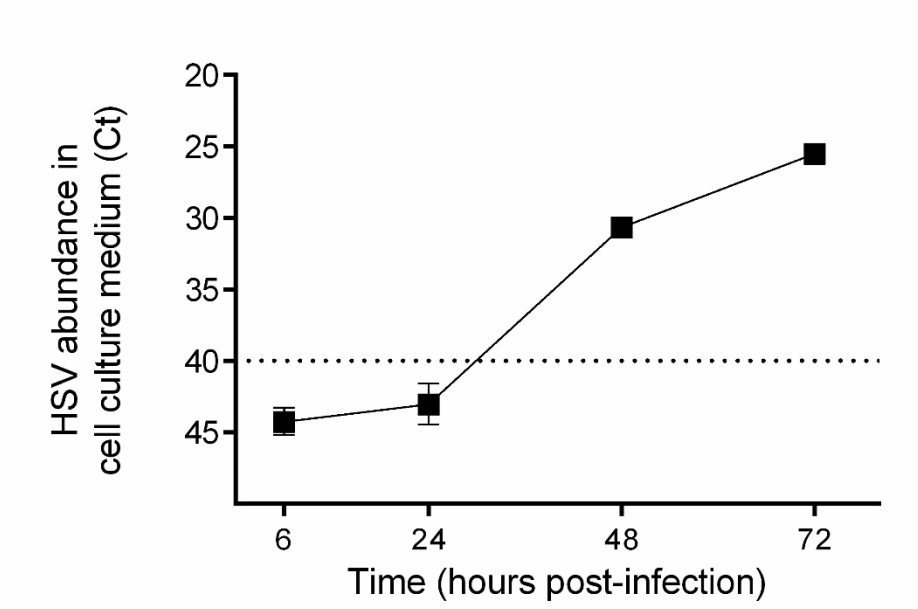

Figure 7.12. HSV DNA abundance in culture medium of microglia co-cultured with HSV-1-infected neuroblastoma cells. HSV-1 infection was done in neuroblastoma cellss at MOI=0.01. HSV DNA abundance was measured in culture medium of microglial cells at 6, 24, 48, and 72 h pi (top compartment-insert). The values represent Ct values after HSV DNA qPCR from culture medium of microglia cells co-cultured with HSV-1-infected neuroblastomas (bottom compartment). Each point represents the mean + 95% CI of data from one experiment. Triplicates were used for each point-time.

7.2.2. HSV-1-infection of primary astrocytes co-cultured with microglia cells

As aforementioned, a co-culture system using both HSV-1-infected astrocytes (at the bottom of the well) and microglial cells (insert-top compartment) was set up to study the influence of remote microglia on HSV-1-infection of astrocytes.

By light microscopy we could observe that astrocyte cell density was not increased at 24 h-72 h pi when co-cultured with microglial cells (seeded at $3x10^5$ cells) (fig7.13-16) . At 72 h pi, the presence of microglia was shown to increase infected astrocyte cell density. This was seen in multiple 10 x magnification pictures (fig 7.15 and fig 7.16). The attached cell area can only be analysed by the software "ImageJ" by using 4 x magnification pictures (fig 7.17-18). The increase in astrocyte cell survival with microglia co-culture was also observed by analysis of attached cell area although more pictures are required for statistical significance (fig 7.18).

At 72 h pi, no significant change in DAD-1 gene expression was detected between astrocytes cultured alone or in co-culture (fig 7.19). Microglia co-culture did not influence HSV-1 DNA abundance neither in astrocytes in culture medium or within astrocytes (fig 7.20-21).

HSV DNA qPCR in microglial cell culture medium showed an increase in HSV DNA abundance over time (6-72 h pi) (fig 7.22). HSV DNA was detected by qPCR within microglial cells co-cultured with infected astrocytes (24 h-72 h pi) (data not shown).

Altogether, there was no decrease in astrocyte cell number, as measured by qRT-PCR, "ImageJ" or observed by light microscopy when astrocytes were grown in co-culture with microglia. There was also no sustained change in HSV DNA abundance among the astrocytes during co-culture.

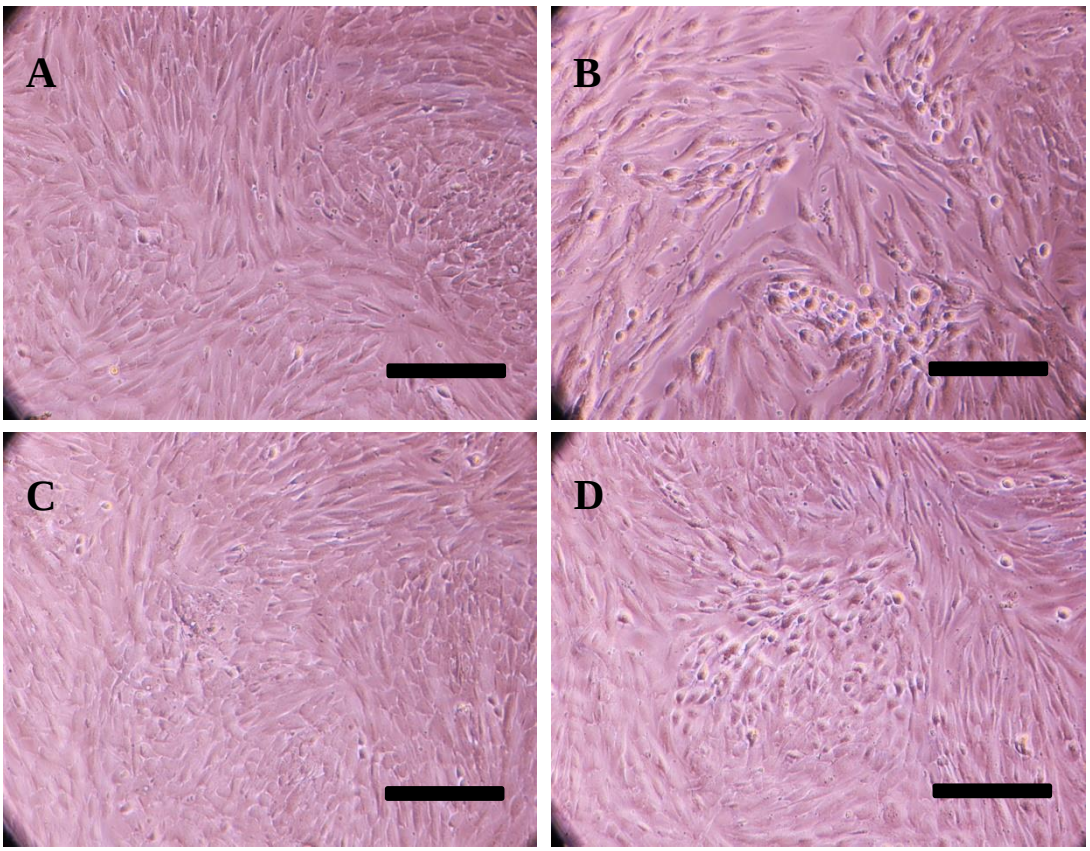

Figure 7.13. Microscopy pictures of HSV-1-infected astrocytes co-cultured with microglia at 24 h post-infection. HSV-1-infection was done in astrocytes at MOI=0.01. Pictures of primary astrocytes were taken 24h pi by light microscopy. **A.** Uninfected astrocytes. Cells are 100% confluent and exhibit classic morphologic features of astrocytes (long, thin, "star-like" ramifications). **B.** HSV-1-infected astrocytes. HSV-1 induced live astrocyte loss (gaps in the monolayer, loss of confluency) and morphologic changes (appearance of rounded cells) have appeared. **C.** Uninfected astrocytes co-cultured with $3x10^5$. The monolayer is intact, similar to the one in A. **D.** HSV-1-infected astrocytes co-cultured with $3x10^5$ microglia cells. The picture is similar as the one in C. 10x magnification. Scale bar: 50 μm.

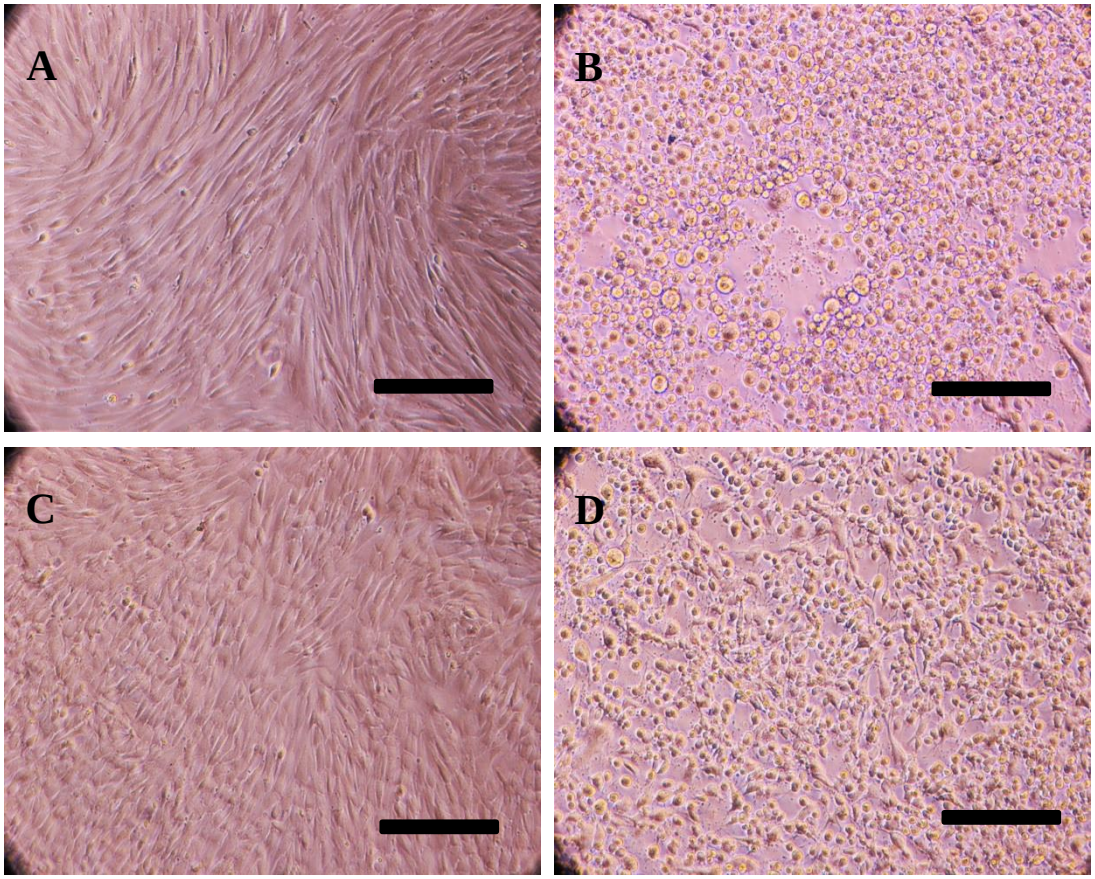

Figure 7.14. Microscopy pictures of HSV-1-infected astrocytes co-cultured with microglia at 48 h post-infection. HSV-1-infection was done in astrocytes at MOI=0.01. Pictures of primary astrocytes were taken 48h pi by light microscopy. **A.** Uninfected astrocytes. Cells are 100% confluent and exhibit classic morphologic features of astrocytes (long, thin, "star-like" ramifications). **B.** HSV-1-infected astrocytes. HSV-1 infection course progressed with bigger gaps between cells and all cells looking round. **C.** Uninfected astrocytes co-cultured with $3x10^5$ microglia cells. The picture is similar as the one in A. **D.** HSV-1-infected astrocytes co-cultured with $3x10^5$ microglia cells. HSV-1 has also induced both live cell loss (gaps between cells, loss of confluency) and morphologic changes with majority cells looking round now. However, there are still some astrocytes with classic morphologic changes and a higher cell density compared to the picture B. Pictures are representative of 2 independent experiments. 10 x magnification. Scale bar: 50 µm.

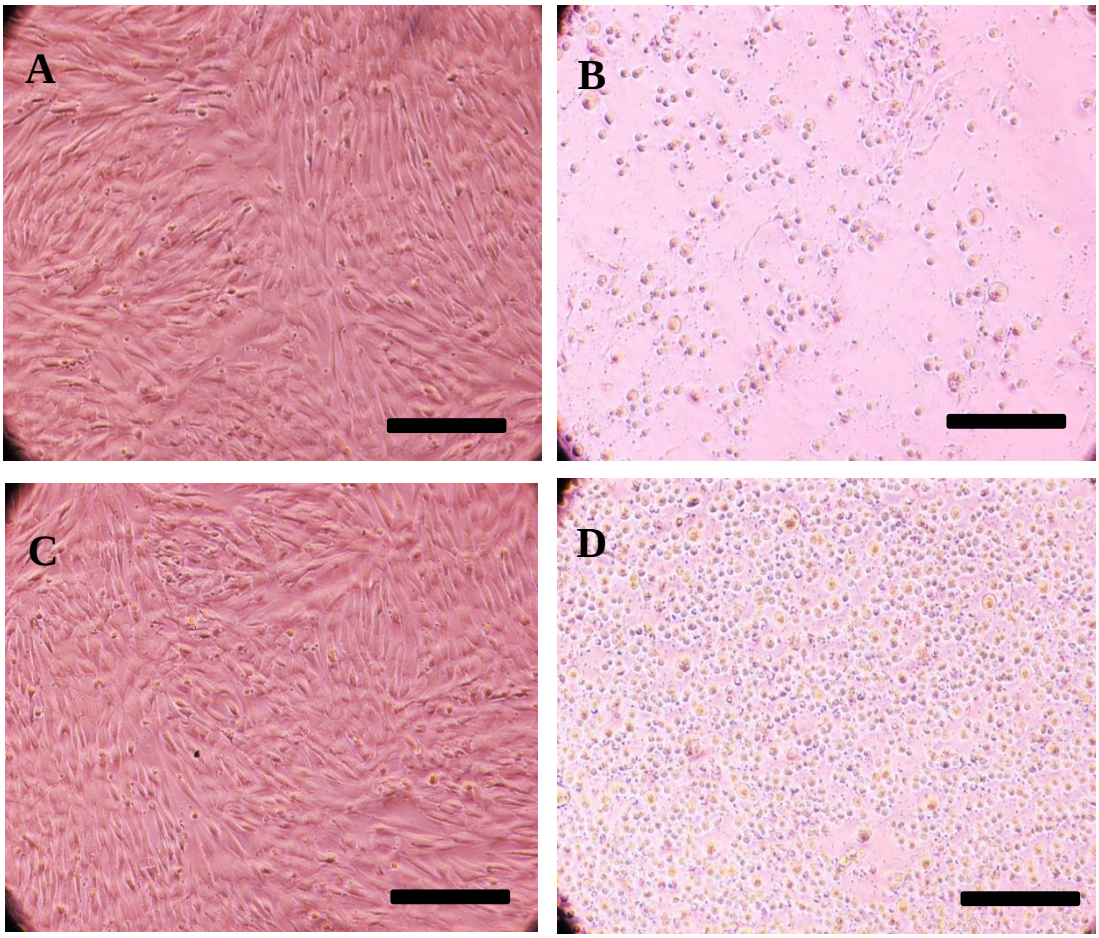

Figure 7.15. Microscopy pictures of HSV-1-infected astrocytes co-cultured with microglia at 72 h post-infection (10 x magnification). HSV-1-infection was done in astrocytes at MOI=0.01. Pictures of primary astrocytes were taken 72h pi by light microscopy. **A.** Uninfected astrocytes. Cells are 100% confluent and exhibit classic morphologic features of astrocytes (long, thin, "star-like" ramifications). **B.** HSV-1-infected astrocytes. HSV-1 infection course has still progressed with only few round cells left attached on the monolayer (around 10% confluent). **C.** Uninfected astrocytes co-cultured with $3x10^5$ microglia cells. The picture is similar as the one in A. **D.** HSV-1-infected astrocytes co-cultured with 3x10^5 microglia cells. All cells look round but many more cells are still alive and attached to the monolayer compared to B and C. Pictures are representative of 2 independent experiments. 10x magnification. Scale bar: 50 µm.

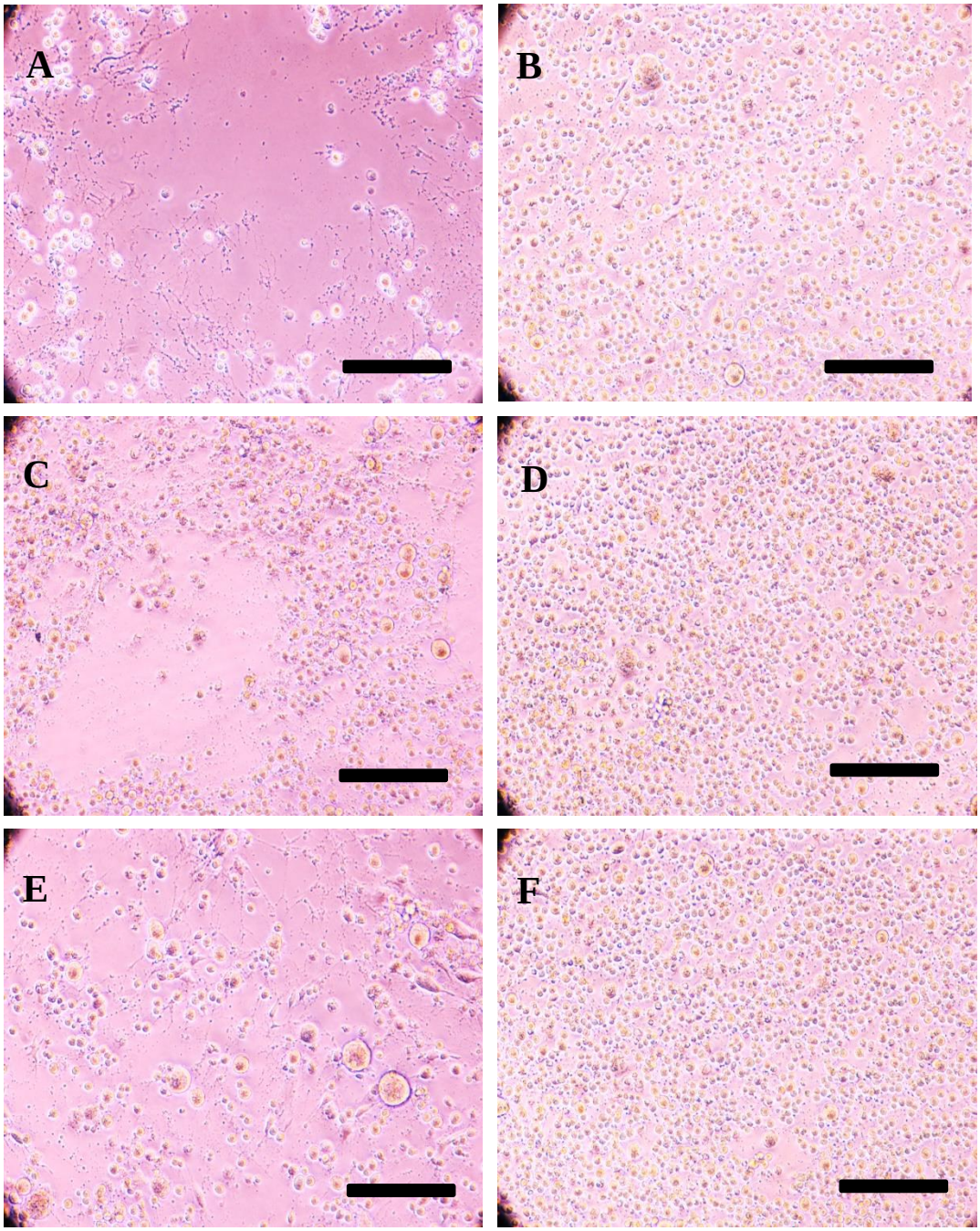

Figure 7.16. Supplementary microscopy pictures of HSV -1-infected astrocytes co-cultured with microglia at 72 h post-infection (10 x magnification). HSV-1-infection was done in astrocytes at MOI=0.01. Pictures of primary astrocytes were taken 72h pi by light microscopy. **A, C, E.** HSV-1-infected astrocytes. HSV-1 infection course has induced extensive cell death. Confluence is around 15-20% confluent in average. **B, D, F.** HSV-1-infected astrocytes co-cultured with $3x10^5$ microglia cells. All cells look round but many more cells are still alive and attached to the monolayer compared to A, C and E (. Pictures are representative of 2 independent experiments. 10 x magnification. Scale bar: 50 µm.

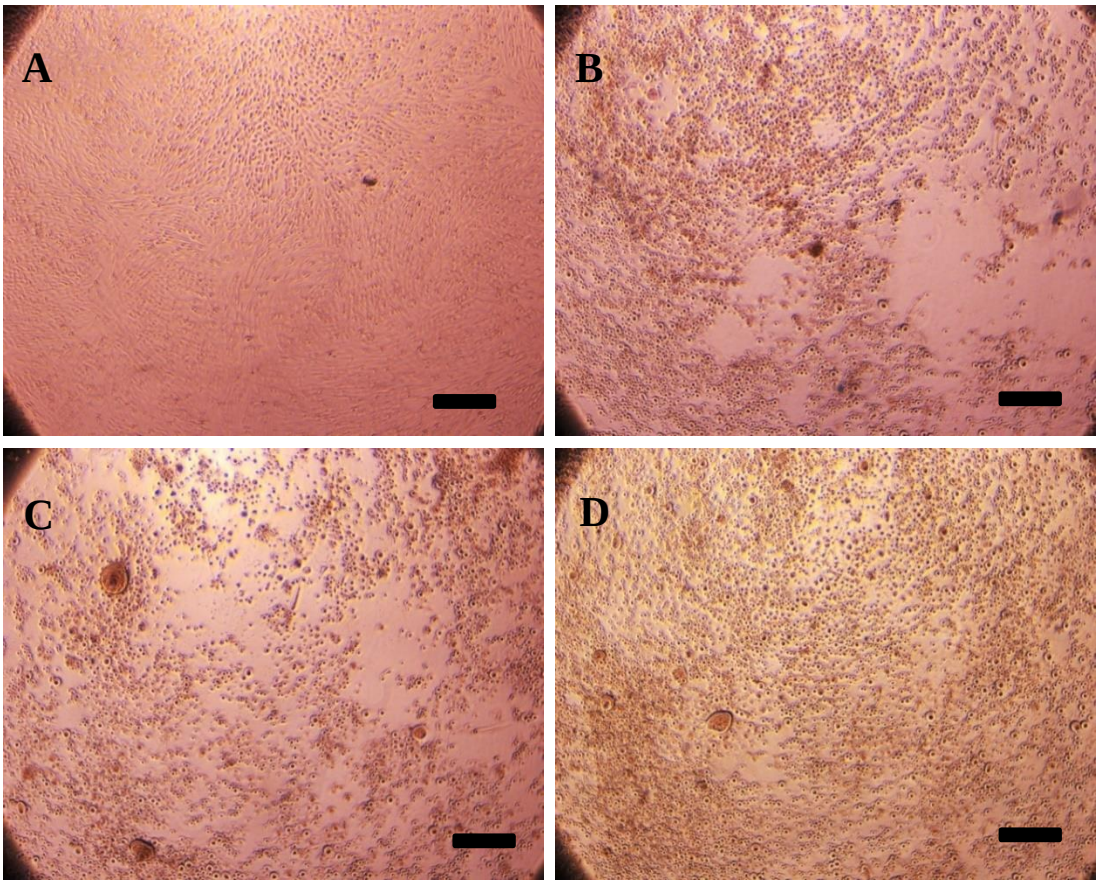

Figure 7.17. Microscopy pictures of HSV-1-infected astrocyte co-cultured with microglia at 72h post-infection (4 x magnification). HSV-1-infection was done in astrocytes at MOI=0.01. Inserts containing microglia cells were added following astrocyte infection. Pictures of primary astrocytes were taken 72h pi by light microscopy. **A.** Uninfected astrocytes. Cells are 100% confluent. **B.** HSV-1-infected astrocytes. HSV-1 infection course has still progressed with big gaps between cells (around 50% confluency). **C.** HSV-1-infected astrocytes co-cultured with 0.5x10^5 microglia cells. The picture is similar as picture B but with slightly lower cell density (around 30% confluency). **D.** HSV-1-infected astrocytes co-cultured with 3x10^5 microglia cells. Confluency is still high (80-90%). Pictures are representative of 2 independent experiments. 4x magnification. Scale: 50 µm.

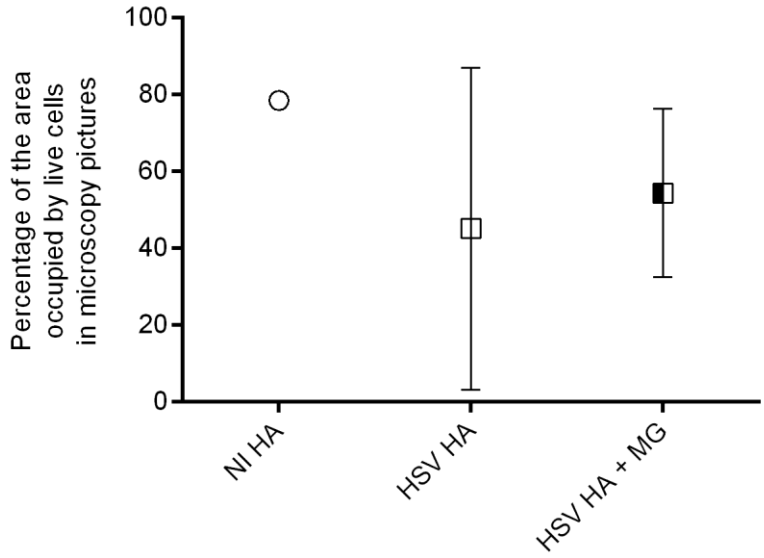

Figure 7.18. The effect of microglia co-culture on live cell area on microscopy pictures of HSV-1-infected primary astrocytes at 72 h post-infection. NI HA: Uninfected Human Astrocytes; HSV HA: HSV-1-infected Human Astrocytes; HSV HA + MG: HSV-1-infected astrocytes co-cultured with 300,000 microglial cells. HSV-1-infection was done at MOI=0.01 in primary astrocytes. Areas of live primary astrocytes were measured by the software ImageJ from pictures taken at 72h post-infection. Data are expressed as mean of the area of live cells +95% CI and were obtained as described in the chapter 2 (Materials and Methods). One picture for NI HSV, two pictures for HSV HA and four for HSV + 300,000 MG were analysed. These pictures are representative of two experiments. Statistical analysis was not performed because of a really low number of replicates.

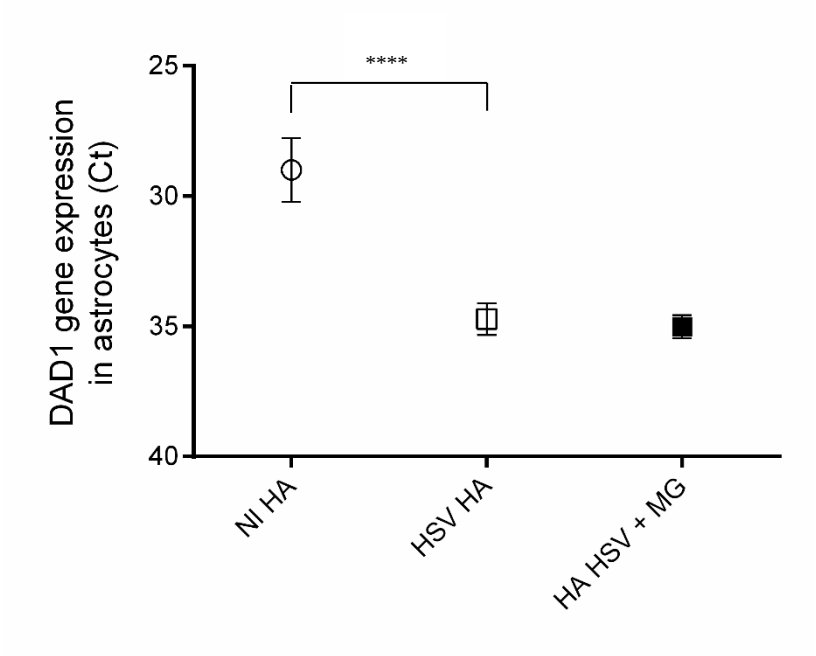

Figure 7.19. DAD-1 gene expression in HSV-1-infected astrocytes co-cultured with microglia. HSV-1-infection was done in astrocytes at MOI=0.01. DAD-1 gene expression was measured by qRT-PCR at 72h pi following nucleic extraction of astrocytes. The values represent Ct values after qRT-PCR targeting DAD-1 in uninfected (circle) or HSV-1-infected (squares) astrocytes co-cultured with microglia cells (filled in black) or not (in white). Each point represents the mean + 95% CI of data from 2 independent experiments. Duplicates (for uninfected and HSV-1-infected populations) and triplicates (for HSV-1-infected cells co-cultured with microglia) were used in each experiment. ANOVA test statistically showed significant differences between the means of the different conditions ($p<0.0001$). (****) $p<0.0005$ (Mann-Whitney test).

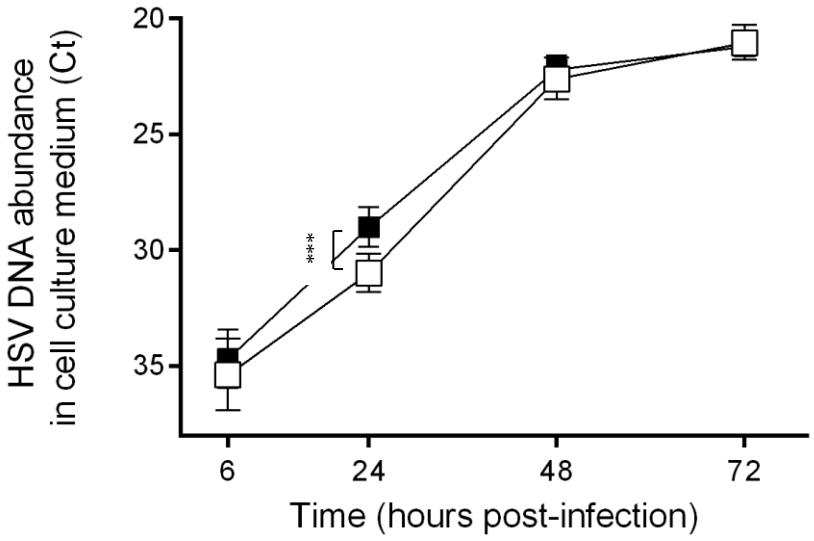

Figure 7.20. The effect of microglia co-culture on HSV DNA abundance in astrocyte culture medium following HSV-1 infection in astrocytes. HSV-1-infection was done in astrocytes at MOI=0.01. HSV DNA abundance was measured in astrocyte culture medium at 6h; 24h; 48h and 72h pi. The values represent Ct values after HSV DNA qPCR from culture medium of HSV-1infected astrocytes cultured with 300,000 microglia cells (squares filled in black), or not co-cultured (white circles). Each point represents the mean + 95% CI of data from 2 independent experiments. Triplicates were used for each point-time in each experiment except for the infected cells cultured alone (duplicates). (***) $p<0.005$ (multiple t-tests).

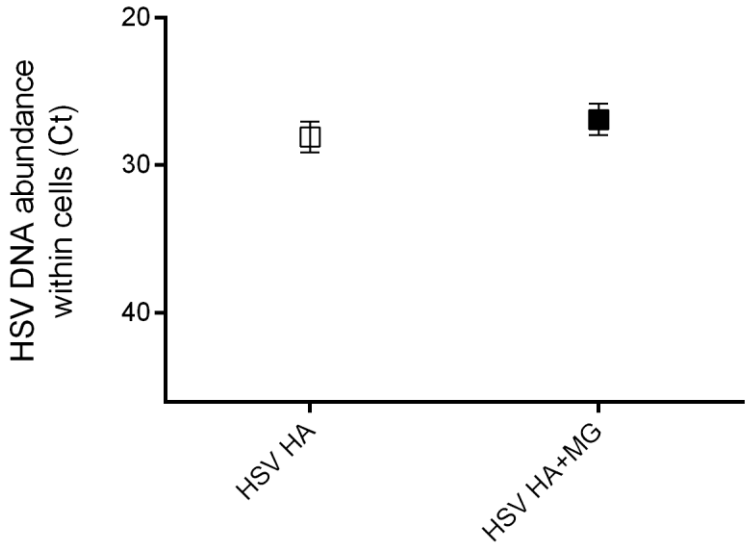

Figure 7.21. The effect of microglia co-culture on HSV DNA abundance within astrocytes following astrocyte HSV-1-infection. HSV HA: HSV-1-infected human astrocytes, HSV HA+MG: HSV-1-infected astrocytes co-cultured with 300,000 microglial cells.HSV-1-infection was done in astrocytes at MOI=0.01. HSV DNA abundance was measured within astrocytes at 72 h pi. The values represent Ct values after HSV DNA qPCR following nucleic extraction from infected astrocytes co-cultured with microglia cells (squares filled in black) or not co-cultured (white squares). Each point represents the mean + 95% CI of data from 2 independent experiments. Triplicates were used in each experiment. P>0.05 (t-test).

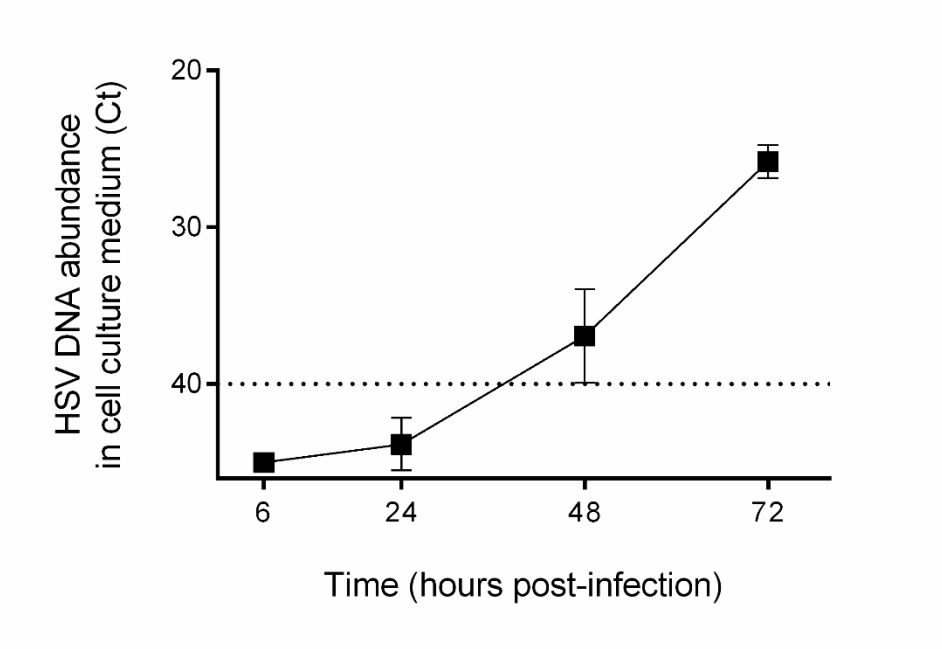

Figure 7.22. HSV DNA abundance in culture medium of microglia co-cultured with HSV-1-infected astrocytes. HSV-1 infection was done in astrocytes at MOI=0.01 (bottom compartment). HSV DNA abundance was measured in culture medium of microglia cells (top compartment) at 6h, 24h, 48h and 72 h pi. The values represent Ct values after HSV DNA qPCR from culture medium of microglia cells co-cultured with HSV-1-infected astrocytes. Each point represents the mean + 95% CI of data from 2 independent experiments. Triplicates were used in each experiment. (***) $p<0.005$; (****) $p<0.0001$ (multiple t-tests).

7.3. Discussion

HSV-1 encephalitis seems to be due to both viral replication and detrimental immune response in brain tissue[45, 49, 169, 37, 85, 170]. The brain cells damaged are not only neurons but also astroglial cells including microglia and astrocytes cells. Crucially, all these brain cells interact between themselves[85, 140]. In HSV-1 encephalitis studies, the role of microglia cells seems crucial, in-part through cytokine/chemokine release and recruitment of neutrophils and lymphocytes[68, 85, 98, 173, 86, 174, 142, 136, 99, 87]. However, they have been shown to be both protective and detrimental during HSV-1 brain infection[90, 136, 99].

There is a crucial need to establish new HSE *in vitro* models using human brain cells to better understand the role of microglia in HSE pathogenesis and protection[90, 136, 99]. Of note, in the literature, there are no HSE *in vitro* studies using co-culture of human brain cells. Indeed, to my knowledge, only two co-culture studies investigated the interaction between two different brain cell type following HSV-1-infection[136, 99]. However, microglia and the brain cells targeted (mixed neural cell culture or neural progenitor cells) were all murine[136, 99]. Hence, in this chapter, I set up new HSV-1 brain infection *in vitro* systems using pore-containing inserts to culture two human brain cell types together (astrocytes/microglia or neuroblastomas/microglia). The major aim of this chapter was to study the remote influence of microglia cells on HSV-1-infected neuroblastomas or primary astrocytes. In each co-culture system, HSV-1-infection was performed at MOI=0.01 in neuroblastoma cells or astrocytes. The effects of the remote microglia co-culture on HSV-1-infected neuroblastoma cells or astrocytes were observed at 24, 48 and 72 h pi.

Firstly, this chapter showed that the co-culture with microglia had no detrimental effect on HSV-1 infection of astrocytes. Indeed, the presence of microglia cells did not induce an increased live astrocyte loss when assessed by light microscopy observations (multiple 10 x magnification microscope pictures) or DAD-1 qRT-PCR. Microglia co-culture also did not

exacerbate HSV replication as observed by qPCR from culture medium and within cells (fig 7.13-21 and fig 7.26-7.28). Of note, although showing the same trend, the analysis of attached cell area by ImageJ was done with too few 4 x magnification (only magnification used for quantifying attached cell area using ImageJ) images for statistical significance (fig 7.18).

The data from the co-culture of infected neuroblastomas with microglia was only preliminary works. Obviously, they have to be interpreted more carefully since only one time-course experiment was performed. The presence of microglia was associated with an increase in infected neuroblastoma cell survival by multiple light microscopy observations and qRT-PCR targeting DAD-1 (fig7.2-7.7 and fig 7.9). Here too, the attached cell area analysis by ImageJ could not lead to trustworthy results as there were not enough 4 x magnification pictures analysed for statistical significance (fig 7.8). Interestingly, microglia culture induced a decrease in HSV DNA abundance within infected neuroblastomas at 72 h pi (fig7.11) but no effect on culture medium HSV DNA abundance (7.10).

HSV DNA abundance was found in culture medium of microglia cells co-cultured with infected neuroblastomas or astrocytes (fig7.12, 7.22) confirming the fact that HSV-1 particles (typically around 200nm of diameter[6]) could pass through the pores (400 nm of diameter) and reach the top compartment (insert). Moreover, HSV DNA was found within microglia cells co-cultured with infected neuroblastomas and astrocytes (data not shown). This suggests that HSV-1 can also infect microglia cells after they reached the top compartment.

The main limitation of this work is the lack of data coming from quantitative and accurate techniques for live cell viability. Indeed, the limitations of DAD-1 qRT-PCR sensitivity have already been stated in the previous chapters. Unfortunately, the WST-1 assay was optimised for 96 well-plates and not 12-well plates and could not be performed on these co-culture experiments. The analysis results of microscopy pictures by ImageJ could not be trusted as there were not enough 4 x magnification microscopy pictures of quality. However, a

reasonable amount of 10 x magnification microscopy pictures was included in this study. Unfortunately, they could not be analysed by "ImageJ" as I could not transform the images into satisfying proper negative pictures due to extensive brightness inside the intracellular compartment. More studies on these co-cultures repeating the same experiments with a better microscope or camera or using other techniques for cell viability quantification such as FACS would be interesting.

Altogether, microglia cells were shown not to exacerbate HSV-1-infection of astrocytes. Although it needs further validation, in neuroblastomas, the presence of microglia appeared to protect against HSV-1-induced cell damage. This may be possible due to exchange of soluble molecules through pores of the membrane separating both compartments. Hence, microglia-release factors are probably responsible for such an effect (if it was confirmed). *In vitro*, it has been shown that microglia cells, following HSV-1-infection, induce the production of TNF-α, IL-1B, IP-10 and RANTES, and to a lesser extent, that of IL-6, IL-8 and MIP-1a[85]. In mice, an TLR2-dependent-increase in the percentage of microglia cells producing TNF was also observed following HSV-1 challenge[90]. Interestingly, IL-6 has already been shown to have a protective role during HSV-1-infection of murine neural Progenitor Cell (NPC) (in a murine co-culture NPC/microglia model; MOI=0.0001, at 4 days pi)[136].

Finally, these two HSV-1 brain infection *in vitro* systems could also be used as platform to assess adjunctive therapies to aciclovir such as dexamethasone or infliximab. This would represent a unique opportunity to assess therapies in more complex HSE *in vitro* human models, closer to *in vivo* conditions.

Chapter 8 Discussion

8.1. Rationale and aim of the thesis.

Herpes simplex encephalitis (HSE) is a lethal brain infection induced by herpes simplex virus subtype 1 (HSV-1). Brain damage associated with HSE is reported to be caused directly by the virus and indirectly by the host immune responses. Aciclovir, the gold standard anti-viral therapy, targets HSV replication, but not brain inflammation. Hence, administration of anti-inflammatory drugs alongside aciclovir may improve outcome in HSE [129, 127, 175, 39].

The debate on using anti-inflammatory drugs, especially corticosteroids, for treating HSE has been ongoing for decades. Several small clinical reports have shown a positive impact of corticosteroids on HSE patient outcome [131, 128, 158, 132, 129, 176]. However, use of corticosteroids is questioned by some clinicians because dampening the immune response could lead to an increased viral replication and further HSV-induced brain damage[177, 124]. To date, there have been no large clinical trials confirming that corticosteroids are beneficial when given in combination with aciclovir in HSE patients.

Murine knock-out models for TNF-α (missing the gene encoding for TNF-α) infected with HSV-1 exhibit more severe encephalitis and increased mortality compared to wild-type mice[178]. Similarly, in a mice model of Japanese Encephalitis, administering the TNF inhibitor etanercept, was shown to significantly increase mouse survival, while reducing brain inflammation[134]. In humans TNF-α is reported to be persistently elevated in the cerebrospinal fluid (CSF) of patients suffering with HSE.[71] Together, these reports suggest anti-TNF agents may be a beneficial treatment for patients with HSE.

The main aim of my thesis was to study the effect of dexamethasone (a corticosteroid) and infliximab (an anti-TNF drug) alone or in combination with aciclovir in human brain cell models of HSE.

My objectives were (i) to set up *in vitro* models of HSE using human brain cells and (ii) to assess the effects of aciclovir/dexamethasone and aciclovir/infliximab in HSV-1-infected neuroblastoma and microglial cells. These effects were assessed at the levels of cell viability, HSV DNA abundance and TNF relative gene expression.

8.2. Main results

In chapter 3, HSV-1 viral load (as measured by HSV DNA in culture medium) increased in the brain cell culture models with time from infection. As viral load increased, there was a decrease in cell mitochondrial activity and cell viability in both neuroblastoma and microglial cells. Different viral replication and mitochondrial metabolism dynamics were observed between microglial and neuroblastoma cells following HSV-1 infection. TNF-α and INF-γ relative gene expression was increased following HSV-1 infection in both cell types. However, no significant change in TNF protein abundance was detected during the infection time-course experiments with either brain cell type. In addition, primary astrocytes also showed decreased cell viability as HSV viral load increased (chapters 3 and 7).

In chapter 4, it was shown that administration of aciclovir to the microglia cell culture model was associated with a reduction in total viral load (as measured by HSV DNA abundance in culture medium). Interestingly, no significant change in HSV DNA abundance was detected following administration of aciclovir into the neuroblastoma cell culture model. However, taking a set volume of culture media (from the infected neuroblastoma cells) and adding this medium to an uninfected culture of Vero cells, showed that medium from the aciclovir-treated neuroblastoma cells was associated with significantly less cell death. This indicates aciclovir

treatment is associated with a reduction in the number of infective (active) viruses released from neuroblastoma cells. However, total HSV DNA (derived from either infective or non-infective virus) can remain the same.

Aciclovir treatment was also associated with an increase in cell viability and mitochondrial activity among both cell types.

In chapter 5, administration of dexamethasone was not seen to be associated with any significant change in HSV DNA load when administered alone or in combination with aciclovir in the human brain cell models. Similarly, dexamethasone was not associated with any significant change in cell viability or mitochondrial activity when administered alone or in combination with aciclovir to the cell cultures.

In chapter 6, infliximab, when administered on its own, was associated with an increase in cell viability and mitochondrial activity (48 h-72 h pi). It was also associated with an early decrease in viral load (HSV DNA) in both neuroblastoma and microglia cultures. The combination of aciclovir and infliximab was associated with a lower HSV DNA abundance in both infected microglial and neuroblastoma cells compared to aciclovir alone. Nonetheless, at 72 h pi, the combination of aciclovir and infliximab was not associated with any statiscally significant increase in cell viability or mitochondrial metabolism compared to aciclovir alone in both infected cell types (or also compared to untreated infected cells for microglia).

In chapter 7, *in vitro* models of HSE were set up using co-culture of astrocytes with microglial cells and co-culture of neuroblastoma cells with microglia cells. Microglia co-culture did not appear to influence cell viability of primary astrocytes following HSV-1 infection. My data suggested that neuroblastoma cells exhibited more sustained cell numbers and less cell damage when grown in association with microglia. However, only a preliminary set of experiments was performed. Further work is required to robustly assess significance of these observations.

8.3. Interpretation of the results and their significance in the literature

HSV-1 induced cell death in Kelly neuroblastoma cells, microglia and primary astrocytes (chapters 3 and 7). Hence, HSV-1-infection is directly responsible for cell death in these human brain cell types individually. It has previously been reported that HSV-1 induces brain cell death by both necrosis and apoptosis[39]. In my brain cell models, increased cell loss was associated with a rise in viral load in the culture medium. Rates of change in cell viability following exposure to HSV1 (MOI=0.01) varied between microglial and neuroblastoma cells. Microglia showed sustained mitochondrial activity and viability for a longer time period following HSV infection compared to neuroblastoma cells. My data also showed HSV DNA load initially increased more rapidly in microglia compared to neuroblastoma cells. However, HSV DNA load was not significantly different at 72 h pi between cell types. The findings suggest microglial cells are potentially more permissive to HSV-1 infection than neuroblastoma cells (microglial cells enable higher HSV-1 loads to be generated without loss of mitochondrial activity). In an *in vitro* study using human fœtal brain cells, HSV-1 was reported to be "extensively replicative" in neurons and astrocytes but exhibit only a "slight and short replication" in microglia[85]. The discrepancy between the former study and my results may reflect the different cell lines, HSV strains and MOI used. Thus, they used primary foetal microglia while I used transformed microglia cell line, originally from adult brains. The differences in the development stage as well the process of transformation may have resulted in the fact they activated different immune signalling pathways and/or that they activated the same but with different intensity. This could explain a different cytokine profile and the different ability of sustaining HSV-1 replication. Otherwise, we did not use the exact same strains neither. These two strains may simply have a difference in virulence that leads to different replication profiles in both studies adding another degree of complexity.

Chapter 4 confirmed that aciclovir effectively impairs HSV-1 infective virus production in both neuroblastoma and microglial cells *in vitro*. The experiments also confirmed aciclovir treatment was associated with increased cell viability and mitochondrial metabolism. In my experiments, aciclovir treatment was associated with a decrease in TNF gene expression in microglia but an increase among neuroblastoma cells.

The observed increases in cell viability and mitochondrial metabolism observed *in vitro* reflect the well-known therapeutic effect of aciclovir in HSE patients[124, 39, 125]. My human brain model results also reflect the findings from previous animal studies. Boivin *et al*. showed that the administration of valaciclovir (oral aciclovir) was associated with reduced inflammation in brain homogenates and a 5-fold decrease in viral DNA in the tissue[133]. Wei *et al.* showed that the administration of aciclovir in a mouse model of HSE was associated with a decrease in TNF gene expression in brain tissue[203].

Chapter 5 showed that administering dexamethasone is not detrimental for HSV-1-infected human brain cells. This is the first time cell viability and HSV DNA load has been assessed in a human brain cell *in vitro* model. There have been several clinical reports and case series retrospectively examining use of glucorticoids as an adjuvant in HSE, that have shown improved patient outcome [130, 160, 128, 177]. A retrospective study showed that glucocorticoid administration was a predictor of good outcome in HSE[130]. One case report observed an improvement in a 16-month old girl with HSE following treatment with high-dose dexamethasone at 9 days after admission; her condition had previously deteriorated on aciclovir treatment alone[128]. The clinical outcomes of few a sample of children (n=3) suffering from HSE also improved with glucocorticoids in a case-report[129]. However, to my knowledge, there have been no human studies with dexamethasone investigating brain cell (or tissue) viability or viral load following HSV-1-infection. A few animal models of HSE have looked at viral load. In an *in vivo* mouse model of HSE, methyl-prednisolone (another glucortocoid)

in combination with aciclovir was compared to aciclovir alone. The study found that combining aciclovir with methyprednisolone reduced long-term (60-180 days pi) magnetic resonance imaging (MRI) abnormalities in mouse brains[94]. Of note, viral load in brain tissue was not exacerbated with methylprednisolone administration. Similarly, a rat model of focal HSE also concluded that adding dexamethasone to aciclovir did not increase brain HSV-1 load compared to aciclovir alone[120]. My viral load findings support these animal studies. Together this information can be used to negate fears that glucocorticoids will exacerbate HSV viral load during HSE treatment.

In contrast to previous animal studies, my acute infection human cell models did not show any benefit of dexamethasone on brain cell viability. One hypothesis for the non-efficacy of dexamethasone in my study is that my *in vitro* models, once again, are a simplified representation of acute phase of HSE infection (up to 72 hours pi). During the acute phase of infection, levels of HSV antigen in the brain are still high and tissue inflammation not extensive yet[143]. Similarly in HSE animal models and clinical studies, there is infiltration of immune cells (beyond microglia) into the brain tissue[35, 143, 71, 69, 179, 180, 68]. Such cell interaction was not captured in my monoculture models.

In chapter 6, the administration of infliximab alone led both to a partial rescue of cell viability and a decrease in HSV DNA abundance in both neuroblastomas and microglia cell models. This is first time that infliximab has been shown to inhibit of HSV-1 replication and protect human brain cells. In a previous *in vivo* study of Japanese Encephalitis, it was shown that use of etanercept was associated with a decrease in Japanese encephalitis virus (JEV) load as well as a reduction in brain inflammation[134]. Interestingly, in a HIV-positive patient with Reiter's syndrome (acute inflammatory arthritis), administering antiretroviral therapy with infliximab for 6 months, was associated with a maintenance of low levels of HIV titres together with the resolution of all complaints, regrowth of nails and rash clearance[204]. Beyond measuring TNF

transcript abundance, the mechanism of action of infliximab was not explored in this thesis. Infliximab may inhibit HSV-1 replication and/or viral release from cells. The reduced viral replication (and/or spread) in brain cells may secondarily limit cell death. The mechanism of action of infliximab now warrants further study. In Inflammatory bowel disease, at molecular and cellular levels, infliximab was shown to be involved in: (i) down-regulating inflammatory cytokines, (ii) inducing apoptosis of activated lymphocytes, (iii) downregulating Th1, (iv) inducing Treg and regulatory macrophages, (v) inhibiting NF-kB and (vi) promoting MAPK signalling[168].

Although infliximab use was associated with an initial decrease in HSV DNA abundance, it was not associated with any sustained improvement in cell viability or mitochondrial activity. A mouse model of HSE, demonstrated that the administration of etanercept combined with valaciclovir (oral aciclovir) led to a significant increase in mouse survival compared to valaciclovir alone[133]. In my *in vitro* HSE models, experiments lasted no more than 3 or 4 days after infection (MOI=0.01) and showed persistent high HSV DNA levels throughout. These experiments are more representative of acute HSE phase, in which viral load is high and inflammation low, than a post-acute phase when inflammation and immune cell infiltration become more apparent and viral load has fallen [71, 143, 35] .

In a clinical study, CSF TNF-α levels were elevated throughout a patient's HSE illness course, but reached maximum levels during the convalescence stage (2-6 weeks after disease onset) [71]. In my study, I did not detect any increase in TNF protein levels in the culture media of neuroblastomas or microglia cells. An *in vitro* study showed that a high concentration of TNF proteins was released by purified human foetal microglia but not by astrocytes or neurons 24-72 h after HSV-1-infection (MOI=1) [85]. The fact they were using human foetal cells, or a 100-fold higher MOI could explain the discrepancy with my results. In this same study, they also observed an early increase in TNF mRNA expression (observed by RNase protein assay) in

human foetal microglia from 3 to 24 h post-infection. Another paper, published by the same group, showed, via real-time qPCR, a 600-fold increase in TNF transcript expression following HSV-1 infection in murine microglial cells at 5 h pi and at MOI=2[86]. My data showed an increase in TNF relative gene expression following HSV-1 infection (MOI=0.01) in human microglial cells, but at 72 h pi (last time-point). Once again, the differences in MOI and cell lines could explain the delay in TNF gene expression between my experiments and these latter publications. Although, there was no consistent trend between TNF gene expression and cell viability in HSV-1-infected neuroblastoma and microglial cells, administering infliximab alone had an impact, albeit transiently, on cell viability. The mechanisms by which infliximab increased cell viability remain uncertain and may be due to a direct anti-HSV-1 action previously unknown, or to the blockage of TNF protein at cell membrane level (undetected by ELISA tests).

Only preliminary studies on the effect of microglial cells on HSV-1-infected neuroblastomas have been performed. The data obtained suggested microglia protected HSV-1-infected neuroblastoma cells. Further studies need to be performed. A microglia-release factor, such as IL-6, could be responsible for this protective effect. Indeed, a HSE model using co-culture of murine brain cells demonstrated that the production of IL-6 by microglia protected neuronal loss upon differentiation of NPC following HSV-1-infection[136].

To my knowledge, this is the first time human-derived primary brain cells have been used in co-culture in HSE *in vitro* models. In my study, microglia co-culture did not exacerbate viral replication or protect primary astrocytes during HSV-1 infection. This may indicate, over the time frame of my study, astrocyte death is driven by viral factors rather than inflammatory factors (secreted by microglia) during HSE. Alternatively, it may suggest astrocyte death is induced by pro-inflammatory molecules released by other immune cells (macrophages, T lymphocytes). The setting up of the co-culture models of HSE offers an opportunity in the

future to assess treatments using different *in vitro* systems that closer model clinical or *in vivo* conditions.

For the first time:

-dexamethasone (0.5 µM) was found not to be detrimental in HSV-1-infected neuroblastoma and microglial cells (alone or combined with aciclovir). However, it did not improve cell viability or decrease HSV-1 replication when combined with aciclovir compared to aciclovir alone.

-infliximab was used in a human HSE model.

-infliximab (0.5mg/ml) was shown to decrease viral load and maintain cell viability in HSV-1-infected microglial and neuroblastoma cells. However, infliximab did not show any additional benefit when used in combination with aciclovir compared to aciclovir alone.

8.4. Technical challenges encountered during my PhD and limitations of my work

8.4.1. Technical challenges encountered during my PhD

During my PhD, a number of technical issues have been encountered and addressed. I started to work with primary astrocytes however their proliferation rate was very slow and their life-time, short. Hence, my experimental design was adapted to the use of transformed cell lines rather than primary cells.

Initially I assessed cell viability by cell counting using Trypan blue exclusion staining. This technique was not well suited to counting infected neuroblastoma cells. The cells formed clusters which were difficult to separate back into single cells. For this reason, the WST-1 assay was introduced as an alternative technique to assess cell viability.

Monitoring infected cells by microscopy was undertaken in each experiment. At each time-point and each condition, numerous 10 x magnification microscopy images were taken. This magnification was used because I could clearly observe viral-induced damage in the cell monolayer. In contrast only a few lower magnification images (4x) were taken for each condition at each time-point, for a wider view of cell damage. However, later during analysis of these images, I discovered that despite a variety of imaging parameters being applied, the 10 x magnification images were not suitable for quantification of attached cell area using the standard imaging software "ImageJ".

8.4.2. Limitations of my work

In-part because of these technical challenges, my work includes limitations:

(i) Use of neuroblastoma cells rather than neurons. Neurons do not multiply in cell culture. Pluripotent stem cells that transform into neurons can also be technically challenging to maintain. Instead, neuroblastomas have been used as proxy neuron-like cells in my models.

(ii) An incomplete set of experimental results using primary astrocytes (explained in the part 8.4.1).

(iii) Use of transformed human microglia rather than primary human microglia. Primary human microglia cells are again slow to culture, and relatively difficult to replace if cultures suffer mycoplasma infection. For these reasons, a human microglia cell line was preferred.

(iv) Low numbers of (4 x magnification) microscopy images systematically analysed for attached cell area (explained in the part 8.4.1).

(v) Limited number of co-culture experiments performed. Due to complexity and time spent preparing these models (including re-passage of cells after mycoplasma infection) only two experiments were undertaken for each co-culture.

(vi) *In vitro* work. The results of my data need to be interpreted cautiously, in the context of a relatively simple *in vitro* human brain cell study performed in three brain cell types (examined mainly in monoculture) during the acute phase of HSV infection (up to 72 h pi).

8.5. Future directions

The future directions of this work could include:

(i) Use a lower MOI to perform the same experiments over a longer time-course (several weeks) so that the models can examine the post-acute HSE phase.

(ii) Consider measuring cell viability by FACS to confirm the data obtained by WST-1 assay and live cell area analysis by ImageJ. I began to explore this technique.

(iii) Repeat experiments using other cell types, including neurons or primary microglia. Although more time-consuming and technically more challenging, the data obtained would potentially be closer to clinical and *in vivo* conditions.

(iv) Assess other anti-inflammatory agents, including IFN-γ drugs, in HSV-1-infected brain cells.

(v) Further develop the *in vitro* HSE human co-culture models.

8.6. Conclusion

Several clinical reports and *in vivo* animal studies suggest that administering anti-TNF or glucocorticoid drugs in combination with aciclovir could have a beneficial impact on HSE patient outcome. There is limited data on the effect of these drugs on cell viability or HSV viral load in human brain cell models. This is the first study to assess the effect of dexamethasone or infliximab alone and in combination with aciclovir, *in vitro*, in HSV-1 infected human neuroblastoma and microglial cells.

My study showed that neither dexamethasone nor infliximab, when combined with aciclovir or alone, impaired cell viability or mitochondrial activity during acute HSV-1-infection among neuroblastoma or microglial cell culture. The study also demonstrated use of these anti-inflammatory agents did not enhance HSV-1 replication in these models. My data on viral load in human brain cell culture supports previous animal studies, indicating these agents can be safely given without exacerbating HSV replication during HSE.

For the first time, I have shown that infliximab (in a single dose) is protective against HSV-1 infection of human neuroblastoma and microglial cells. Infliximab treatment was associated with a rapid reduction of HSV DNA abundance in the culture medium of the infected cells and slowed the reduction in live cell number and mitochondrial activity. Nevertheless, neither dexamethasone nor infliximab, when used in combination with aciclovir showed any increase in cell viability compared to aciclovir alone. Finally, I have begun to set-up models of HSE using primary astrocytes or neuroblastoma cells co-cultured with microglia cells. These models need further investigation. However, my preliminary findings on HSE co-culture systems could be the basis for an interesting non-animal model, closer to *in vivo* conditions, for assessing treatments in the future.

New treatments for HSE are still required. Mortality and morbidity among survivors remain unacceptably frequent in HSE patients worldwide. The results from my thesis offer new insights and new human cell models to be taken forward to further explore anti-inflammatory agents and other novel mediators for the benefit of future HSE treatment.

Bibliography

1. Gru, K. *et al.* Three-Dimensional Structure of Herpes Simplex Virus from Cryo – Electron Tomography, *Science* **302**, 1396-1398 (2003).

2. Eisenberg, R.J. *et al.* Comparative usage of herpesvirus entry mediator A and nectin-1 by laboratory strains and clinical isolates of herpes simplex virus, *Virology*, **322,** 286–299 (2004).

3. Atanasiu, D., Saw, W. T., Cohen, G. H. & Eisenberg, R. J. Cascade of Events Governing Cell-Cell Fusion Induced by Herpes Simplex Virus Glycoproteins gD , gH / gL , and gB, *American Society for Microbiology*, **84,** 12292–12299 (2010).

4. Atanasiu, D. *et al.* Bimolecular complementation reveals that glycoproteins gB and gH / gL of herpes simplex virus interact with each other during cell fusion, *PNAS*, **104**:47, 18718-18723 (2007).

5. Kukhanova, M. K., Korovina, A. N. & Kochetkov, S. N. Human Herpes Simplex Virus : Life Cycle and Development of Inhibitors, *Biochemistry (Moscow)*, **79,** 1635–1652 (2014).

6. Widener, R. W. & Whitley, R. J. Herpes simplex virus. in *Handbook of Clinical Virology* **123,** 251–263 (2014).

7. Nicoll, M. P., Proença, J. T. & Efstathiou, S. The molecular basis of herpes simplex virus latency. *FEMS Microbiol. Rev.* **36,** 684–705 (2012).

8. Besecker, M. I., Furness, C. L., Coen, D. M. & Griffiths, A. Expression of Extremely Low Levels of Thymidine Kinase from an Acyclovir-Resistant Herpes Simplex Virus Mutant Supports Reactivation from Latently Infected Mouse Trigeminal Ganglia, *Journal of Virology*, **81**:15**,** 8356–8360 (2007).

9. Efstathiou et al. The Role of Herpes Simplex Virus Type 1 Thymidine Kinase in Pathogenesis, *Journal of General Virology,* **70,** 869–879 (1989).

10. Jacobson, J. G. *et al.* A Herpes Simplex Virus Ribonucleotide Reductase Deletion Mutant Is Defective for Productive Acute and Reactivatable Latent Infections of Mice and for Replication in Mouse Cells. *Virology*, **173,** 276–283 (1989).

11. Perkins, D., Yu, Y., Bambrick, L. L., Yarowsky, P. J. & Aurelian, L. Expression of herpes simplex virus type 2 protein ICP10 PK rescues neurons from apoptosis due to serum deprivation or genetic defects. *Exp. Neurol.* **174,** 118–22 (2002).

12. Tiley, L. S *et al*. The VP16 transcription activation domain is functional when targeted to a promoter-proximal RNA sequence, *Genes and development*, 6, 2077–2087 (1992).

13. Smibert, C. A., Popova, B., Xiao, P., Capone, J. P. & Smiley, J. R. Herpes Simplex Virus VP16 Forms a Complex with the Virion Host Shutoff Protein vhs. *Journal of Virology*, **68,** 2339–2346 (1994).

14. Wu, T., Monokian, G., Mark, D. F. & Wobbe, C. R. Transcriptional Activation by Herpes Simplex Virus Type 1 VP16 In Vitro and Its Inhibition by Oligopeptides. *Molecular and Cellular Biology*, **14,** 3484–3493 (1994).

15. Goldsmith, B. K., Chen, W., Johnson, D. C. & Hendricks, R. L. Neurovirulence by Blocking the CD8+ T Cell Response. *J. Exp. Med.* **187,** 0–7 (1998).

16. Lyman, M. G. & Enquist, L. W. Herpesvirus Interactions with the Host Cytoskeleton, *Journal of Virology,* **83,** 2058–2066 (2009).

17. Spivack, J. G. & Fraser, N. W. Expression of Herpes Simplex Virus Type 1 Latency-Associated Transcripts in the Trigeminal Ganglia of Mice during Acute Infection and Reactivation of Latent Infection. *Journal of Virology,* **62,** 1479–1485 (1988).

18. Steiner, I., Spivack, J. G. & Boyle, D. R. O. Latent Herpes Simplex Virus Type 1 Transcription in Human Trigeminal Ganglia, *Journal of Virology,* **62,** 3493–3496 (1988).

19. Edward, K. *et al.* Physical Characterization of the Herpes Simplex Virus Latency-Associated Transcript in Neurons, *Journal of Virology,* **62,** 1194–1202 (1988).

20. Deatly, A. M., Spivack, J. G., Lavi, E., R. O. B. & Fraser, N. W. Latent Herpes Simplex Virus Type 1 Transcripts in Peripheral and Central Nervous System Tissues of Mice Map to Similar Regions of the Viral Genome. *Journal of Virology,* **62,** 749–756 (1988).

21. Nicoll, M. P., Connor, V. & Efstathiou, S. Influence of Herpes Simplex Virus 1 Latency-Associated Transcripts on the Establishment and Maintenance of Latency in the ROSA26R Reporter Mouse Model, *Journal of Virology,* **86,** 8848–8858 (2012).

22. Ahmed, M., Lock, M., Miller, C. G. & Fraser, N. W. Regions of the Herpes Simplex

Virus Type 1 Latency-Associated Transcript That Protect Cells from Apoptosis In Vitro and Protect Neuronal Cells In Vivo, *Journal of Virology*, **76,** 717–729 (2002).

23. Nicoll, M. P. *et al.* The HSV-1 Latency-Associated Transcript Functions to Repress Latent Phase Lytic Gene Expression and Suppress Virus Reactivation from Latently Infected Neurons, *Plos Pathogens* **1,** 1–24 (2016).

24. Sawtell, N. M. *et al.* The herpes simplex virus type 1 latency associated transcript locis is required for the maintencance of reactivation competent latent infections. *J Neurovirol* **17,** 552–558 (2012).

25. Raschilas, F. *et al.* Outcome of and prognostic factors for herpes simplex encephalitis in adult patients: results of a multicenter study. *Clin. Infect. Dis.* **35,** 254–260 (2002).

26. Xu, F. *et al.* Seroprevalence and Coinfection with Herpes Simplex Virus Type 1 and Type 2 in the United States , 1988 – 1994. *The Journal of Infectious Diseases* **185**, 1019–1024 (2017).

27. Looker, K. J. *et al.* Global estimates of prevalent and incident herpes simplex virus type 2 infections in 2012. *PLoS One* **10,** 1–23 (2015).

28. Opstelten, W., Neven, A. K. & Eekhof, J. Treatment and prevention of herpes labialis. *Can. Fam. Physician* **54,** 1683–1687 (2008).

29. Tsatsos, M. *et al.* Herpes simplex virus keratitis: an update of the pathogenesis and current treatment with oral and topical antiviral agents. *Clin. Exp. Ophthalmol.* **44,**

824–837 (2016).

30. Beck, R.W. *et al*. Oral Acyclovir for Herpes Simplex Virus Eye Disease. *Arch Opthalmol* **118,** (2015).

31. Jaishankar, D. & Shukla, D. Genital Herpes: Insights into Sexually Transmitted Infectious Disease. *Microb. cell (Graz, Austria)* **3,** 438–450 (2016).

32. Gilden, D. H., Mahalingam, R., Cohrs, R. J. & Tyler, K. L. Herpesvirus infections of the nervous system. *Nat. Clin. Pract. Neurol.* **3,** 82–94 (2007).

33. Zarafonetis, C. J. D. Fatal herpes simplex encephalitis in man. *The american journal of pathology*. *Am. J. Pathol.* **XX,** 429-441 (1943).

34. Smith, M. *et al*., Isolation of the virus of herpes simplex and the demonstration of intranuclear inclusions in a case of acute encephalitis. *The american journal of pathology* XVII, 55-68 (1940).

35. Booss, J. & Kim, J. H. Biopsy histopathology in herpes simplex encephalitis and in encephalitis of undefined etiology. *Yale J. Biol. Med.* **57,** 751–755 (1984).

36. Adams, H. & Miller. Herpes simplex encephalitis : a clinical and pathological analysis of twenty-two cases, *Postgraduate Medical Journal*, **49**, 393–397 (1973).

37. Hatanpaa, K. J. & Kim, J. H. *Neuropathology of viral infections*. *Neurovirology* **123,** 193-214 (2014).

38. Gkrania-klotsas, E. & Lever, A. M. L. Herpes simplex 1 encephalitis presenting as a brain haemorrhage with normal cerebrospinal fluid analysis : a case report. *Journal of Medical Case Reports,* **4,** 1–4 (2008).

39. Whitley, R. J *et al.* Herpes Simplex Encephalitis : an Update. *Curr Infect Dis Re,* **19**:13 (2017).

40. Sayers, C. L *et al*. Herpes Simplex Virus 1 Enters Human Keratinocytes by a Nectin-1- Dependent, Rapid Plasma Membrane Fusion Pathway That Functions at Low Temperature. *Journal of Virology*, **90**:22**,** 10379–10389 (2016).

41. Antinone, S. E. & Smith, G. A. Retrograde Axon Transport of Herpes Simplex Virus and Pseudorabies Virus : a Live-Cell Comparative Analysis, *Journal of Virology*, **84,** 1504–1512 (2010).

42. Drummond, C. W. E., Eglin, R. P. & Esiri, M. M. Herpes simplex virus encephalitis in a mouse model: PCR evidence for CNS latency following acute infection. *J. Neurol. Sci.* **127,** 159–163 (1994).

43. Bradshaw, M. J. & Venkatesan, A. Herpes Simplex Virus-1 Encephalitis in Adults: Pathophysiology, Diagnosis, and Management. *Neurotherapeutics* **13,** 493–508 (2016).

44. Steiner, I. Herpes simplex virus encephalitis: new infection or reactivation? *Curr. Opin. Neurol.* **24,** 268–274 (2011).

45. Whitley, R. J. Herpes simplex encephalitis: Adolescents and adults. *Antiviral Res.* **71,** 141–148 (2006).

46. Dinn, J. Transolfactory spread of virus in herpes simplex encephalitis. *Br. Med. J.* **281,** 1392 (1980).

47. Solomon, T., Hart, I. J. & Beeching, N. J. Viral encephalitis : a clinician ' s guide. *Pract Neurol* **7**, 288–305 (2007).

48. Modi, S., Mahajan, A., Dharaiya, D., Varelas, P. & Mitsias, P. Burden of herpes simplex virus encephalitis in the United States. *J. Neurol.* **264,** 1204–1208 (2017).

49. Steiner, I. & Benninger, F. Update on herpes virus infections of the nervous system. *Curr. Neurol. Neurosci. Rep.* **13**:414, 1-7 (2013).

50. Singh, T. D. *et al.* Predictors of outcome in HSV encephalitis, *Journal of Neurology,* **263,** 277–289 (2016).

51. Kim, Y. S. *et al.* Prognostic value of initial standard EEG and MRI in patients with herpes simplex encephalitis, *Journal of Clinical Neuroligy*, **12,** 224–229 (2016).

52. Chaudhuri, a & Kennedy, P. G. E. Diagnosis and treatment of viral encephalitis. *Postgrad. Med. J.* **78,** 575–583 (2002).

53. McGrath, N., Anderson, N. E., Croxson, M. C. & Powell, K. F. Herpes simplex encephalitis treated with acyclovir: diagnosis and long term outcome, *Journal of*

Neurology, Neurosurgery and Psychiatry, **63,** 321–326 (1997).

54. Hardwicke, M. A. & Sandri-Goldin, R. M. The herpes simplex virus regulatory protein ICP27 contributes to the decrease in cellular mRNA levels during infection, *Journal of Virology,* **68,** 4797–810 (1994).

55. Spencer, C. A., Dahmus, M. E. & Rice, S. A. Repression of host RNA polymerase II transcription by herpes simplex virus type 1, *Journal of Virology,* **71,** 2031–2040 (1997).

56. Zaborowska, J. *et al*. Herpes simplex virus 1 (HSV-1) ICP22 protein directly interacts with cyclin-Dependent kinase (CDK)9 to Inhibit RNA polymerase II transcription elongation, *PLoS One,* **9,** (2014).

57. Perez-Parada, J., Saffran, H. a & Smiley, J. R. RNA degradation induced by the herpes simplex virus vhs protein proceeds 5' to 3' in vitro, *Journal of Virology,* **78,** 13391–13394 (2004).

58. Doepker, R. C., Hsu, W.-L., Saffran, H. a & Smiley, J. R. Herpes simplex virus virion host shutoff protein is stimulated by translation initiation factors eIF4B and eIF4H, *Journal of Virology,* **78,** 4684–4699 (2004).

59. Smiley, J. R. Herpes simplex virus virion host shutoff protein: immune evasion mediated by a viral RNase? *Journal of Virology,* **78,** 1063–1068 (2004).

60. Wilcox, D. R., Muller, W. J. & Longnecker, R. HSV targeting of the host phosphatase

PP1α is required for disseminated disease in the neonate and contributes to pathogenesis in the brain, *Proceedings of National Academy of Sciences,* **112,** E6937–E6944 (2015).

61. Li, Y. *et al.* ICP34.5 protein of herpes simplex virus facilitates the initiation of protein translation by bridging eukaryotic initiation factor 2α (eIF2α) and protein phosphatase 1. *J. Biol. Chem.* **286,** 24785–24792 (2011).

62. Saffran, H. a, Pare, J. M., Corcoran, J. a, Weller, S. K. & Smiley, J. R. Herpes simplex virus eliminates host mitochondrial DNA. *EMBO Rep.* **8,** 188–193 (2007).

63. Wnek, M. *et al.* Herpes simplex encephalitis is linked with selective mitochondrial damage; a post-mortem and in vitro study, *Acta Neuropathologica,* **132,** 433–451 (2016).

64. Zambrano, A. *et al.* Neuronal cytoskeletal dynamic modification and neurodegeneration induced by infection with herpes simplex virus type 1, *Journal of Alzheimers. Disease,* **14,** 259–269 (2008).

65. Piacentini, R. *et al.* Herpes Simplex Virus type-1 infection induces synaptic dysfunction in cultured cortical neurons via GSK-3 activation and intraneuronal amyloid-beta protein accumulation. *Sci Rep* **5,** 15444 (2015).

66. Růžek, D., Piskunova, N. & Žampachová, E. High variability in viral load in cerebrospinal fluid from patients with herpes simplex and varicella-zoster infections of the central nervous system, *Clin. Microbiol. Infect.* **13**, 1217–1219 (2007).

67. Aurelian, L. HSV-induced apoptosis in herpes encephalitis, *Curr. Top. Microbiol. Immunology,* **289,** 79–111 (2005).

68. Marques, C. P. & Lokensgard, J. R. Prolonged Microglia Cell Activation and Lymphocyte Infiltration Following Experimental Herpes Encephalitis, *Journal of Immunology,* **181,** 6417–6426 (2008).

69. Lundberg, P. *et al.* The immune response to herpes simplex virus type 1 infection in susceptible mice is a major cause of central nervous system pathology resulting in fatal encephalitis, *Journal of Virology*, **82,** 7078–7088 (2008).

70. Lima, G. K. *et al.* Toll-like receptor (TLR) 2 and TLR9 expressed in trigeminal ganglia are critical to viral control during herpes simplex virus 1 infection, *The American Journal of Pathology,* **177,** 2433–2445 (2010).

71. Aurelius, E., Andersson, B., Forsgren, M., Sköldenberg, B. & Strannegård, O. Cytokines and other markers of intrathecal immune response in patients with herpes simplex encephalitis, *Journal of Infectious diseases*, **170,** 678–681 (1994).

72. Beland, J. L., Sobel, R. A., Adler, H., Del-Pan, N. C. & Rimm, I. J. B cell-deficient mice have increased susceptibility to HSV-1 encephalomyelitis and mortality, *Journal of Neuroimmunology,* **94,** 122–126 (1999).

73. Nahmias, a J., Whitley, R. J., Visintine, a N., Takei, Y. & Alford, C. a. Herpes simplex virus encephalitis: laboratory evaluations and their diagnostic significance, *Journal of Infectious Diseases*, **145,** 829–836 (1982).

74. Hjalmarsson, A. *et al.* Prognostic value of intrathecal antibody production and DNA viral load in cerebrospinal fluid of patients with herpes simplex encephalitis, *Journal of Neurology,* **256,** 1243–1251 (2009).

75. Michael, B. D. *et al.* The Interleukin-1 Balance during Encephalitis Is Associated with Clinical Severity, Blood-Brain Barrier Permeability, Neuroimaging Changes, and Disease Outcome, *Journal of Infectious Dieases,* **213,** 1651–1660 (2016).

76. Kawai, T. & Akira, S. Toll-like Receptors and Their Crosstalk with Other Innate Receptors in Infection and Immunity, *Immunity,* **34,** 637–650 (2011).

77. Bell, J. K. *et al.* Leucine-rich repeats and pathogen recognition in Toll-like receptors, *TRENDS in Immunology,* **24,** 528–533 (2003).

78. Redecke, V. *et al.* Human TLR9 confers responsiveness to bacterial DNA via species-specific CpG motif recognition, PNAS, **98,** 9237–9242 (2001).

79. Sarkar, S. N. *et al.* Novel roles of TLR3 tyrosine phosphorylation and PI3 kinase in double-stranded RNA signaling, *Nature structural and molecular biology,* **11**:11**,** 1060–1067 (2004).

80. Ozinsky, A. *et al.* The repertoire for pattern recognition of pathogens by the innate immune system is defined by cooperation between Toll-like receptors, *PNAS*, **97**:25 (2000).

81. Broz, P. & Monack, D. M. Newly described pattern recognition receptors team up against intracellular pathogens. *Nature Reviews Immunology,* **13,** 551 (2013).

82. Petterson, T., Jendholm, J., Månsson, A., Bjartell, A. & Riesbeck, K. Effects of NOD-like receptors in human B lymphocytes and crosstalk between NOD1 / NOD2 and Toll-

like receptors, *Journal of Leukocyte Biology*, **89,** 177–187 (2011).

83. Means, T. K., Hayashi, F., Smith, K. D. & Luster, A. D. The Toll-Like Receptor 5 Stimulus Bacterial Flagellin Induces Maturation and Chemokine Production in Human Dendritic Cells, The Journal of Immunology, **170**, 5165-5175. (2003).

84. Yu, Y. *et al.* TLR5-mediated activation of p38 MAPK regulates epithelial IL-8 expression via posttranscriptional mechanism, *American Journal of Physiology-Gastrointestinal and Liver Physiology,* **285,** 282–290 (2003).

85. Lokensgard, J. R. *et al.* Robust expression of TNF-alpha, IL-1beta, RANTES, and IP-10 by human microglial cells during nonproductive infection with herpes simplex virus, *Journal of Neurovirology,* **7,** 208–219 (2001).

86. Aravalli, R. N., Hu, S., Rowen, T. N., Palmquist, J. M. & Lokensgard, J. R. Cutting Edge: TLR2-Mediated Proinflammatory Cytokine and Chemokine Production by Microglial Cells in Response to Herpes Simplex Virus, *Journal of Immunology,* **175,** 4189–4193 (2005).

87. Conrady, C. D. *et al.* Microglia and a Functional Type I IFN Pathway Are Required To Counter HSV-1-Driven Brain Lateral Ventricle Enlargement and Encephalitis, *Journal of Immunology,* **190,** 2807–2817 (2013).

88. Mansur, D. S. *et al.* Lethal encephalitis in myeloid differentiation factor 88-deficient mice infected with herpes simplex virus 1, *American Journal of Pathology,* **166,** 1419–26 (2005).

89. Reinert, L. S. *et al.* Sensing of HSV-1 by the cGAS-STING pathway in microglia orchestrates antiviral defence in the CNS, *Nature Communications*, **7,** 13348 (2016).

90. Wang, J. P. *et al.* Role of Specific Innate Immune Responses in Herpes Simplex Virus Infection of the Central Nervous System, *Journal of Virology*, **86,** 2273–2281 (2012).

91. Kurt-Jones, E. a *et al.* Herpes simplex virus 1 interaction with Toll-like receptor 2 contributes to lethal encephalitis, *Proceedings of the National Academy of Sciences U. S A.*, **101,** 1315–1320 (2004).

92. Tsalenchuck, Y., Steiner, I. & Panet, A. Innate defense mechanisms against HSV-1 infection in the target tissues, skin and brain, *Journal of Neurovirology*, (2016).

93. Kamei, S. *et al.* Prognostic value of cerebrospinal fluid cytokine changes in herpes simplex virus encephalitis, *Cytokine*, **46,** 187–193 (2009).

94. Aurelius, E., Forsgren, M., Sköldenberg, B. & Strannegård, O. Persistent intrathecal immune activation in patients with herpes simplex encephalitis, *Journal of Infectious Diseases*, **168,** 1248–1252 (1993).

95. Mørk, N. *et al.* Mutations in the TLR3 signaling pathway and beyond in adult patients with herpes simplex encephalitis, *Genes and Immunity*, 1–15 (2015).

96. Casanova *et al.* A. Inborn errors of anti-viral interferon immunity in humans, *Current Opinion in Virology*, **1,** 487–496 (2012).

97. Zhang, S. *et al.* TLR3 Deficiency in Patients with Herpes Simplex Encephalitis, *Science*, **317,** 1522–1528 (2007).

98. Marques, C. P., Cheeran, M. C., Palmquist, J. M., Hu, S. & Lokensgard, J. R. Microglia are the major cellular source of inducible nitric oxide synthase during experimental herpes encephalitis, *Journal of Neurovirology*, **14,** 229–238 (2008).

99. Schachtele, S. J., Hu, S., Little, M. R. & Lokensgard, J. R. Herpes simplex virus induces neural oxidative damage via microglial cell Toll-like receptor-2, *Journal of Neuroinflammation*, **7,** 35 (2010).

100. Zolini, G. P. *et al.* Defense against HSV-1 in a murine model is mediated by iNOS and orchestrated by the activation of TLR2 and TLR9 in trigeminal ganglia, *Journal of Neuroinflammation*, **11,** 20 (2014).

101. Hu, S., Sheng, W. S., Schachtele, S. J. & Lokensgard, J. R. Reactive oxygen species drive herpes simplex virus (HSV)-1-induced proinflammatory cytokine production by murine microglia, *Journal of Neuroinflammation*, **8,** 123 (2011).

102. Nguyen, M. L. & Blaho, J. a. Apoptosis during herpes simplex virus infection. *Advances in Virus Research*, **69,** 67–97 (2007).

103. Yu, X. & He, S. The interplay between human herpes simplex virus infection and the apoptosis and necroptosis cell death pathways, *Virology Journal*, **13,** 77 (2016).

104. Jiang, X. *et al.* The herpes simplex virus type 1 latency-associated transcript can protect

neuron-derived C1300 and Neuro2A cells from granzyme B-induced apoptosis and CD8 T-cell killing, *Journal of Virology*, **85,** 2325–2332 (2011).

105. Perkins, D., Gyure, K. a, Pereira, E. F. R. & Aurelian, L. Herpes simplex virus type 1-induced encephalitis has an apoptotic component associated with activation of c-Jun N-terminal kinase, *Journal of Neurovirology*, **9,** 101–11 (2003).

106. Aravalli, R. N., Hu, S. & Lokensgard, J. R. Toll-like receptor 2 signaling is a mediator of apoptosis in herpes simplex virus-infected microglia, *Journal of Neuroinflammation*, **4,** 11 (2007).

107. Adhikary *et al*. C-jun NH2 terminal (JNK) is an essential mediator of Toll-like receptor 2-induced corneal inflammation, *Journal of Leukocyte Biology*, 83(4):991-997 (2008).

108. Perkins, D., Pereira, E. F. R. & Aurelian, L. The herpes simplex virus type 2 R1 protein kinase (ICP10 PK) functions as a dominant regulator of apoptosis in hippocampal neurons involving activation of the ERK survival pathway and upregulation of the antiapoptotic protein Bag-1, *Journal of Virology*, **77,** 1292–305 (2003).

109. DeBiasi, R. L., Kleinschmidt-DeMasters, B. K., Richardson-Burns, S. & Tyler, K. L. Central nervous system apoptosis in human herpes simplex virus and cytomegalovirus encephalitis, *Journal of Infectious Diseases*, **186,** 1547–1557 (2002).

110. S Athmanathan *et al*.. Neuronal apoptosis in Herpes Simplex Virus-1 Encephalitis (HSE), *Indian Journal of Medical Microbiology*, 19(3):127–131 (2001).

111. Sabri, F., Granath, F., Hjalmarsson, A., Aurelius, E. & Sköldenberg, B. Modulation of sFas indicates apoptosis in human herpes simplex encephalitis, *Journal of Neuroimmunology,* **171,** 171–176 (2006).

112. Geiger, K. D. *et al.* Interferon-gamma protects against herpes simplex virus type 1-mediated neuronal death, *Virology,* **238,** 189–197 (1997).

113. Festjens, N., Vanden Berghe, T. & Vandenabeele, P. Necrosis, a well-orchestrated form of cell demise: Signalling cascades, important mediators and concomitant immune response, *Biochimica Biophysica Acta - Bioenergetics,* **1757,** 1371–1387 (2006).

114. Wang, X. *et al.* Direct activation of RIP3/MLKL-dependent necrosis by herpes simplex virus 1 (HSV-1) protein ICP6 triggers host antiviral defense, *Proceedings of the National Academy of Sciences,* **111,** 15438–15443 (2014).

115. Sergerie, Y., Boivin, G., Gosselin, D. & Rivest, S. Delayed but Not Early Glucocorticoid Treatment Protects the Host during Experimental Herpes Simplex Virus Encephalitis in Mice. *Journal of Infectious Diseases,* **2,** 0–8 (2007).

116. Kukla, G. J. Missing link between milankovitch and climate, *Nature,* **253,** 600–603 (1975).

117. Lopez, C. & Dudas, G. Replication of herpes simplex virus type 1 in macrophages from resistant and susceptible mice, *Infection and Immunity,* **23,** 432–437 (1979).

118. Cantin, E., Tanamachi, B. & Openshaw, H. Role for Gamma Interferon in Control of Herpes Simplex Virus Type 1 Reactivation, *Journal of Virology,* **73,** 3418–3423 (1999).

119. Cantin, E., Tanamachi, B., Openshaw, H., Mann, J. & Clarke, K. Gamma Interferon (IFN-gamma) Receptor Null-Mutant Mice Are More Susceptible to Herpes Simplex Virus Type 1 Infection than IFN-gamma Ligand Null-Mutant Mice. *Journal of Virology,* **73,** 5196–5200 (1999).

120. Halford, W. P., Balliet, J. W. & Gebhardt, B. M. Re-evaluating natural resistance to herpes simplex virus type 1. *Journal of Virology,* **78,** 10086–10095 (2004).

121. Mancini, M. & Vidal, S. M. Insights into the pathogenesis of herpes simplex encephalitis from mouse models. *Mammalian Genome* **29,** 1–21 (2018).

122. Shivkumar, M. *et al.* Herpes Simplex Virus 1 Targets the Murine Olfactory Neuroepithelium for Host Entry, *Journal of Virology*, **87,** 10477–10488 (2013).

123. Kollias, C. M., Huneke, R. B., Wigdahl, B. & Jennings, S. R. Animal models of herpes simplex virus immunity and pathogenesis, *Journal of Neurovirology,* **21,** 8–23 (2014).

124. Solomon, T. *et al.* Management of suspected viral encephalitis in adults - Association of British Neurologists and British Infection Association National Guidelines, *Journal of Infection,* **64,** 347–373 (2012).

125. Whitley, R. J. *et al.* Vidarabine versus acyclovir therapy in Herpes Simplex Encephalitis. *New England Journal of Medecine.* **314,** 144–149 (1986).

126. Gnann, J. W. *et al.* Herpes Simplex Encephalitis: Lack of Clinical Benefit of Long-

term Valacyclovir Therapy, *Clinical Infectious Disease*, 1–9 (2015).

127. Sili, U., Kaya, A. & Mert, A. Herpes simplex virus encephalitis: Clinical manifestations, diagnosis and outcome in 106 adult patients, *Journal of Clinical Virology*, **60,** 112–8 (2014).

128. Musallam, B., Matoth, I., Wolf, D. G., Engelhard, D. & Averbuch, D. Steroids for Deteriorating Herpes Simplex Virus Encephalitis, *Pediatric Neurology,* **37,** 229–232 (2007).

129. Maraş Genç, H. *et al.* Clinical outcomes in children with herpes simplex encephalitis receiving steroid therapy. *Journal of Clinical Virology,* **80,** 87–92 (2016).

130. Kamei, S. *et al.* Evaluation of combination therapy using aciclovir and corticosteroid in adult patients with herpes simplex virus encephalitis. *Journal of Neurology, Neurosurgery and Psychiatry*, **76,** 1544–1549 (2005).

131. Meyding-Lamadé, U. K. *et al.* Experimental herpes simplex virus encephalitis: a combination therapy of acyclovir and glucocorticoids reduces long-term magnetic resonance imaging abnormalities, *Journal of Neurovirology*, **9,** 118–125 (2003).

132. Defres, S. *et al.* A Feasibility Study of Quantifying Longitudinal Brain Changes in Herpes Simplex Virus (HSV) Encephalitis Using Magnetic Resonance Imaging (MRI) and Stereology. *PLoS One* **12,** e0170215 (2017).

133. Boivin, N., Menasria, R., Piret, J., Rivest, S. & Boivin, G. The combination of

valacyclovir with an anti-TNF alpha antibody increases survival rate compared to antiviral therapy alone in a murine model of herpes simplex virus encephalitis, *Antiviral Research,* **100,** 649–653 (2013).

134. Ye, J. *et al.* Etanercept Reduces Neuroinflammation and Lethality in Mouse Model of Japanese Encephalitis. *Journal of Infectious Diseases,* **210,** 1–15 (2014).

135. Wnek, M. *et al.* Herpes simplex encephalitis is linked with selective mitochondrial damage; a post-mortem and in vitro study, *Acta Neuropathologica,* **132,** 433–451 (2016).

136. Chucair-Elliott, A. J. *et al.* Microglia-induced IL-6 protects against neuronal loss following HSV-1 infection of neural progenitor cells, *Glia,* **62,** 1418–1434 (2014).

137. Guo, Y. J. *et al.* Effect of Corilagin on anti-inflammation in HSV-1 encephalitis and HSV-1 infected microglias, *European Journal of Pharmacology,* **635,** 79–86 (2010).

138. Preis, P. N., Saya, H., Hochhaus, G., Levin, V. & SadÃ, W. Neuronal Cell Differentiation of Human Neuroblastoma Cells by Retinoic Acid plus Herbimycin A1, *Cancer Research,* **48,** 6530–6534 (1988).

139. Shipley, M. M., Mangold, C. A., Kuny, C. V & Szpara, M. L. Differentiated Human SH-SY5Y Cells Provide a Reductionist Model of Herpes Simplex Virus 1 Neurotropism, *Journal of Virology,* **91** (2017).

140. Liu, W., Tang, Y. & Feng, J. Cross talk between activation of microglia and astrocytes

in pathological conditions in the central nervous system, *Life Sciences*, **89,** 141–146 (2011).

141. Park, L. C. H., Zhang, H. & Gibson, G. E. Co-culture with astrocytes or microglia protects metabolically impaired neurons, *Mechanisms of Ageing and Development*, **123,** 21–27 (2001).

142. Marques, C. P., Hu, S., Sheng, W. & Lokensgard, J. R. Microglial cells initiate vigorous yet non-protective immune responses during HSV-1 brain infection, *Virus Research*, **121,** 1–10 (2006).

143. Esiri, M. M *et al.* Herpes simplex encephalitis: an immunohistological study of the distribution of viral antigen within the brain, *Journal of the Neurological Sciences*, **54,** 209–226 (1982).

144. Stahl, J. P., Mailles, A. & De Broucker, T. Herpes simplex encephalitis and management of acyclovir in encephalitis patients in France, *Epidemiology and Infection*, **140,** 372–381 (2012).

145. Acosta, E. P. & Balfour, H. H. Acyclovir for Treatment of Postherpetic Neuralgia : Efficacy and Pharmacokinetics, *Antimicrobial agents and chemotherapy*, **45,** 2771–2774 (2001).

146. Hamadani, M. Prospective , Controlled Study of Acyclovir Pharmacokinetics in Obese Patients, *Antimicrobial agents and chemotherapy*, **60,** 1830–1833 (2016).

147. King, D. H. & Madera, C. History, pharmacokinetics, and pharmacology of acyclovir, *Journal of the American Academy of Dermatology*, 18:176–179 (1982).

148. Stoeter, D., Michael, B., Solomon, T. & Poole, D. Managing acute central nervous system infections in the UK adult intensive care unit in the wake of UK encephalitis guidelines, *Journal of the Intensive Care Society*, **0,** 1–9 (2015).

149. Gosert, R., Rinaldo, C. H., Wernli, M., Major, E. O. & Hirsch, H. H. CMX001 (1-O-hexadecyloxypropyl-cidofovir) inhibits polyomavirus jc replication in human brain progenitor-derived astrocytes, *Antimicrobial Agents and Chemotherapies,*. **55,** 2129–2136 (2011).

150. Baunbæk-Knudsen, G., Sølling, M., Farre, A., Benfield, T. & Brandt, C. T. Improved outcome of bacterial meningitis associated with use of corticosteroid treatment, *Infectious Diseases. (Auckl)*, **4235,** 1–6 (2015).

151. Gupta, A. & Singh, N. K. Dexamethasone in adults with bacterial meningitis, *The Journal of the Association of Physicians of India*, **44,** 90–92 (1996).

152. Odio, C., McCracken, J. & Al., E. The beneficial effects of early dexamethasone administration in infants and children with bacterial meningitis, *New England Journal of Medecine*, **325,** 1127–1131 (1991).

153. Fitch, M. T. & van de Beek, D. Drug Insight: steroids in CNS infectious diseases--new indications for an old therapy, *Nature Clinical Practice Neurology*, **4,** 97–104 (2008).

154. Molyneux, E. M. *et al.* Dexamethasone treatment in childhood bacterial meningitis in Malawi: A randomised controlled trial, *Lancet*, **360,** 211–218 (2002).

155. Brouwer, M., Mcintyre, P., Prasad, K. & Van De Beek, D. Corticosteroids for acute bacterial meningitis, *Cochrane Database of Systematic Reviews* (2015).

156. Hinkerohe, D. *et al.* Dexamethasone prevents LPS-induced microglial activation and astroglial impairment in an experimental bacterial meningitis co-culture model. *Brain Research*, **1329,** 45–54 (2010).

157. Ramakrishna, C., Openshaw, H. & Cantin, E. M. The case for immunomodulatory approaches in treating HSV encephalitis, *Future Virology*, **8,** 259–272 (2013).

158. Kamei, S. *et al.* Evaluation of combination therapy using aciclovir and corticosteroid in adult patients with herpes simplex virus encephalitis, *Journal of Neurology, Neurosurgery and Psychiatry*, **76,** 1544–1549 (2005).

159. Martinez-Torres, F. *et al.* Protocol for German trial of Acyclovir and corticosteroids in Herpes-simplex-virus-encephalitis (GACHE): a multicenter, multinational, randomized, double-blind, placebo-controlled German, Austrian and Dutch trial [ISRCTN45122933], *BMC Neurology*, **8,** 40 (2008).

160. Genç, H. M. *et al.* Clinical outcomes in children with ‘ Herpes simplex ’ encephalitis receiving steroid therapy, *Journal of Clinical Virology*, **80**, 87-92 (2016).

161. Nestler, U., Winking, M. & Böker, D.-K. The tissue level of dexamethasone in human

brain tumors is about 1000 times lower than the cytotoxic concentration in cell culture, *Neurological Research,* **24,** 479–82 (2002).

162. Thompson, K. A., Blessing, W. W. & Wesselingh, S. L. Herpes simplex replication and dissemination is not increased by corticosteroid treatment in a rat model of focal Herpes encephalitis, *Journal of Neurovirology,* **6,** 25–32 (2000).

163. Dagsdóttir, H. *et al.* Herpes simplex encephalitis in Iceland 1987–2011. *Springerplus* **3,** 524 (2014).

164. Bradford, R. D. *et al.* Herpes Simplex Encephalitis during Treatment with Tumor Necrosis Factor–α Inhibitors, *Clinical Infectious Diseases,* **49,** 924–927 (2009).

165. Crusio, R. H. J., Singson, S. V, Haroun, F., Mehta, H. H. & Parenti, D. M. Herpes simplex virus encephalitis during treatment with etanercept. *Scandinavian Journal of Infectious Diseases,* **3,** 1–3 (2013).

166. Danese, S. Mechanisms of action of infliximab in inflammatory bowel disease: an anti-inflammatory multitasker, *Digestive and Liver Disease,* **40,** 225–228 (2008).

167. Catrina, A. I. *et al.* Evidence that anti-tumor necrosis factor therapy with both etanercept and infliximab induces apoptosis in macrophages, but not lymphocytes, in rheumatoid arthritis joints: Extended report, *Arthritis and Rheumatolgy,* **52,** 61–72 (2005).

168. Guo, Y., Lu, N. & Bai, A. Clinical use and mechanisms of infliximab treatment on

inflammatory bowel disease: A recent update, *Biomed Research International*, **2013,** (2013).

169. Whitley, R. J., Kimberlin, D. W. & Roizman, B. Herpes simplex virus, *Clinical Infectious Diseases*, **26,** (1998).

170. Schachtele, S. J., Hu, S. & Lokensgard, J. R. Modulation of experimental herpes encephalitis-associated neurotoxicity through sulforaphane treatment, *PLoS One* **7,** (2012).

171. Aravalli, R. N., Hu, S., Rowen, T. N., Gekker, G. & Lokensgard, J. R. Differential apoptotic signaling in primary glial cells infected with herpes simplex virus 1, *Journal of Neurovirology*, **12,** 501–510 (2006).

172. Welser, J. V & Milner, R. Use of Astrocyte-Microglial cocultures to examine the regulatory influence of astrocytes on microglial activation, *Astrocytes: methods and protocols, methods in molecular biology*, **814,** 367–380 (2012).

173. Kumaraswamy, G. K., Fu, M. M. & Docherty, J. J. Innate and adaptive host response during the initial phase of herpes simplex virus encephalitis in the neonatal mouse, *Journal of Neurovirology*, **12,** 365–374 (2006).

174. Savarin, C. *et al.* Astrocyte response to IFN-γ limits IL-6-mediated microglia activation and progressive autoimmune encephalomyelitis. *Journal of Neuroinflammation* **12,** (2015).

175. Lahat, E. *et al.* Long term neurological outcome of herpes encephalitis, *Archives of Diseases in. Children,* **80,** 69–71 (1999).

176. Nakano, A. *et al.* Beneficial effect of steroid pulse therapy on acute viral encephalitis. *European Neurology,* **50,** 225–229 (2003).

177. Ramos-Estebanez, C., Lizarraga, K. J. & Merenda, A. A systematic review on the role of adjunctive corticosteroids in herpes simplex virus encephalitis: Is timing critical for safety and efficacy? *Antiviral Therapy,* **19,** 133–139 (2014).

178. Sergerie, Y., Rivest, S. & Boivin, G. Tumor necrosis factor-alpha and interleukin-1 beta play a critical role in the resistance against lethal herpes simplex virus encephalitis, *Journal of Infectious Diseases,* **196,** 853–860 (2007).

179. Zhang, J., Liu, H. & Wei, B. Immune response of T cells during herpes simplex, *Journal of Zhejiang University (Biomedecine and Biotechnology),* **18,** 277–288 (2017).

180. Koyanagi, N. *et al.* Herpes simplex virus-1 evasion of CD8+ T cell accumulation contributes to viral encephalitis, *Journal of Clinical Investigation,* **127,** 507–513 (2017).